Deltares

# Statistical analysis of effects of MSC Zoe incident on populations of protected species in Wadden Sea and North Sea.

**Statistical analysis of effects of MSC Zoe incident on populations of protected species in Wadden Sea and North Sea.**

**Auteur(s)**
Peter Herman
Amrit Cado van der Lelij
Elena N. Ieno
Mardik Leopold
Hans Schekkerman
Karin Troost
Johan Craeymeersch
Allert Bijleveld
Lisanne van de Bogaart

**Statistical analysis of effects of MSC Zoe incident on populations of protected species in Wadden Sea and North Sea.**

| | |
|---|---|
| **Opdrachtgever** | Rijkswaterstaat Noord-Nederland locatie Leeuwarden |
| **Contactpersoon** | De heer Jan Maarten Bakker |
| **Referenties** | |
| **Trefwoorden** | |

| **Documentgegevens** | |
|---|---|
| **Versie** | 1.0 |
| **Datum** | 10-05-2021 |
| **Projectnummer** | 11206109-000 |
| **Document ID** | 11206109-000-ZKS-0004 |
| **Pagina's** | 165 |
| **Classificatie** | Vertrouwelijk tot nader order |
| **Status** | definitief |

| **Auteur(s)** | | |
|---|---|---|
| **Peter Herman** | | |
| **Amrit Cado van der Lelij** | | |

| **Doc. Versie** | **Auteur** | **Controle** | **Akkoord** | **Publicatie** |
|---|---|---|---|---|
| **1.0** | Peter Herman<br>Amrit Cado van der Lelij | Luca van Duren | Toon Segeren | |
| | | | | |

# Summary

On 1-2 January 2019, an incident happened north of the Dutch Wadden Sea, in which the MSC Zoe lost part of her cargo. Among the cargo lost were plastic pellets of two different types: relatively large (several mm) high-density poly-ethylene pellets and small (0.5 mm) polystyrene granules.

As part of the agreement between the Dutch government and MSC, the present study investigated whether significant damage is caused or likely to be caused to the EU protected habitats and species located in Natura 2000 sites, due to the incident with the MSC Zoe. The focus is on the detection of possible effects of ingestion of microplastics at population level. The study is based on many thousands of samples of the macrobenthos in the Wadden Sea (collected in the SIBES monitoring of NIOZ and the WOT shellfish survey of WMR) and the coastal North Sea (collected in the WOT shellfish survey of WMR), on bird counts in the Wadden Sea and North Sea (sea ducks, collected by Rijkswaterstaat and WMR) and bird counts of the Wadden Sea (collected by SOVON). All data span at least one decade. The species selected for analysis are flagship species that are protected through European directives and stand as a model for other species with similar trophic or habitat requirements, or with similar exposure to plastic particles. Only abundant species that can be analyzed with full statistical power have been selected.

The best possible estimation of the spatial distribution of plastics lost by MSC Zoe did not permit to sharply delineate affected areas and use these as fixed factors in the analysis. An exploratory approach had to be used instead. The analysis looked for deviant spatial patterns between the year 2019 and the preceding (for birds also following) year and used expert judgement to evaluate whether any such patterns could be caused by plastic pollution from the MSC Zoe incident.

The available data were modelled with a statistical model that took account of (1) physical cofactors (bottom shear stress due to currents and waves, grain size of the sediment, salinity) through non-linear GAM smoothers, (2) the type of statistical distribution of the data, including the number of zero observations, and (3) the spatial and temporal autocorrelations in the data. A Bayesian approach using R-INLA has been used. Possible effects of the Zoe incident were identified by comparing the unexplained (by physical factors) spatially structured variability in the populations between the samplings before and after the incident.

All populations studied are characterized by relatively high variability in both space and time. Within the bird species, variability was very high for sea ducks (e.g. the Eider duck and the Scoter) and some waders, but more limited in shelducks and bar-tailed godwits. For none of the bird species, any important difference between the observations in early 2019 with those of 2018 or 2020 could be detected. Thus, no evidence for an effect of the MSC Zoe was found. Within the benthic species, recruitment processes that are highly variable from year to year and that dominate the population dynamics of the shellfish, were the prime cause of variability in the data set. Six species were each examined for abundance and biomass, yielding in total 12 analyses. Of these 12 analyses, four showed important differences between the spatial pattern in 2019 with that in 2018. In two cases, the cockle and the razor clam, this was clearly linked to a very high recruitment in 2018. In two other cases, the mussel and the Baltic tellin, the changes in spatial pattern concerned the appearance and disappearance of small-scale spatial hotspots. The important differences concerned only a few percent of the total number of comparisons. In half of the cases the values increased from 2018 to 2019. In the other half, they decreased. This was interpreted as part of the natural dynamics of these species.

The study concludes that no evidence has been found for a negative influence of the MSC Zoe incident on dominant protected flagship species in the Wadden Sea and in the Dutch coastal North Sea.

# Table of Contents

# 1 Introduction

## 1.1 The MSC Zoe incident and the legal context

On the night of January 1st, 2019, the Zoe, a freight ship owned by the Mediterranean Shipping Company, was on its way to the port city of Bremerhaven when it was hit by a storm event in the North Sea. During the storm, the MSC Zoe lost a total of 342 containers (approx. 3.2 million kilos of material). Parts of the containers and their contents washed up on the shores of the North Sea, and part also penetrated into the Wadden Sea.

The Minister of Infrastructure and Water Management and MSC have come to a financial agreement on the coverage of the damage caused by the incident. Besides covering all the costs of the salvage and storage operations, MSC has provided a financial compensation covering the costs that the Dutch Government and any other organization have made to combat the effects of the disaster. Furthermore, MSC settled all claims handed in by over 26 organizations and have provided financial support for ecological/legal research.

This document reports on the scientific investigation requested by Rijkswaterstaat to determine the short- and long-term effects of micro plastics in the Wadden Sea as result of the loss of cargo by MSC Zoe.

The Wadden sea and parts of the North Sea are protected nature reserves under national and European legislation and are classified as Natura 2000 sites. Furthermore, The Wadden Sea is a protected UNESCO biosphere reserve. In accordance with EU legislation, the polluter is responsible for the prevention and remediation of environmental damage. The full legal implications of this status are discussed in Appendix I. In the incident with the MSC Zoe, MSC must bear the cost of the necessary preventive and remedial measures. Rijkswaterstaat, the governmental agency responsible for safeguarding the natural habitat of both the Wadden Sea and the North Sea, is leading the investigation on the ecological effects of the containers and its contents. EU legislation dictates that to determine the effect of any environmental damages, they must be assessed with reference to a baseline condition. The baseline is defined as the condition of a habitat or species, had the incident in question not occurred. It considers all natural fluctuations, influences of other factors or occurrences not caused by the incident. By defining a baseline, it becomes possible to determine if the disturbance, in this case the loss of plastics at sea, has impacted bird species and the habitats including typical macrozoobenthic species that are protected under the Wild Birds and Habitat Directives within the Natura 2000 areas of the Wadden Sea and North Sea coastal zone.

## 1.2 Aim of the research

The aim of this report is to investigate whether due to the incident with the MSC Zoe, significant damage is caused or likely to be caused to the EU protected habitats and species located in Natura 2000 sites. To do so, the project defines a baseline ($T_0$) and a $T_1$ for a number of selected flagship species. In other words, the aim is to describe the situation before and after the incident. For each of the species, monitoring data is statistically analyzed to detect a possible effect of the plastics released during the incident. The purpose of this end report is to present the data and how they have been derived, present the species, the most important aspects of the statistical analyses, and the conclusions.

## 1.3 Selection of species for the analysis

The Wadden Sea and coastal North Sea are biodiverse areas hosting thousands of species. It is not possible to perform a thorough statistical analysis of the populations of all these species. A selection has been made (see full details in Appendix 1) according to the following criteria. First, species were selected if they can act as flagship species, i.e. represent a larger group of organisms that are similar in their exposure to plastic ingestion, to potential damage cause by the plastic or in the options that exist to alleviate or remediate any possible damage. Second, species were selected if they had a protected legal status, either as Natura2000 target species or as species with essential functions in the habitat. And third, species have been selected for which a database exists that allows for in-depth statistical analysis. This implies that the species is sufficiently abundant, and that monitoring has been performed in a systematic and unbiased way over at least the past decade.
The result of the selection process is the following list of flagship protected bird species (see Appendix I). They have different spatial distributions over Wadden and North Sea and therefore different potential exposure to the plastic originating from the MSC Zoe. Due to their different spatial distribution, the bird species are also differentially affected by disturbance from salvage operations, which is an additional potential source of stress from the MSC Zoe incident. Furthermore, they differ in their ability to directly pick up plastic granules, and in their exposure to microplastics through their food.

- Common Scoter (*Melanitta nigra*) is a shellfish-eating duck typical for the coastal North Sea; vulnerable to disturbance by salvage operations; exposed to microplastics through its food, that is swallowed whole. Common Scoters can occur in very large flocks (>100 000 in the early 1990s) over rich feeding grounds, generally banks of Spisula subtruncata. Other shellfish species, such as Ensis spec. are also taken. Numbers have declined to around 40 000 and have been fluctuating around that number since about 2005 (SOVON). In the North Sea, Common Scoters are the main shellfish eating seabird; other species often join the flocks of Common Scoters (Velvet Scoter, Eider, Great Scaup) and Common Scoters are a flagship species for this guild.
- Common Eider (*Somateria mollisima*) is a shellfish-eating duck typical for the Wadden Sea; exposed to microplastics through its food, that is swallowed whole. The Wadden Sea is the core area for this large duck in The Netherlands; the North Sea Coastal Zone is mainly used during periods of food shortage in the Wadden Sea. Eiders are, in terms of biomass and food consumption, the most important consumers of shellfish (mussels, cockles, etc.) in the Wadden Sea and are an indicator species of ecosystem functioning of the area.
- Shelduck (*Tadorna tadorna*) is a filter-feeding duck feeding at the surface of intertidal flats in the Wadden Sea and likely to ingest indigestible particles of similar size as the microplastics lost by MSC Zoe. The Dutch Wadden Sea is an important area for breeding, moulting and wintering Shelduck. In summer, over 80% of the total flyway population moults in the international Wadden Sea. The Dutch part harbors about one third of this population in autumn and about 10% in mid-winter. The species has some ecological similarities with other dabbling duck, such as the mallard *Anas platyrhynchos* and wigeon *Mareca penelope*.
- Red Knot (Calidris canuta) is a shellfish-eating small wader known to feed on prey of sizes similar to the microplastics lost. The Dutch Wadden Sea is an internationally important area for two subspecies of Red Knot. In winter the area holds about 15% of the world population of Nearctic Red Knots *C.c.islandica*. Numbers of Afrosiberian Red Knots are probably largest in late summer (July-August) when they may represent a similar proportion of that population. The species has some ecological similarity to other shellfish-eating waders (e.g. oystercatcher), but these usually take other size classes as prey.

- Bar-tailed Godwit (*Limosa lapponica*) as a worm-eating bird specializing in predation on the lugworm Arenicola marina that has been observed to ingest microplastic particles. The Wadden Sea is one of the most important wintering sites of the *lapponica* subspecies of Bar-tailed Godwit, harboring close to 50% of the total population in winter. For the *taimyrensis* subspecies, the area forms a key stopover site during both spring (Rakhimberdiev et al. 2018) and autumn migration; numbers present in the Wadden Sea at one time may represent up to roughly 20-30% of that population. The species is a flagship species resembling other worm-feeding birds such as the Eurasian Curlew *Numenius arquata*, Black-tailed Godwit *Limosa limosa*, Grey Plover *Pluvialis squatarola*, and Oystercatcher *Haematopus ostralegus*, as well as some smaller sandpipers.
- Northern Pintail (*Anas acuta*) has been added to the original list as a duck species known to feed on seeds of saltmarsh plants, and therefore possibly exposed to floating microplastic particles that it could mistake for food. The international Wadden Sea can harbor in excess of 50% of the Pintail in the East-Atlantic flyway population, of which about 20% in the Dutch part.

All these bird species have a protected status through the Bird Directive, part of the Natura 2000 legislation, as well as a protection under the Dutch Nature Conservation Act. Targets for the species have been set for the Wadden Sea and/or the coastal zone of the North Sea.

As major food items for these (and similar) birds, and major constituents of the habitat quality, the following macrobenthic species have been selected:

- Lugworm (*Arenicola marina*), a worm species known to ingest microplastics and a preferred food of the bar-tailed godwit; strong bioturbator structuring the sediment and affecting occurrence of other species
- Baltic Tellin (*Limecola balthica*, formerly called *Macoma balthica*), a major food item for red knot and other shellfish-eating waders, and a very important grazer of phytoplankton and microphytobenthos (benthic algae) in the Wadden Sea
- Common cockle (*Cerastoderma edule*), a shellfish grazing on phytoplankton; food source for waders such as the red knot and the oystercatcher; commercial species supporting a limited industry of hand collectors in the Wadden Sea; biomass dominant of the macrobenthos in the Wadden Sea intertidal zone
- Blue mussel (*Mytilus edulis*), food for shellfish-eating waders and staple food for eider ducks; ecosystem engineer building reefs that are home to a suite of epibenthic species attracting a diversity of bird and fish predators; commercial species supporting an important shellfish industry in the Netherlands
- Razor clam (*Ensis leei)*. Invasive shellfish species in the coastal zone of the North Sea, that has become the biomass dominant since the early 2000s. As juveniles staple food for common scoters. Occurs in dense beds that are also commercially exploited.
- Surf clam (*Spisula subtruncata*), one of the most important shellfish species in the North Sea coastal zone; staple food of the common scoter; commercial species for shellfish exploitation, although actual exploitation has been minimal in past decade.

The selected four macrobenthic species from the Wadden Sea together represent 49 % of the total macrobenthic biomass in the intertidal Wadden Sea (Compton et al., 2013). The ranking is as follows: cockle 27%, lugworm 10 %, Baltic tellin 6 %, blue mussel 6 %. Together they represent the food base for higher trophic levels, and they determine to a large extent the fate of primary production and the ecosystem functioning in the Wadden Sea. Through their ecosystem engineering activity, especially the case for the reef-building mussel and the strongly bioturbating lugworm, they co-determine the occurrence, food and density of many other species.

Therefore, the ecological functions of the chosen species are essential for the preservation of the protected habitat values in this Natura 2000 area. For the North Sea coastal zone, the razor clam and surf clam are the two species dominating biomass. They are a major food source for sea ducks but also for many internal predators in the system, such as shrimp and fish. In turn, together they are major grazers on the phytoplankton and remineralizers of nutrients, thus shaping the ecosystem functioning in the coast. As such, they also characterize the values of the habitat for this Natura 2000 protected zone.

## 1.4 Spatial and temporal distribution of plastics lost by MSC Zoe

Plastic pollution affects marine species in two main ways, through entanglement and ingestion. In this report the focus is on potential damage due to ingestion of microplastics, which can be direct (purposefully ingestion by mistaking it for food) or indirect (inadvertently consuming plastic while foraging on other prey items). Two different types of microplastics were lost from the MSC Zoe: over 11 metric tons of semi-transparent 0.5 mm diameter polystyrene (PS) granules and an unknown quantity of white HDPE (High Density Polyethylene) pellets, with a diameter of a few millimeters. Foekema et al. (2021) established that at the time they were lost to sea, both plastics were in pure form, and were not mixed with any toxic colorants, flame-retardants, or plasticizers. As is the case with all microplastics, adsorption of toxic components is likely to have occurred once the particles were drifting in the sea. Given the quantity and size of the plastics, it was *a priori* deemed possible that the plastics were inadvertently ingested by filter feeding shellfish, shellfish eating birds, deposit-feeding macrobenthos and other N2000 species.

In a parallel study to this statistical analysis, Foekema et al. (2021) have extensively searched for plastic particles from the MSC Zoe incident in sediments and biota of Wadden Sea and coastal North Sea. Very few microplastics were detected in the digestive tracts of macrobenthos. In fish, birds and mammals microplastic fragments were regularly found, but the fragments found could not be ascribed to the MSC Zoe incident.
The ingestion and physiological damage of particles with the size and composition of the particles lost by MSC Zoe was investigated experimentally by Foekema et al (2021). Mesocosm experiments with differing doses of the particles showed some differences in abundance of some benthic populations, but more than half of the significant differences were increases at higher doses. This provided no direct evidence for harmful effects of the microplastics on the communities at population level. Individual animals introduced experimentally into the mesocosms, showed no uptake of the microplastic particles (mussel, cockle, mud snail) or limited uptake at high dosage of the particles (lugworm). No effect on their survival or physiological condition was found. It was remarked that mussels do filter the microplastic particles from the water. They disposed of it in their pseudofaeces, as they do with other inorganic particles.
Using a hydrodynamic model of the North Sea, the trajectories of particles and distribution of the plastics has been calculated by Foekema et al. (2021) (see Chapter 2). They show that within 17 days all HDPE pellets are washed up onshore, hereby decreasing their potential to impact the environment substantially. For the polystyrene granules the model is less conclusive, as there are two likely scenarios. Either the granules have been distributed over a very wide area in a negligible concentration, or they have been accumulated in higher concentration in an unknown smaller area.

## 1.5 Approach

Due to the large uncertainty on the spreading of the particles in nature, it is not possible to propose a most likely spatio-temporal distribution and use that in the statistical analysis in a regression-like approach. Therefore, a data exploration approach has been preferred. For the different target species, a statistical model has been constructed to describe their spatial distribution as accurately as possible. The spatial statistical model incorporates different independent variables. The model is then used to estimate the distribution of species in space and time. The year or years after the incident is compared to the years before the incident, in order to detect any spatial pattern and to see if it deviates from what could be expected by looking at previous years. Such a deviation is no proof of causality, but would, if detected, form the starting point of a more directed search in the data for possible indications of causal links to MSC Zoe.

## 1.6 Available ecological data

Data used in this report have been collected as part of regular monitoring programs. The following programs contributed:

- SIBES, run by NIOZ, is a synoptic monitoring of the macrobenthos of the intertidal in the Wadden Sea. Data on the lugworm *Arenicola marina*, the cockle *Cerastoderma edule* and the Baltic tellin, *Limecola balthica* have been used.
- WOT shellfish survey, run by Wageningen Marine Research, monitors shellfish in the coastal zone and in the Wadden Sea. Data on the razor clam *Ensis* and the cut-through shell *Spisula subtruncata* in the coastal zone, and on the blue mussel *Mytilus edulis* in the Wadden Sea have been used.
- Sea duck monitoring by Rijkswaterstaat and by Wageningen Marine Research, has been used as the source for data on the Eider Duck *Somateria mollissima* and the common scoter *Melanitta nigra*.
- Monitoring of birds in the Wadden Sea by SOVON was the source of data on the common shelduck *Tadorna tadorna*, the red knot *Calidris canutus*, the northern pintail *Anas acuta* and the bar-tailed godwit *Limosa lapponica*.

Full references to these monitoring programs, as well as an account of the field and laboratory methods used, are provided in Chapter 3.

In addition to these ecological data, information on the physical environment was used as co-factors in the analysis of the macrozoobenthic populations. Macrobenthos is known to respond to physical factors in the environment, because the species have preferences for particular hydrodynamic or sediment conditions (e.g. Ysebaert et al., 2002; Compton et al. 2013). By providing the physical information as co-factors, any variation in abundance or biomass caused by these factors is compensated for, and the analysis can concentrate on what is left as variation in the dataset. This enhances the power of the analysis to detect changes.

In order to obtain a consistent set of physical variables, these were extracted from a hydrodynamical and mud dynamics model run and validated by Deltares (Vroom et al., 2020). The procedure for extraction of the co-factors is detailed in a separate report (Herman and van Weerdenburg, 2020). In short, many different physical variables, related to water depth, salinity, current velocity and bottom shear stress were extracted from the model by averaging the values over a spring-neap tidal cycle simulation. The model ran simulations using conditions of March of 2017. This year has been validated, and March was chosen as it has meteorological conditions that are similar to the year-average (Vroom et al., 2020).

One value for each variable was available per model cell. In order to use these for the statistical analysis, a nearest-neighbor interpolation using the coordinates of the ecological data and of the model cells was performed.
Sediment grain size was not extracted from the model but from existing monitoring databases. For the Wadden Sea, grain size information from the SIBES program was used. For the North Sea, sediment grain size information available at TNO (www.dinoloket.nl) was used. Nearest-neighbor interpolation was used here too.

## 1.7 Structure of the report

Underlying this report is a much more extensive report of the statistical analysis by Highland Statistics Ltd (Zuur and Ieno, 2021). This report is the source for all the statistical results presented here. It contains all information on the model building process for each species and documentation of the R code used. Readers requiring more details on the statistical methods used are referred to this report. If even more detail would be required, all scripts used to produce the Highland Statistics report and the statistical results are available from the repository where the database underlying this report has been archived (see Chapter 4.6 for details).
In this document, we have summarized the most essential parts of the Highland Statistics report, complementing it with ecological information that helps in the interpretation of the results. The structure of this report is that it first contains several general chapters, followed by a chapter per investigated species. The general chapters discuss the field and laboratory methods underlying the data sets analyzed here, and an introductory description of the approach used in the statistical analysis. The chapters per species introduce the biology and ecology of the species concerned, summarize the results of the statistical analysis, discuss the results and conclude about possible effects of the MSC Zoe.
The chapters on the individual species are followed by a general discussion summarizing the most important results.

## 1.8 Review and interaction with stakeholders

The role of the authors and institutions in the work was as follows. The institutions holding the data (NIOZ, WMR, SOVON) were responsible for preparing a clean data file with the data on the species investigated. One or more specialists per species have supervised the data file preparation and compared the files with known information on the species. They have informed the statisticians of Highland Statistics on the details of the sampling, the possible exposure of the species to disturbance by MSC Zoe and on the characteristics of the species that were relevant to the statistical model. After statistical examination of the data and building of a preliminary statistical model, the statisticians have consulted the species specialists with further questions and discussion on the preliminary results. On this basis the final results have been prepared. The species specialists have delivered ecological information on the species and contributed to the discussion of the results. The editors of the report (Deltares) have been in continuous contact with the statisticians and the species specialists and have written the final version of the report based on the received input and the detailed report of Highland Statistics. Deltares has also delivered physical co-factors to be included in the models.
The report has been reviewed by Rijkswaterstaat and by the scientific consultation board of the project. In response to questions and remarks of the review the report has been adapted. The final text remains the full responsibility of the authors.
MSC has received a copy of the draft report and has been invited to give a written reaction to it. If they would have reacted, a copy of their reaction and a response on how this might have led to changes in the report would have been added as appendix. However, MSC has preferred not to react to the draft report.

# 2 Dispersal and uptake of MSC Zoe plastics

For the statistical analysis of possible effects of the MSC Zoe incident on natural populations, abundance and biomass data of the populations before, during and after the incident will be compared. In order to link possible patterns in the populations to the incident, it is very important to have as many details as possible on the spatial distribution of the plastic material lost by MSC Zoe, and on possible mechanisms by which populations have been in contact with this material. In this chapter we review the available evidence with the aim of formulating hypotheses underlying the statistical analysis.

## 2.1 Available information

The trajectory of the MSC Zoe during the storm in the area north of the Wadden Islands is known. Also known are the places where many containers and lost goods have been found. These correspond most likely to the places where larger quantities of goods have been lost overboard. Four points on the trajectory have been identified as hotspots for material loss. It is approximately known which plastic material has been lost from the ship. This information is summarized by van der Molen et al. (subm.) from which we derived the following summarizing information.

Over 11 metric tons of semi-transparent 0.5 mm diameter polystyrene granules have been lost, but the container containing this material has remained on board. It is therefore unknown where the cargo has been lost and whether that has been a gradual or a sudden process. The granules have a density of 1.04 to 1.08 $kg.dm^{-3}$ and an estimated sinking velocity of 0.004 $m.s^{-1}$. Although in several places the sediment and biota have been searched for the occurrence of the granules, none have been found with certainty. Further search in field samples is ongoing.

An unknown quantity of white HDPE (High Density Polyethylene) pellets, with a diameter of a few millimeters, has been found along the North Sea beaches of the Wadden Islands and the mainland coast of the Wadden Sea. Some pellets were still packaged in plastic bags, others were found as individual pellets. It is unknown where these pellets were lost from the ship. It is also unknow whether the container in which they were packed has opened upon falling onto the sea bed or earlier. Therefore, it is unsure whether all pellets have been released from the same point or not. The pellets have a density of 0.94-0.97 $kg.dm^{-3}$, causing them to float with a vertical raising velocity in sea water of 0.05 $m.s^{-1}$. A project seeking co-operation from the general public (waddenplastic.nl) has collected data on the spatial distribution and numerical density of these pellets in many places along the coasts of the Wadden Islands and the mainland. Most pellets have been found in the eastern Wadden Sea, where the density was much higher than in the western part of the Wadden Sea.

## 2.2 Model calculations

Van der Molen et al. (subm.) have used a hydrodynamic model of the North Sea to calculate the trajectories of particles released in the model at different points. The model has been calibrated for the period of early 2019. The spatial resolution is limited (5 km), causing the Wadden Islands to be represented rather schematically in the model. The model formulates the vertical movement of the particles as a function of their (density-driven) sinking or floating velocity and an additional vertical random walk component that scales with vertical turbulence intensity. The effect of wind waves has been parameterized in that term. The horizontal movement is described as a function of water velocity, into which the wind shear stress effects on the 3D currents is incorporated, as well as a parameterization of wave effects. In the model, the particles have no interaction with the sediment.

Particles sinking to the bottom are reinjected into the water column and continue their journey. They can only leave the model when they reach one of the lateral boundaries, either open sea or (in most cases) beaches and coasts.
For the floating HDPE pellets, the model has been used to determine the most likely place where the material has been lost from the MSC Zoe. This is a location north of the tidal inlet between Ameland and Schiermonnikoog. For these pellets, the model predicts a residence time at sea of a few weeks only. After that, all pellets are caught on beaches and coasts. After one week, approximately half of the pellets were still moving. This is reduced to 10% after two weeks, and all pellets were lost from the model after 17 days. The model prediction corresponds to the observations in the field. The most likely trajectory of the pellets is from the point of loss to the southwest and close to the coast, after the turning of the dominant wind direction, more towards the southeast. Figure 2.1 shows where the pellets in the model end up and illustrates the trajectories for a random selection of particles.

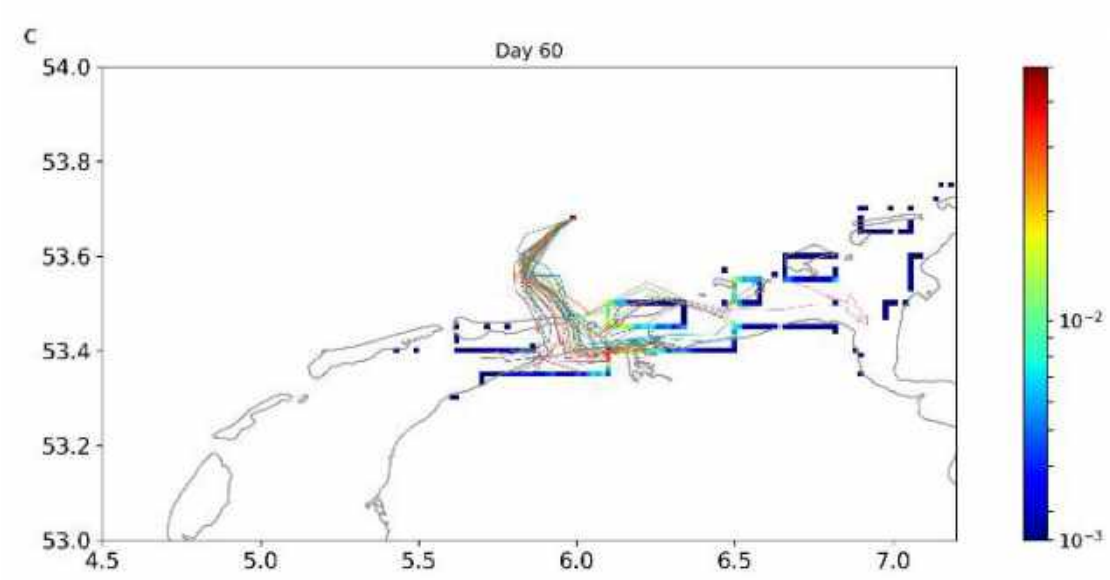


*Figure 2.1 Results of the particle tracking of HDPE particles in the model. The color coding along the coasts shows how many particles have washed ashore at the different places. These are relative numbers (number of particles in the model simulation) and not absolute numbers in reality. For a random selection of particles, the trajectory in the model is shown. This figure illustrates the most likely scenario, i.e. the scenario with a point of loss of cargo that best explains the observed distribution of pellets along the coasts of the Wadden Sea.*

The modelling of the sinking, small PS granules is much more uncertain than that of the HDPE pellets. According to the most recent information available, there are no observations that can be used to validate the model. There are no (external) indicators that can help identifying the place where the granules have been lost. There is no information on how these granules interact with the sediment. Their sinking speed in seawater is of the same order of magnitude as that of mud particles: 4 $mm.s^{-1}$ for the granules, 1 $mm.s^{-1}$ for typical mud particles. For mud we know that it returns relatively quickly (few days) to the sediment after it has been eroded in a resuspension event (van der Hout et al., 2017). For the PS granules with a sinking speed of 4 $mm.s^{-1}$, it would take approximately 1.5 hours to sink to the bottom in a water column of 20m, if vertical turbulence is neglected. They have a relatively high chance of contacting the bed in a relatively short time. Their subsequent fate depends on how they interact with the sediment. The particles have the diameter of (coarse) sand grains, but the sinking speed of mud. If they are incorporated into the sand bed, e.g. in moving sand ripples, their spatial distribution is most likely restricted to the immediate surroundings of the point where they were lost.

However, if that incorporation usually fails because the particles are too light to behave like sand, and too large to enter the interstitial spaces between the sand grains, they may remain in the water column and eventually wash ashore as is predicted in the model.
The particles in the model keep moving for a very long time. After six weeks, half of the particles was still moving. In accordance with that, the spatial distribution is over a wide area (Figure 2.2). Four simulations have been made, releasing the granules continuously in the first, second, third and fourth quarter of the MSC Zoe trajectory in the Netherlands. Depending on the release scenario, 25 to 95 % of the particles end up in the German Wadden coast.

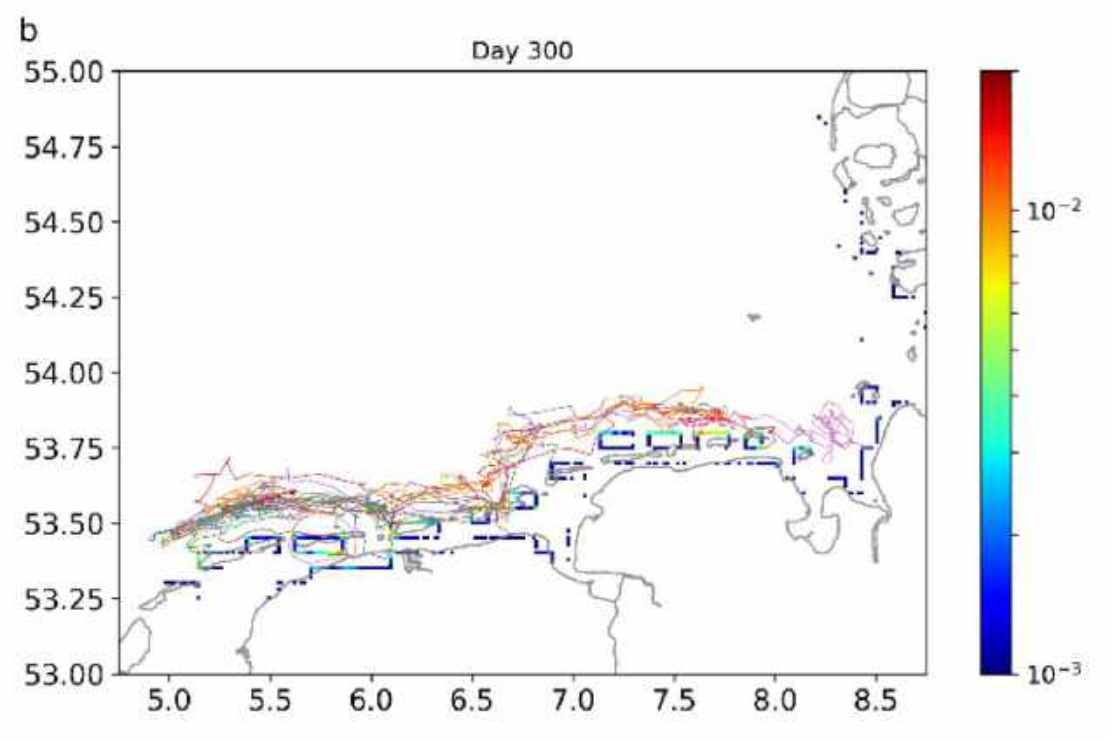


*Figure 2.2 Spatial distribution of the PS granules released from the second quarter of the MSC Zoe trajectory.*

From the model, it is concluded that the granules distribute over a very large area. The surface of the international Wadden Sea is approximately $10^4$ km$^2$. The simulations suggest that the particles could end up in at least half that surface and, in addition, to a considerable area outside of the Wadden Sea. This leads to an extreme dilution of the particles, making it very unlikely that they would have a direct effect on biological populations. With a diameter of 0.5 mm, the particles have a volume of 6.5 $10^{-11}$ m$^3$. 11 metric tons of particles have been lost. With a density of 1.06 kg.dm$^{-3}$, this corresponds to 10.38 m$^3$. We calculate that 1.6 $10^{11}$ particles have been released. If they end up over an area of $10^4$ km$^2$ = $10^{10}$ m$^2$, we expect 16 particles per m$^2$ over the Wadden Sea and coastal area. This is an extremely low concentration, when compared with the numerical density of macrobenthic animals, which usually is in the order $10^3$ m$^{-2}$. With two orders of magnitude difference in density between animals and particles, only approximately 1 % of the animals could be affected at most, even assuming that the ingestion of a single microplastic particle would have notable effects on the individual.
If, in contrast to this scenario, the particles have a much stronger interaction with the sediment, they will disappear much faster from the water column and they will be distributed over a much smaller area. As an extreme, we can consider the case where they sink out within 1.5 hours and remain in the sediment.

That would distribute them over an area of approximately 10 $km^2$, where the concentration could then reach 1.6 $10^4$ $m^{-2}$, or almost 2 per $cm^2$. Foekema et al. (2021) show that at this concentration some uptake by one species (the lugworm *Arenicola marina)* is found, but without physiological effects on the animals. In search of such effects, out study is hampered by the fact that we have no information where the point or trajectory of release has been, and for biological populations we only have information on filter feeding shellfish. Shellfish are known to filter out very efficiently any particles in the size range of sand grains.
In summary, there are two possibilities for the PS granules. Either they have been distributed over a very wide area in a negligible concentration, or they have been accumulated in higher concentration in an unknown smaller area. For neither of the two cases it is easy to formulate hypotheses that are statistically testable.

## 2.3 Uptake of plastic particles in the food web

The plastic particles lost by the MSC Zoe can have entered the food web in different ways. Particles can have been taken up by benthic organisms, e.g. shellfish, that serve as food for birds. If plastic particles are contained in the food, this might have been a source of disturbance for the birds. In addition, birds may also have taken up the plastic particles directly, either by mistaking them for food particles, or by accidently swallowing them during feeding on other items.

### 2.3.1 Uptake of plastic particles by shellfish

The shellfish examined in this report, have similar mechanisms through which particles are ingested. Bivalves feed on phytoplankton, zooplankton, protists and dead particulate organic matter (Fréchette et al., 1989; Riera, 2007; Vaquer et al., 2000). Particles around 2-7 µm can be retained on the gills efficiently (Møhlenberg & Riisgård, 1978), as long as they do not escape (Troost et al., 2008). In larvae, the ciliated velum functions in swimming and feeding (Widdows, 1991).

Particles retained on the gills are transported to the labial palps, where sorting takes place (Ward et al., 1998; Warvolumd & Shumway, 2004). The palps select the edible particles and transport them toward the mouth for further digestion (Bayne, 1976). The rejected particles are covered in mucus and excreted as pseudofaeces (Payne et al., 1995; Ward et al., 1998). The volume of water cleared of all particles per time unit is defined as the clearance rate, while the volume of water pumped is defined as the filtration rate (Riisgård, 2001). Clearance rates observed for Macoma in the field were mostly between 0.1-0.6 l/h/g (Hummel, 1985b), which is comparable to the range found in a laboratory study (maximum of 1.2 l/h/g) (Hummel, 1985a). The maximum clearance rate (l/h) depends on weight and follows the allometric equation: 7.45w0.66 (Møhlenberg & Riisgård, 1979).

Ingested particles by bivalves may be excreted in the form of pseudofaeces during the filtration process (Payne et al., 1995; Ward et al., 1998). Contamination by microplastics may cause alterations in the endocrine and circulatory system of bivalves (Browne et al., 2008; Guilhermino et al., 2018) and can get stuck in the mucus on the outer side of the gills epithelium (Guilhermino et al., 2018; Paul-Pont et al., 2016). Note however, that ‘microplastics’ is a very heterogeneous group of stressors, and that some of these effects are described for much smaller particles than the MSC Zoe granules, and therefore not necessarily applicable to the current study case.

An outdoor mesocosm experiment has been conducted to assess the effects of polystyrene (PS) granules (0.5 mm) and polyethylene (HDPE) pellets (5 mm) on bivalves, which were lost by the container ship MSC Zoe in January 2019 and ended up in the sea (Foekema et al., 2021). The organisms (e.g. cockles and mussels) and ecosystem in the experiment were exposed to different concentrations of 0.1, 0.8, 8.0 and 80 gram PS granules per $m^2$ and monitored during 56 days. The highest dose (80 gram per m2) would be applicable to a field situation where all PS granules lost by the MSC Zoe (11,000 kg) are spread homogenous to 0.01% of the surface area of the Wadden Sea, which is very unlikely. Mussels and cockles were examined at the end using a stereomicroscope for the presence of PS granules in the digestive system. No granules were found inside the mussels and cockles, which was also the case for the shellfish collected from the field after the MSC Zoe lost her cargo. Survival and growth were not affected by the PS granules, nor did the benthic community change in species richness and diversity. The granules were however found in the pseudofaeces of mussels, which consists of non-edible particles that are expelled before digestion. The mesocosm experiment can be considered a worst-case scenario; the mesocosm is a stagnant system, while water movement in the field will ensure the PS granules to disperse rapidly. In conclusion, no negative effects on shellfish are expected.

### 2.3.2 Uptake of plastics by other benthic organisms

In this study, the lugworm *Arenicola marina* is studied as a flagship benthic worm. The species is known to feed by ingesting sediment and digesting the organic fraction of the ingested material. However, ingestion by *Arenicola marina* is not indifferent for the nature of the particles. The animals use their proboscis to select and take up particles. The maximum size of particles taken up is determined by the size of the proboscis, which is smaller for smaller animals. In general, it is thought that *A. marina* can take up particles up to a size of 500 µm (Gebhardt and Forster, 2018). That would place the particles lost by MSC Zoe at the margin of what could be taken up, even by the largest worms. In the mesocosm experiments by Foekema et al. (2021) uptake of microplastic particles was observed in the experiments with the highest concentration, confirming that they could be taken up.

### 2.3.3 Direct uptake of plastics by birds

For the drifting HDPE pellets, only limited possibilities exist for direct uptake by birds. Only the northern pintail is known to feed on drifting seeds of saltmarsh plants. For that reason, the species was added to our study. Shelducks do not pick up drifting particles but are known to feed on mud snails and could therefore pick up pellets from the surface of tidal flats. For sea ducks (eider, common scoter) there is no mechanism by which they could have come into contact with the pellets.

For the small PS granules, direct uptake by birds is even less likely. Exposure in sizable amounts could only have come through the food web, if the prey of the birds would have ingested the particles in relatively large amounts. This is unlikely for shellfish and lugworms, as discussed above, but not entirely excluded for other species of prey.

## 2.4 Likely distribution patterns of damage by plastic particles

#### 2.4.1.1 HDPE pellets

Model calculations and field research have shown that these pellets have arrived in the drift line debris and have largely been buried in the sand at those locations. It is possible that they have undergone secondary transport from there, but we have no evidence for that.

None of the animals investigated in our study have a relation with the drift line, e.g. as habitat or foraging area. For most species we know that they will not pick up drifting particles from the water. Given that the pellets would be transported along the surface of water, it seems unlikely that the particles could reach benthic shellfish. Only the northern pintail is known to feed on drifting seeds of saltmarsh plants.

For that reason, the species was added to our study. Shelducks do not pick up drifting particles but are known to feed on mud snails and could therefore pick up pellets from the surface of tidal flats where the DHPE could have stranded. For sea ducks (eider, common scoter) there is no mechanism by which they could have come into contact with the pellets. The only possible disturbance for these species is by disturbance during the salvage activities following the MSC Zoe incident.

#### 2.4.1.2 PS granules

The basic hypothesis for this material is that an elevated concentration of the granules in the food of the benthic animals or birds, decreases their digestion efficiency and affects the ecosystem through the food web. This is the mechanism experimentally investigated by Foekema et al. (2021), who found, however, only traces of the PS granules in the digestive track of lugworms but not in shellfish, and only when the particles were present in high concentrations.

Due to the large uncertainty on the spreading of the particles in nature, it is not possible to propose a most likely spatio-temporal distribution and use that in the statistical analysis in a regression-like approach. Therefore, a data exploration approach has been adopted.

# 3 Field and laboratory methods

This chapter documents the field and laboratory methods used to generate the datasets that have been analyzed for possible effects of the MSC Zoe incident. From some data sets, e.g. the SIBES data set collected by NIOZ, several species have been extracted and analyzed. The methodology for all these species has been the same. For that reason, the methodology is specified per dataset in this chapter. In the chapters on individual species, reference will be made to the name of the dataset and coupled methodology.

## *3.1* SIBES – used for *Arenicola marina*, *Cerastoderma edule* and *Limecola balthica*

### 3.1.1 Background

In 2008, the NIOZ, together with the gas exploitation company NAM, initiated a synoptic intertidal benthic survey (SIBES) across the entire Dutch Wadden Sea with the goal of monitoring mud-dwelling organisms or macrofauna for their abundance, biomass and composition. To tease apart effects of subsidence, due to gas drilling, from the inherent natural variation in the system, this survey has been conducted over extensive temporal and spatial scales. Prior to implementing SIBES, the best sampling design for monitoring macrofauna at these scales was identified (Bijleveld et al. 2012).

### 3.1.2 Sampling and study site

Sampling design encompasses the entire intertidal Dutch Wadden Sea, with sampling at 500 m intervals and additionally 20% random sample points (see Figure 3.1). The random points fall off the grid and are additional to the regular grid. They are added to the grid in order to cover the full range of inter-sample distances, which helps in establishing the spatial autocorrelation structure of the data.

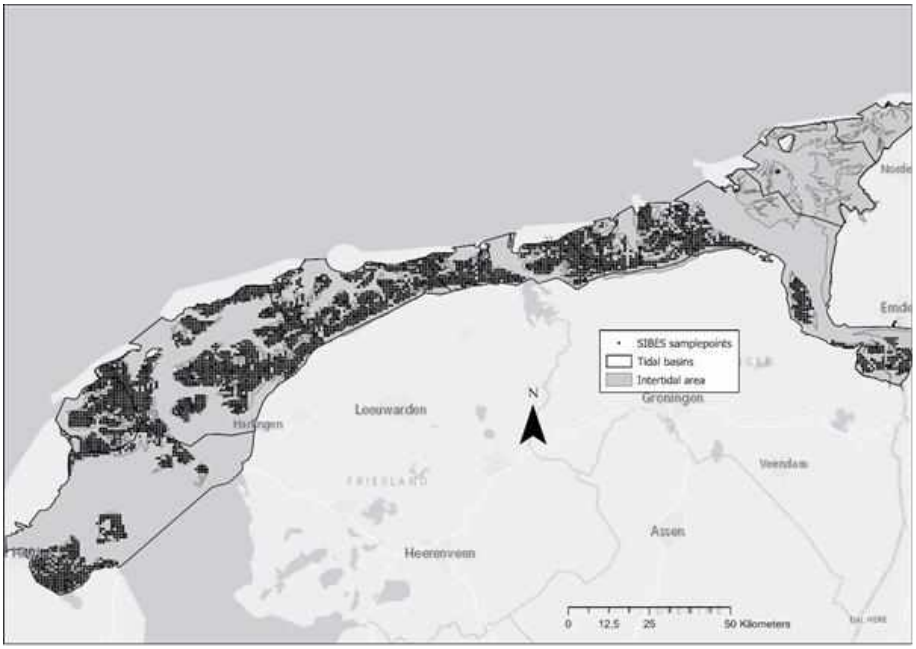


*Figure 3.1 The sampling grid of the SIBES project in the intertidal zone of the Wadden Sea.*

Sampling was completed on an annual basis in summer from June to October, depending on weather conditions. The NIOZ research vessel, Navicula, was used as a platform to access the sample areas across the Wadden Sea. During low tide samples were taken by foot. In areas where it was too deep or muddy to access by foot, small inflatable boats were used to sample the SIBES sites. Sampling locations, ~4500 in total, were found with a handheld GPS (WGS84 as map datum). At each site sampled by foot, a single core of 0.0175 $m^2$ was taken to a depth of ~25 cm. By boat, two cores of 0.018 $m^2$ were taken to a depth of ~25 cm.
All macrobenthos samples were sieved on a 1 mm mesh in the field (Compton et al. 2012, 2013). After sieving, bivalves were separated from the other macrobenthic species for later analysis in the laboratory. The bivalve samples were frozen, whereas the remaining macrobenthic species were preserved using a 4% buffered formalin solution. Sediment samples were taken using a centrifuge tube to a depth of 4 cm and then frozen at -20°C. The sediment samples were taken at all sample points.

### 3.1.3 Selection of samples for the present analysis

For the present analysis, it was very important that a complete time series until at least 2019 was available. As the entire grid sampling of 2019 was not yet analyzed, the analysis was restricted to the random points only. These have all been sorted and identified until the year 2019. In order not to cause any unbalance in the sampling effort, only random points were taken for the previous years too.

### 3.1.4 Sample processing

All shellfish were identified to species level (Hayward & Ryland 1995) and measured for their maximum length using digital calipers (precision of 0.01 mm). An ash free dry mass (AFDM) was then determined for each individual greater than 8 mm in size or for multiple individuals together when their size was smaller than 8 mm in length. To determine the AFDM, the wet meat of an organism is placed into a crucible and then dried at 60°C for a minimum of 48 hours. Once dried, the dry sample goes into a desiccator to cool prior to weighing to an accuracy of four decimal places in the NIOZ weighing robot (Mettler Toledo WKC204C). The dried organism is then put into an incinerator where the organic matter is burnt, so that only the ashed matter remains (560°C for 5 hours). Once incinerated, the ashed sample goes into a desiccator to cool prior to weighing the ashed mass to an accuracy of four decimal places.

## *3.2* WOT Shellfish survey Wadden Sea – used for *Mytilus edulis*

### 3.2.1 Background information survey

Every year, Wageningen Marine Research carries out shellfish surveys in the Dutch coastal waters (Wadden Sea, Oosterschelde, Westerschelde and Coastal Zone), investigating the distribution and size of the most important commercial shellfish species. The survey in the Wadden Sea is mainly focused on mussels (*Mytilus edulis*), cockles (*Cerastoderma edule*) and Pacific oysters (*Crassostrea gigas*). These surveys are part of the annual shellfish inventories, as commissioned by the Dutch Ministry of Agriculture, Nature and Food Quality (LNV) and carried out by Wageningen Marine Research, in collaboration with the ministry of LNV. These surveys are crucial to support policy makers regarding the shellfish industry and are an important source of information for a range of ecosystem studies. These surveys have been performed on an annual basis since 1990.

### 3.2.2 Sampling and study site

The study area of the survey is the littoral zone in de Dutch Wadden Sea (Figure 3.2). Sampling points are distributed across the area using a stratified sampling grid. In order to get an efficient distribution of the sampling effort, the area is divided into a number of strata; areas with a different expected occurrence of either cockles or mussels and Pacific oysters. In areas with a high chance of encountering a target species, the density of sampling stations is higher (and the distance between sampling stations is smaller). In areas where mussels are expected, mainly within the known contours of intertidal beds, sampling stations are 0.25 geographic minutes apart (corresponding to 463 m in latitude and 280 m in longitude) (purple in Figure 3.2). Here, each station represents a surface area of 12.84 ha. In the areas outside the intertidal mussel and oyster beds, a stratification is made based on the expected occurrence of cockles, with the highest density stratum in areas with a high chance of encountering cockles (red dots in Figure 3.2) and a lower density stratum in areas with a smaller chance (green dots in Figure 3.2). In the remaining area the lowest density stratum can be found (blue dots in Figure 3.2). The aim of stratification is to increase the reliability of the stock assessment and to minimize shipping time.

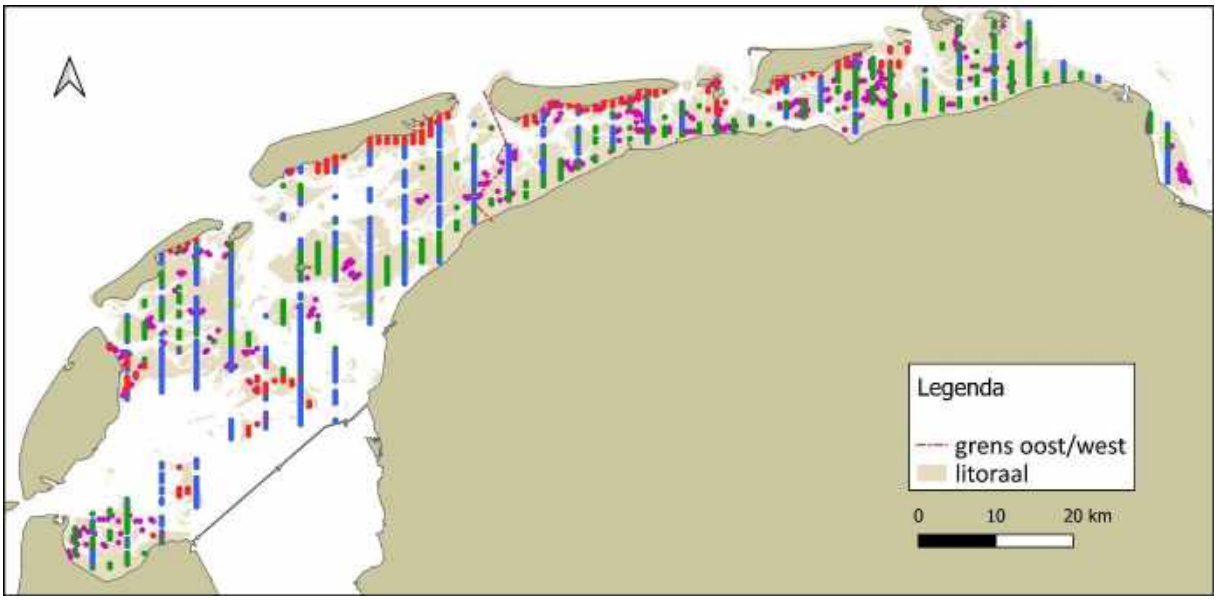


*Figure 3.2: Study Area of the survey: Dutch Wadden Sea with the littoral zone ('litoraal') and the boundary between East and West. All points sampled in 2020 are displayed followed; purple dots are located on mussel or oyster beds, red and green dots are located in areas with probability of high cockle density and blue dots are located in the remaining area.*

### 3.2.3 Data collection

The main vessel used to carry out the annual survey in the Wadden Sea is a former cockle fishing boat owned by Roem van Yerseke B.V. (YE42, "Anna Elizabeth"). In addition, some samples are collected by the Wadden Unit of the Ministry of Agriculture, Nature and Food Quality using vessels of the governmental shipping company (MS Phoca, MS Asterias, MS Krukel and MS Harder). Positions of sampling stations are determined using GPS equipment in combination with the navigation systems MaxSea and TimeZero. A handheld GPS (Garmin) is used to find sample locations reached by foot or dinghy. Several sampling devices are used during the survey (Figure 3.3):

- "Stempelkor": most locations are sampled with the use of a device particularly developed for this survey. A cockle dredge was modified to a haul length restricted to 0.8m, taking samples of 0.4m$^2$ (2.0m x 0.2m) to a depth of 7 cm, and with a mesh width of 0.5cm. The samples are collected by a suction tube into sieve containers on deck. This device is used since 1998 in the Wadden Sea to restrict the sampling impact on tidal flats, especially on mussel beds.

- Corer: the corer is used in the Wadden Sea during low tide at locations that are too shallow to reach by vessel and are sampled on foot. Two PVC corers (24.4cm in diameter) are used to get two samples of each 10cm depth. The sediment is scooped out, into a sieve. Total sampled area is 0.1m$^2$.
- Hydraulic grab: this grab is used for sampling on dense oyster beds. The hydraulically operated grab is controlled by a crane on the ship (YE42). The sampled area is 1.06m$^2$ and the maximum depth is 34cm. The sample is dumped into a large sieve on deck with a mesh size of 5mm.
- Cockle-sampling device: used in shallow places reached by dinghy. Position is determined with a handheld GPS. On every location, three samples are taken with a total surface area of 0.1m$^2$ and depth of 7cm.

*Figure 3.3. : "Stempelkor" (top left), hydraulic grab (top right), corer with sieve (bottom left) and cockle-sampling device (Photographers: Karin Troost, Douwe van den Ende and Herman Troost).*

### 3.2.4 Sample processing

Samples collected by Wageningen Marine Research are processed on board during the survey. Samples collected by Wadden Unit are frozen, transported to Wageningen Marine Research in Yerseke and processed further in the lab. Since freezing and thawing of mussels can result in a decrease of fresh weight because the dead animals release seawater that was contained within the closed shell, the samples are sorted by species and location and sealed in plastic bags before transport. After defrosting in the lab, also the sea water remaining in the bags is weighed since this can only originate from within the shells.

Samples are sieved over 5mm and all shellfish, crabs and echinoderms are recorded. Of large samples, subsamples may be taken based on the total volume, on the condition that at least 100 individuals of the target species are retained, or at least 50 individuals of another species. All living shellfish are collected from the (sub)samples, biofouling of mussels is removed, and the shellfish are sorted by size or age class. Broken shells are included when the hinge is completely present (i.e. both sides of the hinge ligament between both valves) and meat residues are present. Mussels are sorted in three classes based on appearance and shell length: seed (on appearance, generally < 20mm), half-grown mussels (on appearance and always < 45mm) and full-grown mussels (always > 45mm). Per size class the total wet weight and total number of individuals is determined per sample.

#### 3.2.5 Data analysis

The species abundance (number per $m^2$) and biomass (weight per $m^2$) are estimated for every location. Weights of broken mussels are estimated based on the average weight of shellfish of the same species and age class. This average is based on all intact shellfish in the sample, on the samples collected during the day or on all samples collected during the entire survey, depending on the amount of intact shellfish collected.

## *3.3* WOT Shellfish survey Coastal Zone – used for *Spisula subtruncata* and *Ensis leei.*

#### 3.3.1 Background

The exploitation of wild shellfish has developed from free fisheries to a strongly regulated commercial activity, in which economic and ecological objectives are both aimed for. Within the framework of this policy, an annual stock estimate is made for the economic important species razor shell (*Ensis* sp.) and surf clam (*Spisula subtruncata*). The survey covers the entire Dutch coastal zone and is commissioned by the Ministry of Agriculture, Nature and Food Quality. The main objective of this survey is the assessment of the stock sizes of the economically important species *Ensis* sp., *Spisula subtruncata*, *Cerastoderma edule and Mytilus edulis* in the Dutch coastal zone. In addition to these species, this survey also reports on the occurrence of other shellfish species, crabs and echinoderms.

#### 3.3.2 Sampling and study site

The study area of the survey is the Dutch coastal zone, including the Natura-2000 areas: “Noordzeekustzone”, “Voordelta”, “Vlakte van de Raan”, and the mouth of N2000 area “Westerschelde” (Figure 3.4). Sampling stations are distributed across the study area using a stratified sampling grid. To get an efficient distribution of the sampling effort, the area is divided into several strata based on the occurrence probability of the Surf Clam. In strata where higher densities are expected, a finer grid (with a higher density of sampling stations) is used compared to strata where low densities are expected. Sampling effort is lowest in strata where no shellfish are expected. Due to the complex geomorphology of the Voordelta (gullies and flats), a finer grid is used in this area compared to other areas.

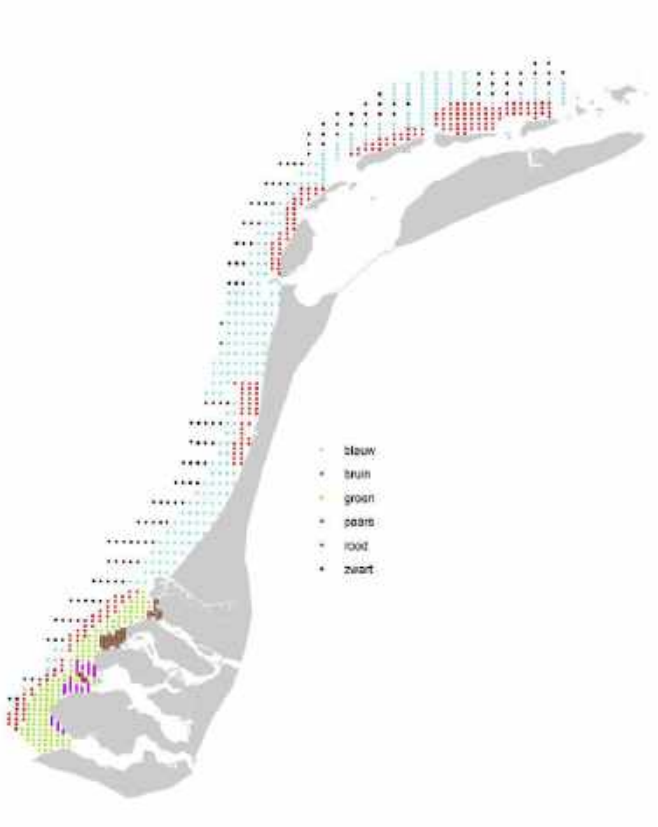


*Figure 3.4. Study area of the survey in the Dutch coastal zone (Perdon et al., 2019). Colors refer to subdivisions of the data set that are not important for our study.*

The survey is carried out annually in the period April-June. Vessels used during the survey are a former cockle fishery boat owned by Roem van Yerseke B.V. (YE42, “Anna Elizabeth”) and the RV Isis owned by the governmental shipping company. The sample locations are determined using GPS equipment in combination with the navigation systems MaxSea and TimeZero. Several sampling devices are used during the survey (Figure 3.5):

- Trawled dredge: this is the most commonly used device during the survey. The trawled dredge consists of a cage equipped with a 9.4cm wide blade at the bottom that penetrates the sediment (10cm depth). The cage acts as a sieve during fishing (mesh size 5mm), when the trawled dredge is dragged across the bottom.
- Modified hydraulic dredge: this device is used in the shallow areas of the Voordelta, on board of the YE42. The dredge is equipped with a 21.4cm wide blade that penetrates the sediment (7.0cm depth). The dredge is dragged across the sediment by a suction tube, collecting the sample onto deck where the sampled gets sieved (5mm) in a rinsing machine.
- Hydraulic grab: the hydraulically operated grab is controlled by a crane on the ship (YE42) and mainly used in rocky areas west of Texel. The sampled area is 1.06m2 and the maximum depth is 34cm. In previous years (before 2019), a Van Veen grab was used instead (1 sample consisted of 5 grabs of 0.1m2 each).

*Figure 3.5. Trawled dredge (left), modified hydraulic dredge (middle) and hydraulic grab(right) (Photographers: Karin Troost and Jack Perdon).*

The trawled dredge and modified hydraulic dredge take samples over a distance of approximately 150m, except in the Voordelta, where the maximum distance is approximately 75m (due to geomorphological conditions). The exact distance is determined by means of a DGPS (Differential Global Positioning System) or by using an electronic mechanism connected to a measuring wheel that is dragged across the bottom during fishing. The sampled surface per location is app. 15m2 when using the trawled dredge (Voordelta ± 7.5m2) and ± 30m2 using the modified hydraulic dredge.

### 3.3.3 Sample processing

Depending on sample size, all living organisms from the total sample or a subsample are identified and counted. Shellfish are identified at species level, except for razor shell. Very often only the tips or siphons of razor shells are sampled, which makes it impossible to identify at species level due to absence of specific identification characteristics. Intact individuals are sorted per sample by species and weighed (fresh weight, 0.1gr accuracy). Broken shells are included when both the hinge (i.e. both sides of the hinge ligament between both valves) and meat residues are present. Shell lengths of all individuals are measured. When the shells are broken or only the siphon is presented, width is estimated based on expert judgement. Surf Clams are also sorted in two classes based on shell length: small (< 19 mm) and big (> 19 mm), roughly corresponding to respectively 1-year old and older cohorts.

The species abundance (number per $m^2$) and biomass (weight per $m^2$) are estimated for every location. The biomass of broken shells is estimated based on average weights of intact specimens at that location or, in case no intact shells are present in the sample, based on average weights of the day or entire survey.

With the use of current sampling devices, sampling efficiency for deep-burrowing species such as Ensis sp. and otter shell is not optimal (Beukema, 1974; Craeymeersch et al., 2007). The modified hydraulic dredges penetrate 7 to 10cm into the seabed, resulting in only partial collection of deep-living or deep-burrowing specimens (tips of *Ensis* sp. and siphons of other shells). Therefore, not all specimens will be considered, resulting in an underestimation of the actual stocks. Comparison between years is yet still possible.

Sample efficiency of the trawled dredge used in this survey is estimated to be 50%, based on 400 stations sampled in 2004 and 2005 (unpublished data IMARES and Netherlands Institute of Ecology) (Sala et al., 2016).

The sampling grid is specially developed to estimate biomass and abundance of target species (*e.g. Spisula subtruncata*) and therefore caution is needed to interpret the stock development of non-target species. The grid is less suitable for stock estimates of mussels, which can occur locally in very high numbers after high spat fall.

## 3.4 Sea ducks – used for *Somateria mollissima and Melanitta nigra*

### 3.4.1 Background

Every year, since 1993, an inventory is made of the total numbers of several species of sea duck, most notably eiders (*Somateria mollissima*), common and velvet scoters (*Melanitta nigra* and *M. fusca*) and scaup (*Aythya marila*) in the Wadden Sea, North Sea coastal waters and in the Delta area in the southwest of the country. This is done in the context of the yearly assessment of the conservation status of a large range of species in the monitoring program "Biologische Monitoring van de zoute rijkswateren (MWTL)". The results are yearly reported, in a series of reports, see the latest by Sluijter *et al*. (2020). The aim is to have a yearly, synoptic mid-winter count in January, but weather conditions sometimes prevent this and counting the ducks is sometimes done in December or February. In addition, IMARES (now: Wageningen Marine Research) conducted a series of counts of eiders between 2000 and 2012 (see Smit & de Jong 2011), to answer questions by the Ministry of Agriculture, Nature and Food Quality, on the relationship between shellfish stocks and numbers of eiders in the Wadden Sea and in the adjacent North Sea, and the interactions between ducks and humans. Additional counts of common scoters in North Sea coastal waters were conducted through various project assignments, commissioned either by the Ministry of Agriculture, Nature and Food Quality, or by the Ministry of Infrastructure and Water Management, to assess possible effects of human impacts in the North Sea coastal waters, e.g., from coastal nourishment, or fisheries (see e.g., Leopold *et al*. 2014; Prins *et al*. 2014; Fijn *et al*. 2017)

### 3.4.2 Sampling and Study site

The study area of the surveys is the Dutch coastal zone, from IJmuiden to the Dutch/German border, and the Dutch Wadden Sea. The study area is divided in 10 sub-areas to which all ducks are assigned (Figure 3.6).

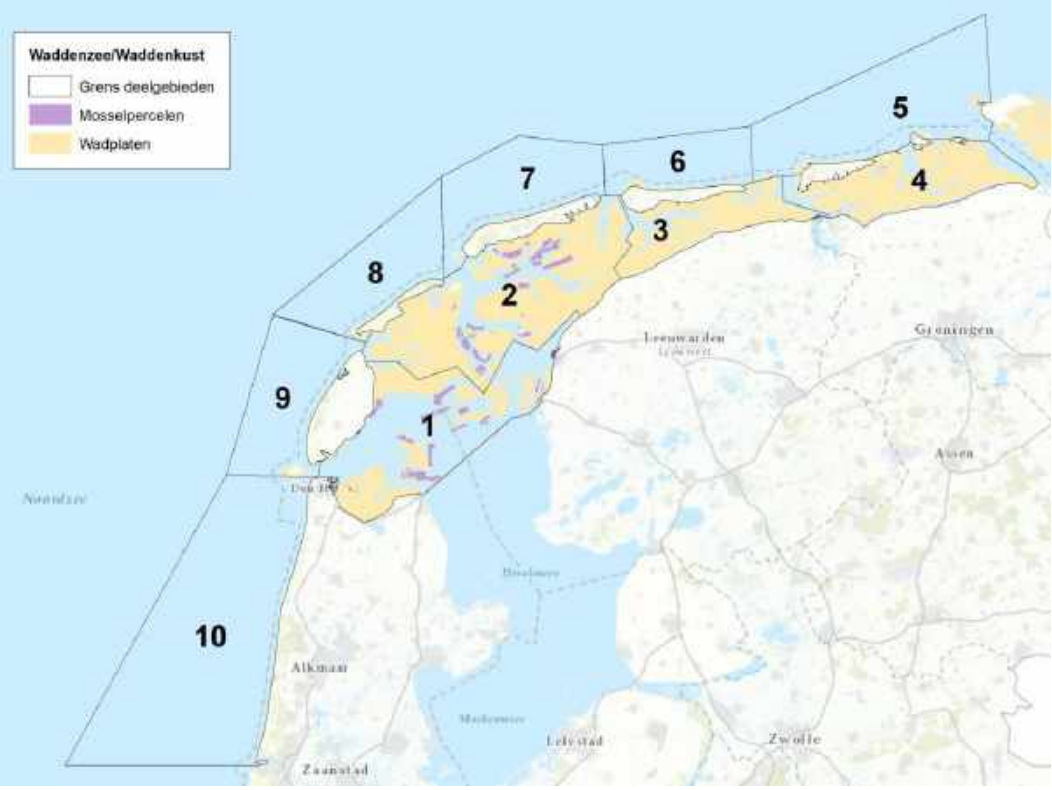


*Figure 3.6. Spatial positions of the 10 areas. For each area we have a time series on counts of eider ducks and common scoters (map taken from Sluijter et al. 2020).*

The ducks were counted by aerial survey, using a high-winged aircraft and pre-determined transect lines. Only when time was short, or in presumed low density areas where the ducks usually occurred in a few large concentrations, a transect parallel to the coastline was flown until a concentration of ducks was detected, which was then circumnavigated, and counted. All teams consisted of two counters (left and right side of the aircraft), a pilot and a navigator. Each count normally lasted 2-3 days due to the numbers of transects flown and the extent of the area to be counted. Transect lines were set so far apart that the counters could see all ducks, presumably without overlap between neighboring transects, i.e., the counts are total counts. Altitudes flown were circa 150 m (500 ft), and ground speeds were between 140 and 190 km/hour, depending on head- and tailwinds.

### 3.4.3 Sample processing

Care was taken to examine the GPS tracks of all counts, from the various reports on these counts. Sub-areas that were incompletely covered, or not covered at all were identified, and given the label “not data”. Sub-areas that were fully covered but devoid of ducks (of a given species) were given the count value 0 (zero).

## 3.5 Wadden Sea Birds – used for shelduck, red knot, northern pintail and bar-tailed godwit.

Data on the abundance of Common Shelduck, Northern Pintail, Red Knot and Bar-tailed Godwit in the Dutch Wadden Sea originate from systematic waterbird counts which have been carried out since the 1970s. Today they are part of the Network Ecological Monitoring (NEM), the Dutch government's system of nature monitoring schemes.

The waterbird monitoring network is a partnership between Sovon Bird Research Netherlands, Statistics Netherlands (CBS) and several Dutch government agencies. The 'midwinter' counts in January, which go back furthest in time, also contribute to the International Waterbird Census (IWC) coordinated by Wetlands International.
Since 2002, the monitoring scheme consists of a combination of monthly counts in a number of sample areas, and five integral counts per year in which the entire Wadden Sea area is counted in one weekend (largely on the same day). Four of these integral counts take place in fixed months (September, November, January, May), the fifth in a rotating scheme so that all months are covered at least once in every eight years. See (van Roomen et al. 2002) for a rationale and validation of this setup. The counts are organized and coordinated by Sovon, and almost fully carried out by volunteers, of which approximately 150 are involved during an integral count of the Dutch Wadden Sea (e.g. Hornman *et al.* 2012, 2020).
All waterbirds that forage on the intertidal mudflats and in saltmarshes are counted in fixed areas visited around the time of high tide, when they are concentrated on a limited number of 'high tide roosts' (HVP's). Most roosts are located on salt marshes and in polders of the mainland coasts and the Wadden Islands. Some important roosts are located on elevated sand bars that are not completely submerged during most high tides; these are visited by ship. Counts are usually carried out by one or two experienced observers per site, using tripod-mounted telescopes. Birds are counted individually or, in lager flocks, by determining the number of subunits of e.g. 10, 50 or 100 birds making up the flock. Methodological studies indicate that the random error in estimates of roosting wader flocks is about 37%, largely independent of flock size, but errors decease across larger areas by averaging out over multiple flocks (Rappoldt *et al.* 1985).
Because most sites are not counted in every month and there are occasional missing site counts also during the integral months (with the share of 'gaps' in the data increasing further back in time), a procedure has been developed to augment ('impute') data for the missing counts so that trends are always based on the same counting areas. This procedure uses the ratios between the average numbers in (a) the counting area to be imputed and the other areas, (b) the missing month and the other months of the year, and (c) the missing year and the other years in the series. The procedure is carried out with the computer package U-index (Bell 1995).

## 3.6 Overview of species and data sets used in the analysis

Table 3.1 summarizes the list of species, the data sets used for the analysis and the time period covered by the analysis. The backward extent of the data set is limited to that period for which a methodologically uniform time series could be obtained. Whether or not 2020 is included in the analysis depends on the working up of the samples. This was done for the bird counting series and for the WOT shellfish survey in the Wadden Sea, but not for the other two data sets. It is presently not known when the SIBES and North Sea shellfish samples of 2020 will be available, as sample processing has been hampered considerably by Covid restrictions on laboratory work.

*Table 3.1 Overview of species, the data set analyzed and the time period used in the analysis*

| Species | Data set | Start year | End year |
|---|---|---|---|
| ***Arenicola marina*** | SIBES | 2009 | 2019 |
| ***Cerastoderma edule*** | SIBES | 2009 | 2019 |
| ***Limecola balthica*** | SIBES | 2009 | 2019 |
| ***Mytilus edulis*** | WOT shellfish WS | 2012 | 2020 |
| ***Ensis leei*** | WOT shellfish NS | 2010 | 2019 |
| ***Spisula subtruncata*** | WOT shellfish NS | 2010 | 2019 |
| ***Melanitta nigra*** | RWS / WMR sea ducks | 1993 | 2020 |
| ***Somateria mollisima*** | RWS / WMR sea ducks | 1993 | 2020 |
| ***Tadorna tadorna*** | SOVON water birds | 1976 | 2020 |
| ***Calidris canuta*** | SOVON water birds | 1976 | 2020 |
| ***Anas acuta*** | SOVON water birds | 1976 | 2020 |
| ***Limosa lapponica*** | SOVON water birds | 1976 | 2020 |

# 4 Statistical analysis: general set-up of the analysis and workflow

## 4.1 Basic structure of the analysis.

The aim of the statistical analysis is to determine whether there is a significant influence of the MSC Zoe incident on the abundance (number per counting area), or biomass (gram per $m^2$) of each species, causing an offset from the values in previous (baseline) years. However, it is not possible to make a reliable quantitative prediction about how the plastic has been dispersed in the environment of the species (Chapter 2). The uncertainty on the fate of the plastic materials differs between the two types of material (HDPE and PS) lost. For neither of the two is it possible to apply a regression-like approach to estimate the relationship between a population statistic (a dependent variable) and the intensity of the disturbance (an independent variable). For that reason, the approach used is data exploration. A statistical model is carefully constructed to estimate the distribution of the species in space and time, allowing for spatial and temporal correlation. Subsequently the model is investigated by looking for a pattern in 2019 (and for some species also 2020) that is deviant from what can be expected based on the previous years. Such deviations can be suspected to be caused by the MSC Zoe incident and deserve closer examination should they be found.
All statistical models are constructed and analyzed by species. No species interaction has been taken into account.
The statistical model prescribes that the observation $Y_{t,s}$ at point *s* and time *t* is a randomly drawn variate from a statistical probability distribution. The probability distribution is specified by its type (e.g. a normal distribution, Poisson distribution etc.) and by its parameters. For example, a normal distribution is characterized by the parameters μ, the mean, and σ, the standard deviation. The statistical model attempts to predict the expected value $E[Y_{ts}]_s$ at time *t* and spatial position *s* as a function of external information available for the model building. The external information available to estimate the statistical model consists of control parameters (e.g. the year and month of sampling, the organization that took the sample, the surface of the sample) and environmental information. We expect more lugworms in silty sand than in very coarse sand or in pure mud. Therefore, the median grainsize at a sampling point contains information that is useful to predict the abundance of the lugworm. Several cofactors are available for the Wadden Sea and coastal area. Details are given in Herman & van Weerdenburg (2020).
The procedure for fitting a statistical model can be explained with the simple example of a linear regression as a starting point. When applying a regression analysis, the following model is fitted to the data:

$$Y_i \sim N\left(\mu_i, \sigma^2\right)$$

$$E(Y_i) = \mu_i = \alpha + \beta \times X_i$$

The model states that every observation $Y_i$ is drawn randomly and independently from a normal distribution with mean $\mu_i$ and variance $\sigma^2$ that is common to all observation points. The expected value $E(Y_i)$ is defined as a linear function of an independent variable X; the i-th expected value of observation $Y_i$ is calculated from the i-th value of the independent variable X. The linear relation has two parameters α and β that are estimated during the model fitting. For a standard linear regression this estimation is done through linear least-squares estimation.

In the statistical analyses used in this report, the basic model building as exemplified by the simple regression approach is extended in different ways. These extensions are summarized as specified below.

### 4.1.1 Use of non-linear smoothers (GAMs)

Following the class of models known as General Additive Models (GAMs), the simple linear function of an independent variable X is replaced by a generic function of several variables $X_j$:

$$F = \alpha + \beta * X_i \quad \Rightarrow \quad F = \alpha + f_1(X_1) + f_2(X_2) + \ldots + f_m(X_m)$$

Here, the functions $f_j$ belong to a broad class of smooth functions. They can represent the influence of a categorical factor on the observations (e.g. which observer has made the counting?), or the (possibly non-linear) influence of a continuous variable on the counts (e.g. the lugworm abundance is a unimodal, roughly Gaussian response curve on median grain size). The smoother functions follow the patterns present in the data, without imposing a fixed functional form. However, they are constrained not to show discontinuities. How 'flexible' they are in following small wiggles in the data depends on the choice of smoother function type and parameters determining the flexibility. Appropriate fitting of GAM smoothers requires choosing functions that are following the real structure in the data without overfitting every small wiggle. Figure 4.1 demonstrates the difference with linear regression. A linear regression model has a fixed shape (straight line). If the data do not follow this shape, as is the case in the example, a pattern will appear in the residuals (the difference between observations and fitted values). A GAM is flexible in following the pattern in the data, and its residuals do no longer show a clear pattern.

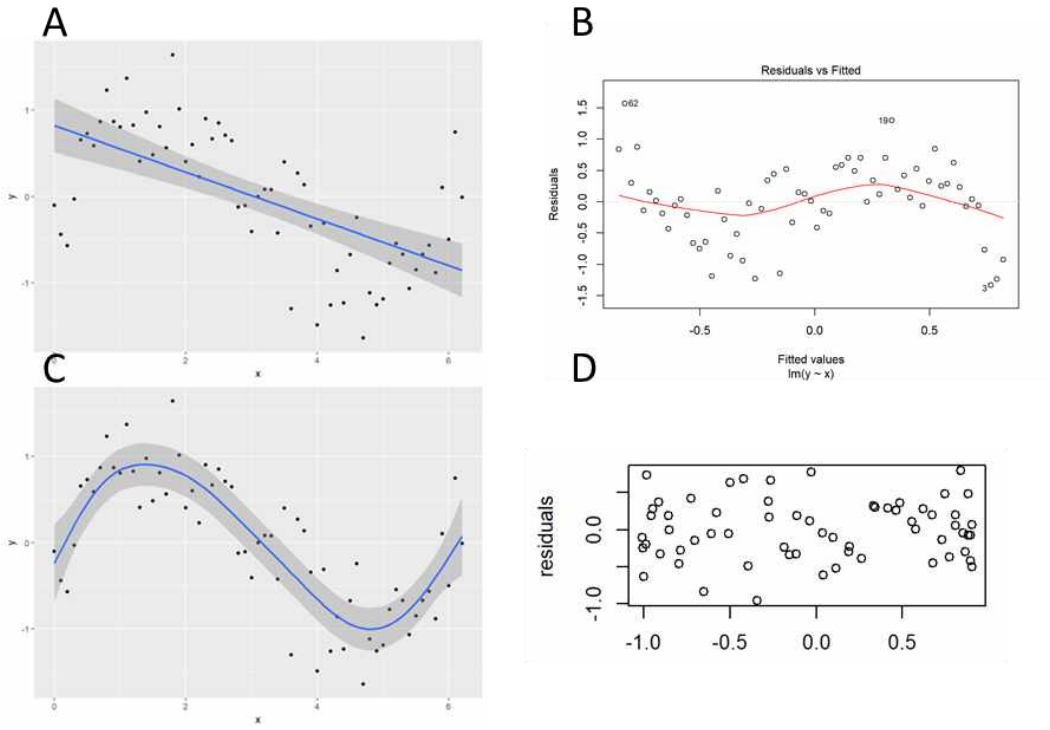


*Figure 4.1. A dataset fitted with a linear regression model (A). Residuals versus fitted values show clear patterns (B). After fitting the same dataset with a non-linear GAM smoother (C), the residuals do no longer show a pattern when plotted versus the fitted values (D). Figures from http://environmentalcomputing.net/intro-to-gams/*

### 4.1.2 The use of a link function

The expected value of the response variable $E(Y_i)$ itself does not need to be a linear function of the smoothers. It can be *linked* to the smoothers via a link function. In general, equation (2) becomes:

$g(E(Y)) = \alpha + f_1(X_1) + f_2(X_2) + \ldots + f_m(X_m)$

where g() is the link function. If the link function is a log link, we have by using the fact that logarithms are the inverse of exponentiation:

$E(Y) = \exp(\alpha + f_1(X_1) + f_2(X_2) + \ldots + f_m(X_m)) = \exp(\alpha) * \exp(f_1(X_1)) * \ldots$

### 4.1.3 The use of different statistical distributions

The distribution in eq.(1) does not need to be a normal distribution. Other distributions used are Poisson, negative binomial and gamma distributions. The choice of a link function is co-determined by the choice of distribution, in order to operate within the class of generalized linear models.

### 4.1.4 Accounting for spatial and/or temporal autocorrelation

The observations do not need to be independent of one another. Observations in space and time often have spatial and/or temporal autocorrelation. Nearby observations (in space or time) can be more similar to one another than observations far apart. They can, inversely, also be more dissimilar the closer they are, but in any case, distance influences the similarity of pairs of observations. This can be a consequence of the underlying process (e.g. highly mobile populations will spread out over space and generate higher than expected values in an area around a population hotspot) or a consequence of an incomplete description of the environment. As an example, it is possible to summarize the environment of the lugworm by grain size and current velocity, but neglect bathymetry. Yet lugworms have a preferred zone in the intertidal window. Neighboring points on tidal flats tend to have similar height in the intertidal, hence their residuals will be spatially correlated if we had not incorporated height in the model. Where observations are known to be correlated (this feature can be tested), the procedure is to add a term to the deterministic part of the model. This term is called a spatio-temporal field. It contains an additional element to be added to the model for every point in space and time, representing whatever spatio-temporally correlated information that was not yet incorporated into the model. It can be considered as a 'latent variable'. By mapping the spatio-temporal field for every moment in time it is possible to infer which environmental factor could be behind the pattern. However, sometimes this remains unknown.

### 4.1.5 Use of a Bayesian approach

A Bayesian approach is used for model fitting. The essence of the approach is that information available prior to the estimation of the statistical model is incorporated into the model building and fitting process. Apart from the technical and computational consequences, this has also effects on how the model is evaluated. Instead of calculating the 'statistical significance' the emphasis is on optimizing the model fit, with a premium on a parsimonious model. Once fitted, the relevance of the model terms is evaluated by checking their *posterior* probability distribution. This is the probability distribution of the fitted parameter, after taking the prior information as well as the data into account. In this report, the posterior probability distribution of parameters is usually summarized as the 95 % credible intervals, i.e. the interval expected to contain the true parameter in 95 % of the cases. If 0 is included in the credible interval, i.e. is considered as one of the likely values for the term, the term is considered not to contribute to explaining the variation in the data.

## 4.2 Model building

In the model fitting, a gradual build-up of complexity has been used as a general strategy. Starting from a relatively simple model assuming no autocorrelation in the error terms and simple GAM functions, the model complexity is increased through several cycles of fitting, testing residuals, increasing model complexity etc., until a model is found that represents the data well without apparent anomalies in the residuals. Anomalies that were checked are: relations between residuals and predicted values, autocorrelation in space and/or time between residuals, non-conformity to the assumed error distribution (e.g. excessive number of zeroes).
As an example, the following sequence of checks, model specifications, fits and renewed checks was performed to model the abundance (count data) of the lugworm *Arenicola marina* (chapter 5):

### 4.2.1 General data exploration

Check for outliers, errors in the data file and other abnormalities

### 4.2.2 Fit of a Poisson General Linear Mixed Model GLMM

The model assumes independent Poisson-distributed observations and a linear function of categorical and continuous variables for the deterministic part of the model. The model is specified as follows:

$$\begin{aligned} Counts_{is} &\sim Poisson\,(\mu_{is}) \\ E[Counts_{is}] &= \mu_{is} \\ var[Counts_{is}] &= \mu_{is} \\ \log(\mu_{is}) &= \beta_1 + Covariates_s + u_i \\ u_i &\sim N(0, \sigma_u^2) \end{aligned}$$

In this and the following equations, the subscript i refers to points in space, the subscript s to time. Poisson denotes the Poisson distribution with one parameter, the mean and variance μ. The operator E[] expresses the expected value, the operator var[] the variance. μis, the expected value, is linked through a log-link function to a predictive equation that contains an overall intercept, a linear function of covariates and a place-specific intercept $u_i$, modelled as independent (spatially and temporally uncorrelated) variates from a normal distribution.

### 4.2.3 Check of the residuals

It was found that the linear nature of the relationship of the residuals with the environmental variables was not adequate, by the tests specified earlier (no relation of residuals with fitted values, no overdispersion, no excessive number of zero values). Moreover, spatial correlation in the random terms was detected and the model did not correctly predict the large number of zero observations. In the next step the first problem (linear nature of the response) was tackled, while the other points remained as points of attention.

### 4.2.4 Fit of a Poisson General additive mixed model.

Similar to the model in 4.2.2, but the simple linear function of the environmental variables is replaced by GAM smoothers.

$$
\begin{aligned}
Counts_{is} &\sim Poisson\,(\mu_{is}) \\
E[Counts_{is}] &= \mu_{is} \\
var[Counts_{is}] &= \mu_{is} \\
\log(\mu_{is}) &= \beta_1 + fYear_s + fMonth_s + fTotSurf_{is} + \\
&\quad f(tauFlood_i) + f(tauWave_i) + f(Salinity_i) + \\
&\quad f(GrainSize_i) + u_i \\
u_i &\sim N(0, \sigma_u^2)
\end{aligned}
$$

Where all terms are as in the previous model, except for the functions of the environmental variables, that are now GAM smoothers.

### 4.2.5 Check of the Poisson GAM residuals

Although the non-linear nature of the relation with environmental factors is much better represented by the GAM smoothers, this does not resolve the problem of spatial correlation in the residuals.

### 4.2.6 Fit of a Poisson GAM with spatial correlation

Similar to the model in 4.2.4, but an additional spatial field is added to represent the autocorrelation.

$$
\begin{aligned}
Counts_{is} &\sim Poisson\,(\mu_{is}) \\
E[Counts_{is}] &= \mu_{is} \\
var[Counts_{is}] &= \mu_{is} \\
\log(\mu_{is}) &= \beta_1 + fYear_s + fMonth_s + fTotSurf_{is} + \\
&\quad f(tauFlood_i) + f(tauWave_i) + f(Salinity_i) + \\
&\quad f(GrainSize_i) + u_i \\
u_i &\sim N(0, \Omega)
\end{aligned}
$$

Where the only difference with the model in 4.2.4 is that the random intercepts for the points are no longer considered to be drawn independently, but are now modelled to have a spatial covariance structure specified by the covariance matrix Ω.

### 4.2.7 Check of the residuals of the spatial Poisson GAM

It was found that the model cannot cope with the excessive number of zero counts and that the model was over-dispersed. Therefore, other models than the Poisson model were tried.

### 4.2.8 Fit of different GAM models with spatial correlation

Apart from the Poisson model in step 4.2.6, also a Zero-inflated Poisson model, a negative binomial model and a zero-inflated negative binomial were tried. All were combined with GAM smoothers and spatial correlation. A DIC comparison (Deviance information criterion, the Bayesian equivalent to the well-known Akaike Information Criterion) was used to select the best model. The negative binomial GAM with spatial correlation turned out to be the best fitting model. This model is specified as follows:

$$
\begin{aligned}
Counts_{is} &\sim NB(\mu_{is}, \theta) \\
E[Counts_{is}] &= \mu_{is} \\
var[Counts_{is}] &= \mu_{is} + \frac{\mu_{is}^2}{\theta} \\
\log(\mu_{is}) &= \beta_1 + fYear_s + fMonth_s + fTotSurf_{is} + \\
&\quad f(tauFlood_i) + f(tauWave_i) + f(Salinity_i) + \\
&\quad f(GrainSize_i) + u_i \\
u_i &\sim N(0, \Omega)
\end{aligned}
$$

Here the negative binomial (NB) distribution has replaced the Poisson distribution. It has two parameters, the mean μ and dispersion parameter θ. All other terms are identical to the model in 4.2.6.

### 4.2.9 Check the residuals of the selected model

No problems were found. For a GAM model with spatial dependency, the binomial distribution is the optimal choice.

### 4.2.10 Fit a model that includes temporal dependency

The model as specified in 4.2.8 calculates a single spatial random field, that is assumed to remain the same over time. In such a model, changes due to the Zoe incident would not be visible. It is therefore needed to allow the random field to change from year to year. This can be done in several ways. One generic method is to include an autoregressive process in the sequence of random fields. A random field in year t is assumed to be composed of two parts: the random field of year t-1, plus a new part of spatially correlated variation that is unrelated to last year's field. A parameter ρ expresses how strong the correlation with last year was. By putting ρ=0 in an extreme case, the model assumes no temporal correlation. The random fields are called replicate fields. Such independent fields have the 'freedom' to reflect a pattern due to the Zoe incident, should that be present in the data. Therefore, this is the model of choice in this case. *A. marina*, however, is a long-lived species and some serial correlation of the random fields is likely. In fact, the data corroborate that this is the case. It was nevertheless omitted from the model to maximize the chance of detecting a possible Zoe effect. The model then becomes:

$$
\begin{aligned}
Counts_{is} &\sim NB(\mu_{is}, \theta) \\
E[Counts_{is}] &= \mu_{is} \\
var[Counts_{is}] &= \mu_{is} + \frac{\mu_{is}^2}{\theta} \\
\log(\mu_{is}) &= \beta_1 + fYear_s + fMonth_s + fTotSurf_{is} + \\
&\quad f(tauFlood_i) + f(tauWave_i) + f(Salinity_i) + \\
&\quad f(GrainSize_i) + v_{is} \\
v_{is} &= \rho \times v_{i,s-1} + u_{i,s} \\
\rho &= 0 \\
u_{i,s} &\sim N(0, \Omega)
\end{aligned}
$$

This model differs from the model in 4.2.8 because instead of a purely spatial random field, a spatio-temporal random field has been defined. This field takes different values in each of the years. The spatio-temporal field is expressed (in principle) as an autoregressive process in time and a spatially correlated process in space. In this special case, in order to be able to investigate a possible Zoe effect, the autoregressive parameter ρ is set to zero, so that a replicate model in time is used that can reveal sudden changes.

#### 4.2.11 Checks of the residuals of the model

The fitting proved that incorporating temporal correlation of the spatial fields for the different years, technically by specifying an autoregressive component in time, was a better (more parsimonious) model than the model with replicate spatial fields. However, the latter was used for further analysis because it is the only model that provides answers to the scientific question. If an effect of the MSC Zoe incident is available, this will be an effect that is uncorrelated to any signal in the previous year. A statistical model assuming autocorrelation will not show the signal – a sudden disturbance – to the full extent, as it will be constrained to show the part of variation that is linked through autocorrelation with variation in the surrounding years.

## 4.3 Results of the model fitting and detection of MSC Zoe effect

The final model has GAM smoothers with respect to environmental factors, and spatial random fields for the different years. We refer to the chapters on the different species for the form of the smoothers representing the relation with environmental factors. We give an example of a random field (*A. marina* in 2019) to explain how these maps should be interpreted (Figure 4.2).

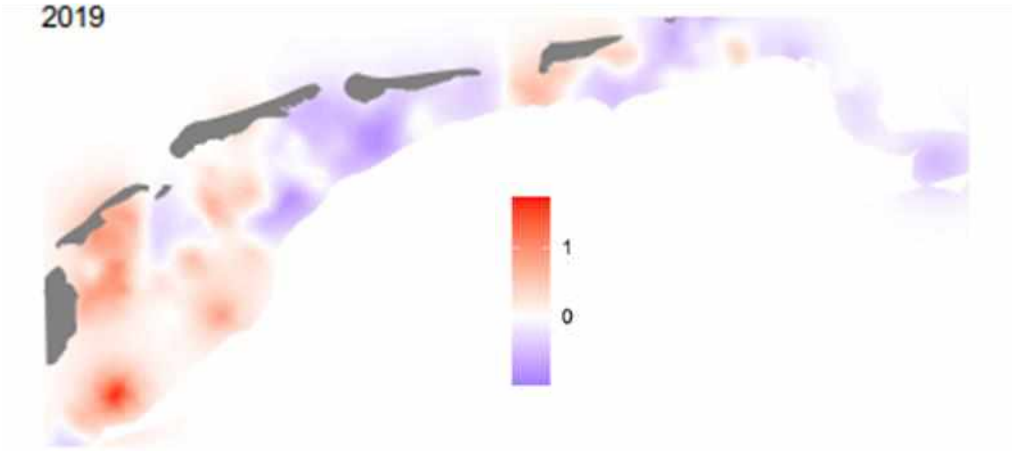


*Figure 4.2. Spatial random field of A. marina in 2019, as an example. See text for interpretation of this map.*

In the red areas the observed counts were higher than expected based on the environmental parameters, and these consistently high observations were correlated in space. For the blue areas the reverse is true. Using the scale, the darkest red area has a multiplication factor of approximately exp(1.5)=4.5. For the darkest purple-blue areas it is approximately exp(-1)=0.4.

The other model terms describe the prediction well in the white areas. However, the red areas require an additional multiplicative term that can go up to a factor 4-5 in order to arrive at the correct prediction. In the dark blue areas, the prediction needs to be corrected by a factor of 0.4.

A possible Zoe effect is detected by comparing the random fields for the year 2019, with the random field of 2018 and, if available, of 2020. Any deviation is examined for its possible relation with the incident. Where such a relation cannot be excluded, closer examination of the data is called for.

## 4.4 Adaptation of workflow for variables measured on a continuous scale

Some of the variables studied are not counts (which are measured on a discrete scale, i.e. only assume integer values) but measurements on a continuous scale. This is the case for all biomass values of benthic species, but also for some abundance values. In the WOT data, abundance values are calculated to numbers per $m^2$, based on subsampling protocols and calculations of the length of the sampling path. The result is a decimal number that cannot be reduced to an integer.
The 'natural' distribution to use for these variables is the Gamma distribution, but this cannot cope with the often very large proportion of zero observations in the data sets. For this reason, a zero-altered Gamma (ZAG) distribution is used. This distribution is composed of two parts. A Bernouilli distribution models the probability of presence (non-zero) values and a gamma distribution models the value of the variable at places where the species is present. The ZAG distribution thus has three parameters: the parameter π of the Bernouilli part, representing the probability of being present, and the parameters μ and *r* of the gamma part, where μ is the mean of the gamma distribution and *r* is its shape parameter. The ZAG is represented as follows:

$$\begin{aligned} Obs_i &\sim ZAG(\mu_i, \pi_i, r) \\ E[Obs_i] &= \pi_i \times \mu_i \\ Var[Obs_i] &= \frac{\pi_i \times r + \pi_i - {\pi_i}^2 \times r}{r} + \mu_i^2 \end{aligned}$$

In accordance with the two-step structure of the model, also the fitting procedure to the data set is done in two steps. First, the Bernouilli model is fitted to the data, using a logit link function and formulating a model that contains an intercept, smoothers of the physical cofactors and a spatial random field per year. Only afterwards can the gamma model be fitted to the subset of the data where the species was present. This fitting uses a log-link. Besides separate smoothers of the physical cofactors, it also yields a spatially random field per year, which in principle is different from the spatial field obtained by fitting the Bernouilli model. However, fitting two spatial fields per year is problematic because it is not guaranteed that enough relevant data will be available for both, and also because it is reasonable to assume that the latent variable described by the random field will affect both presence/absence and numerical abundance or biomass. For these two reasons, it was decided to fit a single spatial random field per year that is shared by both parts of the model. The detailed explanation is given in an appendix of the Highland Statistics report. For this end report, the most important aspect to consider is that the ZAG can be fitted yielding one spatial random field per year. Besides, the analysis yields two sets of smoothers for the cofactors, one set expressing the influence of the cofactors on presence/absence and one set describing the influence on the numerical value where the species has been found.
With this adjustment, the full model fitted is given as:

$$
\begin{aligned}
Obs_{is} &\sim ZAG(\mu_{is}, \pi_{is}, r) \\
E[Obs_{is}] &= \pi_{is} \times \mu_{is} \\
Var[Obs_{is}] &= \frac{\pi_{is} \times r + \pi_{is} - {\pi_{is}}^2 \times r}{r} + \mu_{is}^2 \\
logit(\pi_{is}) &= \gamma_1 + f(tauFlood_{is}) + f(tauWave_{is}) + f(Salinity_{is}) + \\
&\quad f(Grainsize_{is}) + Year_s + b \times u_i \\
log(\mu_{is}) &= \beta_1 + f(tauFlood_{is}) + f(tauWave_{is}) + f(Salinity_{is}) + \\
&\quad f(Grainsize_{is}) + Year_s + u_{is} \\
u_{is} &\sim N(0, \Omega)
\end{aligned}
$$

Where the subscript i denotes space and the subscript s time and all symbols are as used before. One new symbol in this formulation is the proportionality factor b between the spatial random fields of the Bernouilli and gamma parts of the model. This factor is needed because the two different link functions result in a scaling difference between the two parts of the model fitting.
As was done in the other analyses, the possible effect of the MSC Zoe effect was investigated by comparing the spatial random field of 2019 with that of 2018.

## 4.5 Adaptation of workflow for bird species

The analysis steps followed for *A. marina* are an example of the workflow generally applied to the benthic species. Not all species have been modelled with exactly the same model. Variations are discussed in the chapters of the species. The most common cause for changing the model was an excessive number of zero observations, beyond what is probable given a negative binomial distribution. In those cases, a zero-inflated negative binomial (ZINB) distribution is used. Comparable to the ZAG, also this distribution is characterized by a third parameter, π, expressing the fraction of observations that were zero, but were not expected to be zero based on the negative binomial. The other fraction (1- π) of the observations is distributed according to a negative binomial distribution with mean and dispersion parameter specified by the other two parameters (μ and θ) of the ZINB.
For the bird species much less spatial resolution is available, as the birds are counted in large plots. However, whereas benthic species only had one observation per year, the bird species have a higher resolution in time. For these cases the workflow is adapted by emphasizing the time series analysis. Instead of treating 'year' as a categorical control variable, a smoother for the effect of time is used and allowance is made for temporal autocorrelation.
The time trend is modelled as a special smoother of the time of observation. This smoother, a special case of the group of autoregressive processes, is termed a Random Walk trend. It specifies that a trend value at time *s* is equal to the trend value one time step before, plus a new random noise term that is drawn from a normal distribution:

$$\mathrm{Trend}_{is} = Trend_{i,s-1} + v_{is}$$

Where the subscript i denotes space (areas) and the subscript s time. The random noise term $v_{is} \sim N(0, \sigma^2)$ is characterized by the variance $\sigma^2$ that is estimated during the fitting procedure and determines the flexibility of the trend. The higher the random noise added at each time step, the lower the influence of the previous time step and the more flexible the trend term will appear.
In some species the trends of neighboring areas show strong correlation. Analyzing spatial correlation with just 10 to 13 series is not easy, but it proved useful to improve the fit sometimes. The spatial correlation between the random intercepts of neighboring areas was modelled as a CAR (conditional auto-regressive correlation) model. In this formulation, the random intercept of an area is constrained to be a weighted average of the random intercepts of the neighboring areas.

For the detection of an MSC Zoe effect, the smoother trend values of 2019 are compared to the smoother trend values of 2018 and 2020. To do so, the *posterior* distribution of the difference between 2019 and 2018, and between 2020 and 2019, is obtained from the fitting procedures. If the 95 % credible interval of the difference does not encompass zero, the trends are examined closer to see if the Zoe incident could cause the pattern. The 'credible interval' is, loosely speaking, the Bayesian equivalent of a confidence interval. It depicts the range where 95 % of the cases in the *posterior* distribution has been found by the analysis.

## 4.6 Data archiving

The data used for this analysis are maintained in dynamic web-connected databases. In order to guarantee full replicability of the analyses reported here, a frozen data set has been archived at the 4TU repository under the following permanent url: https://doi.org/10.4121/14364194.v1.

The frozen data set contains the following elements:

- Data files as delivered by the research institutes to the statistical expert of Highland Statistics
- Data files as worked up in preliminary analysis by Highland Statistics, and used in this form as input for the statistical analysis
- Documented analysis scripts, one per species. These are R Markdown documents that contain all code used for the statistical analysis and are fully self-documenting. The detailed descriptions of the analysis (reports of Highland Statistics) are directly generated from these files
- Files containing the output of the statistical analyses, if different from the graphs and tables contained in the R Markdown documents

Access to the data files and analyses is restricted for the sole purpose of controlling, replicating or improving the analyses presented in this report. Access will be granted to everybody upon sending a motivated request. Use of the data files for any other scientific or other purpose will not be allowed. It remains the sole privilege of the data owner to grant access outside the context of the present analysis.

# 5 The Lugworm (*Arenicola marina*)

## 5.1 Biology and ecology

*Arenicola marina* (Eng: Lugworm, Ned: Wadpier) is a polychaete worm that can attain a body length of maximally 20 cm and an age of about 6 years. The body is relatively thick and bears bristles and gills, the thinner tail lacks both bristles and gills. The animals live buried into the sediments of estuarine waters, predominantly in intertidal areas, although low densities may be found in shallow subtidal sediments. They are generally found in areas with salinities of 10-35 ‰ S. They prefer mixed to sandy sediments, where densities up to 70 adults per m² can be attained. The animals make a typically J-shaped burrow, and normally live in the deepest part, down to a depth of about 40 cm in large adults.

### 5.1.1 Feeding

*Arenicola marina* feeds, during periods the sediment is covered by seawater, by collecting sediment with accumulated organic matter by protruding the papillate proboscis. The ingested sediment passes the alimentary tract and the digestible organic matter from it is retained in the gut. The undigestible parts leave the body via the anus at the tail end and are defecated on top of the sediment. For this purpose, the animal moves up in its burrow, tail upward, to the surface. There the gut is emptied in a few seconds, leaving a characteristic faecal cast, and the animal moves downward as rapid as possible to resume feeding and to minimize predation. While feeding and defecating, above the head of the active animal the sediment forms a depression as a result of sediment removal near the head, and in this depression diatoms and organic matter accumulates. In this sinking enriched sediment bacteria live on the accumulated organic matter, and both diatoms and bacteria form the main digestible fraction of the ingested sediment. The animals pump oxygen-rich seawater into their burrow via the tail-end downward. At the head-end the water flows into the organically enriched sediment, which is oxygenated and by this the bacterial growth on downward moving organic matter is promoted. This process is sometimes called ‘gardening’. This results in an increased amount of easily digestible bacteria near the head. Feeding activity and thus defecation frequency is temperature dependent. In summer, this frequency can go up to once per 30 minutes, in winter this frequency is much lower. In a relatively dense population the total amount of reworked sediment, i.e. sediment ingested in deeper layers and put on top of the sediment, can be 30 cm per year. As the size of the papillae of the proboscis increases with the size of the animal, the largest animals can live in coarser sediments than small animals.

### 5.1.2 Reproduction

In the Wadden Sea *Arenicola marina* reproduces in late summer and early autumn, September to November. The females lay their eggs in their tube, and these are fertilized by the sperm of the males that is present in the oxygen-rich water which is pumped into the burrows by the females. Fertilization takes place in the burrows of the females; the fertilized eggs develop in the burrows into so-called trochophore larvae. After around 4 weeks the larvae leave the female burrow. During the presence of eggs and larvae in the burrow the females do not feed, and thus do not emerge to the sediment surface to produce faecal casts. After leaving the female burrow, the larvae expose themselves to tidal currents to be transported to sheltered sites where they over-winter. In early spring they migrate for a second time to move to areas with fine-grained nearshore sediments. After the summer, at a length of around 6 cm, they move again to courser sediments.

### 5.1.3 Population in the Wadden Sea

The populations of *Arenicola marina* in the Wadden Sea are, compared with other macrobenthos species, very stable, especially in terms of biomass. At Balgzand, during a 50-y monitoring program, the mean winter biomass is 4.7 ± 0.2 (s.e.) $g.m^{-2}$ ash-free dry mass without clear temporal trends, although during recent years (2015-2019) the highest biomass values in the entire study period are found. This is partly the result of the relatively long lifespan and their deep-living habit, which makes that the species suffers predation only from very few specialized predators. Bar-tailed godwits have a strong preference for *Arenicola marina*, and juvenile plaice preys upon their tail-ends.

## 5.2 Interaction with plastics

*Arenicola marina* is found to accumulate micropollutants that can be taken up from the water via the skin and the gills, and from the food and sediment via the gut. Copper is found to inhibit oxygen uptake in juveniles. Accumulation of poly-aromatic carbohydrates is relatively strong, although there is little known of the effects of these chemicals. A. marina are able to take up particles up to 500 µm (Gebhardt and Forster, 2018).
Microplastics are found to influence *Arenicola marina* in two ways: reduction of microalgae in the sediment, and thus reduction of food, while metabolic activity increased, but faecal cast production, and thus total feeding activity, decreased with increasing concentrations (up to 2% of wet sediment weight) of microplastics in outdoor mesocosm experiments. Not all microplastics gave the same level of effect (Green *et al*., 2016). A field study along the Belgian coast (Van Cauwenberghe *et al*., 2015) showed a presence of microplastics in natural *Arenicola marina* populations. Laboratory experiments with high concentrations of polystyrene microspheres did not result in adverse effect on the energy budget. A laboratory study (Besseling et al., 2013) on the effect of polystyrene microparticles on *Arenicola marina* showed increased microplastic intake and increased weight loss with increasing polystyrene concentrations. Moreover, increased polystyrene levels increased the accumulation of polychlorinated biphenyls. Note that this study used smaller particles than the ones coming from the MSC Zoe.
Foekema et al. (2021) found up to 30 microplastic granules in the lugworms added to the experimental mesocosms with the highest microplastic concentrations. No effect on their physiological conditions was detected.
It can be concluded that experimental high levels of microplastics in a size range that can easily be taken up will negatively influence both behavior and condition of *Arenicola marina*. The present low ambient levels found in Northwest European coastal waters are thought not to be harmful for *Arenicola marina* populations.

## 5.3 Data collection and analysis

Data were collected within the SIBES sampling program (Chapter 3.1). The analysis is documented in the R Markdown file **02SIBESData1.Rmd.** From this markdown file the report of Highland Statistics (chapter 2, Arenicola marina) was automatically generated.
The data set comprises 6882 samples in the years 2009 to 2019. The species was found in appr. 35 % of the samples. The counts per sample ranged from 0 to 20, corresponding to densities of 0-1500 ind. $m^{-2}$, but high counts were very rare. The biomass was in the range 0-1 gram AFDW per sample, or 0-80 $g.m^{-2}$.
The covariates provided as environmental factors had a high degree of collinearity. Therefore, a limited set of variables was selected that represent the condition of the sediment (median grain size), the current (maximum bottom shear stress during flood), effects of waves (median bottom shear stress due to waves), and salinity.

### 5.3.1 Analysis of Numerical Abundance

A series of statistical models with increasing complexity was fitted to the data. These models have already been discussed as part of the general introduction to the statistical analysis. The final model fitted to the data is a negative binomial GAM with spatial and temporal correlation fields.

The model is specified as follows:

$$
\begin{aligned}
Counts_{is} &\sim NB(\mu_{is}, \theta) \\
E[Counts_{is}] &= \mu_{is} \\
var[Counts_{is}] &= \mu_{is} + \frac{\mu_{is}^2}{\theta} \\
\log(\mu_{is}) &= \beta_1 + fYear_s + fMonth_s + fTotSurf_{is} + \\
&\quad f(tauFlood_i) + f(tauWave_i) + f(Salinity_i) + \\
&\quad f(GrainSize_i) + v_{is} \\
v_{is} &= \rho \times v_{i,s-1} + u_{i,s} \\
\rho &= 0 \\
u_{i,s} &\sim N(0, \Omega)
\end{aligned}
$$

In this equation, the subscript *i* refers to points in space, the subscript *s* to time. NB denotes the negative binomial distribution with two parameters, the mean μ and the dispersion parameter θ. The operator E[] expresses the expected value, var[] the variance. Expressions for expected value and variance are the standard formulations for the negative binomial distribution. The expected value at a particular time and place $\mu_{is}$ is linked through a log-link function to a predictive equation that contains a number of factors (year, month, surface sampled) that vary in time and/or in space. Further the linear term contains smoothing functions for the environmental factors median bottom shear stress during flood, median wave bottom shear stress, salinity and grainsize, which all vary in space. Finally, the linear term contains a spatio-temporal random field that represents the correlation in space and time of the variable. The spatio-temporal field is expressed (in principle) as an autoregressive process in time and a spatially correlated process in space. In this special case, in order to be able to investigate a possible Zoe effect, the autoregressive parameter $\rho$ is set to zero, so that a replicate model in time is used that can reveal sudden changes.

The categorical factors year, month and sampled surface allow for spatially averaged effects of the year and month of sampling, as well as for a methodological compensation for the

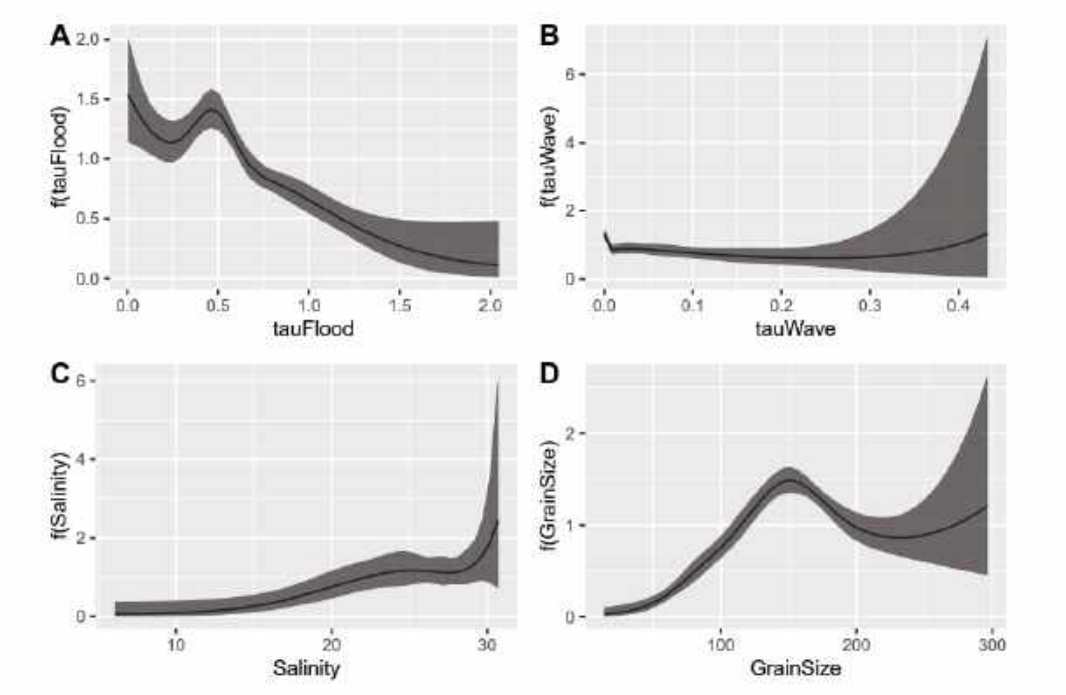


*Figure 5.1. Posterior mean values and 95 % credible intervals for the smoothers obtained by the negative binomial GAM with spatial correlation applied on the A. marina count data. Each smoother is an unpenalized cubic regression spline with 5 df.*

unequal size of the samples. They are control variables and compensations for year effects that are not very interesting in the present analysis. In fact, we do not expect the MSC Zoe effect, if it occurs, to be entirely homogeneous across the entire Wadden Sea.
The smoothers of the environmental factors describe clear effects for three out of the four variables, as shown in Figure 5.1.

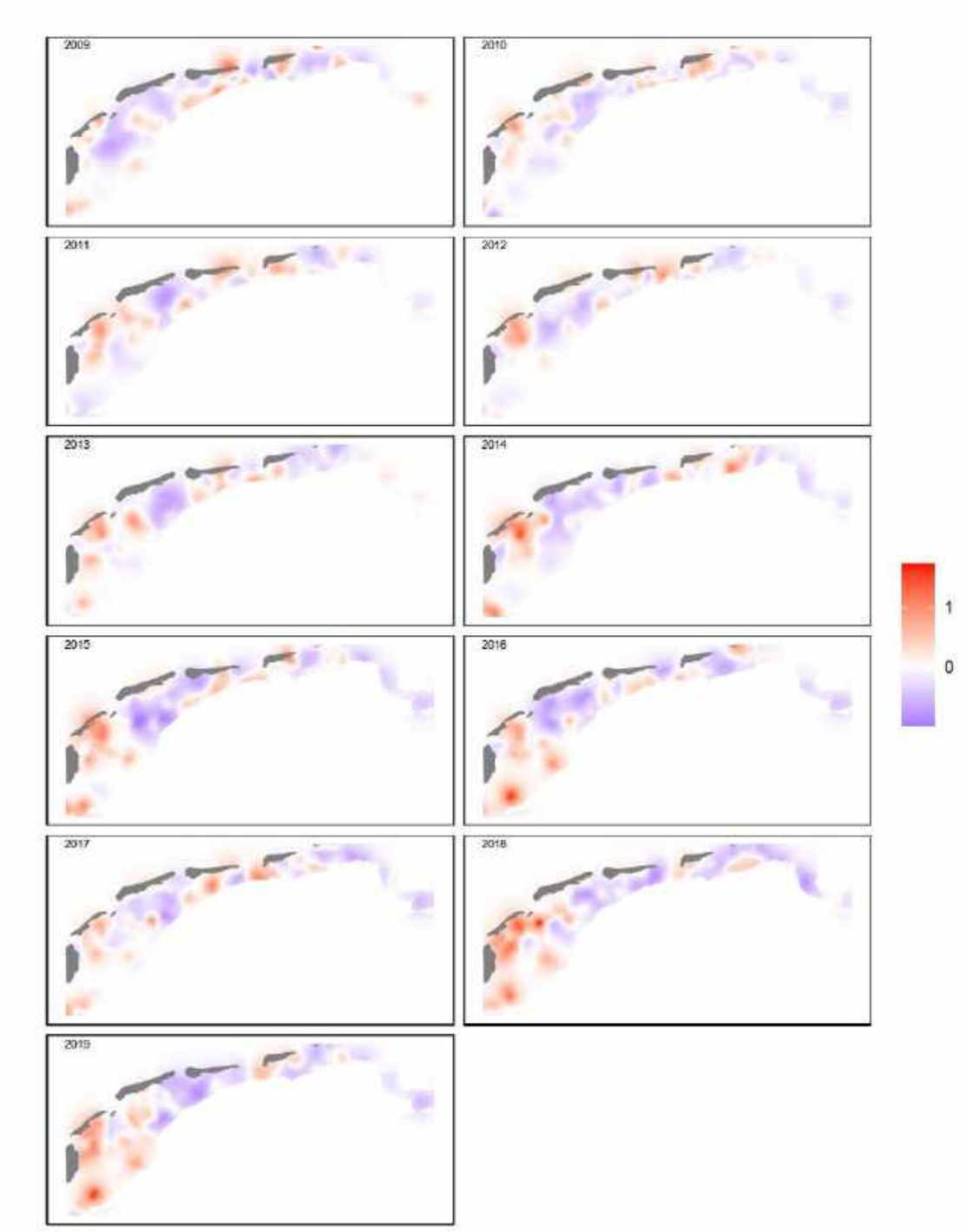


*Figure 5.2. Spatial random fields for each year obtained by the negative binomial GAM with the spatial-temporal replicate correlation applied on the A. marina count data.*

The spatial fields of all years for this species are shown in Figure 5.2, from which we concluded that there was a slow change of hotspots for the species from the Eastern to the Western Wadden Sea in the course of the decade that was sampled.
The effect of the MSC Zoe incident was estimated by comparing two statistical models that differ in the specification of the random fields. In the first model, every year has a separate spatial correlation field. In the second model, only a single spatial field was used for both the years 2018 and 2019. Based on DIC, the latter model was clearly to be preferred. (Table 5.1).

*Table 5.1. DIC values of two NB GAM models with spatial-temporal replicate correlation. The full model in the first row contains a spatial random field for each year. The sub-model in the second row also contains a spatial random field for each year, except for the 2018 and 2019 data. These are modelled by 1 spatial random field.*

| Model | DIC |
|---|---|
| NB GAM + replicate SRF (2018 and 2019 separate) | 13735.84 |
| NB GAM + replicate SRF (one field for 2018 and 2019) | 13682.68 |

This implies that there was very little information in the data that justified the use of extra parameters to separate the fields of 2018 and 2019, or more generally put, that there was no reason to conclude that the spatial pattern of the species in 2019 was different from the pattern in 2018.

The year effect, which is one of the categorical factors included in the statistical model, shows that 2018 was quite an exceptional year for the species, with the highest counts found during the decade. This may be related to the exceptional weather conditions during 2018. However, this difference between years is not interpreted as a possible effect of the MSC Zoe incident, as it is homogeneously present over the entire Wadden Sea and cannot be found back in an exceptional pattern in the spatial field.
The conclusion based on the comparison of the model with and without a common field for the two years 2018 and 2019, was further corroborated by analyzing the posterior probability distribution of the differences $\delta_i$ between the spatial fields of 2018 and 2019 for each of the sampling locations that were sampled in both years. This can be done because the Bayesian estimation procedure not only finds the expected value for the spatial field, but also calculates its probability distribution, called the ‘posterior’ distribution because it is obtained after fitting. With an additional targeted run of the program, the credibility interval (comparable to the confidence interval in more traditional statistics) for the difference of the spatial fields of 2018 and 2019 can be calculated and plotted. Of the more than 1000 comparisons, only 6 had a 95% credibility interval that did not include 0.

### 5.3.2 Analysis of Biomass

Biomass (g AFDW per sample) is a variable measured on a continuous scale. A Zero-altered Gamma (ZAG) model was used to model the data. A ZAG is composed of two parts: a Bernouilli part for presence/absence and Gamma part for numerical value when present. Both parts are brought together, with a common spatio-temporal random field, in the full ZAG model. Computationally, several steps are involved. The Bernouilli part of the model is fitted first, with its own spatiotemporal field. Subsequently, the Gamma part is fitting to the non-zero observations. Finally, a model with a common spatio-temporal random field is fitted to the data. The latter is a computationally very demanding task. It was omitted in this case, as both the Bernouilli and Gamma parts of the model showed the total absence of a possible MSC Zoe effect on the dataset, and moreover such an absence of effect was also concluded from the analysis of abundance.

The Bernouilli part of the model is formulated as:

$$
\begin{aligned}
Obs_{is} &\sim Bernouilli(\pi_{is}) \\
E[Obs_{is}] &= \pi_{is} \\
Var[Obs_{is}] &= \pi_{is} \times (1 - \pi_{is}) \\
logit(\pi_{is}) &= \gamma_1 + f(tauFlood_{is}) + f(tauWave_{is}) + f(Salinity_{is}) + \\
&\quad f(Grainsize_{is}) + Year_s + u_{is} \\
u_{is} &\sim N(0, \Omega)
\end{aligned}
$$

The Gamma part of the model is formulated as:

$$
\begin{aligned}
Obs_{is} &\sim ZAG(\mu_{is}, r) \\
E[Obs_{is}] &= \pi_{is} \\
Var[Obs_{is}] &= \frac{\mu_{is}^2}{r} \\
log(\mu_{is}) &= \beta_1 + f(tauFlood_{is}) + f(tauWave_{is}) + f(Salinity_{is}) + \\
&\quad f(Grainsize_{is}) + Year_s + v_{is} \\
v_{is} &\sim N(0, \Omega)
\end{aligned}
$$

In this equation, the subscript *i* refers to points in space, the subscript *s* to time. Bernouilli denotes the Bernouilli distribution with parameter π, ZAG is the Zero-adjusted Gamma distribution with parameters μ and r. The expected value at a particular time and place $\mu_{is}$ is linked through a logit link in the case of the Bernouilli part of the model, and through a log-link for the ZAG part. The linear predictive equation contains the factor year and smoothing functions for the environmental factors median bottom shear stress during flood, median wave bottom shear stress, salinity and grainsize. Finally, the linear term contains a spatio-temporal random field that is a replicate model in time.

For both parts, it was tested whether a model with separate spatial fields for 2018 and 2019 performed better (according to DIC criterion) than a model with a joint spatial field for these two years. The results are summarized in Table 5.2. In both cases, the results show that a model with a joint spatial field for the years 2018 and 2019 is performing better than a model with separate fields for the two years. This leads to the conclusion that no effect of the MSC Zoe can be detected in the data.

*Table 5.2. DIC values of two models comparing 2018 and 2019 spatiotemporal fields, both for the Bernouilli and for the Gamma part of the model. The full model contains a spatial random field for each year. The sub-model also contains a spatial random field for each year, except for the 2018 and 2019 data. These are modelled by 1 spatial random field. Note that comparison of DIC values is only meaningful within the parts (Bernouilli or Gamma) of the model.*

| Model | DIC |
|---|---|
| Bernouilli part | |
| Bernoulli GAM + replicate SRF (full model | 13736.54 |
| Bernoulli GAM + replicate SRF (sub model) | 13682.69 |
| Gamma part | |
| Gamma GAM + replicate SRF (full model) 13709.32 | 13736.54 |
| Gamma GAM + replicate SRF (sub model) | 13682.69 |

## 5.4 Discussion

The relationships with environmental variables found here correspond closely to the patterns found in earlier studies summarizing sampling in the S.W. Netherlands (Ysebaert et al., 2002; Cozzoli et al., 2013).

*Arenicola marina* is known from field studies to have a preference for a median grainsize of around 150 µm (compare the distribution in Oosterschelde and Westerschelde, reported by Cozzoli et al., 2013, in Figure 5.3) The species reacts positively to a moderate bottom shear stress (tauFlood) but negatively to excess current – as was also seen by Ysebaert et al. 2002 (in that study current velocity was used. Bottom shear stress is roughly proportional to velocity squared). The species distribution is restricted to salinity values above 15, as also reported by Ysebaert et al. 2002. It has little reaction to wave stress, as the multiplication factor is around 1 overall. In Ysebaert et al., 2002 and Cozzoli et al, 2013, wave stress was not considered as an environmental predictor.

The conclusions of the statistical model with respect to the influence of environmental factors is thus corroborated by other studies and appears to be quite robustly estimated in this analysis, even across systems.

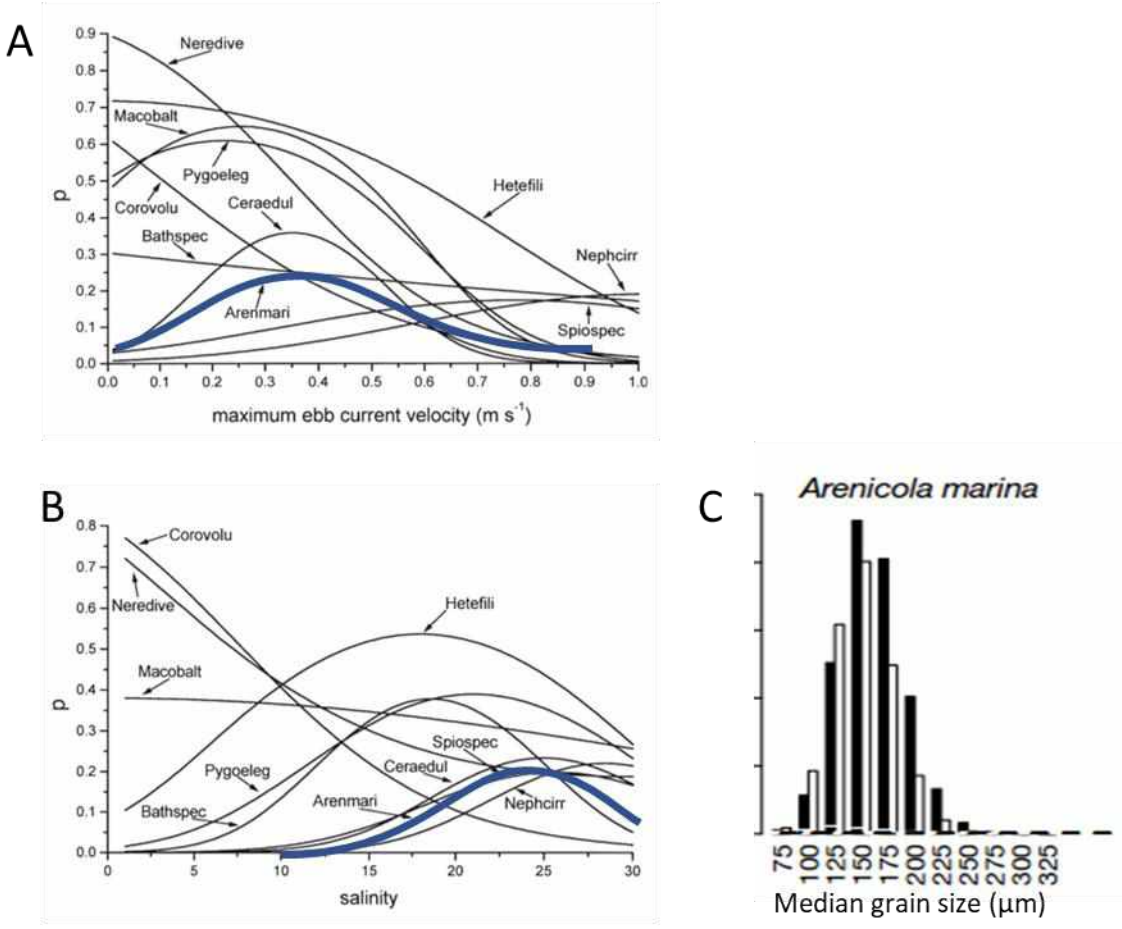


*Figure 5.3 Comparison material from the literature on response of A. marina to environmental variation. A: probability of occurrence in the Westerschelde as a function of current velocity. B. Probability of occurrence in the Westerschelde as a function of salinity. C. Expected 95$^{th}$ percentile of biomass (based on quantile regression) for the Westerschelde (white bars) and Oosterschelde (black bars) as a function of sediment median grain size. A and B based on Ysebaert et al., 2002. C based on Cozzoli et al, 2013.*

The sediment selected and subsequently ingested by *Arenicola marina* during feeding is dependent on its size. Smaller animals have smaller papillae on the proboscis than large adults, hence large animals can process coarser sediments. In general, particles larger than 500 µm are rejected and accumulate in the sediment at depths where the worms forage (Cadée, 1976; Gebhardt & Forster, 2018). Experimental studies showed, that microplastics in the size range ingested by *A. marina* may be harmful at elevated concentrations. In the MSC Zoe case the spilled microplastics had size ranges of 2-5 mm (HDPE-pellets (high-density polyethene)), and possibly polystyrene pellets (PS) in the size range 0.5 – 1 mm. Both kinds of spilled microplastics are of sizes that exceed the reported maximum ingested size-range of *A. marina*, and are therefore not supposed to directly influence metabolism, growth rate and survival of *A. marina*. However, in the mesocosm experiments by Foekema et al. (2021) some uptake of PS granules in this size range was reported when the particle concentration in the experiments was high, suggesting that either the size limit is not absolute, or that the particle size was variable and contained smaller particles in an ingestible range. No negative effect of this particle ingestion on the physiology of the species was reported from these experiments.

The densities of *A. marina* in the Wadden Sea in the summer of 2019, about half a year after the MSC-Zoe accident, appear to be very comparable to the densities in 2018. This underlines the probable absence of any direct effect of the spilled microplastics on the *A. marina* populations in the Wadden Sea.

*Arenicola marina* is a long living species. As the reproduction period of *A. marina* is in late summer and early autumn, i.e. after the summer 2019 SIBES sampling campaign, possible effects on reproduction cannot be seen in this analysis. The time series of abundance is too short, after the incident, to completely rule out the occurrence of long-term effects.

*Arenicola marina* is a species actively modifying its environment. The feeding activity of the species causes mixing of the upper 20 cm of the sediment. Microplastics that are not taken up by the worms as a result of their selective feeding behavior, may end up in deeper parts of the Wadden Sea sediments. The possible effects of this process of long-term burial of larger microplastic particles in deeper layers of estuarine sediments, are poorly known (Van Cauwenberghe *et al*., 2015). The present study does not document any such possible effects.

## 5.5 Conclusion

No evidence has been found for effects of the MSC Zoe incident on the population abundance or biomass of *Arenicola marina* in the Wadden Sea. The time series of abundances is too short to completely rule out possible effects on longer term, but the probability of such effects is considered small, particularly as *A. marina* is unable to ingest the HDPE particles and most PS granules are unlikely to be ingested due to their size.

# 6 The Cockle (*Cerastoderma edule*)

## 6.1 Biology and ecology

Description: the inequilateral, solid and thick shell is slightly longer than high and can be up to 50mm long (Tebble, 1966) (Figure 6.1). The outer shell surface is off-white, yellowish or brownish and has 22-28 conspicuous ribs with short, flat spines on top. Growth lines, due to reduced or negligible winter growth, are clearly distinguishable. The inner surface is white, with two adductor muscle scars (Tyler-Walters, 2007).

*Figure 6.1. Cerastoderma edule* (Common cockle). Photographer: Oscar Bos

Distribution and habitat: found from the western Barents Sea and northern Norway to the Iberian Peninsula, and south along the coast of west Africa to Senegal (Tyler-Walters, 2007). *C. edule* occur from the intertidal to the shallow subtidal areas in estuaries and coastal zones (Cardoso, 2007). They live totally burrowed (infaunal) in muddy to sandy sediments, up to a depth of 5cm (Tyler-Walters, 2007).

Feeding: cockles are filter-feeders (suspension-feeders), collecting their food by filtering and sorting particles from the water column (Gosling, 2003). The ciliated gills create a water current which flows into the inhalant siphon, between the gills. The inhalant and exhalant siphons extend several millimeters beyond the margin of the shell (Gosling, 2003

Predators: during all benthic stages, bivalves are vulnerable to benthic predators (Troost, 2009). In early stages they are preyed upon by small crabs and shrimps (Hiddink, 2002; Jensen & Jensen, 1985; van der Veer et al., 2006) and in later stages by crabs, starfish and birds (Leonard et al., 1999; Meire, 1993). Predation pressure decreases with cockle growth. European flounder (*Platichthys flesus*) predates on cockle seed and also shore crab (*Carcinus maenas*) prefers cockles < 15 mm in length (Sanchez-Salazar et al., 1987). Higher on shore oystercatchers (*Haematopus ostralegus*) are present in winter and prefer cockles of at least 20 mm in length (Sanchez-Salazar et al., 1987).

Reproduction and development: Sexual maturity in cockles is generally reached during their second summer, when they are about 18 months old and 15-20 mm in length. Reproduction can occur sooner in big cockles (Seed & Brown, 1977). *C. edule* is a broadcast-spawning bivalve with separate sexes. Males may release about 15 million sperm per second and females about 1900 eggs per second in the water through the exhalant syphon (Tyler-Walters, 2007). Fertilization occurs in the water column and depends on sperm concentration.

At high water flow rates, fertilization is only likely between close individuals. This might be compensated for by synchronous spawning of a large proportion of the dense populations (André et al., 1993). Fertilized eggs (50-60µm) will develop to form a veliger larva which lives in the water column and feeds on algae with its velum. After about 3-4 weeks the foot develops and the veliger metamorphoses into a juvenile cockle (pediveliger), which will settle in the sediment after 3-5 weeks (Creek, 1960). Settlement and recruitment success have a significant impact on the dynamics of cockle populations. Adult suspension feeders may reduce settlement of larvae by ingestion of settling larvae (André & Rosenberg, 1991). Post-settlement mortalities of 60-96% have been reported, resulting from intra- and interspecific mortality and predation (De Montaudouin & Bachelet, 1997; Guillou & Tartu, 1994; Sanchez-Salazar et al., 1987). In the Dutch Wadden Sea, a big spat fall events occurs roughly every seven years, after which the population ages and declines (van Asch, 2019). Natural mortality is high, annually about 59% of cockles dies, where 28% dies during summer (Kamermans et al., 2004). However, in summer 2018 until 2020, extremely high mortalities were observed during summer, probably due to heat waves (Suykerbuyk et al., In prep.; Troost & Van Asch, 2018). *C. edule* usually lives 2-4 years but may live up to 9 years (Tyler-Walters, 2007).

Abiotic tolerances: *C. edule* is sensitive to low winter temperatures (Beukema, 1990; Hancock & Urquhart, 1964; Kristensen, 1958). The lower thermal tolerance limit was determined between -2.4 ºC after 24 hours (Kristensen, 1958) and -6.2 ºC (Compton et al., 2007). Upper tolerance limits are described by assessing median lethal temperatures. Ansell et al. (1981) reported such temperatures to be 37 ºC for short exposure (6h). Compton et al. (2007) observed median lethal temperatures between 32 and 34 ºC and Verdelhos et al. (2015) found such temperatures to be about 32 ºC for 52h of exposure. *C. edule* usually lives at salinities between 10-35 psu (Brock, 1980; Kater et al., 2006; Tyler-Walters, 2007). Larvae prefer salinities between 30 and 35 psu but can survive at salinities of 5 psu (Kingston, 1974). Current velocity effects larval settlement and growth of adult bivalves (Kater et al., 2006). Cockles get easily dislodged by storms, inhabiting the surface of sediments to a depth of 5 cm (Smaal et al., 2013).

### Historical trends Wadden Sea

Cockles are harvested on the mud flats in the tidal regions using a hand-rake to which a net is attached. The cockle stock varies greatly from year to year, both in the western and eastern part of the Wadden Sea (Troost et al., 2012). There is no significant upward or downward trend. The big fluctuations in cockle density are mainly caused by incidental big spat fall events, which occur roughly every seven years (van Asch, 2019), as was the case in 1997, 2003 and 2011. The spat fall of 1997 did not extend to Balgzand, which illustrates that recruitment can vary not only in time, but also in space (Troost et al., 2012). After harsh winters or warm summers, the stock declines due to extreme temperatures often in combination with parasitic infections (Thieltges et al., 2013). This was the case in 2018 and 2019, when extreme cockle mortalities were observed during heat waves (Suykerbuyk et al., In prep.; Troost & Van Asch, 2018). In the Wadden Sea, mortality was estimated to be around 60% in 2018 and around 70% in 2019 (Troost & Van Asch, 2018). During summer 2020, there were no indications of extreme mortality in the Wadden Sea (Troost et al., 2021). This will be assessed during the annual shellfish survey in 2021.

## 6.2 Data collection and analysis

Data were collected within the SIBES sampling program (Chapter 3.1). The analysis is documented in the R Markdown file **03SIBESData2.Rmd.** From this markdown file the report of Highland Statistics (chapter 3, *Cerastoderma edule*) was automatically generated.
The data set comprises 6882 samples in the years 2009 to 2019. The species was found in appr. 29 % of the samples. The counts per sample ranged from 0 to 200, but high counts were rare (25 counts were over 50).

The covariates provided as environmental factors had a high degree of collinearity. Therefore, a limited set of variables was selected that represent the condition of the sediment (median grain size), the current (maximum bottom shear stress during flood), effects of waves (median bottom shear stress due to waves), and salinity.

### 6.2.1 Analysis of Numerical Abundance

A series of statistical models with increasing complexity was fitted to the data, including Poisson, zero-inflated Poisson, negative binomial and zero-inflated negative binomial. The final model fitted to the data is a zero-inflated negative binomial GAM with spatial and temporal correlation fields.
The model is specified as follows:

$$
\begin{aligned}
Counts_{is} &\sim ZINB(\mu_{is}, \theta, \pi) \\
E[Counts_{is}] &= (1-\pi) \times \mu_{is} \\
var[Counts_{is}] &= (1-\pi) \times \mu_{is} \times (1 + \pi \times \mu_{is} + \frac{\mu_{is}}{\theta}) \\
\log(\mu_{is}) &= \beta_1 + fYear_s + fMonth_s + fTotSurf_{is} + \\
&\quad f(tauFlood_i) + f(tauWave_i) + f(Salinity_i) + \\
&\quad f(GrainSize_i) + v_{is} \\
v_{is} &= \rho \times v_{i,s-1} + u_{i,s} \\
\rho &= 0 \\
u_{i,s} &\sim N(0, \Omega)
\end{aligned}
$$

In this equation, the subscript *i* refers to points in space, the subscript *s* to time. ZINB denotes the zero-inflated negative binomial distribution with three parameters, the mean μ and the dispersion parameter θ of the negative binomial part, and the parameter π that is used to model the zeroes that cannot be explained with the covariates in the count part of the model. The operator E[] expresses the expected value. $\mu_{is}$, the expected value conditional on not being an excess zero value, is linked through a log-link function to a predictive equation that contains a number of factors (year, month, surface sampled) that vary in time and/or in space. Further the linear term contains smoothing functions for the environmental factors median bottom shear stress during flood, median wave bottom shear stress, salinity and grainsize, which all vary in space. Finally, the linear term contains a spatio-temporal random field that represents the correlation in space and time of the variable. The spatio-temporal field is expressed (in principle) as an autoregressive process in time and a spatially correlated process in space. In this special case, in order to be able to investigate a possible Zoe effect, the autoregressive parameter $\rho$ is set to zero, so that a replicate model in time is used that can reveal sudden changes.
The categorical factors year, month and sampled surface allow for spatially averaged effects of the year and month of sampling, as well as for a methodological compensation for the unequal size of the samples.
The smoothers of the environmental factors describe clear effects for three out of the four variables, as shown in Figure 6.2. The effect of waves is not very clear.

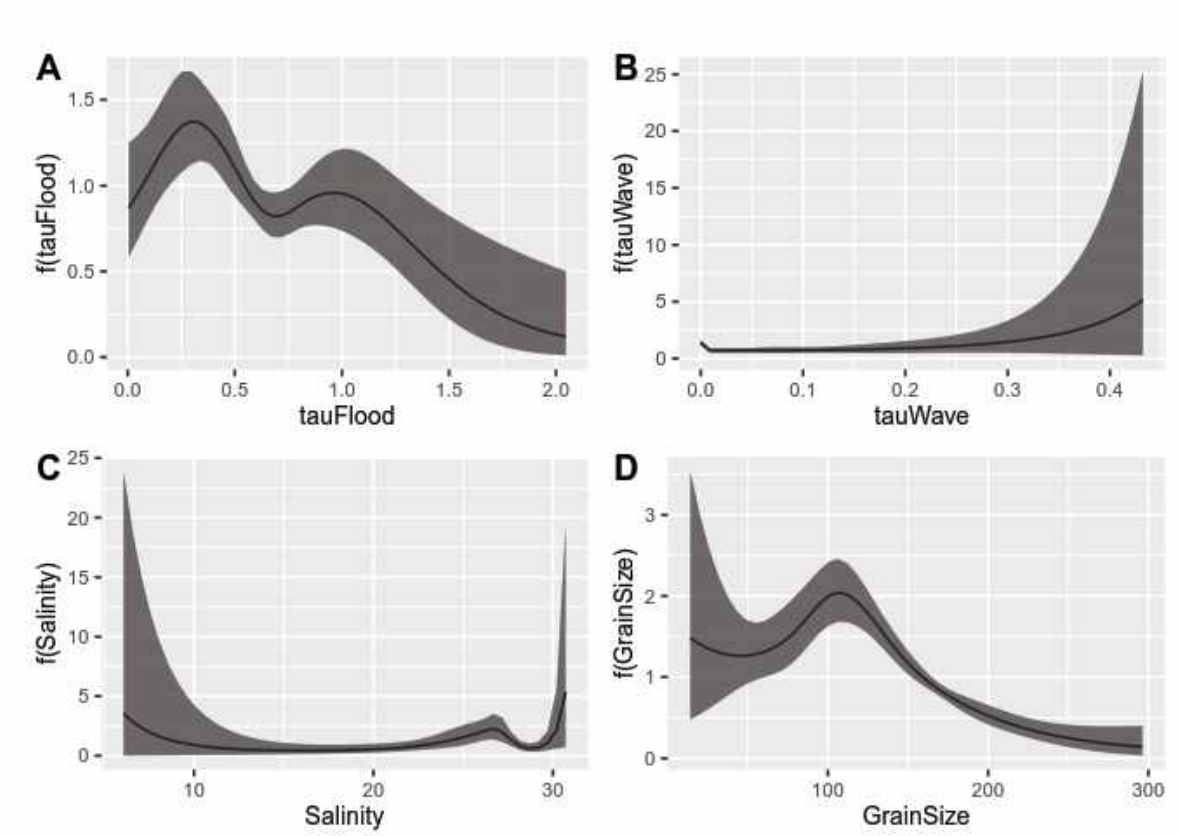


*Figure 6.2. Posterior mean values and 95 % credible intervals for the smoothers obtained by the ZINB GAM with spatial correlation applied on the* C. edule *count data. Each smoother is an unpenalized cubic regression spline with 5 df.*

The spatial fields of all years for this species are shown in Figure 6.3. Over the years, we see some variability in the hotspots and coldspots for the species, but the pattern remains relatively stable. Good recruitment years (in this series especially 2011 and 2018) see hotspots developing in the area between the Vlie, Marsdiep and Eijerlandse Gat basins. These disappear gradually in subsequent years. Balgzand is a consistent hotspot throughout the years, as are some areas along the Groningen coast and south-east of Ameland.

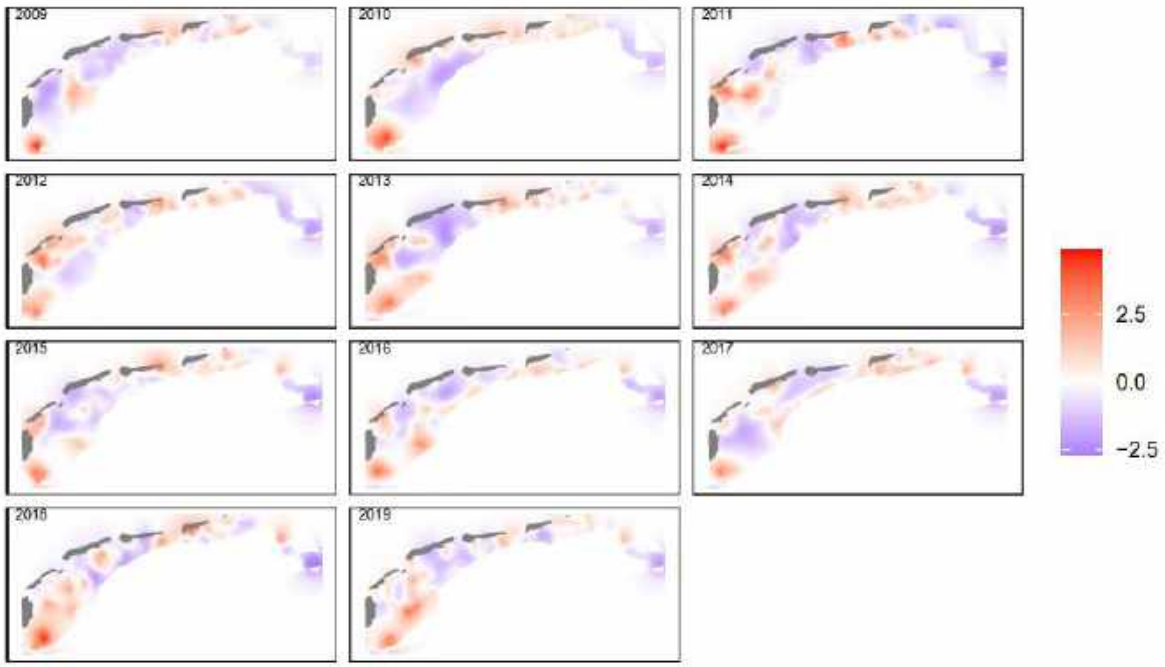


*Figure 6.3. Spatial random fields for each year obtained by the ZINB GAM with the spatial-temporal replicate correlation applied to the* C. edule *count data.*

The effect of the MSC Zoe incident was estimated by comparing two statistical models that differ in the specification of the random fields. In the first model, every year has a separate spatial correlation field. In the second model, only a single spatial field was used for both the years 2018 and 2019. Based on DIC, the latter model was clearly to be preferred. (Table 6.1).

*Table 6.1. DIC values of two ZINB GAMs with spatial-temporal replicate correlation. The full model in the first row contains a spatial random field for each year. The sub-model in the second row also contains a spatial random field for each year, except for the 2018 and 2019 data. These are modelled by 1 spatial random field.*

| Model | DIC |
|---|---|
| ZINB GAM + replicate SRF (2018 and 2019 separate) | 17732.41 |
| ZINB GAM + replicate SRF (one field for 2018 and 2019) | 17689.50 |

This implies that there was very little information in the data that justified the use of extra parameters to separate the fields of 2018 and 2019, or more generally put that there was no reason to conclude that the spatial pattern of the species in 2019 was different from the pattern in 2018.

The conclusion based on the comparison of the model with and without a common field for the two years 2018 and 2019, was further corroborated by analyzing the posterior probability distribution of the differences $\delta_i$ between the spatial fields of 2018 and 2019 for each of the sampling locations that were sampled in both years. Differences are deemed ‘important’ if 0 is not included in the 95 % credible interval for the difference.

There were 34 stations with an important difference between the spatial random fields of 2019 and 2018. The total number of stations compared is 1047, of which 3.25 % fall outside the 95 % credible intervals, which have not been corrected for multiple testing. It is very likely that such a pattern arises due to chance, so it should not be the basis for far-reaching conclusions.

The stations with large differences between the spatial fields are highlighted in Figure 6.4. They are spatially clustered in four groups, three of which saw a decrease between 2018 and 2019. These are most likely places that saw peaks in counts during the high-spatfall year 2018, but rapid subsequent decrease of the numbers because the locations are too exposed to maintain high numbers of cockles in the sediment.

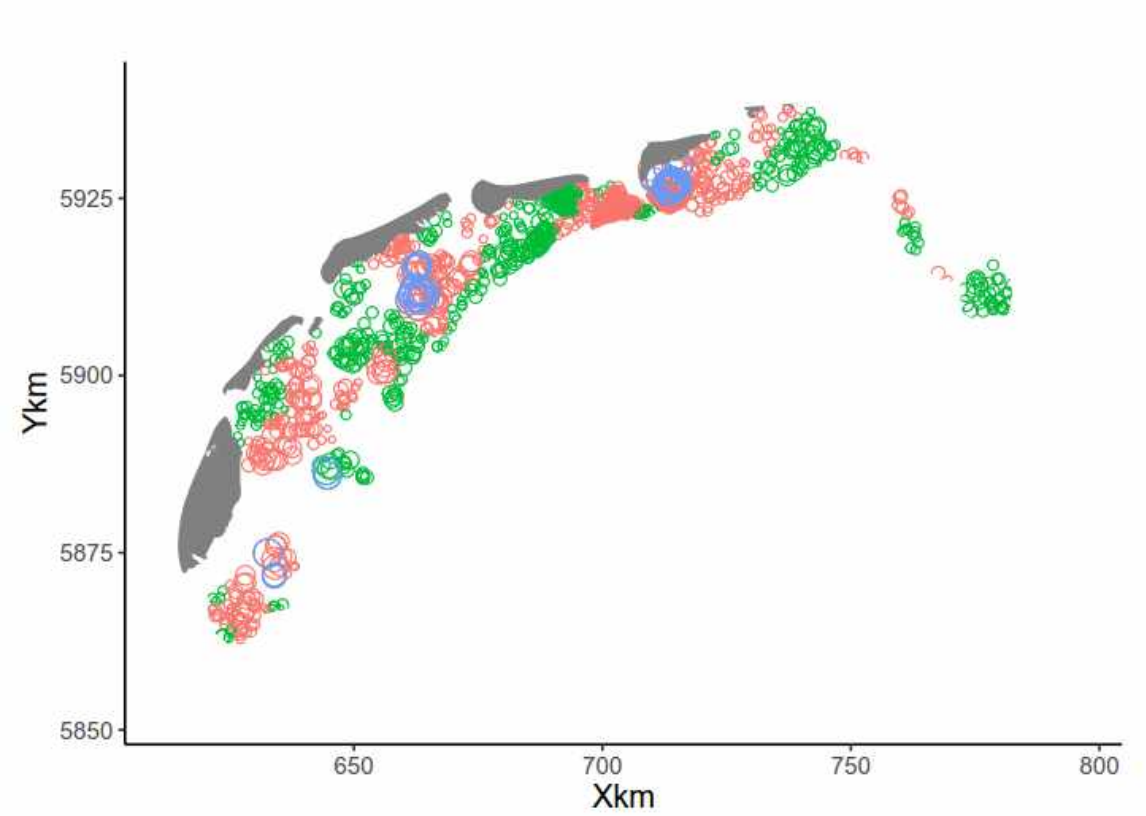


*Figure 6.4. Posterior mean values of $\delta_i = w_{i,2019} - w_{i,2018}$ for all stations $i$ that were sampled in 2019 and 2018. Green and red circles represent positive and negative values of the posterior mean of $\delta_i$, respectively. The size of a circle is proportional to the posterior mean value of $\delta_i$. The circles in purple are $\delta_i$s for which the 95% credible interval does not contain 0 (no correction for multiple testing has been applied).*

### 6.2.2 Analysis of Biomass

Biomass data of *C. edule* were modelled with a ZAG distribution (chapter 4.4). This model is composed of a Bernouilli part and Gamma part, that share common spatio-temporal fields, up to a constant. The model is specified as:

$$
\begin{aligned}
Obs_{is} &\sim ZAG(\mu_{is}, \pi_{is}, r) \\
E[Obs_{is}] &= \pi_{is} \times \mu_{is} \\
Var[Obs_{is}] &= \frac{\pi_{is} \times r + \pi_{is} - {\pi_{is}}^2 \times r}{r} + \mu_{is}^2 \\
logit(\pi_{is}) &= \gamma_1 + f(tauFlood_{is}) + f(tauWave_{is}) + f(Salinity_{is}) + \\
&\quad f(Grainsize_{is}) + Year_s + b \times u_i \\
log(\mu_{is}) &= \beta_1 + f(tauFlood_{is}) + f(tauWave_{is}) + f(Salinity_{is}) + \\
&\quad f(Grainsize_{is}) + Year_s + u_{is} \\
u_{is} &\sim N(0, \Omega)
\end{aligned}
$$

Where ZAG stands for Zero-adjusted Gamma model with three parameters. Subscript i denotes space and subscript s denotes time. The expected value at a particular time and place is linked through a logit link in the case of the Bernouilli part of the model, and through a log-link for the Gamma part.

The linear predictive equation contains the factor year and smoothing functions for the environmental factors median bottom shear stress during flood, median wave bottom shear stress, salinity and grainsize. Finally, the linear term contains a spatio-temporal random field that is a replicate model in time and that is shared (up to a constant) between the two parts of the model.

The smoothers for the environmental variables are derived separately for the Bernouilli and Gamma parts of the model. The strongest effect, both on presence/absence and on numerical value when present, is shown by TauFlood, the maximum bottom shear stress caused by the tidal current during flood. Especially for the numerical values, the form of the response is an optimum curve at intermediate to relatively high values of bottom shear stress. Presence/absence is also influenced by grain size, with an optimum in slightly muddy fine sand (median grain size around 100 µm). Once established, grain size has no notable influence on biomass values. The contrary is true for salinity, that does not seem to influence presence/absence, but has a positive influence on the numerical values where the species is present.

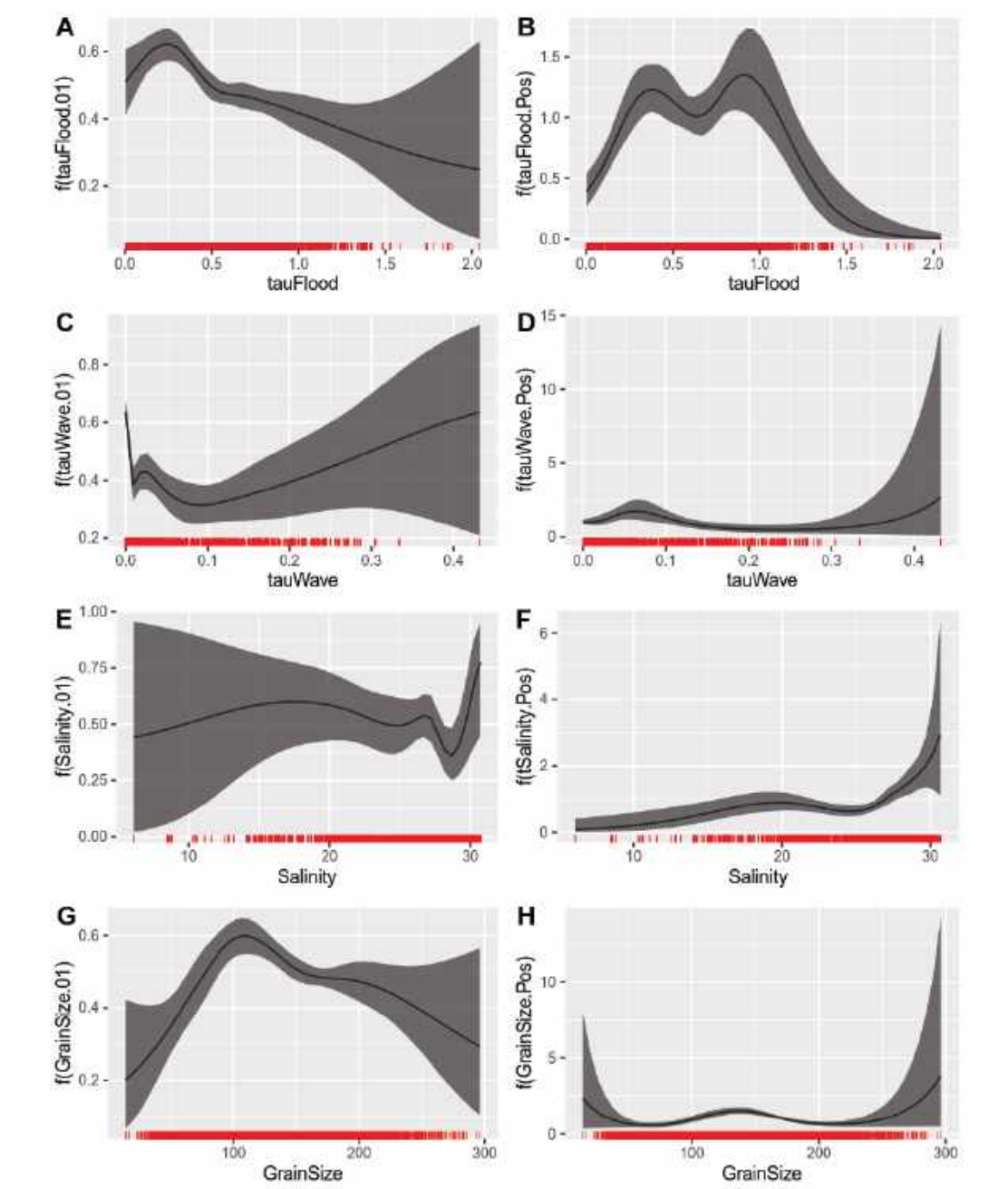


*Figure 6.5. Posterior mean values and 95% credible intervals for all smoothers obtained by the ZAG model with a shared spatial-temporal replicate correlation. The figures on the left are for the binary part and the figures on the right are for the Gamma part of the ZAG model applied to the* C. edule *biomass data.*

The year effects (results not shown) show that the probability of presence was very high in the year 2018, which was a year with a strong spatfall. However, the average biomass when present was especially low in 2018. A very similar pattern was observed in 2011, also a very good spatfall year. In 2019 the fraction present declined again, but the numerical values increased in places where the species was present.

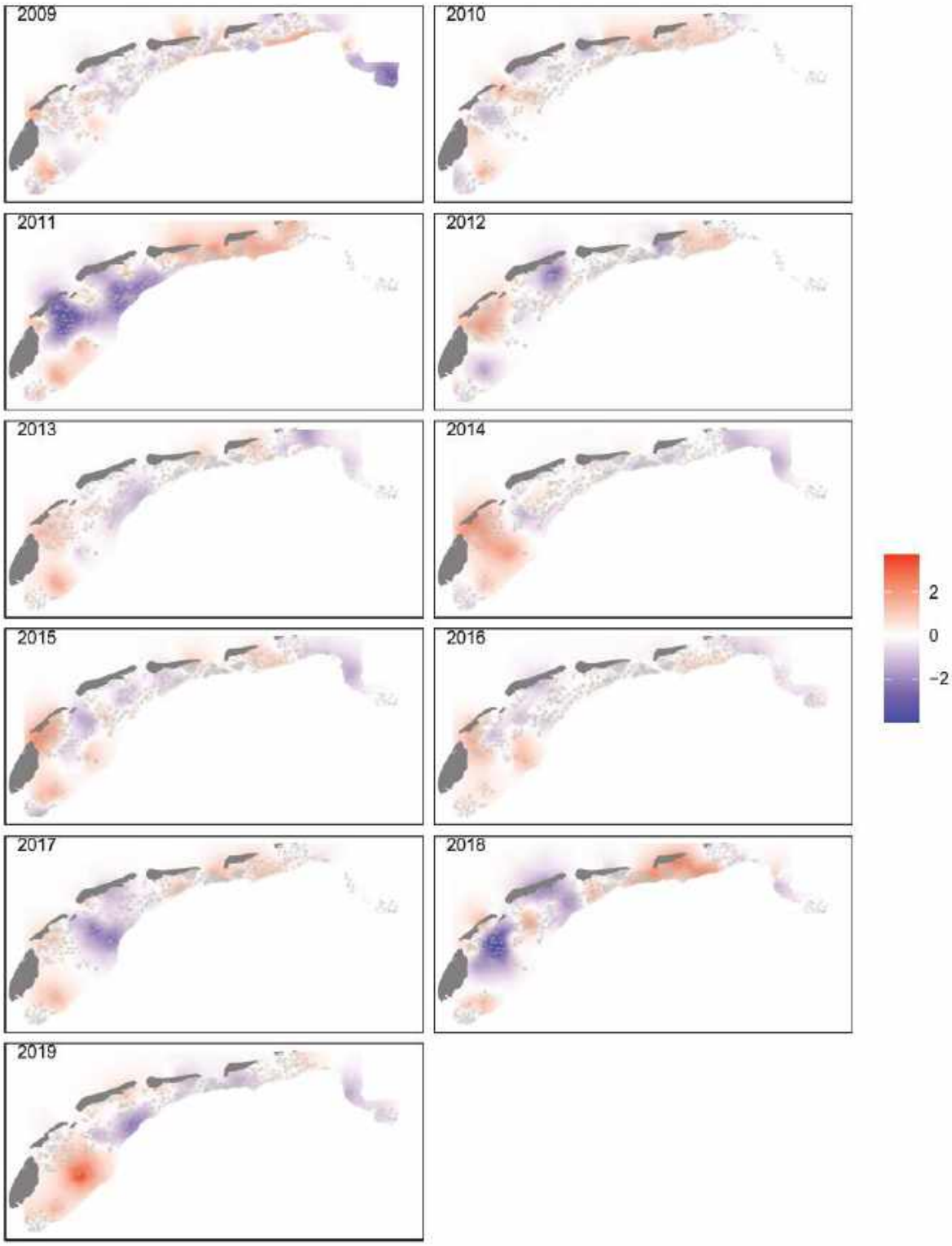


*Figure 6.6. Posterior mean values of the shared spatial-temporal random fields obtained by the ZAG model applied on the* C. edule *biomass data.*

Also, in the spatio-temporal random fields (Figure 6.6), a similarity can be seen between the years 2018 and 2011, both years with a high spatfall. Compared with other years the north-eastern part of the Wadden Sea is a relative hotspot, whereas the western central part of the Wadden Sea is a coldspot. In both cases, the pattern disappears in the subsequent year: the hotspot in the north-east disappears, and the values in the central-western part increase.

Presumably, survival and/or growth differences between the different subregions of the Wadden Sea are responsible for these patterns.
A comparison between a model with a separate spatial-temporal random field for every year, and a model with a common field for the years 2018 and 2019, shows that the latter model is better (Table 6.2). This contrasts with the result of the analysis of numerical abundance. It highlights the differences between the spatial fields of 2018 and 2019.

*Table 6.2. DIC values of two ZAG GAMs with spatial-temporal replicate correlation. The full model in the first row contains a spatial random field for each year. The sub-model in the second row also contains a spatial random field for each year, except for the 2018 and 2019 data. These are modelled by 1 spatial random field.*

| Model | DIC |
|---|---|
| ZAG GAM + replicate SRF (2018 and 2019 separate) | 4386 |
| ZAG GAM + replicate SRF (one field for 2018 and 2019) | 4479 |

When examining the posterior mean values of the difference in the spatial random field between 2018 and 2019, there are 125 stations where the difference $\delta_i = u_{i,2019} - u_{i,2018}$ is important (i.e. 0 is not included in the 95 % credible interval). This represents 21.82% of the stations. From these 125 changes, 50 changes are an increase, and 75 (13.1 % of all stations) are a decrease from 2018 to 2019.

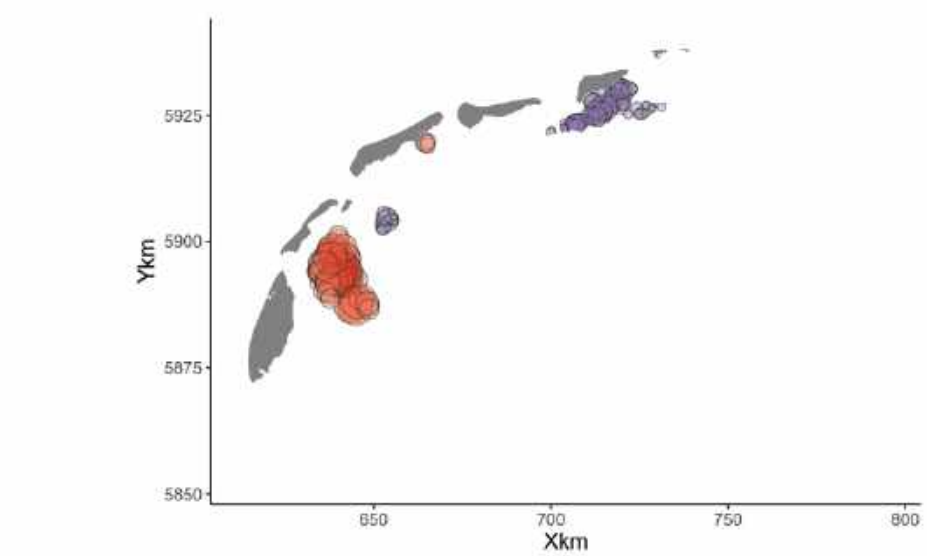


*Figure 6.7. Posterior mean values of $\delta i = u_{i,2019} - u_{i,2018}$ for stations $i$ that were sampled in 2019 and 2018, and for which the 95% credible interval does not contain 0 (no correction for multiple testing has been applied). Red symbols are increases from 2018 towards 2019, purple symbols are decreases.*

The areas of important increase and decrease are spatially clustered. Decreases are mainly observed in the north-eastern part of the Wadden Sea, whereas increases are observed in the central-western part. This corresponds to the pattern that was noted earlier, and that was also found back in 2011.

## 6.3 Discussion

The positive response to salinity, intermediate response to currents, and broad preference for relatively fine sediment, correspond to published responses of the species in Westerschelde and Oosterschelde. The response to bottom shear stress from currents in Figure 6.2 and Figure 6.5 suggests a bimodal form. There is no immediate explanation for this pattern.

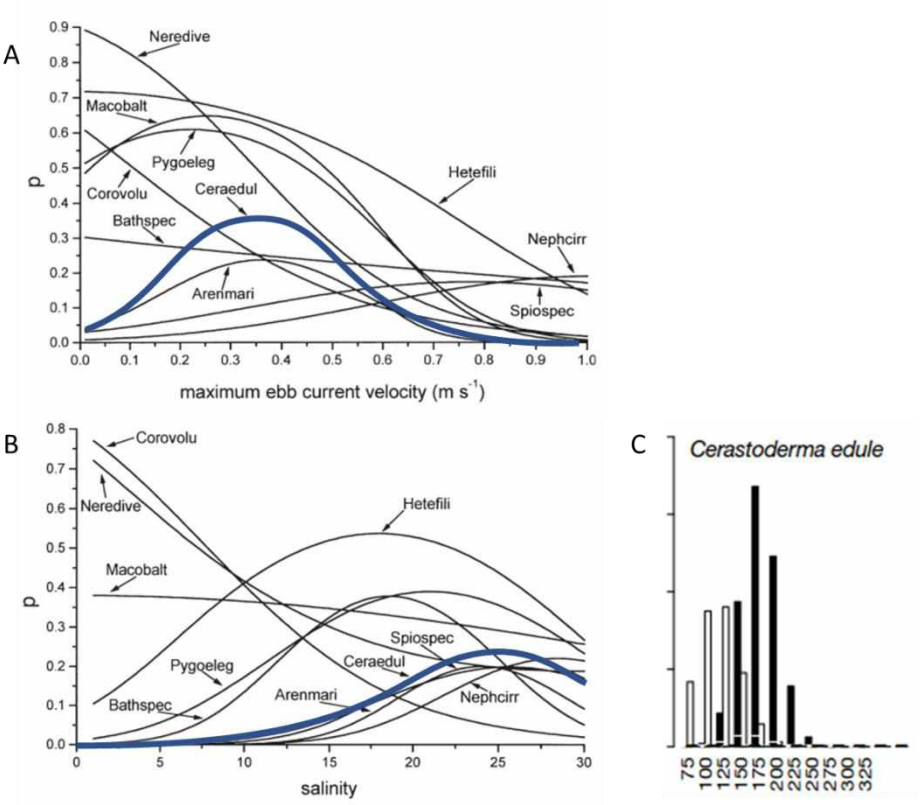


*Figure 6.8. Comparison material from the literature on response of* C. edule *to environmental variation. A: probability of occurrence in the Westerschelde as a function of current velocity. B. Probability of occurrence in the Westerschelde as a function of salinity. C. Expected 95$^{th}$ percentile of biomass (based on quantile regression) for the Westerschelde (white bars) and Oosterschelde (black bars) as a function of sediment median grain size. A and B based on Ysebaert et al., 2002. C based on Cozzoli et al, 2013.*

The spatial and temporal development of the cockle population is strongly influenced by the large recruitment events, that occur roughly every seven years but are not strictly periodic (van Asch, 2019). Successful recruitment depends negatively on adult population strength. It can be triggered after harsh winters or warm summers, when the stock declines due to extreme temperatures often in combination with parasitic infections (Thieltges et al., 2013). In the years of study, a strong recruitment event occurred in 2018, and moreover the hot summers of 2018 and 2019 caused very high cockle mortality during heat waves (Troost and Van Asch, 2018). These events can be found back in the density and biomass data analyzed here. The strong recruitment of 2018 has led to a spatiotemporal field that was very similar to the field in 2011, when recruitment was also high. Hotspots and coldspots in high-recruitment years are in different locations, compared to other years.

Whereas no large difference between the spatial random fields of 2018 and 2019 were found in numerical abundance, such difference was present for biomass. A relatively large number of sampling points showed an important difference between the two years (Figure 6.7). We recognize here the pattern described in the spatial random fields for high-recruitment years. Hotspots are found in the eastern Wadden Sea, and coldspots in the central-western part during the year of peak recruitment. However, in subsequent years the eastern hotspot and the central-western coldspot disappear, presumably due to differential survival or growth in these areas. Because of the recurrence of this pattern, especially in the comparison 2011-2012 that is similar to the comparison 2018-2019, it is difficult to ascribe the observed differences to an effect of the MSC Zoe incident. Of the changes illustrated in Figure 6.7, only the change in the east is a decrease. In contrast, the change in the central-western part is an increase.

As we are only looking for decreases as possible MSC Zoe effects, only one out of two changes could in principle qualify. Linking both phenomena to strong recruitment and differential growth and survival afterwards, as has been observed earlier in the time series, is a more straightforward explanation for the observation that does encompass both the decrease in the east and the increase in the center.

## 6.4 Conclusion

The dataset on the cockle *Cerastoderma edule* in the Wadden Sea shows that for abundance, no great year-to-year changes have been observed and the spatial pattern in 2018 was very similar to the pattern in 2019. In contrast to the abundance data, the biomass showed stronger changes, also in the comparison of 2018 and 2019. Some decreases were observed in the eastern Wadden Sea, but strong changes in the central-western part were increases. Both phenomena have already been observed earlier in 2011-2012, after the successful recruitment in 2011. We conclude that the shifts in patterns between 2018 and 2019 in biomass of the cockle are linked to the high recruitment in 2018, and that a causal link with the MSC Zoe incident is very unlikely.

# 7 The Baltic Tellin (*Limecola balthica*)

## 7.1 Biology and ecology

### Appearance of the shell

Description: The shell of the *L. balthica* (previously referred to as *Macoma balthica)* the shell is almost circular and can be up to 25mm long (Figure 7.1). The posterior of the shell may be slightly tapered roughly in the middle. Color varies from yellow-white to pink and can be uniform or in concentric bands. Outer surface may be blackened in sulfide-rich sediments. It has a strong external hinge (Bruyne et al., 2013; Budd & Rayment, 2001).

*Figure 7.1. Limecola balthica* (Baltic tellin). Photographer: Oscar Bos.

Distribution and habitat: *L. balthica* occurs from temperate to arctic coastal waters in both the North Atlantic and North Pacific oceans. It lives buried in the sediment, at a depth of a few centimeters. The Baltic tellin occurs particularly on tidal flats and in estuaries and occupies a variety of sediment types, from soft mud to muddy gravel (Bruyne et al., 2013; Budd & Rayment, 2001). It can be found from the upper regions of the intertidal zone into the sublittoral, up to 35m. Juveniles are mainly found on the high intertidal flats, while adults are also found in the subtidal area of the Wadden Sea and North Sea (Beukema, 1993).

Feeding: all *Macoma* species (formerly the genus name of *Limecola balthica*) were by Yonge (1949) classified as deposit feeders. However, a variability in feeding behavior within this group has been observed since then and *L. balthica* is now considered a facultative deposit/suspension feeder (Brafield & Newell, 1961; Bubnova, 1972; Hummel, 1985b; Olafsson, 1986; Skilleter & Peterson, 1994). Deposit-feeding behavior can be recognized by the extended inhalant siphon sucking in material on the sediment surface and the burrow entrance (Yonge, 1949). When filter-feeding, *L. balthica* collects its food by filtering and sorting particles from the water column (Gosling, 2003). The ciliated gills create a water current which flows into the inhalant siphon, between the gills.

Predators: like for the cockle, predators of the Baltic tellin include crabs, flat fish and birds (Costil et al., 2006). Juvenile Baltic tellins are under high predation pressure in the low intertidal by shrimps, crabs and small fish and spend their first juvenile stage in the higher intertidal where they outgrow these predators (see next paragraph) (Beukema, 1993; Hiddink & Wolff, 2002). *L. balthica* is an important food source for oystercatchers and red knot, but they only take individuals bigger than 11 mm (Hulscher, 1982; Piersma et al., 1994; Zwarts et al., 1996). The common shrimp preys on *L. balthica* smaller than 5 mm but prefers individuals of 1-2 mm (Keus, 1986).

Reproduction and development: *L. balthica* is a broadcast-spawning bivalve with separate sexes (Costil et al., 2006). There are two spawning periods: the first (primarily) in spring and the second (to a lesser extent) in autumn (Budd & Rayment, 2001). Females produce 0.02-0.07 million eggs per spawning (Honkoop & Van der Meer, 1998). Fertilization occurs in the water column. Fertilized eggs will develop to form a veliger larva which lives in the water column and feeds on algae with its ciliated velum. Veligers continue to develop into the pediveliger stage, in which the larvae develop a foot and the velum degenerates (Gosling, 2003). After about 3-4 weeks the veliger metamorphoses and is ready to settle (Drent, 2004). Juveniles settle in spring in the low intertidal and migrate to the high intertidal in June, where they stay until winter. In winter, they migrate back again to the low intertidal and the North Sea (Armonies & Hellwig-Armonies, 1992). They migrate by byssus drifting, which decreases the sinking rate (Sörlin, 1988). This migration may be seen as an adaptation to avoid epibenthic predation in the low intertidal zone (Hiddink & Wolff, 2002). The results from a laboratory experiment indicate that timing of metamorphoses is depending on food availability; larvae offered high food levels grew significantly faster (6.9 µm/day), and metamorphosed earlier (16.5 days) and at greater length (264 µm) than larvae subjected to low food level (4.4 µm/d, 19.3 days and 244 µm, respectively) (Bos et al., 2006). Settlement and recruitment success have a significant impact on the dynamics of populations. Larval mortality is very high mainly due to predation or unsuccessful settlement of spat. The life expectancy of the Baltic tellin is 6 to 7 years (Costil et al., 2006).

Abiotic tolerances: *L. balthica* tolerates wide variations in temperature and salinity (Costil et al., 2006). Baltic tellin can tolerate temperatures up to 49˚C (Oertzen (1969) in Budd & Rayment (2001)). Ratcliffe et al. (1981) showed that juveniles could survive at temperatures up to 39°C (6 hours), while 30% of the adults died at the same temperature. *L. balthica* is found in brackish and in fully saline waters, but is more common in brackish waters (Clay (1967) in Budd & Rayment (2001)).

### Historical trends Wadden Sea

The Baltic tellin stock shows great variability in time. The stock in the Western Wadden Sea increased until the end of the 1980s and then decreased again. The biomass decreased to significantly lower numbers than at the beginning of the series in the 1970s. In the Eastern Wadden Sea, the stock has also been declining since the mid-1980s but increased again around 2000. After this short increase, the stock declined again and reached the lowest biomass in 2011. This development is in accordance with spat fall, which has been very low since 2000. After this, the stock size has been more or less constant, with some higher numbers from 2012 to 2017 (Schelpdiermonitor, 2021). Analysis based on growth rings also shows that the adult survival has decreased. This in combination with low spat fall, leads to small stocks (Troost et al., 2012). No good explanations exist for the long-term variations in the population strength.

## 7.2 Data collection and analysis

Data were collected within the SIBES sampling program (Chapter 3.1). The analysis is documented in the R Markdown file **04SIBESData3.Rmd.** From this markdown file the report of Highland Statistics (chapter 4, *Limecola balthica*) was automatically generated.

The data set comprises 6882 samples in the years 2009 to 2019. The species was found in appr. 47 % of the samples. The counts per sample ranged from 0 to 800, but high counts were rare and most counts were well below 100.
The covariates provided as environmental factors had a high degree of collinearity. Therefore, a limited set of variables was selected that represent the condition of the sediment (median grain size), the current (maximum bottom shear stress during flood), effects of waves (median bottom shear stress due to waves), and salinity.

### 7.2.1 Analysis of Numerical Abundance

A series of statistical models with increasing complexity was fitted to the data, including Poisson, zero-inflated Poisson, negative binomial and zero-inflated negative binomial.
The final model fitted to the data is a zero-inflated negative binomial GAM with spatial and temporal correlation fields.
The model is specified as follows:

$$
\begin{aligned}
Counts_{is} &\sim ZINB(\mu_{is}, \theta, \pi) \\
E[Counts_{is}] &= (1-\pi) \times \mu_{is} \\
var[Counts_{is}] &= (1-\pi) \times \mu_{is} \times (1 + \pi \times \mu_{is} + \frac{\mu_{is}}{\theta}) \\
\log(\mu_{is}) &= \beta_1 + fYear_s + fMonth_s + fTotSurf_{is} + \\
&\quad f(tauFlood_i) + f(tauWave_i) + f(Salinity_i) + \\
&\quad f(GrainSize_i) + v_{is} \\
v_{is} &= \rho \times v_{i,s-1} + u_{i,s} \\
\rho &= 0 \\
u_{i,s} &\sim N(0, \Omega)
\end{aligned}
$$

In this equation, the subscript *i* refers to points in space, the subscript *s* to time. ZINB denotes the zero-inflated negative binomial distribution with three parameters, the mean μ and the dispersion parameter θ of the negative binomial part, and the parameter π that is used to model the zeroes that cannot be explained with the covariates in the count part of the model. The operator E[] expresses the expected value. $\mu_{is}$, the expected value conditional on not being an excess zero value, is linked through a log-link function to a predictive equation that contains a number of factors (year, month, surface sampled) that vary in time and/or in space. Further the linear term contains smoothing functions for the environmental factors median bottom shear stress during flood, median wave bottom shear stress, salinity and grainsize, which all vary in space. Finally, the linear term contains a spatio-temporal random field that represents the correlation in space and time of the variable. The spatio-temporal field is expressed (in principle) as an autoregressive process in time and a spatially correlated process in space. In this special case, in order to be able to investigate a possible Zoe effect, the autoregressive parameter $\rho$ is set to zero, so that a replicate model in time is used that can reveal sudden changes.
The categorical factors year, month and sampled surface allow for spatially averaged effects of the year and month of sampling, as well as for a methodological compensation for the unequal size of the samples.
The smoothers of the environmental factors (Figure 7.2) describe clear effects of bottom shear stress by tidal currents (tauFlood) and of grain size. The effect of salinity and of waves is not important.

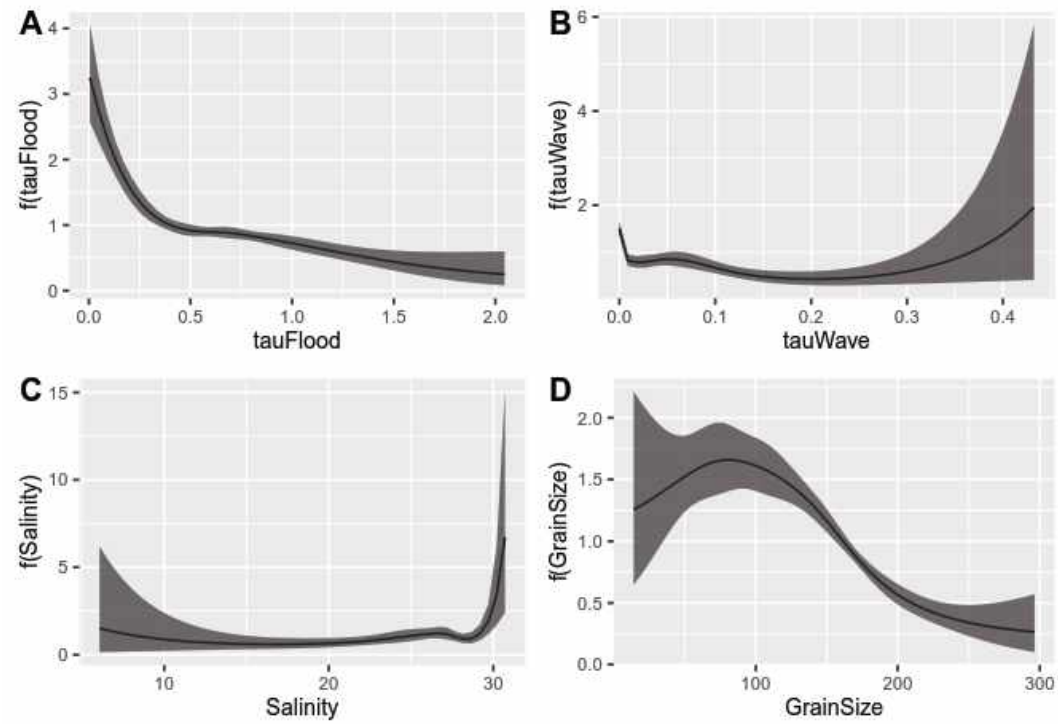


*Figure 7.2. Posterior mean values and 95 % credible intervals for the smoothers obtained by the ZINB GAM with spatial correlation applied on the* L. balthica *count data. Each smoother is an unpenalized cubic regression spline with 5 df.*

The spatial fields of all years for this species are shown in Figure 7.3. Over the years, we see variability in the hotspots and coldspots for the species. Although patterns are sometimes carried over from one year to the next, no recurrent pattern is present. The spatial variability of hotspots and coldspots is dominating the visual image. Good recruitment years (2018 and 2014 stand out from the other years) do not have similar spatial fields.

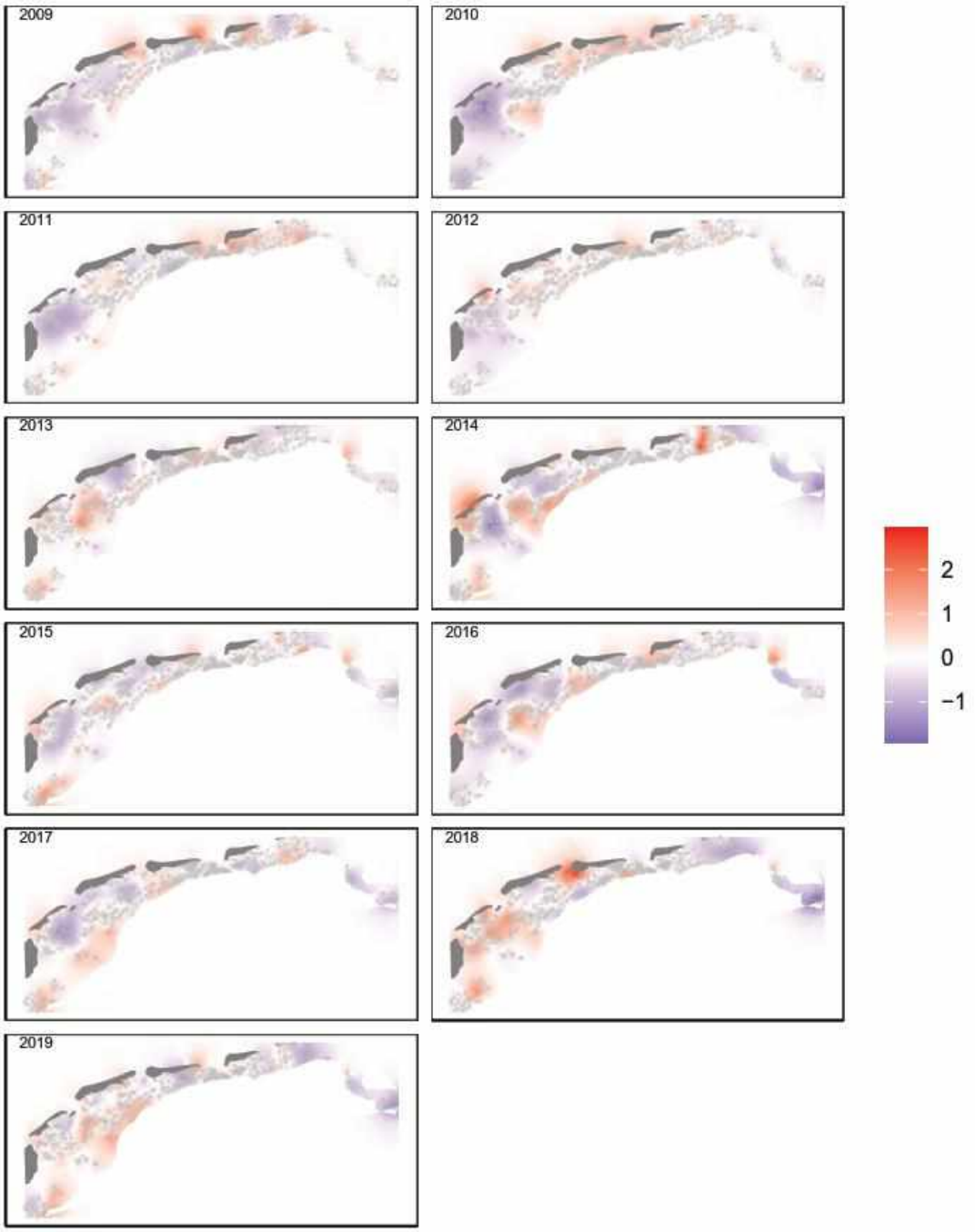


*Figure 7.3. Spatial random fields for each year obtained by the ZINB GAM with the spatial-temporal replicate correlation applied to the* L. balthica *count data.*

The effect of the MSC Zoe incident was estimated by comparing two statistical models that differ in the specification of the random fields. In the first model, every year has a separate spatial correlation field. In the second model, only a single spatial field was used for both the years 2018 and 2019 (

Table *7.1*). Based on DIC, no differences between the two models were found. If no difference in DIC is found, it is advisable to select the simpler model, which in this case is the model with a common spatial field. In any case, no strong evidence for an effect of the MSC Zoe incident has been found.

*Table 7.1. DIC values of two ZINB GAMs with spatial-temporal replicate correlation. The full model in the first row contains a spatial random field for each year. The sub-model in the second row also contains a spatial random field for each year, except for the 2018 and 2019 data. These are modelled by 1 spatial random field.*

| Model | DIC |
|---|---|
| ZINB GAM + replicate SRF (2018 and 2019 separate) | 24288 |
| ZINB GAM + replicate SRF (one field for 2018 and 2019) | 24285 |

The conclusion based on the comparison of the model with and without a common field for the two years 2018 and 2019, was further corroborated by analyzing the posterior probability distribution of the differences $\delta_i$ between the spatial fields of 2018 and 2019 for each of the sampling locations that were sampled in both years. Differences are deemed 'important' if 0 is not included in the 95 % credible interval for the difference.
Out of 573 stations for which the comparison could be made, there were 16 stations with an important difference between the spatial random fields of 2019 and 2018 (Figure 7.4). All important differences found were decreases between 2018 and 2019. They occurred in three small spatial clusters.

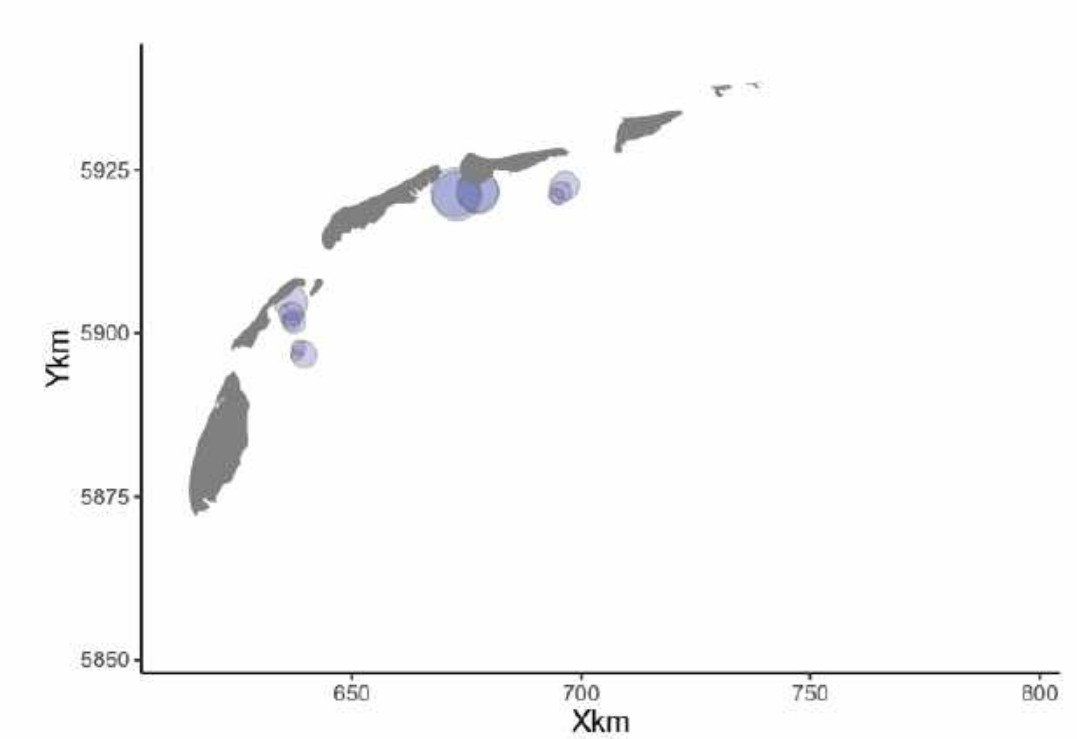


*Figure 7.4. Posterior mean values of $\delta_i = w_{i,2019} - w_{i,2018}$ for all stations $i$ that were sampled in 2019 and 2018. Only stations with important differences are shown. The size of a circle is proportional to the posterior mean value of $\delta_i$. The circles in purple are decreases, in red (not occurring in this figure) increases between 2018 and 2019. No correction for multiple testing has been applied.*

### 7.2.2 Analysis of Biomass

Biomass data of *L. balthica* were modelled with a ZAG distribution. This model is composed of a Bernouilli part and Gamma part, that share common spatio-temporal fields, up to a constant. The model is specified as:

$$
\begin{aligned}
Obs_{is} &\sim ZAG(\mu_{is}, \pi_{is}, r) \\
E[Obs_{is}] &= \pi_{is} \times \mu_{is} \\
Var[Obs_{is}] &= \frac{\pi_{is} \times r + \pi_{is} - {\pi_{is}}^2 \times r}{r} + \mu_{is}^2 \\
logit(\pi_{is}) &= \gamma_1 + f(tauFlood_{is}) + f(tauWave_{is}) + f(Salinity_{is}) + \\
&\quad f(Grainsize_{is}) + Year_s + b \times u_i \\
log(\mu_{is}) &= \beta_1 + f(tauFlood_{is}) + f(tauWave_{is}) + f(Salinity_{is}) + \\
&\quad f(Grainsize_{is}) + Year_s + u_{is} \\
u_{is} &\sim N(0, \Omega)
\end{aligned}
$$

Where ZAG stands for Zero-adjusted Gamma model with three parameters. Subscript i denotes space and subscript s denotes time. The expected value at a particular time and place is linked through a logit link in the case of the Bernouilli part of the model, and through a log-link for the Gamma part. The linear predictive equation contains the factor year and smoothing functions for the environmental factors median bottom shear stress during flood, median wave bottom shear stress, salinity and grainsize. Finally, the linear term contains a spatio-temporal random field that is a replicate model in time and that is shared (up to a constant) between the two parts of the model.

The smoothers for the environmental variables are derived separately for the Bernouilli and Gamma parts of the model (Figure 7.5). Presence/absence is influenced by currents (tauFlood), waves (tauWave) and median grain size. Numerical values of biomass, conditional on presence, are only influenced by waves, as the response curves for the other variables are very flat or the credible intervals very wide.

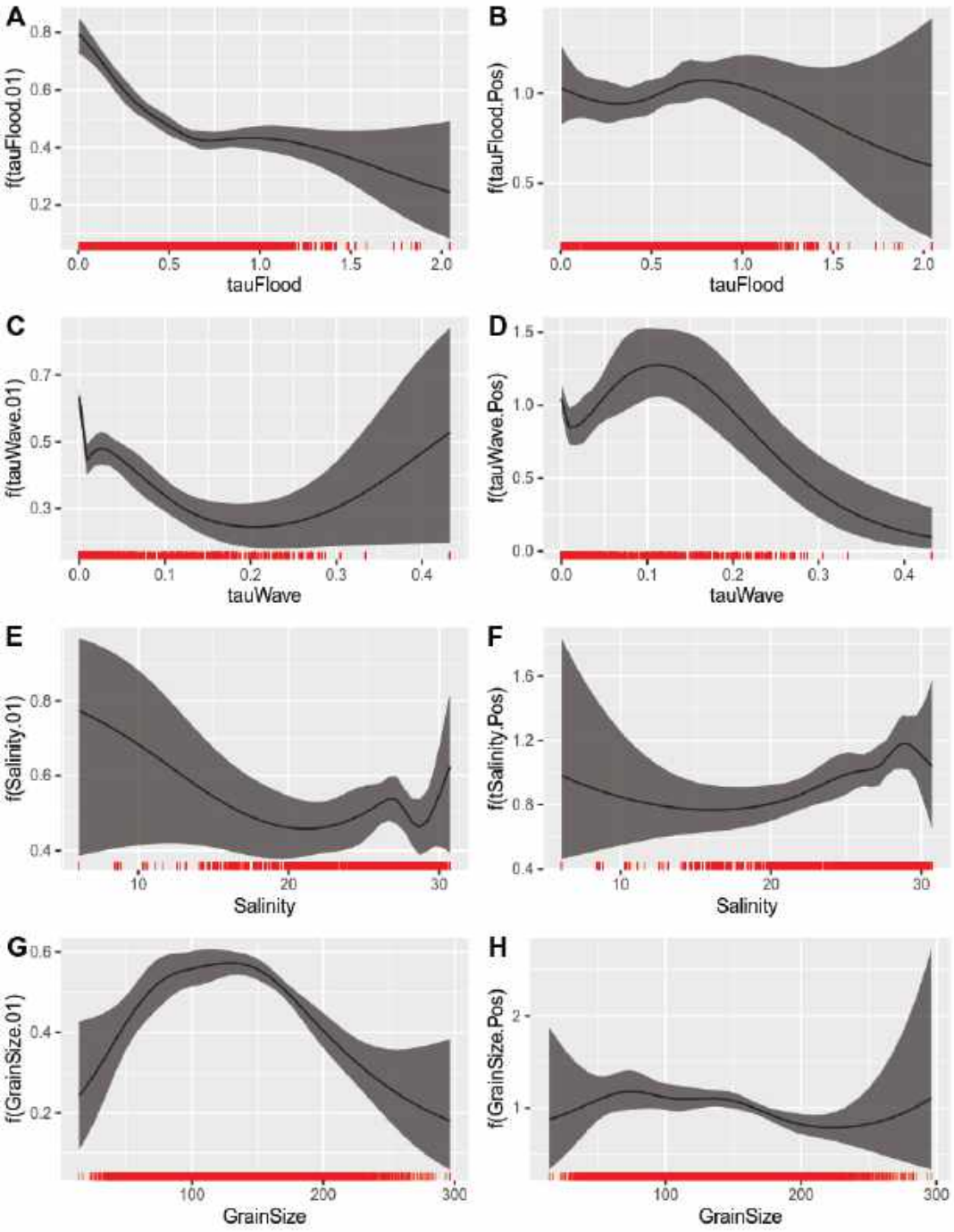


*Figure 7.5. Posterior mean values and 95% credible intervals for all smoothers obtained by the ZAG model with a shared spatial-temporal replicate correlation. The figures on the left are for the binary part and the figures on the right are for the Gamma part of the ZAG model applied to the* L.balthica *biomass data.*

The year effects (results not shown) indicate that the probability of presence was highest in the years 2012-2014 and in 2018. The average biomass when present showed variability within each year, but little differences between the years.

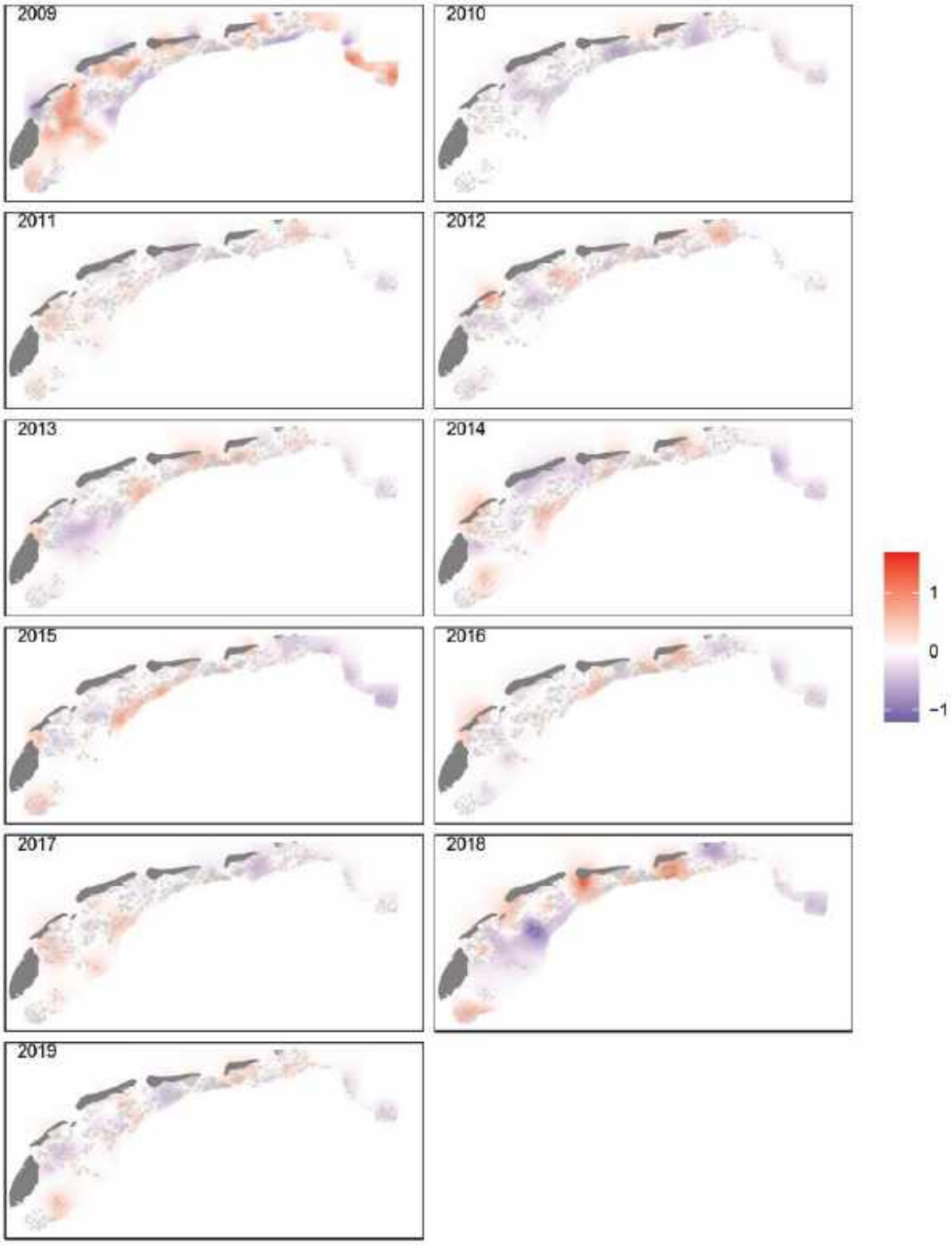


*Figure 7.6. Posterior mean values of the shared spatial-temporal random fields obtained by the ZAG model applied on the* L. balthica *biomass data.*

The spatio-temporal random fields (Figure 7.6) show relatively little variation. Note that the range of the scale is considerably smaller than for other species. It is also much lower than the range for the fields of numerical abundance of this species. As was the case for abundance, no clear patterns that are sustained over several years emerge.
A comparison between a model with a separate spatial-temporal random field for every year, and a model with a common field for the years 2018 and 2019, shows that the latter model is better (Table 7.2). An important difference between the spatial random fields of 2018 and 2019 has been found.

*Table 7.2. DIC values of two ZAG GAMs with spatial-temporal replicate correlation. The full model in the first row contains a spatial random field for each year. The sub-model in the second row also contains a spatial random field for each year, except for the 2018 and 2019 data. These are modelled by 1 spatial random field.*

| Model | DIC |
|---|---|
| ZAG GAM + replicate SRF (2018 and 2019 separate) | -6925 |
| ZAG GAM + replicate SRF (one field for 2018 and 2019) | -6903 |

When examining the posterior mean values of the difference in the spatial random field between 2018 and 2019, there are 16 stations where the difference $\delta i = ui,2019 - ui,2018$ is important. This represents 2.79% of the stations. From these 16 changes, 7 changes are an increase, and 9 are a decrease from 2018 to 2019.

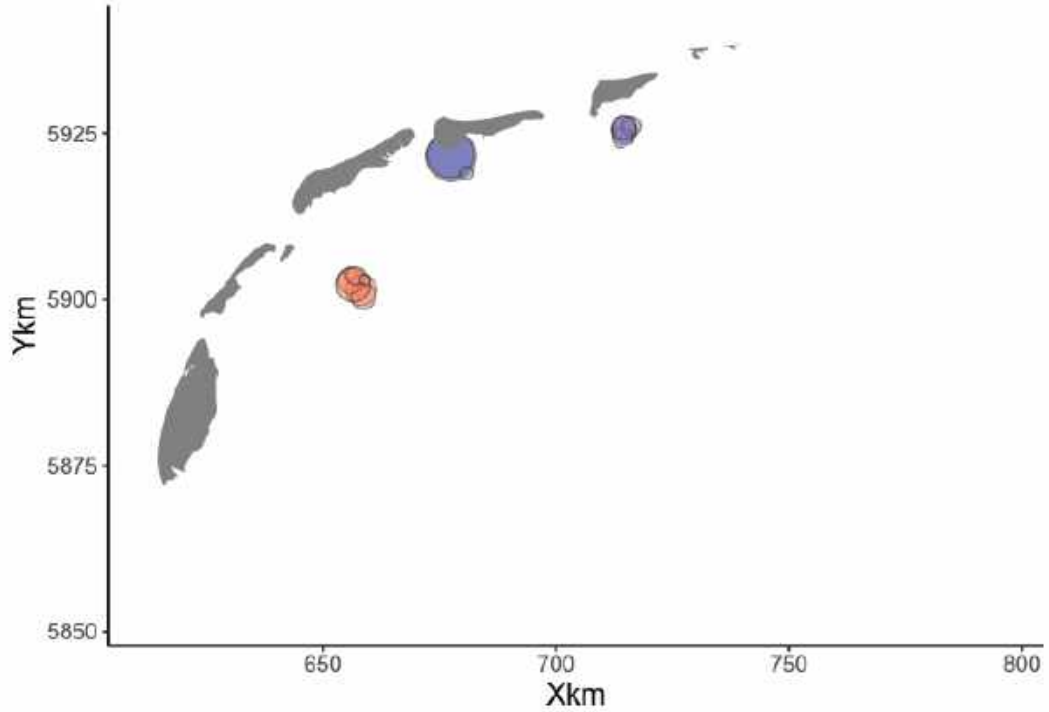


*Figure 7.7. Posterior mean values of $\delta i = u_{i,2019} - u_{i,2018}$ for stations $i$ that were sampled in 2019 and 2018, and for which the 95% credible interval does not contain 0 (no correction for multiple testing has been applied). Red symbols are increases from 2018 towards 2019, purple symbols are decreases.*

The areas of important increase and decrease are spatially clustered. Decreases are mainly observed in the north-eastern part of the Wadden Sea, whereas increases are observed in the central part. The three locations with strong changes correspond to features that are unusually sharply expressed in the random field of 2018: two strong and relatively small hotspots in the north-eastern Wadden Sea, and one strong coldspot in the central part. In 2019 the spatial field is much more homogeneous and close to zero everywhere. Strong changes as illustrated in Figure 7.7, correspond to the loss of well-expressed features of 2018, rather than to the acquisition of particular features in 2019.

## 7.3 Discussion

The environmental preferences of *Limecola balthica* generally show an indifferent response to salinity over quite a broad range, a preference for relatively low currents and bottom shear stress, and a preference for a range of rather fine sediments with an optimum median grain size between 100 and 150 µm. In comparison with earlier studies in Westerschelde and Oosterschelde, the present analysis from the Wadden Sea confirms most aspects. However, in the Wadden Sea a stronger preference for very small current velocity conditions was found.

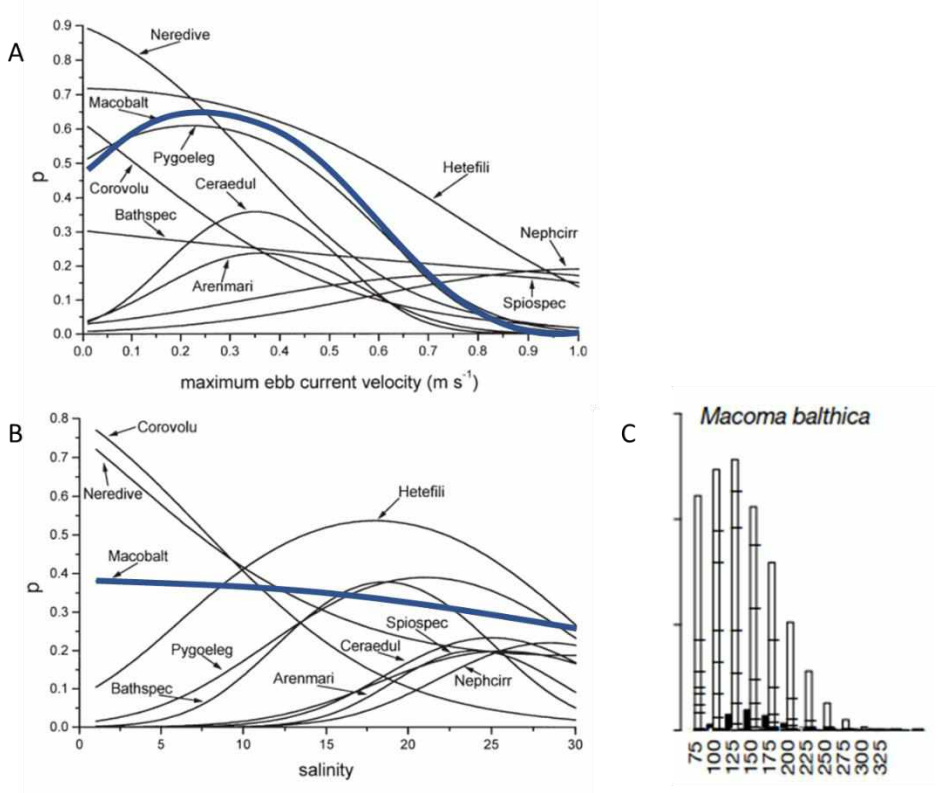


*Figure 7.8. Comparison material from the literature on response of* Limecola balthica (*note: previously called* Macoma balthica) *to environmental variation. A: probability of occurrence in the Westerschelde as a function of current velocity. B. Probability of occurrence in the Westerschelde as a function of salinity. C. Expected 95$^{th}$ percentile of biomass (based on quantile regression) for the Westerschelde (white bars) and Oosterschelde (black bars) as a function of sediment median grain size. A and B based on Ysebaert et al., 2002. C based on Cozzoli et al, 2013.*

Within the period 2009-2019 covered by this data set, no clear temporal trend can be found back in the numbers or biomass of *L. batlhica* in the Wadden Sea. There is some year-to-year variation in numbers, with 2014 and 2018 standing out as years of high recruitment, but variation in biomass is much more restricted. As shown by the random spatio-temporal fields, spatial patterns are generally well explained by the covariables (especially bottom shear stress and grain size) and the spatial random fields show small, local and non-persistent highs and lows.

The analysis found no difference between the spatial random fields of abundance in 2018 and 2019, but for biomass important differences were found. These differences are linked to the fact that, in contrast to the general picture, the year 2018 showed relatively strong hotspots and coldspots.

Where these patterns were lost again in the transition to 2019, important local differences have been detected. It is unlikely that these differences are linked to effects of the MSC Zoe incident. The changes are not only losses, but also gains, which would be difficult to explain if they were caused by the MSC Zoe incident. Moreover, the spatial field of 2019 is quite homogeneous compared to that of 2018, which is the inverse of what would be expected if the MSC Zoe incident had caused significant, but spatially inhomogeneous, changes in 2019.

## 7.4 Conclusion

Abundance and biomass of *Limecola balthica* in the Wadden Sea are fluctuating during the study period, without a strong temporal trend. Two years of strong recruitment are found in 2014 and 2018. Spatial patterns are mostly well explained by environmental cofactors. There is limited spatio-temporally autocorrelated variation around the average values. A limited number of statistically important changes were found in the spatial fields of biomass between 2018 and 2019. These correspond to the loss of well-expressed features in the high-recruitment year 2018, rather than to the acquisition of unusual patterns in 2019. Influence of the MSC Zoe incident on this population is very unlikely.

# 8 The Atlantic razor clam (*Ensis leei*)[1]

## 8.1 Biology and ecology

**Appearance of the shell**

Description: the Atlantic razor clam has an elongate, curved and fragile shell with a length up to 19cm (Bruyne et al., 2013; Hill, 2006) (Figure 8.1). The shell is smooth on the outside, whitish in color with horizontal and vertical purplish-brown markings separated by a diagonal line. The periostracum is olive-green and the inner surface is white with a purple tinge and the foot is pale red-brown (Hill, 2006).

*Figure 8.1. Ensis leei* (Atlantic razor clam). Photographer: Oscar Bos.

Distribution and habitat: the Atlantic razor clam is an invasive species and originates from the Eastern American coast (Richards (1938) in Houziaux et al. (2011)) with the first confirmed record from the German Bight in 1979 (Von Cosel et al., 1982). Now widely distributed along Europe, from Norway to the Atlantic coast of Spain (Gollasch et al., 2015). In the Netherlands it was first observed in the Dutch coastal zone in 1982 (De Boer & De Bruyne, 1983) and is now widely spread among the Dutch coast (De Mesel et al., 2011; Troost & Van Asch, 2018). *Ensis leei* occurs both in the intertidal zone and in the subtidal zone, up to 15m (Bruyne et al., 2013). It occurs in fine to coarse sand and silty areas and can thus be independent of sediment characteristics (Dauvin et al., 2007). It lives in deep, vertical, permanent burrows several centimeters deep (Bruyne et al., 2013).

[1] In the WOT surveys not all razor clam – like organisms are identified with certainty to species level. Reflecting this uncertainty, they are indicated as "*Ensis* sp.". The vast majority of these individuals belong to the species *Ensis leei*. Therefore, we give here the ecological description of that species. Even if occasionally, an observed individual may belong to other, autochtonous *Ensis* species, the spatial and temporal patterns found in the statistical analysis can fully be ascribed to *Ensis leei.*

The presence of razor shells in sand is indicated by keyhole-shaped openings made by the short, united siphons which extend just above the sediment surface when the animal is feeding (Hill, 2006). When disturbed, pressure in the cavity produces powerful jets of water which assist quick downward movement of the shell by loosening the adjacent sand (Trueman, 1967). It can dig rapidly in the sediment down to about 50cm (Richards (1938) in Houziaux et al. (2011)). According to Holland & Dean (1977) razor clams (*Tagelus plebeius*) can dig to 70 cm.

Feeding: Atlantic razor clams are filter-feeders (suspension-feeders), collecting their food by filtering and sorting particles from the water column (Gosling, 2003). In the intertidal, it will move to the surface during high tide to expose its siphon to filter the water (Tulp et al., 2010). In deeper waters, it mainly filters at the surface at night, avoiding predation from predators relying on vision (Gollasch et al. (1999) in Tulp et al. (2010)).
Predators: fish such as sole, plaice and flounder in the Voordelta are found to predate especially on small razor clams (Wijsman et al., 2006). Eiders and common scoters have been noted to eat *Ensis*, however, adult specimens are often too big or have been buried too deep in the sediment (Leopold et al., 2001; Swennen et al., 1985; Tulp et al., 2010). Juvenile specimens or individuals that have emerged from the sediment can be predated more easily by eiders (Leopold et al., 2001). Small Atlantic razor clams are also preyed on by oystercatchers and (Muir, 2003; Swennen et al., 1985) seagulls (Cadée, 2001).

Reproduction and development: *Ensis leei* is a broadcast-spawning bivalve with separate sexes. Spawning occurs in May or June and fertilization occurs in the water column after release of sperm and eggs (Kenchington et al., 1998). It was shown that a second spawning may occur in the Wadden Sea in July/August (Wijsman et al., 2006). Fertilized eggs will develop to form a veliger larva which lives in the water column and feeds on algae with their velum. The earliest larvae of the Atlantic razor clams measure 92 x 78 µm, the umbo appears in larvae of 115 µm in length and is well developed in larvae 135 µm long (Loosanoff & Davis (1963) in Von Cosel (2009)). Loosanoff & Davis observed a duration of free-swimming larval phase of 10-27 days (10 days at 24˚C). They settle at a length of 210-270 µm, depending on environmental conditions. After settlement, they grow fast (depending on food availability and temperature), reaching a length of on average 3.5cm in their first year (Wijsman et al., 2006). Especially during the first years of life, mortality is high due to predation by fish, birds and crustaceans (Wijsman et al., 2006). They live on average 3-4 years (Bruyne et al., 2013).

Abiotic tolerances: *Ensis leei* shows large temperature tolerances, but low winter temperatures seem to limit its development (Essink, 1994). High mortality rates were observed during cold winters, suggesting that the clams lose the ability to burrow at low temperatures (Crisp, 1964). Its salinity tolerance is 7–32 psu (Maurer et al., 1974), which means that it occurs in both marine and estuarine areas (Beukema & Dekker, 1995). *E. leei* shows a limited tolerance to reduced oxygen conditions (Schiedek and Zebe, 1987).

### Historical trends Wadden Sea

At the start of the annual shellfish survey, *Spisula subtruncata* was an abundant species (Perdon et al., 2019). However, the *S. subtruncata* stock collapsed in 2002 and the fishery switched to the Atlantic razor clam. *Ensis* is an invasive species, which rapidly increased in number since 2002. The *Ensis* stock varies greatly from year to year but shows a long-term gradual increase (Schelpdiermonitor, 2021; Troost et al., 2021). The number of *Ensis* sharply increased in 2019 compared to the year before and has never been that high since the start of the surveys (1995). The stock almost tripled compared to the stock size in 2018. This increase is caused by a big spat fall event in 2018 (Perdon et al., 2019).

## 8.2 Data collection and analysis

The data have been collected in the WOT shellfish survey (chapter 3.3). They are available as abundance data ('density', N.m$^{-2}$) and biomass data ('biomass', g WW m$^{-2}$), where WW stands for 'wet weight'. Because of subsampling and different sample size per haul, abundance data cannot be recalculated to integer numbers. Both abundance and biomass are therefore modelled with statistical distributions for continuous-scale variables.
Physical co-factors are derived from the same source as the cofactors for the SIBES data in the Wadden Sea. The available co-factors in the dataset show a high degree of collinearity. Therefore, only a subsample of a few, relatively independent, cofactors can be used. For the sake of consistency, the same variables as used in the Wadden Sea analysis (SIBES data) have been used for the WOT data in the coastal zone. Note, however, that a different set of (highly correlated) independent physical variables would have yielded more or less the same result. The degree of collinearity within the set of cofactors used is limited.

### 8.2.1 Analysis of numerical abundance

A ZAG (Zero-altered Gamma) distribution was used to model the data. As explained in Chapter 4.4, such distribution is composed of two parts, a Bernouilli distribution modelling the presence/absence of the species, and a gamma distribution modelling the value of the abundance provided the species is present. Both model parts share a common spatial random field, up to a constant b that is needed because both parts use different link functions: logit for the Bernouilli part and log for the gamma part. The smoothers of the cofactors are kept separate between the Bernouilli and gamma parts.
The model fitted is specified as follows:

$$
\begin{aligned}
Abundance_{is} &\sim ZAG(\mu_{is}, \pi_{is}, r) \\
E[Abundance_{is}] &= \pi_{is} \times \mu_{is} \\
Var[Abundance_{is}] &= \frac{\pi_{is} \times r + \pi_{is} - {\pi_{is}}^2 \times r}{r} + \mu_{is}^2 \\
logit(\pi_{is}) &= \gamma_1 + f(tauFlood_{is}) + f(tauWave_{is}) + f(Salinity_{is}) + \\
&\quad f(Grainsize_{is}) + Year_s + b \times u_i \\
log(\mu_{is}) &= \beta_1 + f(tauFlood_{is}) + f(tauWave_{is}) + f(Salinity_{is}) + \\
&\quad f(Grainsize_{is}) + Year_s + u_{is} \\
u_{is} &\sim N(0, \Omega)
\end{aligned}
$$

Where ZAG stands for Zero-adjusted Gamma model with three parameters. Subscript i denotes space and subscript s denotes time. The expected value at a particular time and place is linked through a logit link in the case of the Bernouilli part of the model, and through a log-link for the Gamma part. The linear predictive equation contains the factor year and smoothing functions for the environmental factors median bottom shear stress during flood, median wave bottom shear stress, salinity and grainsize. Finally, the linear term contains a spatio-temporal random field that is a replicate model in time and that is shared (up to a constant) between the two parts of the model.
The results of the model fitting consist of the relation with the cofactors, and the spatial random fields for all years of observation.
The relation with the cofactors is very similar, per cofactor, between the Bernouilli part and the gamma part of the model (Figure 8.2). Presence and abundance peak at a value of bottom shear stress from flow of appr. 0.6 Pa, are only little influenced by waves, are restricted to nearshore areas with slightly depressed salinity (< 31.5) and have some preference for grain size around 250 µm.

Presence/absence did not differ much between years, but the value of the year factor was much higher (approximately a factor 3) in 2019 than in the other years. Indeed, 2019 was a year when an exceptional spatfall of *Ensis*, that happened during the hot and dry summer of 2018, was first recorded in the samples of the WOT, which are taken in Spring before the recruits of the year are retained on the sieve. Even though these recruits had already survived their first winter, with all the mortality involved, they still outnumbered normal abundance factors at an exceptionally high level.
The spatial random field of 2019 reflects this very high recruitment peak with the presence of very strong hotspots in the near-coastal zone (Figure 8.3). Hotspots in other years occasionally are shared by consecutive years, e.g. between 2017 and 2018, but in general have little similarity from one year to another. Hotspots of abundance are mostly determined by spatfall, which is a spatially heterogeneous process that leads to extremely high abundances in some areas, but very low numbers in other areas where the cloud of settling larvae has not hit the bottom.

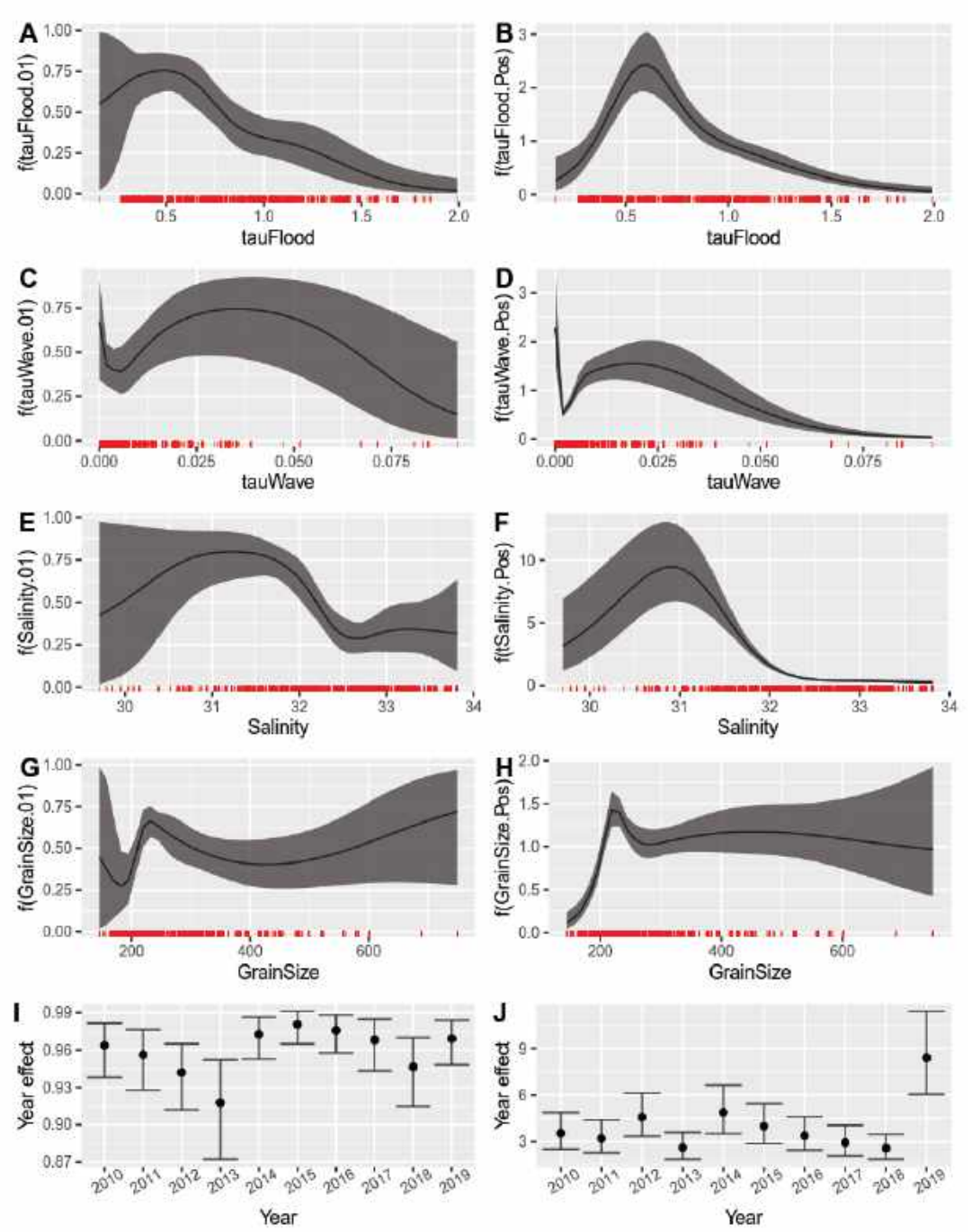


*Figure 8.2. Posterior mean values and 95 % credible intervals for all smoothers and the year effect obtained by the ZAG model with a shared spatial-temporal replicate correlation. The figures on the left are for the binary part and the figures on the right are for the Gamma part of the ZAG model applied to the* Ensis *abundance data.*

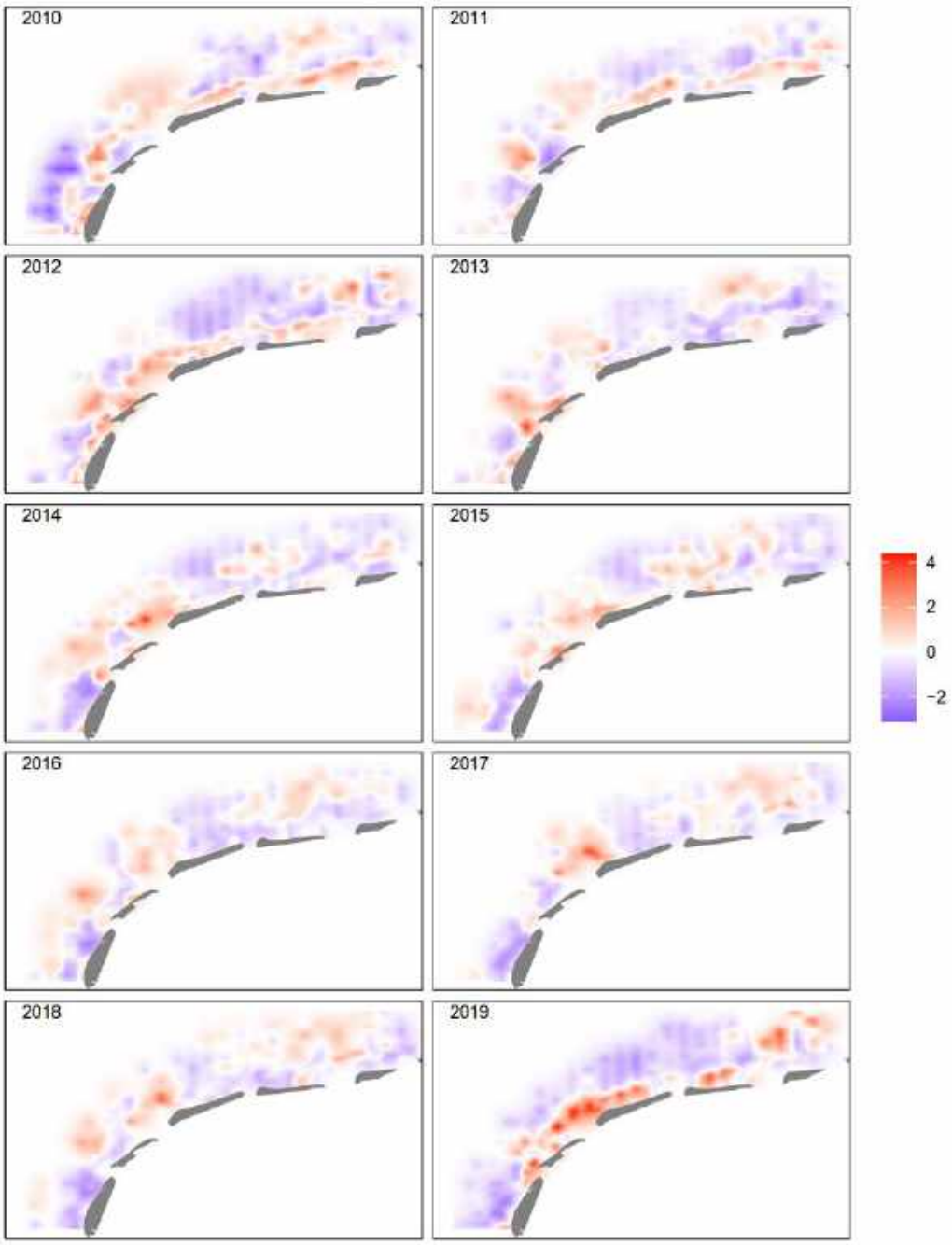


*Figure 8.3. Posterior mean values of the shared spatial-temporal random fields obtained by the ZAG model applied to the* Ensis *abundance data.*

The presence of an MSC Zoe effect is investigated by comparing two models, one with a shared random field for 2018 and 2019, and one with separate random fields for both these years. A DIC comparison of both models (Table 8.1) shows that a model with separate spatial random fields for 2018 and 2019 is clearly better than the model with a shared field. This means that the random fields of 2018 and 2019 substantially differ from one another.

*Table 8.1. DIC values of two ZAG GAMs with spatial-temporal replicate correlation. The full model in the first row contains a spatial random field for each year. The sub-model in the second row also contains a spatial random field for each year, except for the 2018 and 2019 data, which are modelled by 1 common spatial random field.*

| Model | DIC |
|---|---|
| ZAG GAM + replicate SRF (2018 and 2019 separate) | 16162.60 |
| ZAG GAM + replicate SRF (one field for 2018 and 2019) | 16364.69 |

When the differences between the spatial random fields of 2018 and 2019 are analyzed per station, there were relatively many stations where the 95 % credible intervals of the posterior distribution did not contain 0. Although this large number may have been influenced by the fact that no correction for multiple testing has been applied, it corroborates the previous conclusion that the spatial random fields of both years are substantially different. The spatial location of the sites with large differences shows the correspondence with the hotspots of recruitment in the year 2019. All large ('credible') differences were actually *increases*, with the 2019 value substantially higher than the 2018 value.

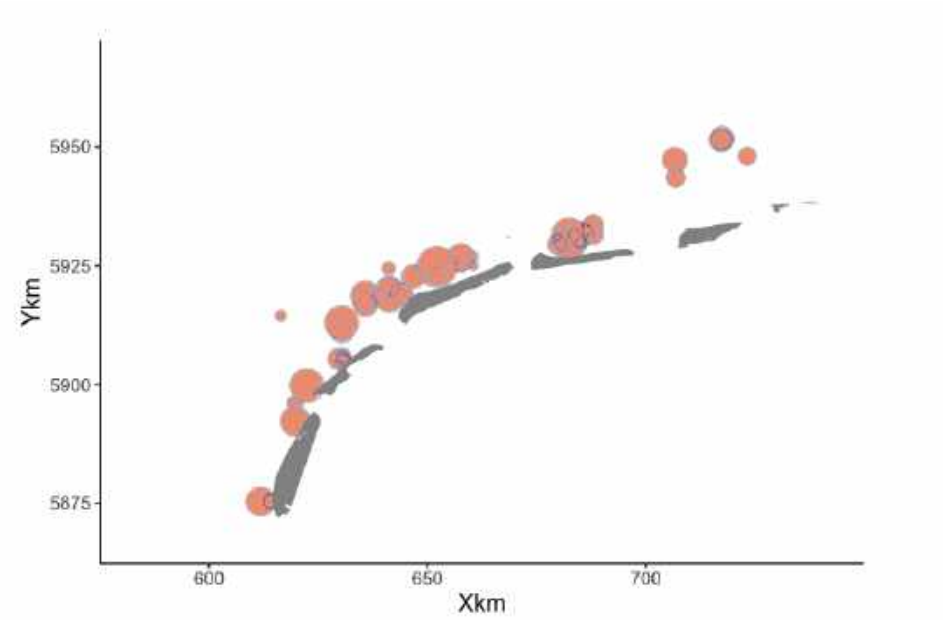


*Figure 8.4. Posterior mean values of $\delta_i = u_{i,2019} - u_{i,2018}$ for stations I that were sampled in 2019 and 2018, and for which the 95 % credible interval does not contain 0 (no correction for multiple testing has applied).*

### 8.2.2 Analysis of Biomass

The same model as for the abundance data was used. The response to the cofactors (Figure 8.5) was qualitatively similar to the response of the abundance data, but in general patterns were quantitatively less expressed: less variation in space and time was present in the biomass data, leading to lower coefficients for the regression on cofactors. The strong year effect of 2019 was also seen in biomass, but also here the relative strength of the year 2019 is less expressed than in the abundance data: a factor 1.5-2 difference, instead of 3-4.

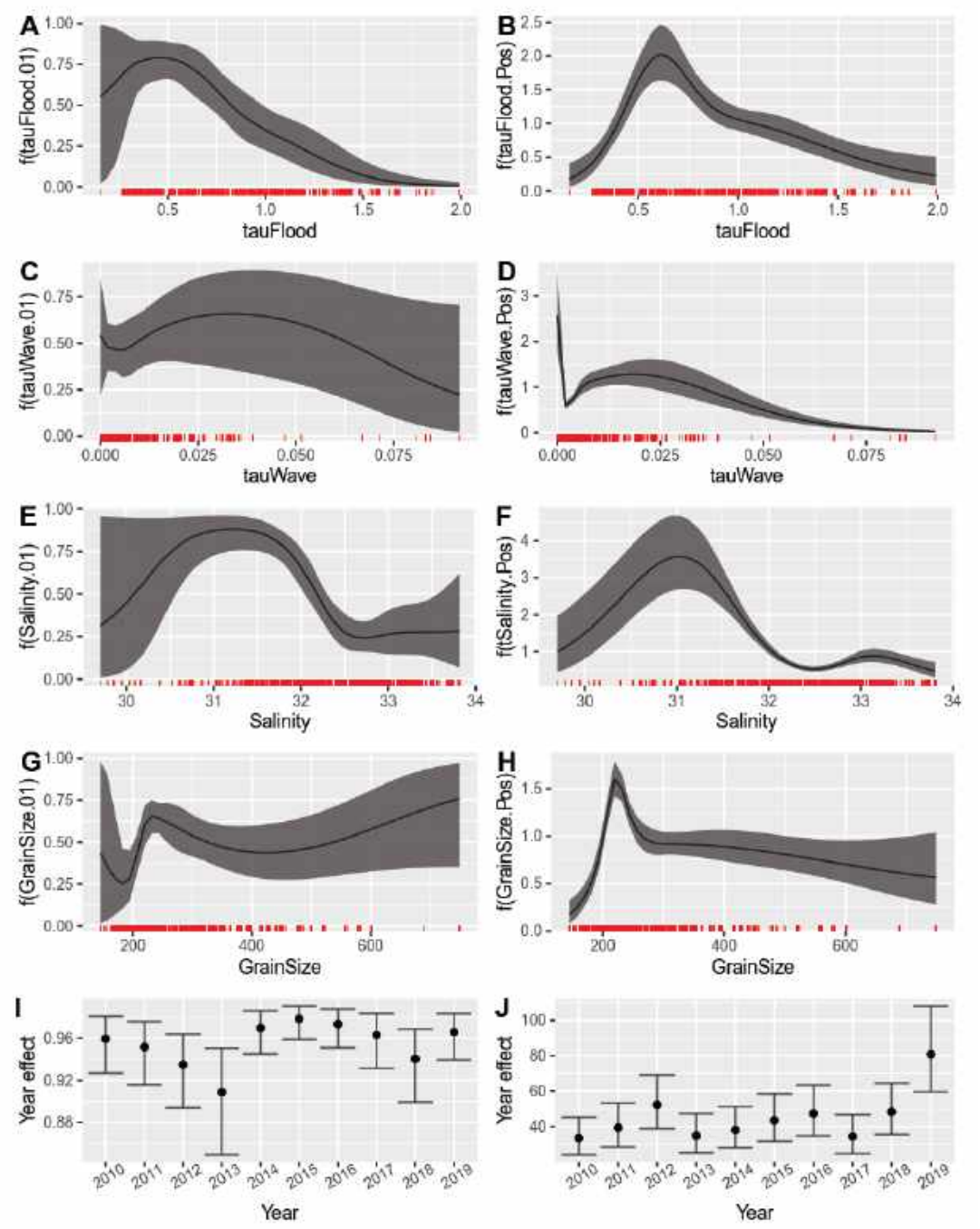


*Figure 8.5. Posterior mean values and 95 % credible intervals for all smoothers and the year effect obtained by the ZAG model with a shared spatial-temporal replicate correlation. The figures on the left are for the binary part and the figures on the right are for the Gamma part of the ZAG model applied to the* Ensis *biomass data.*

The spatially random fields for biomass differ with respect to the fields for abundance (Figure 8.6).In the model building for abundance, it was concluded that a model with separate spatial random fields for each year was substantially better than a model with one common spatial random field. The reverse is true for biomass. The spatial random fields of the different years are quite similar in the position of hotspots and coldspots. A formal DIC test shows that a model with a common spatial field is better than a model with spatial-temporal random fields.

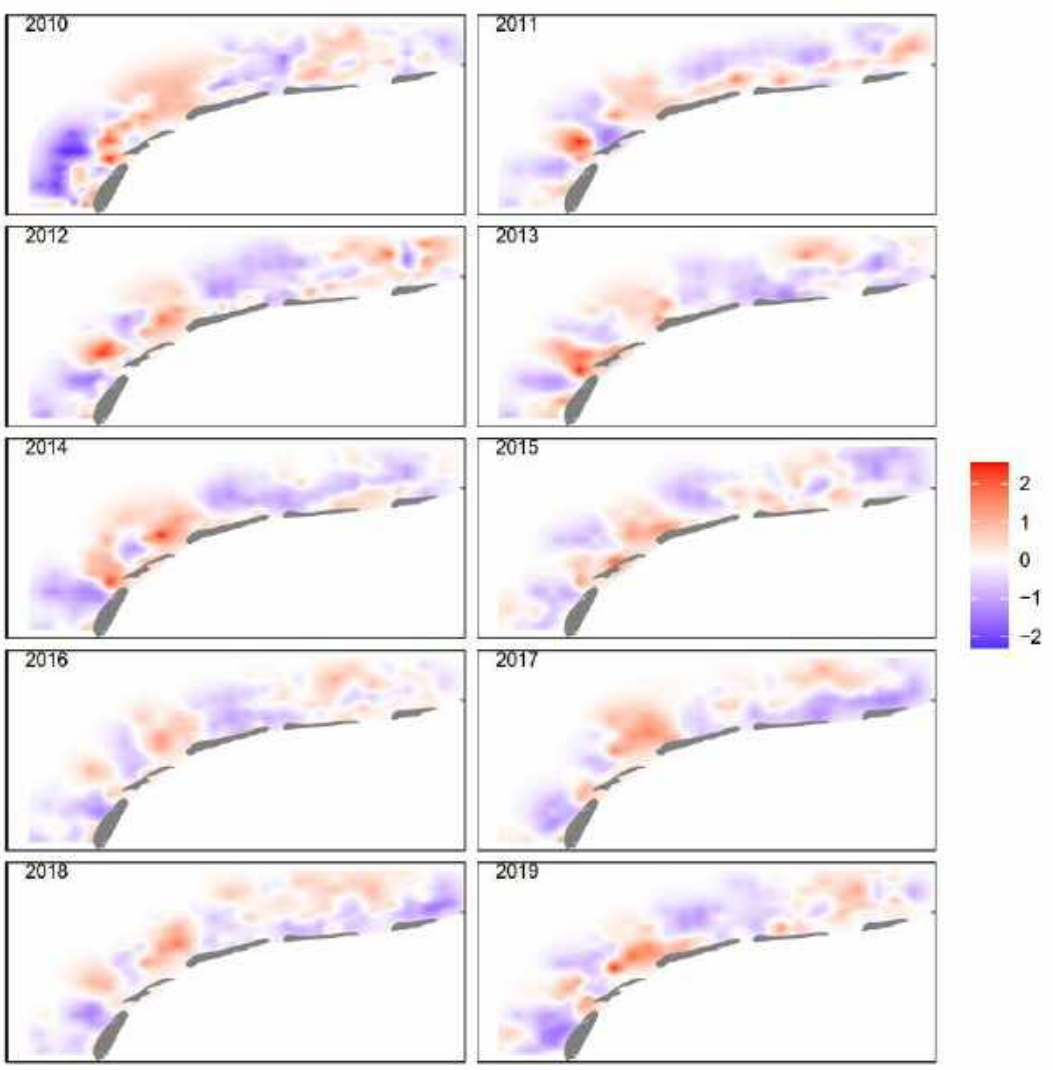


*Figure 8.6. Posterior mean values of the shared spatial-temporal random fields obtained by the ZAG model applied to the* Ensis *biomass data.*

The comparison between abundance and biomass data shows that abundance is very much influenced by the spatial and temporal vagaries of recruitment, where high numbers of recruits are found in different places from year to year. However, biomass is much more influenced by the heavy older animals. In order to be present as an older individual, animals have to survive and grow for several years. Biomass is therefore much more influenced by the factors that correlate to growth and survival. These factors are much more constant in space and time. Much of the information has been 'absorbed' by the cofactors. The spatial field is mostly a latent variable showing spatially organized information not covered by the available cofactors but persistent in time.
In contrast to the abundance data, A DIC comparison (Table 8.2) shows that a model with separate spatial random fields for 2018 and 2019 is worse than a model with a shared field. This means that the random fields of 2018 and 2019 are essentially the same and no Zoe effect can be seen.

*Table 8.2. DIC values of two ZAG GAMs with spatial-temporal replicate correlation. The full model in the first row contains a spatial random field for each year. The sub-model in the second row also contains a spatial random field for each year, except for the 2018 and 2019 data, which are modelled by 1 common spatial random field.*

| Model | DIC |
|---|---|
| ZAG GAM + replicate SRF (2018 and 2019 separate) | 28937.77 |
| ZAG GAM + replicate SRF (one field for 2018 and 2019) | 28830.64 |

When analyzed by station, only three stations show a substantial difference (with a credible interval not encompassing 0). All three concern increases in 2019, compared to 2018.

## 8.3 Discussion

*Ensis leei* has a high reproductive capacity, short generation time, rapid growth and, thus, has all characteristics of a successful “r” strategist invader (Gollasch et al 2015). Pelagic larvae of *E. leei* are present almost year-round (Witbaard et al 2015). It further has little requirements regarding its environment (Houziaux et al 2011). Thus, the Dutch coastal area is very suitable for this species. This is in agreement with habitat suitability mapping of the WOT data from the period 1995-2009 (De Mesel et al 2011). Only some areas in the south-west and north-west of Texel and Vlieland appeared less suitable (Figure 8.7).
In the study of De Mesel et al (2011), the most important environmental variables explaining the presence/absence were mean salinity, minimum salinity, depth, median grainsize, maximum current velocity and the bathymetric position index. The response curves show a preference for higher salinities (>22 psu) with a slight decrease at 32 psu. The lower limit is in agreement with Skov et al (2008) who did not find razor clams at salinities below 20 psu. Maximum velocities should not be too high: < 0.4 m/s. There is a positive response for sediments with median grain sizes up to 200 µm, a negative response above 400 µm. Variables reflecting impact of waves were not available at that time. Thus, the present results are in line with the results of De Mesel et al (2011), except for median grain size. The range in the present study is smaller.

Variability in recruitment is a striking feature of the life histories of most marine invertebrates with a major impact on the population dynamics. Recruitment dynamics of *E. leei* is not regular and shows strong year-to-year variability (Armonies and Reise, 1999; Beukema and Dekker, 1995). In most years there seems to be a rather low recruitment, and from time to time a strong one (Perdon et al 2019). The year 2018 was such a year. The stock of razor shells showed an increase in numbers with a factor 3 due to a relatively large amount of small specimens, mostly between 3 and 5 cm length (Perdon et al 2019). More than 80% of the stock was found north of the Wadden islands, of which 98% were small specimens. But also in other parts of the Dutch coastal zone the stocks were dominated by small individuals, about 80%. Houziaux et al (2011) noticed that largest abundance patches of juveniles occur just next to larger abundance patches of adults. The authors suggest that the distribution of juveniles near the adult patches would then mirror optimum habitat for post-settlement survival, pointing at areas suitable and available for colonization. The larvae likely find a suitable ground to grow as older specimens die and are expelled.

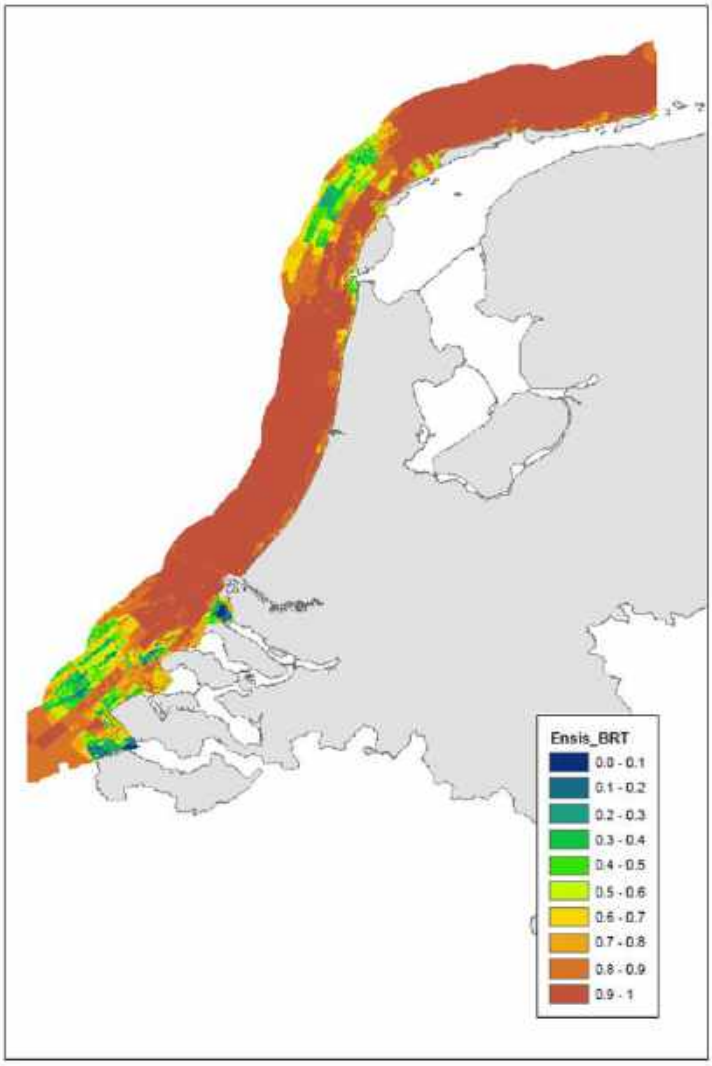


*Figure 8.7. Probability of occurrence of Ensis sp.in the Dutch coastal zone as predicted by the BRT-model (De Mesel et al 2011).*

However, yearly changes of areas with high recruitment might also be related to other factors. In the Voordelta (south-west Netherlands) successful recruitment was often restricted to different subareas, independent of presence of older specimen (Craeymeersch et al 2015). This might be environmentally driven but could also be human activity related. Tulp et al (2020 report an increase in *E. leei* after an experimental fishery in the Wadden Sea. This apparently is a response of this species to relocate and quickly colonize space, that became vacant because the original inhabitants were disturbed, removed or died. Thus, recruitment might be enhanced due to disturbance of the sediment or removal of competitors or predators (Prins et al 2020).

## 8.4 Conclusions

In conclusion, the results from the statistical analyses indeed reflect spatial and temporal differences in recruitment success, resulting from very heterogeneous processes. And the differences between 2018 and 2019 are most likely due to natural phenomena and not a Zoe effect.

# 9 The Cut Through shell, *Spisula subtruncata.*

## 9.1 Biology and ecology

Description: the asymmetrical triangular (more rounded on one side) and thick shell can be up to 35mm long (Figure 9.1). The outer shell surface is off-white with a grey-yellowish epidermis and growth lines are clearly distinguishable. Hinge mainly internal (Bruyne et al., 2013).

*Figure 9.1. Shell of* Spisula subtruncata*. Source: Wikimedia.*

Distribution and habitat: *S. subtruncata* is a common species occurring in shallow coastal waters from Norway to Western Africa, the Canary Islands and the Mediterranean (Hayward & Ryland, 2017). It occurs mainly between 2 and 20m depth (Rueda & Smaal, 2004). It can be found along the entire Dutch coast (De Mesel et al., 2011; Troost et al., 2021) and lives buried in shallow soft bottoms (Cardoso et al., 2007), from fine to coarse sand and mud (Degraer et al., 2006). It can burrow quickly using a thick pointed foot (Yonge, 1948).

Feeding: *S. subtruncata* is a filter-feeding bivalve (suspension-feeder) (Rueda & Smaal, 2004). No information has been found about the specific mechanism of filter-feeding by *S. subtruncata*, but it will be similar to other filter-feeding bivalves. Filter-feeding bivalves collect their food by filtering and sorting particles from the water column (Gosling, 2003; Troost, 2009). The siphons extend to a maximum length of 8mm and when burrowed, only the tips can be visible above the surface (Yonge, 1948). The inner lobe of the inhalant siphon is represented by a ring of large, with intermingled small, tentacles around the opening. The tentacles prevent large particles from entering with the inhalant current (Yonge, 1948). The ciliated gills create a water current which flows into the inhalant siphon, between the gills (Gosling, 2003).

Predators: *S. subtruncata* is an important food source for shrimps (Pihl & Rosenberg, 1984), demersal fishes (Braber & De Groot, 1973) and diving sea ducks like the common scoter (Christensen et al., 1993; Leopold et al., 1995).

Reproduction and development: *S. subtruncata* is a broadcast-spawning bivalve with separate sexes. Spawning of *S. subtruncata* in Dutch coastal waters occurs in June or July at a water temperature of about 15-17˚C (Cardoso et al., subm. ms in Cardoso et al., 2007), which is in accordance with observations of Rueda and Smaal (2004), who found active gonads from April to June. All individuals of *S. subtruncata* above 12mm shell length (corresponding to the end of first year of life) developed gonads, suggesting that sexual maturity is a function of size and not of age (Cardoso et al., 2007). Fertilization occurs in the water column. Fertilized eggs (oocyte diameter 57.43µm (Cardoso et al., 2007)) will develop to form a veliger larva which lives in the water column and feeds on algae with its velum. It takes about one month after spawning for larvae to settle on the seafloor (Cardoso et al., 2007). Settlement and recruitment success have a significant impact on the dynamics of *S. subtruncata* populations. Adult suspension feeders may reduce settlement of larvae by ingestion of settling larvae (André & Rosenberg, 1991). Unsuccessful settlement of spat or predation during the first months might lead to a decline in population size (Cardoso et al., 2007). *S. subtruncata* is a very fast-growing species (reaching 8-10 mm during the first 4-5 months, Kiorboe & Mohlenberg, 1981) with a life span of 1 to a maximum 5 years (Bruyne et al., 2013; Kiorboe & Mohlenberg, 1981).

Abiotic tolerances: little is known about the abiotic tolerances of *S. subtruncata*. Salinity should not be too low, which is probably related to the preferred depth of > 5m (De Mesel et al., 2011). *S. subtruncata* seems to be sensitive to freezing temperatures (1998). Flow rates are preferably lower than 0.45m/s (Craeymeersch et al., 2007).

### Historical trends coastal zone

The *S. subtruncata* stock in the Dutch coastal zone has been assessed since 1995. The large stock in the coastal zones in 1996 declined until 1999. In 2000 there was a short-lived peak but after 2001 there was hardly any stock left. Fisheries switched in this period from *S. subtruncata* to the invasive species *Ensis leei*, which was first introduced in the Dutch coastal zone in 1982 (De Boer & De Bruyne, 1983). In spring 2017 the stock of *S. subtruncata* had sharply increased due to an extremely large spatfall in the summer of 2016. The estimated biomass of 2017 has never been higher since the beginning of the time series. The reason for this sudden increase after such a long period of virtual absence is not known (Perdon et al., 2019).

## 9.2 Data collection and analysis

The data have been collected in the WOT shellfish survey (chapter 3.3). They are available as abundance data ('density', $N.m^{-2}$) and biomass data ('biomass', g WW $m^{-2}$), where WW stands for 'wet weight'. Because of subsampling and different sample size per haul, abundance data cannot be recalculated to integer numbers. Both abundance and biomass are therefore modelled with statistical distributions for continuous-scale variables.
Physical co-factors are derived from the same source as the cofactors for the SIBES data in the Wadden Sea. The available co-factors in the dataset show a high degree of collinearity. Therefore, only a subsample of a few, relatively independent, cofactors can be used. For the sake of consistency, the same variables as used in the Wadden Sea analysis (SIBES data) have been used for the WOT data in the coastal zone. Note, however, that a different set of (highly correlated) independent physical variables would have yielded a similar result. The degree of collinearity within the set of cofactors used is limited.

### 9.2.1 Analysis of Numerical Abundance

The raw data show that there are many stations with zero observations. The species is only present in a limited subset of the stations. From year to year, the absolute values of the abundance in the stations where the species is present can vary substantially. However, spatially the presence of the species is very predictable from year to year. The zone north of the island of Ameland is the core area for the presence of the species. To a lesser degree, also the zone north of Terschelling often has stations with presence of the species.

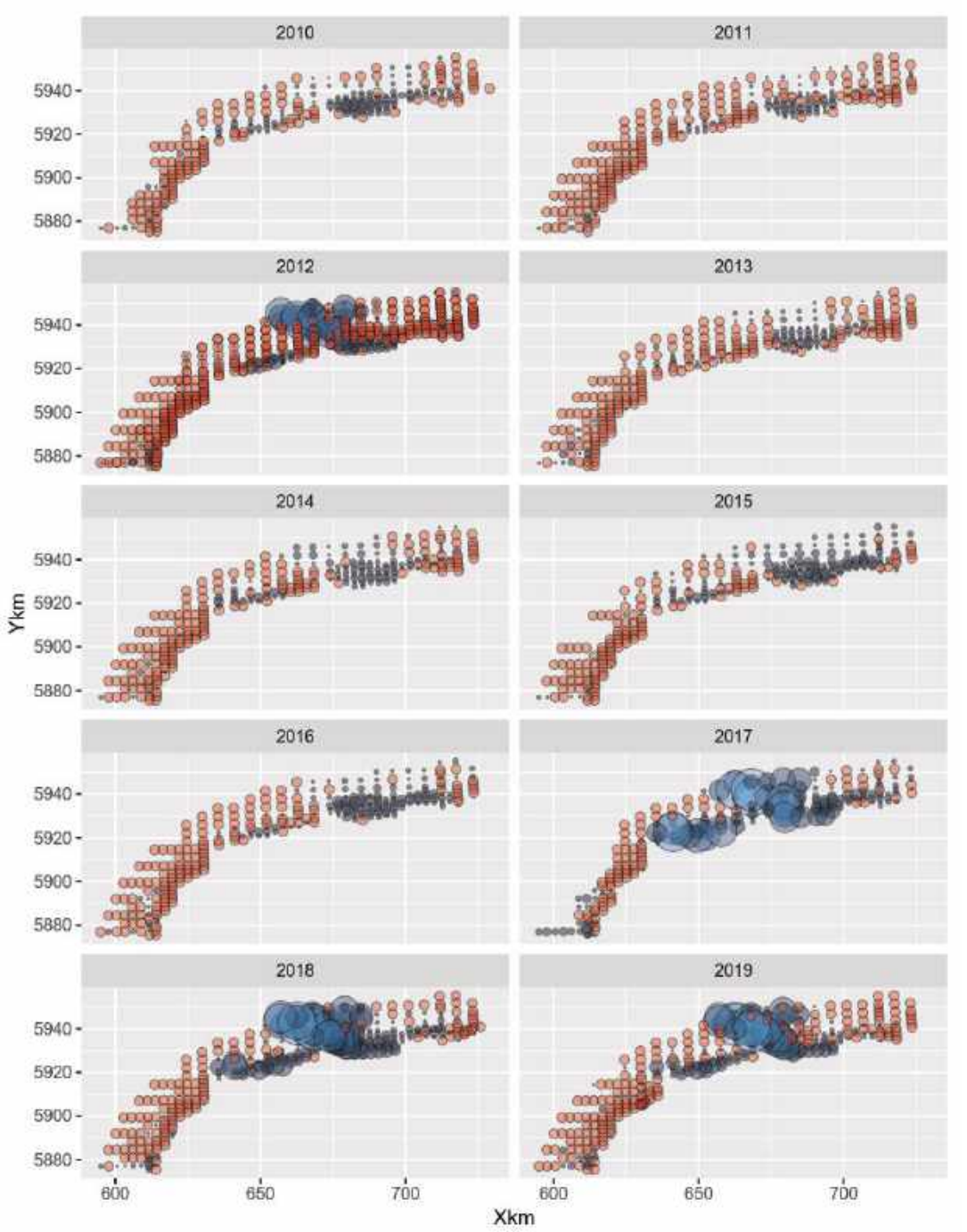


*Figure 9.2. Abundance of Spisula subtruncata in the coastal zone. Spatial locations of the absence-presence and presence-only abundance data. Red dots are stations with zero abundance. The size of the blue dots is proportional to the abundance values.*

A ZAG (Zero-altered Gamma) distribution was used to model the data. As explained in Chapter 4.4, such distribution is composed of two parts, a Bernouilli distribution modelling the presence/absence of the species, and a gamma distribution modelling the value of the abundance provided the species is present. Both model parts share a common spatial random field, up to a constant b that is needed because both parts use different link functions: logit for the Bernouilli part and log for the gamma part. The smoothers of the cofactors are kept separate between the Bernouilli and gamma parts.
The model fitted is specified as follows:

$$
\begin{aligned}
Abundance_{is} &\sim ZAG(\mu_{is}, \pi_{is}, r) \\
E[Abundance_{is}] &= \pi_{is} \times \mu_{is} \\
Var[Abundance_{is}] &= \frac{\pi_{is} \times r + \pi_{is} - {\pi_{is}}^2 \times r}{r} + \mu_{is}^2 \\
logit(\pi_{is}) &= \gamma_1 + f(tauFlood_{is}) + f(tauWave_{is}) + f(Salinity_{is}) + \\
&\quad f(Grainsize_{is}) + Year_s + b \times u_i \\
log(\mu_{is}) &= \beta_1 + f(tauFlood_{is}) + f(tauWave_{is}) + f(Salinity_{is}) + \\
&\quad f(Grainsize_{is}) + Year_s + u_{is} \\
u_{is} &\sim N(0, \Omega)
\end{aligned}
$$

Where ZAG stands for Zero-adjusted Gamma model with three parameters. Subscript i denotes space and subscript s denotes time. The expected value at a particular time and place is linked through a logit link in the case of the Bernouilli part of the model, and through a log-link for the Gamma part. The linear predictive equation contains the factor year and smoothing functions for the environmental factors median bottom shear stress during flood, median wave bottom shear stress, salinity and grainsize. Finally, the linear term contains a spatio-temporal random field that is a replicate model in time and that is shared (up to a constant) between the two parts of the model.
In contrast to what was the case for *Ensis* in these same samples, the effect of the cofactors on the presence and abundance of *Spisula subtruncata* shows clear differences for the Bernouilli part and the gamma part of the model (Figure 9.3). Waves have little impact on either of the two parts. Bottom shear stress and sediment grain size are important factors determining presence/absence of the species, but once present have little or no influence on the numerical abundance. Salinity, in contrast, has a sharper influence on the numerical abundance than on presence/absence. Provided the species is present, it will only show high values of abundance in offshore, relatively saline waters. This pattern can also be seen in Figure 9.2.
There are year-to-year variations in the probability of presence of the species, but much wider variability between the years in the actual values of abundance. High abundance is found in the years 2012, 2017, 2018 and 2019, with by far the highest peak in 2017. As was the case for *Ensis* in 2019, this marks an exceptional spatfall year. However, in contrast to the situation for *Ensis*, the places where this spatfall was mostly recorded, are the places characterized with semi-permanent presence of the species, although some niche-broadening may have taken place during the exceptional spatfall.
The spatial-temporal random fields mostly show hotspots of abundance during the four high-abundance years in the zones where the peaks of abundance occurred (Figure 9.4). These zones then turn into coldspots during the low-abundance years.

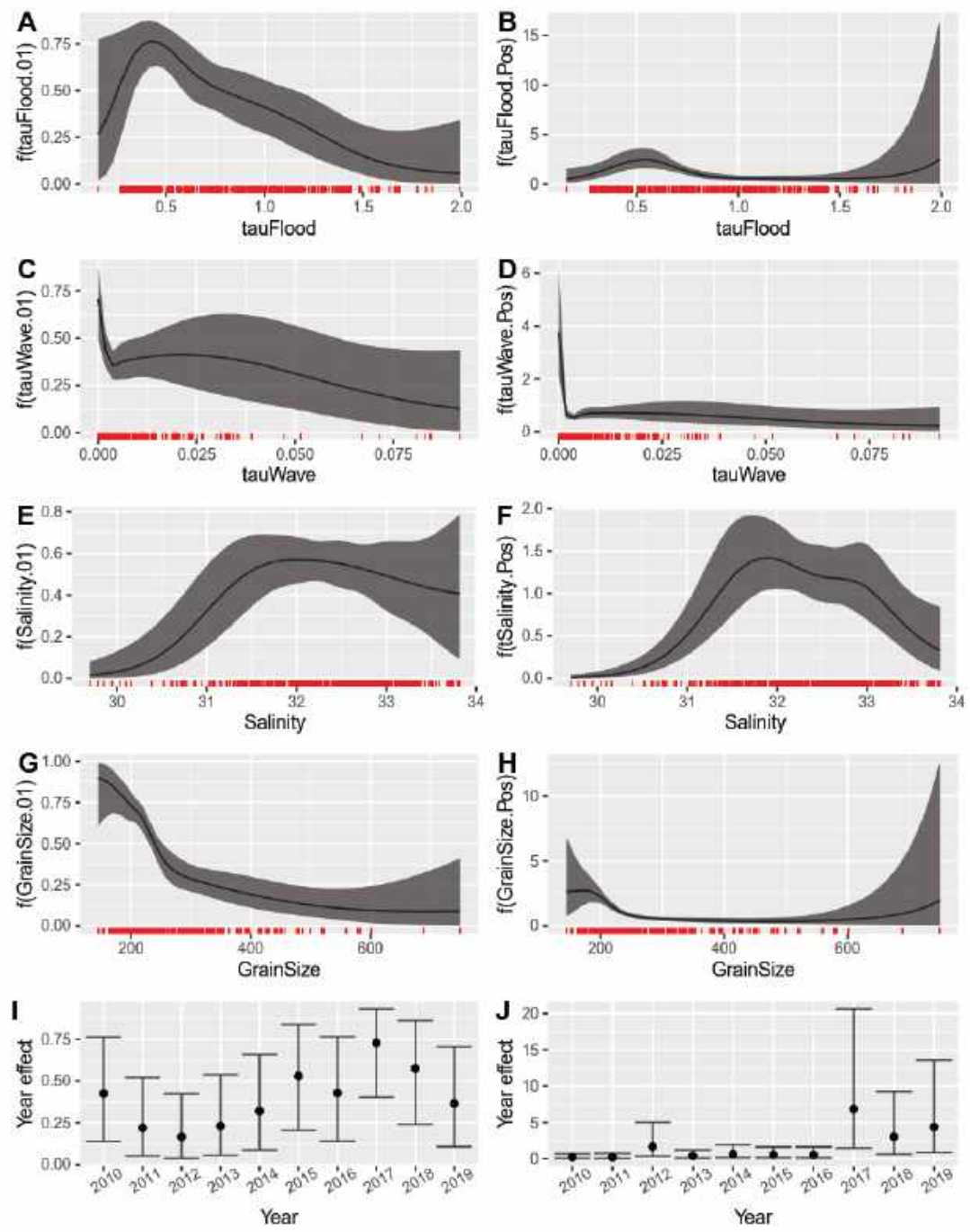


*Figure 9.3. Posterior mean values and 95 % credible intervals for all smoothers and the year effect obtained by the ZAG model with a shared spatial-temporal replicate correlation. The figures on the left are for the binary part and the figures on the right are for the Gamma part of the ZAG model applied to the* Spisula subtruncata *abundance data.*

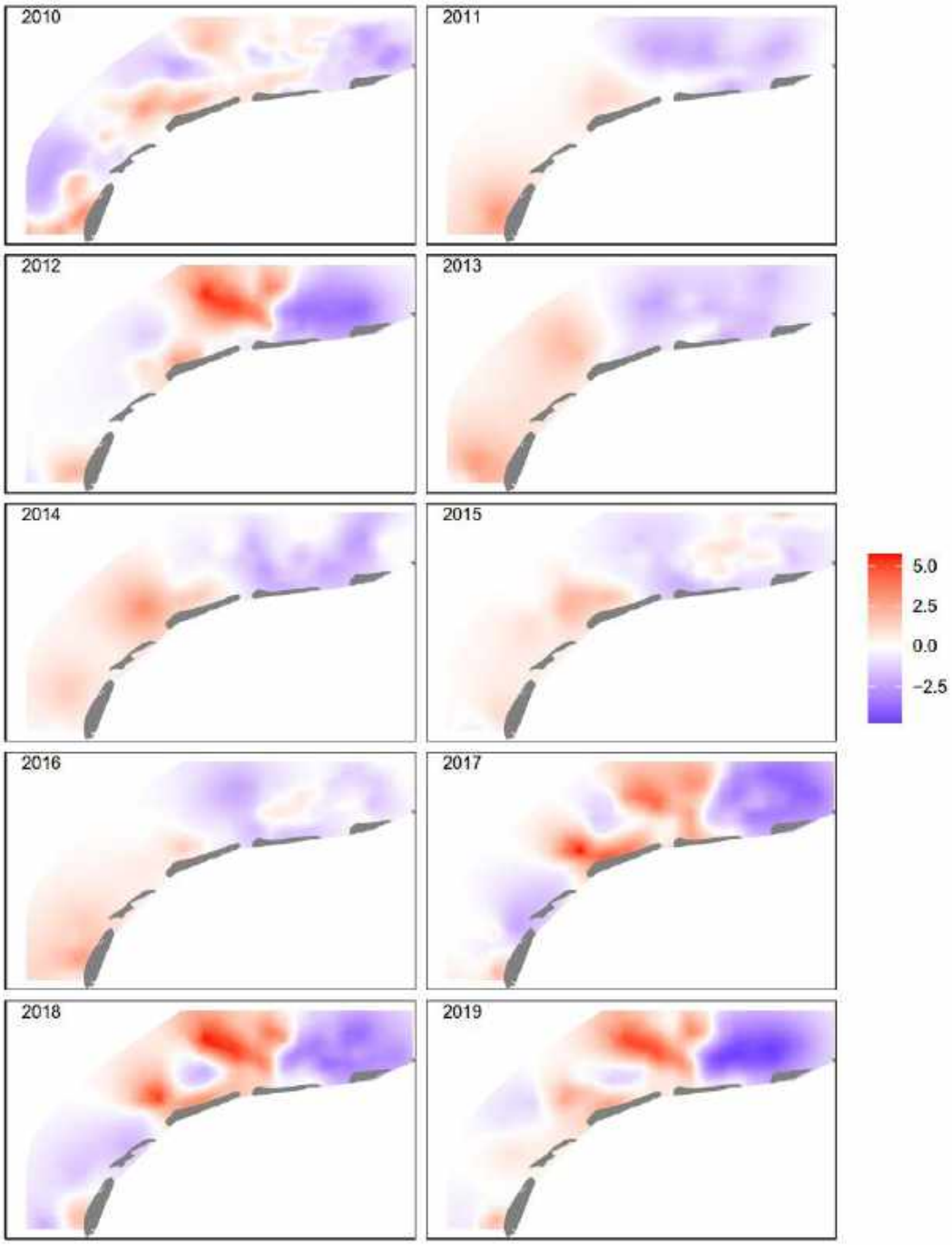


*Figure 9.4. Posterior mean values of the shared spatial-temporal random fields obtained by the ZAG model applied to the* Spisula subtruncata *abundance data.*

The presence of a Zoe effect is investigated by comparing two models, one with a shared random field for 2018 and 2019, and one with separate random fields for both these years. A DIC comparison of both models (Table 9.1) shows that a model with a common spatial random field for 2018 and 2019 is clearly better than the model with separate fields. This means that no difference is detected between the random fields of 2018 and 2019.

*Table 9.1. DIC values of two ZAG GAMs with spatial-temporal replicate correlation. The full model in the first row contains a spatial random field for each year. The sub-model in the second row also contains a spatial random field for each year, except for the 2018 and 2019 data, which are modelled by 1 common spatial random field.*

| Model | DIC |
|---|---|
| ZAG GAM + replicate SRF (2018 and 2019 separate) | 8218.4 |
| ZAG GAM + replicate SRF (one field for 2018 and 2019) | 8115.5 |

An evaluation by station shows that only three stations have a credible posterior interval for the difference that does not encompass 0, thus confirming this conclusion. There is no statistical evidence for a possible Zoe effect.

### 9.2.2 Analysis of Biomass

In contrast to what was the case for Ensis, biomass and abundance data of Spisula subtruncata are highly correlated. A Pearson correlation coefficient of 0.9 between the two data sets was found. As a consequence, the results of the analysis of the biomass data were very similar to the results of the abundance data. We will not repeat the results on the cofactors and the spatial random fields but concentrate only on the detection of a possible Zoe effect.

Table 9.2 shows that a model with separate spatial random fields for 2018 and 2019 is worse than a model with a shared field. This means that the random fields of 2018 and 2019 are essentially the same and no Zoe effect can be seen. This result is the same as that for abundance of *Spisula subtruncata*.

*Table 9.2. DIC values of two ZAG GAMs with spatial-temporal replicate correlation. The full model in the first row contains a spatial random field for each year. The sub-model in the second row also contains a spatial random field for each year, except for the 2018 and 2019 data, which are modelled by 1 common spatial random field.*

| Model | DIC |
|---|---|
| ZAG GAM + replicate SRF (2018 and 2019 separate) | 10174 |
| ZAG GAM + replicate SRF (one field for 2018 and 2019) | 10056 |

When analyzed by station, only two stations show a substantial difference (with a credible interval not encompassing 0).

## 9.3 Discussion

As with many other benthic species in the marine environment, the spatial and temporal distribution and abundance of *Spisula subtruncata* is highly variable (Craeymeersch et al 2001, Degraer et al., 2007, Baptist & Leopold 2009). *Spisula* was very abundant along large parts of the Dutch coast in the 1990s, but during the period 2000–2005 numbers declined (Craeymeersch et al 2001, Baptist & Leopold 2009). Only recently a new successful recruitment was reported, in 2016 (Troost et al 2017).
In 2017, the biomass stock was the highest since 1995 and further increased the years after, up to 2019. In that year 70% of the biomass was found north of the Wadden islands. In 2020 the stock started decreasing again (Troost, pers. comm.).
In general, recruitment dynamics of *S. subtruncata* are much more stochastic than that of *E. leei*. In the twentieth century, high densities of *S. subtruncata* were found in the 1930s, early 1960s, at the end of the 1970's and early 1980s and the 1990s. Low population sizes might result from unsuccessful settlement and/or severe predation by benthic predators during the first months of life (Cardoso et al 2007).

One of the factors that influences the settlement success is the wind direction and force during the pelagic larval phase, which for *Spisula* lasts one month (Cardoso et al., 2007). The resulting hydrographic patterns determine where the postlarval stage ends up, so where the spatfall takes place. If spatfall takes place in a favorable environment, a new Spisula bed may be formed (Belgrano et al., 1995; Armonies et al., 2001; Ellien et al., 2004; Baptist & Leopold, 2009). Craeymeersch and Perdon (2006) tried to link data on wind direction and wind force to the reproduction success of North Sea *S. subtruncata* but did not find a good correlation.

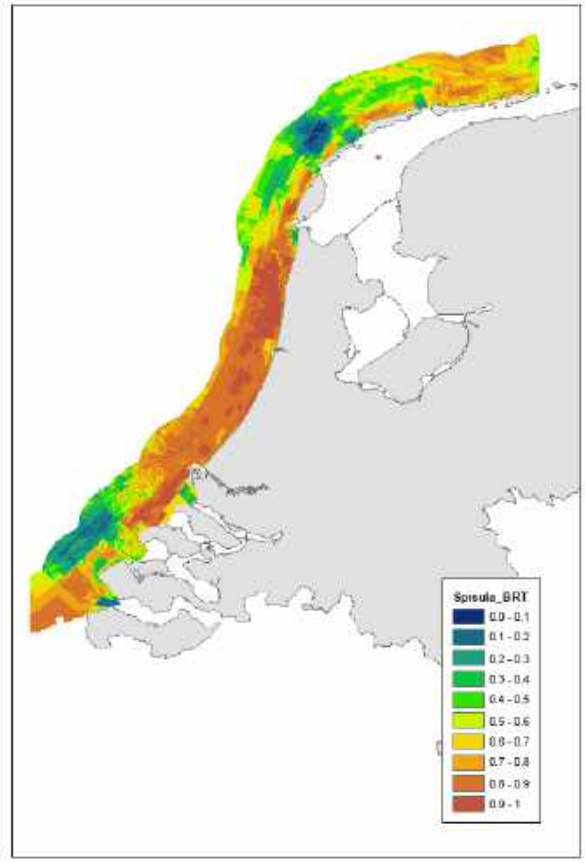


*Figure 9.5. Probability of occurrence of Spisula subtruncata in the Dutch coastal zone as predicted by the BRT-model (De Mesel et al 2011)*

In contrast to *Ensis leei*, high concentrations of *S. subtruncata* are only found in some areas. This could also be seen in the habitat suitability map made on the basis of the WOT data over the period 1995-2009 (De Mesel et al 2011) (Figure 9.5). In the study of De Mesel et al (2011), the most important environmental variables explaining the presence/absence of *S. subtruncata* were minimum current direction, mean salinity, median and maximum current velocity, minimum salinity, bathymetric position index, slope, depth and median grain size. The response curves show an optimum salinity between 20 and 28 psu. Maximum velocities should not be too high: median values < 0.4 m/s and maximum values < 0.45 m/s. They do not like sediments with a median grain size above 400 µm. Variables reflecting impact of waves were not available at that time. Skov et al (2008) found a negative relation with median grain size. Minimum current direction should be interpreted as a proxy for geographical position: high north of the Wadden islands, low in the coastal areas of North and South Holland. The species is mostly found at relatively flat seabed bottoms (BPI-zone 7, slope < 1%). Thus, the present results are in line with the results of De Mesel et al (2011).

## 9.4 Conclusions

The recruitment dynamics of *S. subtrun*cata are rather stochastic, resulting in only a few years with high recruitment. Moreover, such successful recruitment is not always in the same areas, although some zones are certainly more suitable than others. The last good recruitment north of the Wadden islands was in 2016. Population structure and stock size are determined by growth and mortality of that year class in the subsequent years. In line with this trend, the population in 2019 was not really different from that in 2018, except that biomass stock still increased. No Zoe effect could be detected in the data of this species.

# 10 The Mussel (*Mytilus edulis*)

## 10.1 Biology and ecology

Description: the inequilateral and elongated triangular shell has a smooth surface with a sculpturing of concentric lines, but no radiating ribs (Figure 10.1). The shell color varies from blue or purple to brownish. Length varies usually between 50 – 100 mm (Tyler-Walters, 2008). On the inside is a small anterior adductor scar and a large posterior adductor muscle scar (Bruyne et al., 2013).

*Figure 10.1. Mytilus edulis* (Blue mussel). Photographer: Oscar Bos.

Distribution and habitat: *M. edulis* is a widely distributed species in the boreal regions of the northern hemisphere, from the western border of the Kara Sea, South to the Mediterranean. Western coast of Canada South to Carolina, California, Japan and several regions in South-America (Tyler-Walters, 2008). It occurs from the high intertidal (to ca. 5 m) to the shallow subtidal area. In Europe it can be found on all coasts with suitable substrate, where it is attached by fibrous byssus threads to rocks and piers, within harbors and estuaries. It can also occur on rocky shores of the open coast, where they can occur in dense beds (Tyler-Walters, 2008). Mussel beds provide refuge and habitat for a range of other species (Bouma et al., 2009). As such, they contribute to biogenic reefs that are considered an essential quality element of the protected habitats under Natura2000. In the Dutch Wadden sea mussels mainly occur in mussel beds formed on the muddy to sandy bottoms in the intertidal and subtidal (Dankers & Fey-Hofstede, 2015; Folmer et al., 2017).

Feeding: mussels are filter-feeders (suspension-feeders), collecting their food by filtering and sorting particles from the water column (Gosling, 2003). The ciliated gills create a water current which flows into the inhalant siphon, between the gills. The inhalant and exhalant siphons extend several millimeters beyond the margin of the shell (Gosling, 2003). Mussel larvae have maximum retention efficiencies for particles (algae) of 2-6 µm (Sprung, 1984) and particles > 9 µm are not retained (Riisgard et al., 1980).

A review study reported clearance rates for 1 g M. edulis varying from app. 1 to over 7 l/h (Riisgård, 2001). Clearance rate of C. edule was found to be higher than M. edulis at comparable body weight (Møhlenberg & Riisgård, 1979). Mussels feed on phytoplankton, zooplankton, protists and dead particulate organic matter (Bayne, 1976, 1998). Particles larger than 4 µm are filtered by the gills of mussels with 100 percent efficiency (Møhlenberg & Riisgård, 1978), as long as they do not escape (Troost et al., 2008).

Predators: mussels are an important food source for a variety of predatory species. The Wadden Sea intertidal mussels are preyed on by shore birds (e.g. oystercatchers, herring gulls) and crabs, while subtidal mussels are a food source for mainly starfish, molluscivorous ducks, and also crabs and different fish species (Agüera García, 2015; Cervencl et al., 2015; Tyler-Walters, 2008).

Reproduction and development: *M. edulis* is a broadcast-spawning bivalve with separate sexes. Females may produce about 5-12 million eggs per spawning (Helm, 2004). Spawning occurs usually in early summer, when the water temperature exceeds 12˚C (Dankers & Fey-Hofstede, 2015). Fertilization occurs in the water column. Fertilized eggs (60-90 µm) will after about 2 days develop into a veliger larva (Gosling, 2003). In this stage, the larvae obtain their nutrition by active feeding using their ciliated velum (Widdows, 1991). Veligers continue to develop into the pediveliger stage, in which the larvae develop a foot and the velum degenerates (Gosling, 2003). The larvae will settle on a suitable substrate and metamorphose into the benthic juvenile stage, app. 3 weeks after fertilization (Bayne, 1971). Settlement and recruitment success have a significant impact on the dynamics of mussel populations. Adult suspension feeders may reduce settlement of larvae by ingestion of settling larvae (De Montaudouin & Bachelet, 1997). Adult edible cockles, blue mussels and Pacific oysters filter and for a large part ingest M. *edulis* and *C. gigas* larvae (Troost, 2009). High shore populations can be composed of numerous year classes (Seed, 1969).

Abiotic tolerances: *M. edulis* is well acclimated for temperatures between 5-20˚C, with an upper thermal tolerance of about 29˚C (Read & Cumming, 1967). They can survive occasional sharp freezing temperatures (Tyler-Walters, 2008). *M. edulis* is tolerant to a wide range of salinities, varying from 5-40psu (Tyler-Walters, 2008). Survival of larvae at salinities from 15 to 40 psu is good at temperatures between 5-20˚C; optimal growth occurs at 20˚C and salinities between 25 and 30 psu (Brenko & Calabrese, 1969).

### Historical trends Wadden Sea

In the early 1990s, almost no mussel beds remained on the tidal flats in the Wadden Sea (Troost et al., 2012). In about 10 years' time, the intertidal area of mussel beds had increased again to about 2000 ha and remains about this size. The majority can be found in the Eastern Wadden Sea (Troost et al., 2012). Around 2000, with the rise of the Pacific oyster (*Crassostrea gigas*) major changes occurred because the oysters settled in mussel beds, creating 'mixed' beds (Troost et al., 2021). The composition of intertidal mussel/oyster beds is highly dependent on the amount of mussel spatfall. In the few years following a major spatfall in 2016, the composition shifted toward more than half of the beds consisting of mussels only. (Troost et al., 2021). The average life span of pure mussel beds is 3,43 years and survival chances significantly increase when mixed with Pacific oysters (van der Meer et al., 2018). In the Western Wadden Sea, an analysis of long-term recruitment from 1955–2002 showed that abundant recruitment occurs on average once every two years in the subtidal and once every four years in the intertidal areas (Van Stralen, 2002).

## 10.2 Data collection and analysis

The data have been collected in the framework of the WOT shellfish survey in the Wadden Sea. Details of the field methods are given in Chapter 3.2.
The data set comprises 10972 samples in the years 2012 to 2020. Data prior to 2011 were not considered, as the number of samples in 2011 was much lower than in the other years. A subset of samples in 2011, mostly in the Western part of the Wadden Sea, was rejected on quality grounds.
The species was found in appr. 25 % of the samples. Abundance data were given as numbers per $m^2$ but were not reducible to counts as various methods of subsampling and recalculating to a $m^2$ basis were used. This excluded the use of distributions (Poisson, negative binomial) for discrete variables. Instead, Zero-adjusted Gamma distribution was used for modelling of both abundance and biomass data.
The same covariates as for the SIBES data were used. Model-derived variables were interpolated from the model grid to the sampling locations. No measured grain size information was available. The mean median grain size of the SIBES campaigns between 2012 and 2020 were spatially interpolated to the mussel sampling locations.

### 10.2.1 Analysis of Numerical Abundance

The numerical abundance was modelled with a ZAG model with spatio-temporal correlation fields. The model used is specified as follows:
A series of statistical models with increasing complexity was fitted to the data, including Poisson, zero-inflated Poisson, negative binomial and zero-inflated negative binomial.
The final model fitted to the data is a zero-inflated negative binomial GAM with spatial and temporal correlation fields.
The model is specified as follows:

$$
\begin{aligned}
Obs_{is} &\sim ZAG(\mu_{is}, \pi_{is}, r) \\
E[Obs_{is}] &= \pi_{is} \times \mu_{is} \\
Var[Obs_{is}] &= \frac{\pi_{is} \times r + \pi_{is} - {\pi_{is}}^2 \times r}{r} + \mu_{is}^2 \\
logit(\pi_{is}) &= \gamma_1 + f(tauFlood_{is}) + f(tauWave_{is}) + f(Salinity_{is}) + \\
&\quad f(Grainsize_{is}) + Year_s + b \times u_i \\
log(\mu_{is}) &= \beta_1 + f(tauFlood_{is}) + f(tauWave_{is}) + f(Salinity_{is}) + \\
&\quad f(Grainsize_{is}) + Year_s + u_{is} \\
u_{is} &\sim N(0, \Omega)
\end{aligned}
$$

Where ZAG stands for Zero-adjusted Gamma model with three parameters. Subscript i denotes space and subscript s denotes time. The expected value at a particular time and place is linked through a logit link in the case of the Bernouilli part of the model, and through a log-link for the Gamma part. The linear predictive equation contains the factor year and smoothing functions for the environmental factors median bottom shear stress during flood, median wave bottom shear stress, salinity and grainsize. Finally, the linear term contains a spatio-temporal random field that is a replicate model in time and that is shared (up to a constant) between the two parts of the model.

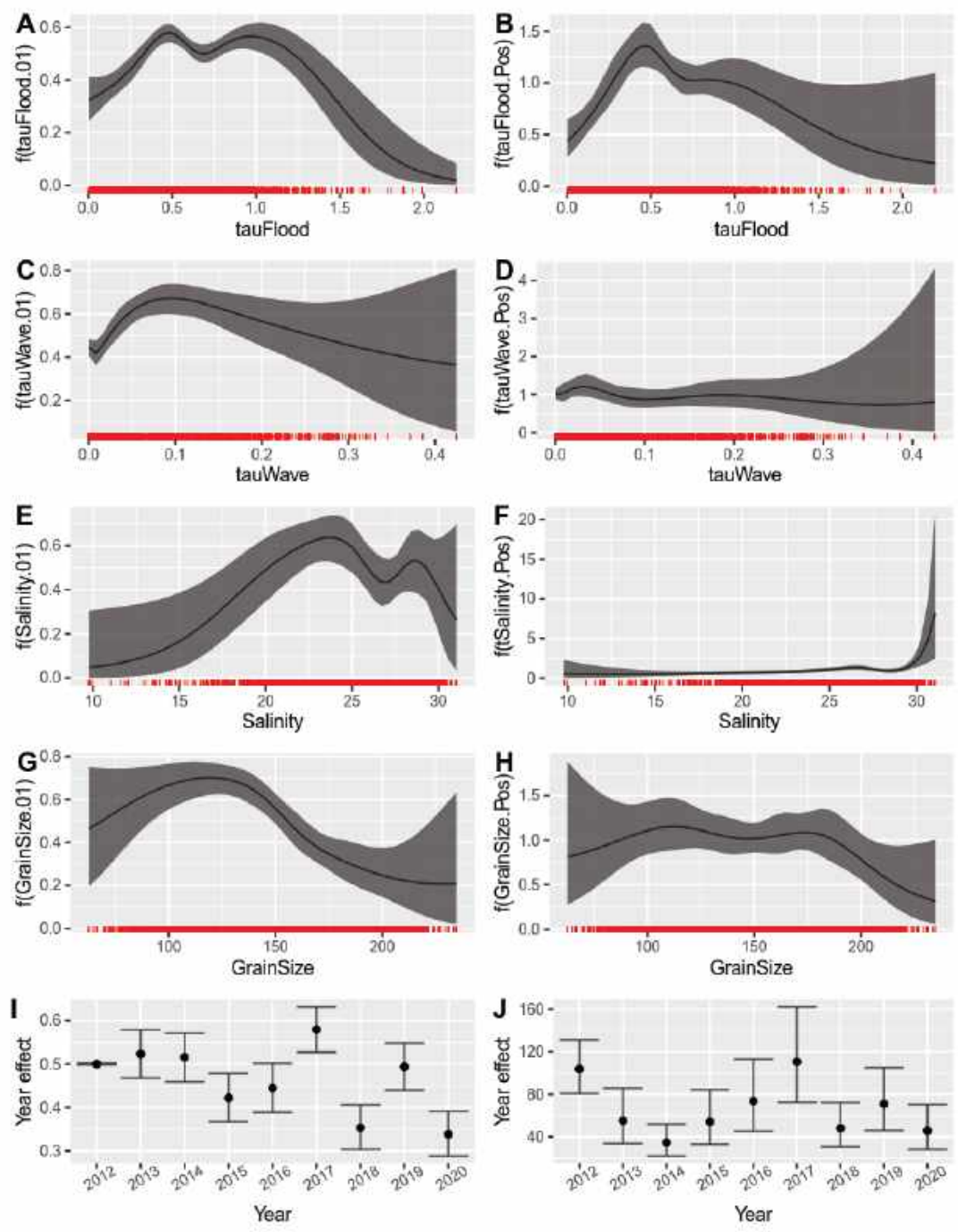


*Figure 10.2. Posterior mean values and 95% credible intervals for all smoothers and the year effect obtained by the ZAG model with a shared spatial-temporal replicate correlation. The figures on the left are for the binary part and the figures on the right are for the Gamma part of the ZAG model applied on the* M. edulis *abundance data.*

The smoothers of the environmental factors all affect the presence/absence of the species as shown in the left-hand column of
Figure 10.2. However, only tauFlood affects the numerical value of the abundance in places where the species is present.
The categorical factor year allows for spatially averaged effects of the year of sampling. It shows high average probability to be present in the years 2017 and 2019. Where the species was present, the average numerical abundance was highest in the years 2012 and 2017.

Between 2018 and 2019, there was an increase in the average probability of occurrence, and an increase in the average numerical abundance in places with presence.
The spatial fields of all years for this species are shown in Figure 10.3. These fields are characterized by a patchy set of hotspots and coldspots with a limited spatial scale. From year to year, the pattern is rather variable.

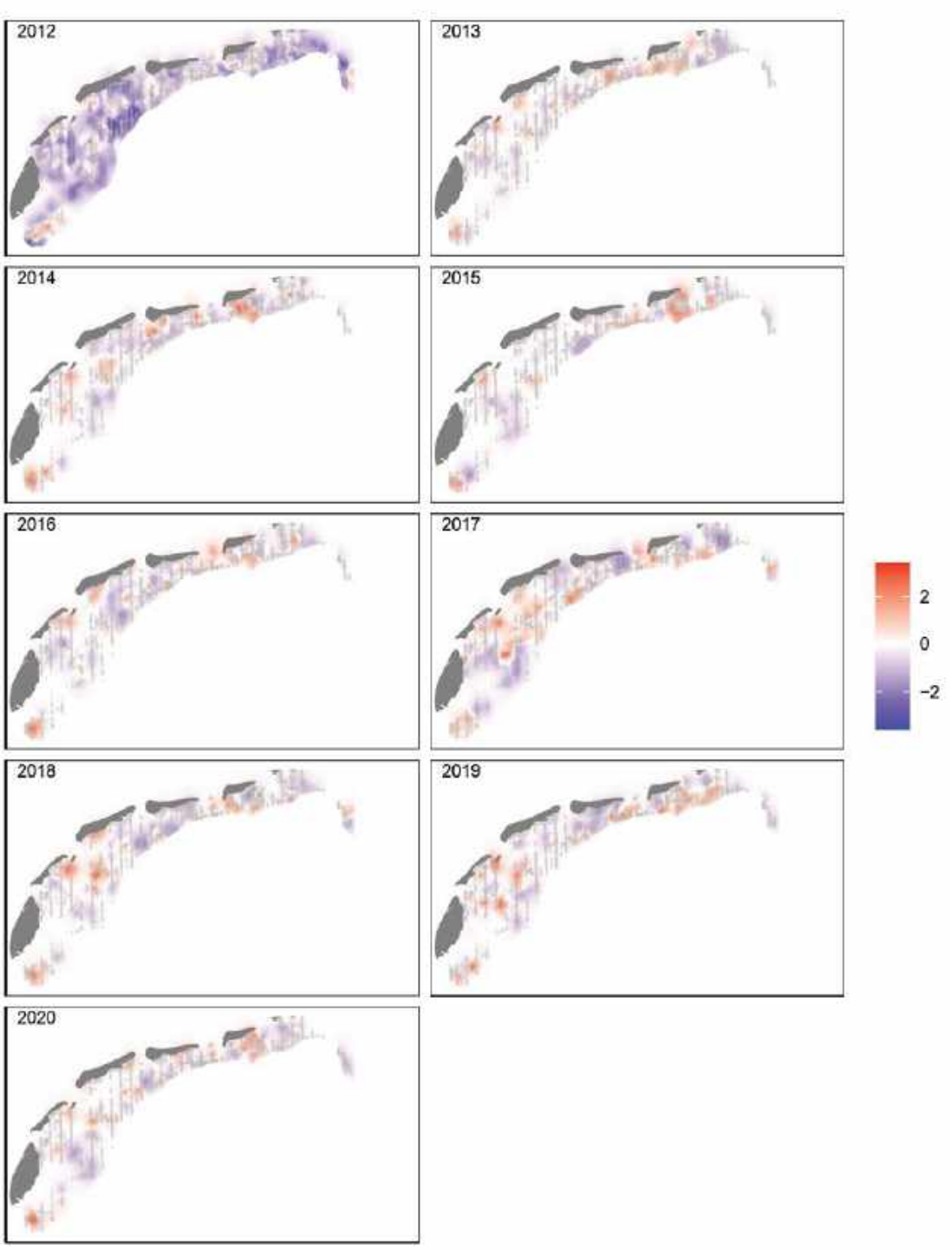


*Figure 10.3. Posterior mean values of the shared spatial-temporal random fields obtained by the ZAG model applied on the M. edulis abundance data.*

The effect of the MSC Zoe incident was estimated by comparing two statistical models that differ in the specification of the random fields. In the first model, every year has a separate spatial correlation field. In the second model, only a single spatial field was used for both the years 2018 and 2019. Based on DIC, the latter model was clearly to be preferred. (Table 10.1).

*Table 10.1. DIC values of two ZINB GAMs with spatial-temporal replicate correlation. The full model in the first row contains a spatial random field for each year. The sub-model in the second row also contains a spatial random field for each year, except for the 2018 and 2019 data. These are modelled by 1 spatial random field.*

| Model | DIC |
|---|---|
| ZAG GAM + replicate SRF (2018 and 2019 separate) | 39362 |
| ZAG GAM + replicate SRF (one field for 2018 and 2019) | 39903 |

This implies that there was very little information in the data that justified the use of extra parameters to separate the fields of 2018 and 2019, or more generally put that there was no reason to conclude that the spatial pattern of the species in 2019 was different from the pattern in 2018.
The conclusion based on the comparison of the model with and without a common field for the two years 2018 and 2019, was further corroborated by analyzing the posterior probability distribution of the differences $\delta_i$ between the spatial fields of 2018 and 2019 for each of the sampling locations that were sampled in both years. Differences are deemed 'important' if 0 is not included in the 95 % credible interval for the difference.
There were 30 stations where the difference $\delta_i = u_{i,2019} - u_{i,2018}$ was important. This represents 2.49% of the stations. From these 30 changes, 24 changes were an increase, and 6 were a decrease from 2018 to 2019.
The stations with large differences between the spatial fields are highlighted in Figure 10.4. They are spatially clustered in four groups, three of which saw an increase between 2018 and 2019. Most important differences are spatially concentrated in the eastern Wadden Sea.

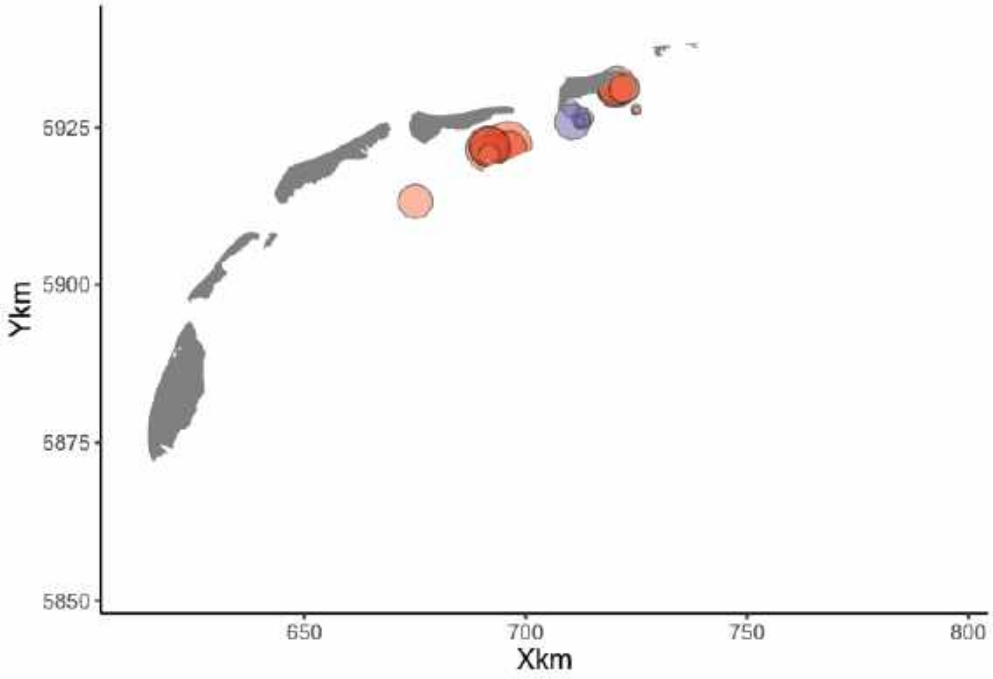


*Figure 10.4.* Mytilus edulis *abundance: Posterior mean values of* $\delta i = u_{i,2019} - u_{i,2018}$ *for stations* $i$ *that were sampled in 2019 and 2018, and for which the 95% credible interval does not contain 0 (no correction for multiple testing has been applied). Red symbols are increases from 2018 towards 2019, purple symbols are decreases.*

### 10.2.2 Analysis of Biomass

Biomass data of *M. edulis* were also modelled with a ZAG distribution, with exactly the same model formulation as used for abundance.

The smoothers for the environmental variables (Figure 10.5 )are very similar to the smoothers of the abundance data (Figure 10.2). All factors affect presence/absence of mussels, while only the bottom shear stress due to currents has a substantial influence on the numerical value of the biomass in places where the species is present.

The year effects and the spatial-temporal random fields (Figure 10.6) are also similar to the results obtained for abundance data.

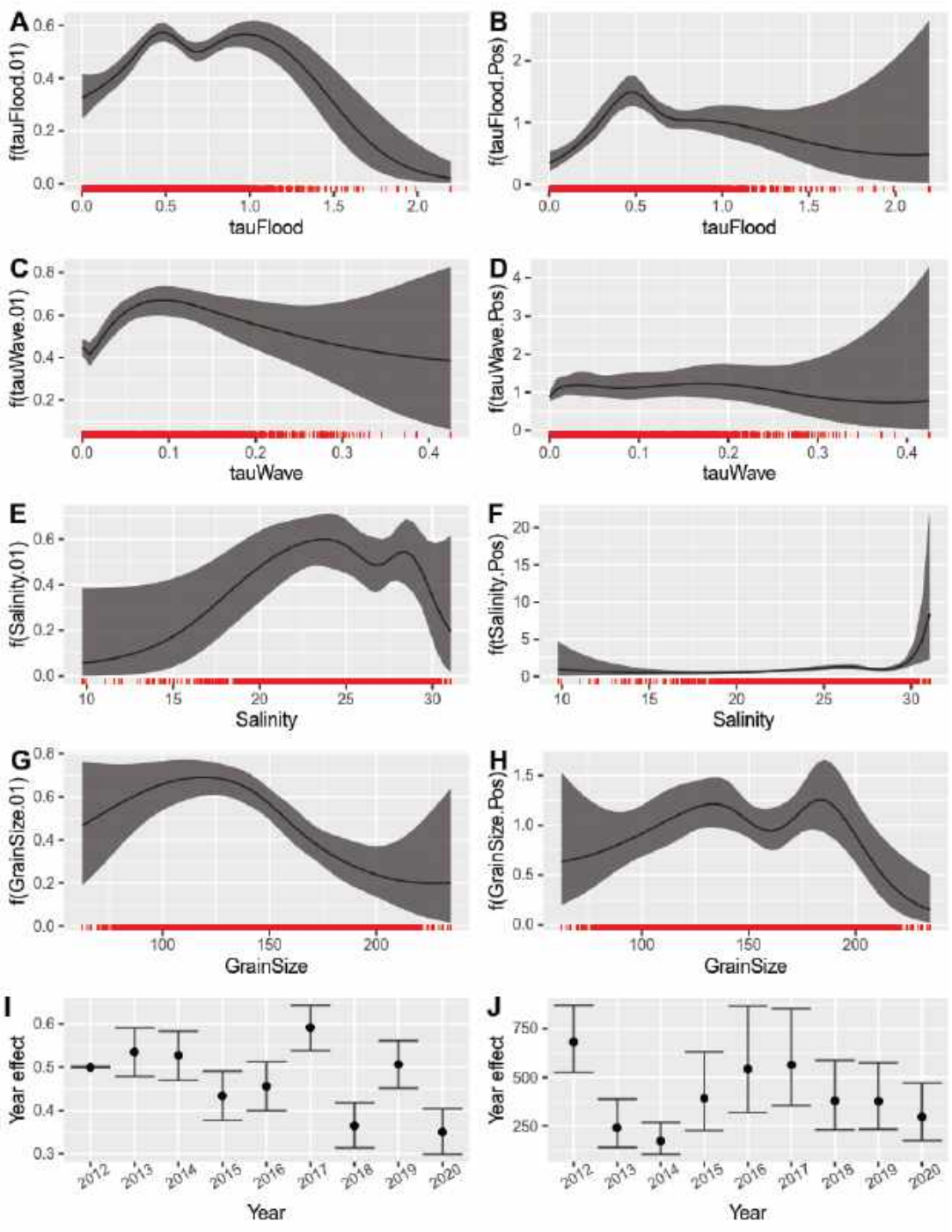


*Figure 10.5. Posterior mean values of all smoothers and the year effect obtained by the ZAG model with a shared spatial random effect. The figures on the left are for the binary part, and the figures on the right are for the Gamma part of the ZAG model applied on the biomass data of* M. edulis*.*

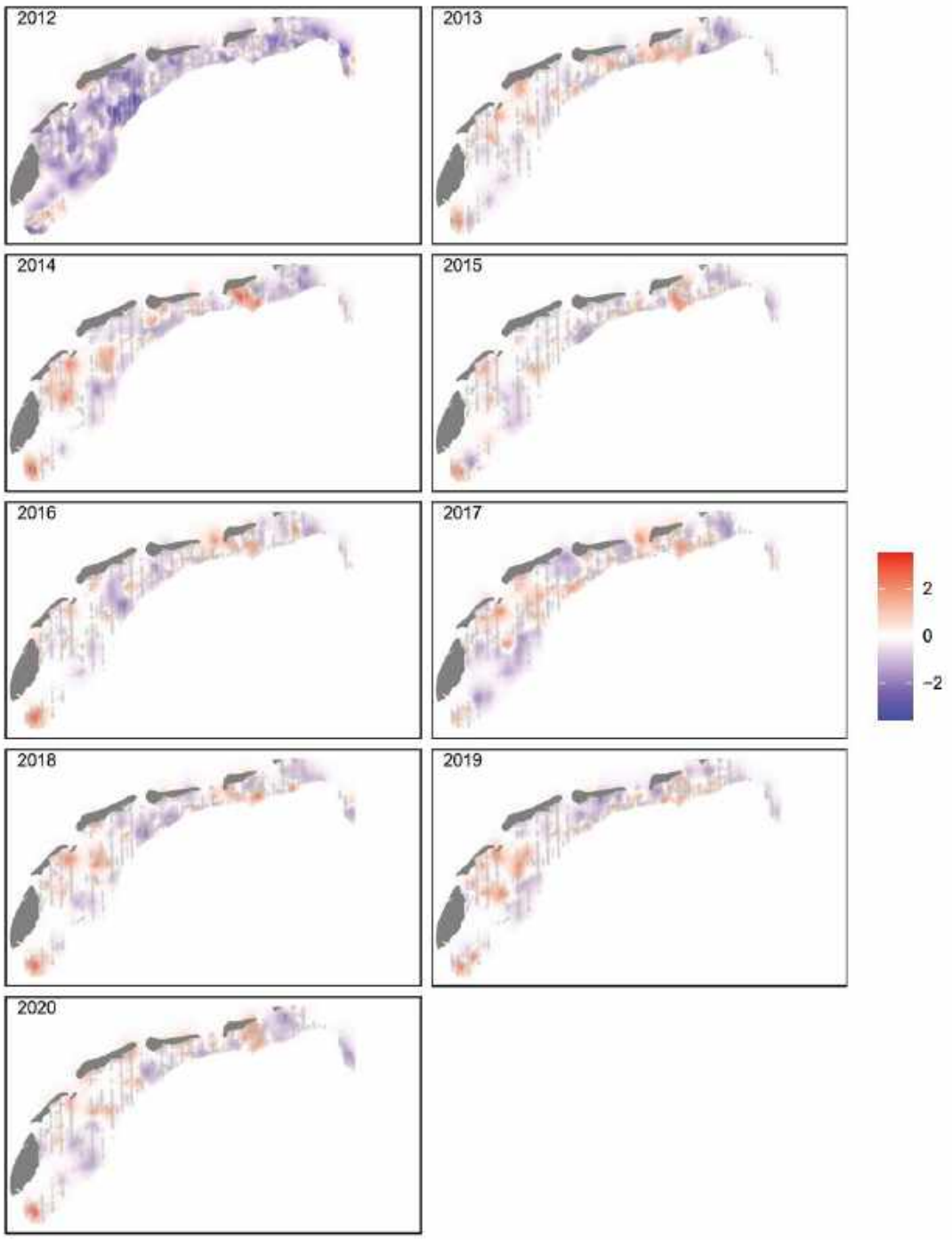


*Figure 10.6. Posterior mean values of the shared spatial-temporal random fields obtained by the ZAG model applied on the* M. edulis *biomass data.*

A comparison between a model with a separate spatial-temporal random field for every year, and a model with a common field for the years 2018 and 2019, shows that the latter model is a worse fit to the data ( Table 10.2). This contrasts with the result of the analysis of abundance and highlights the differences between the spatial fields of 2018 and 2019.

*Table 10.2. DIC values of two ZAG GAMs with spatial-temporal replicate correlation. The full model in the first row contains a spatial random field for each year. The sub-model in the second row also contains a spatial random field for each year, except for the 2018 and 2019 data. These are modelled by 1 spatial random field.*

| Model | DIC |
|---|---|
| ZAG GAM + replicate SRF (2018 and 2019 separate) | 48042 |
| ZAG GAM + replicate SRF (one field for 2018 and 2019) | 48122 |

When examining the posterior mean values of the difference in the spatial random field between 2018 and 2019, there are 12 stations where the difference $\delta i = vi,2019 - vi,2018$ is important. This represents 0.99% of the stations. From these 12 changes, 7 changes are an increase, and 5 are a decrease from 2018 to 2019.

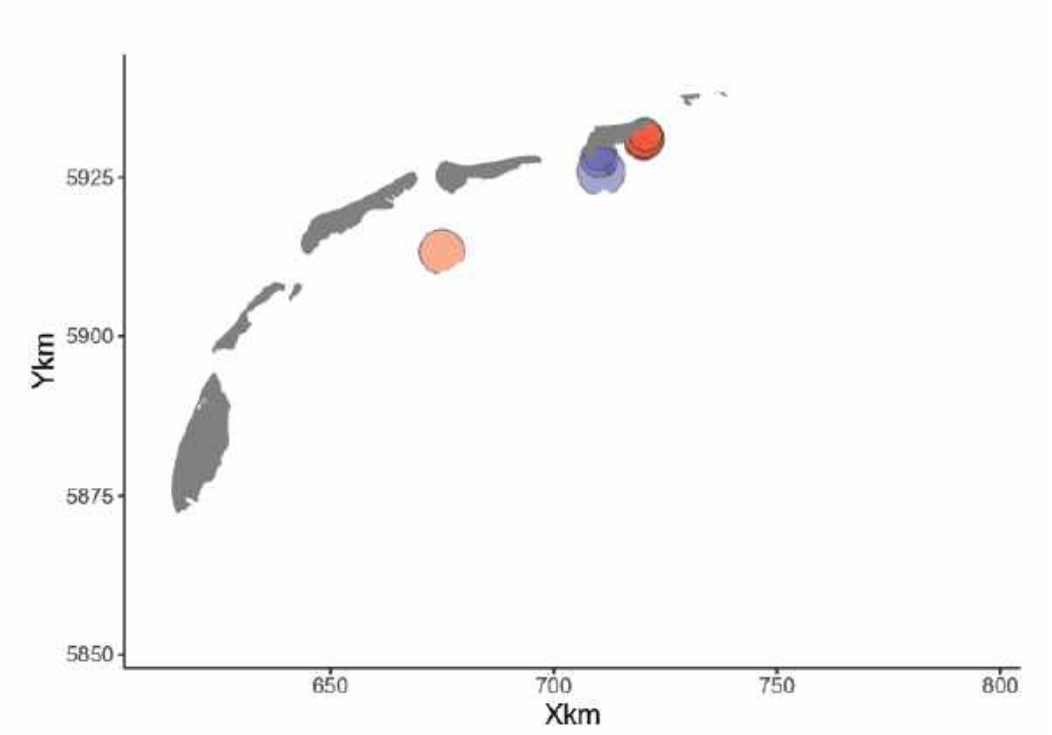


*Figure 10.7.* Mytilus edulis *biomass: posterior mean values of* $\delta i = u_{i,2019} - u_{i,2018}$ *for stations* $i$ *that were sampled in 2019 and 2018, and for which the 95% credible interval does not contain 0 (no correction for multiple testing has been applied). Red symbols are increases from 2018 towards 2019, purple symbols are decreases.*

As for abundance, the areas of important increase and decrease are spatially clustered and mainly observed in the north-eastern part of the Wadden Sea (Figure 10.7).

## 10.3 Discussion

As is the case for most shellfish species, the population of mussels in the Wadden Sea is strongly determined by the stochasticity of the recruitment process. The fact that recruitment is unsuccessful in most years, especially in the intertidal (Van Stralen, 2002), and the low survival of young, recently settled beds (van der Meer et al., 2018), was the cause for the very long restoration time after the near-disappearance of intertidal mussel beds in the early 1990s. However, after the recovery, mussel populations have remained stable on the long run, but strongly fluctuating at the year-to-year scale (Troost et al., 2021).
In the data set studied here, the highest recruitment was found in 2016. Judging from the probability of presence and the average number when present in 2019, recruitment in 2018 was smaller than in 2016, but higher than in other years.
As mussels are gregarious animals, high density values are always spatially concentrated in mussel beds. Locally, very high biomass values are attained. Many places in the Wadden Sea are suitable for settlement of mussels (Brinkman et al., 2002), but as the total area of mussel beds is restricted and relatively constant on the long run, only a fraction of these are actually occupied with mussels. The spatial fields, that have relatively small hotspots and coldspots, reflect this pattern.
The spatial fields of biomass showed some differences between 2018 and 2019. When analyzed per sampling point, this appeared to be the case in only a very limited number of points, but the local differences were sometimes large. In half the cases, the difference was an increase, in the other half it was a decrease. Such a pattern is to be expected where the population numbers and biomass are either high (within a mussel bed) or very low (outside the beds) and the precise occurrence of the beds cannot be accurately predicted by the cofactors. The spatial random fields then show the occurrence of beds. Comparison of the fields show that hotspots tend to remain for a number of years before they disappear, in accordance to the dynamics of the beds.
In the background of these dynamics, the small differences between the spatial random fields of 2018 and 2019, cannot be interpreted as a consequence of the MSC Zoe incident, as natural causes for the variability are much more likely.

## 10.4 Conclusion

The dynamics of the mussel population in the Wadden Sea are determined by the stochastic nature of recruitment processes, and by the gregarious occurrence of mussels in organized beds. Small differences found between the spatial random fields of 2018 and 2019 can well be explained by these dynamics. It is very unlikely that any difference found was caused by the MSC Zoe incident.

# 11 The Eider Duck (*Somateria mollissima*)

## 11.1 Biology and ecology

Eiders are large, robust seaducks that live along rocky shores and sandy coastlines and estuaries in the North Atlantic and North Pacific. There is probably very little, if any exchange between these two separate populations (Voous 1960). Eiders do migrate, but over relatively small distances. The Wadden Sea is nearly at the southern breeding range of the species, with only small numbers breeding further south, in the Dutch Delta area (Smit 2018), Belgium and France (Keller *et al.* 2020), only very few migrate further south than France and reach the Mediterranean and the Black Sea: some have even bred here (Ardamatskaya 2001; BirdLife International 2021). The European strongholds of the species are in the Baltic, along the coasts of Norway and in the international Wadden Sea. Within the Netherlands, most birds are found in the central and eastern Wadden Sea (Swennen *et al*. 1989; Smit 2018). Birds breeding in northern Europe, e.g., in the Faroes, in Iceland and Svalbard have a slightly different appearance and belong to a different subspecies than the nominate that breeds and winters in the Netherlands (BirdLife International 2021). Although some of these northern birds may reach the British Isles in winter, their occurrence in the Netherlands is, at best, exceptional (Leopold 2005).

Eiders, being seabirds, have a long potential lifespan. From ringing records, the oldest known bird was >36yrs (Fransson *et al*. 2017). Their potential for population growth is large for seabirds, with their average clutch size of about 5 eggs (Bregnballe 2002). However, eiders only started breeding in the Netherlands in 1906, on Vlieland (Swennen 1976) and their numbers increased only slowly to a peak of 10800 breeding pairs around the year 2000 (Kats 2007), after which numbers declined again (Smit 2018). In the Netherlands eiders have suffered several mass mortality events, from pollutants (Swennen & Spaans 1970) oil spills (Swennen 1972) and food shortages (Camphuysen *et al*. 2002). The sizes of the wintering population in the Netherlands is much larger than the breeding population, as large numbers of birds from further north (mainly from the Baltic) come to the Wadden Sea to winter. Numbers have increased greatly in the 20$^{th}$ century, probably aided by both nature conservation (protection) and an ample food supply at mussel culture plots (Swennen 1976; Swennen *et al*. 1989; Kats 2007). However, wintering numbers have decreased recently, from ca. 100-150 000 birds in the years 1993-2005, to ca. 50-100 000 in 1996-2020 (Sluijter *et al*. 2020). The conservation status in Europe of the eider has recently been uplisted to Near Threatened because of the moderate declines seen in many parts of its range (BirdLife International 2021); the current decline in the Netherlands is not just a local phenomenon.

## 11.2 Interaction with plastics and salvage operations after the MSC Zoe incident

In the Netherlands, Eiders prefer marine, relatively sheltered and shallow waters, rich in bivalves. Their principal habitats are in the Wadden Sea, where mussels (preferably the thin-shelled ones on culture plots) and cockles are the preferred foods (Swennen 1976; Kats 2007). When these preferred foods are scarce, or other bivalves are abundantly present, eiders may switch to e.g., through shells (*Spisula*) or razor clams (*Ensis*) (Leopold *et al*. 2001; Ens *et al*. 2006; Tulp *et al*. 2010). The diet is broad, however, and includes, besides bivalves also gastropods, crustaceans, echinoderms, and even fish (Leopold et al. 2001). If any of these prey animals contain contaminants, e.g. plastic particles from the Zoe spill, eiders might ingest these. As eiders are used to foods that are hard-shelled, with lots of indigestible material, they might also ingest plastic particles directly, if these cover shellfish beds, or lie between shellfish on the sea floor.

The large-scale, post-spill salvage operations, aimed at recovering as many lost containers as possible, will have disturbed seaducks, including eiders, in the area of operation, and hampered feeding in the North Sea coastal waters north of the Dutch Wadden isles.

## 11.3 Data collection and analysis

The data set consists of aerial counts of the species (see chapter 3.4) collected between 1993 and 2020 by the observers Rijkswaterstaat and WMR. In the observation years, not all months are covered with countings. For the species, only the winter months are relevant. In order to avoid an excessive number of unavailable observations, the analysis has been restricted to the months December, January and February. In this series, there are also missing observations.
The countings have been grouped in 10 areas, 4 in the Wadden Sea (A1 to A4) and 6 in the North Sea coastal area (A5 to A10).

The raw time series in the different areas reveal that there are large differences between areas in the average number of birds counted. Moreover, the trend in time seems to be very different for North Sea areas (virtual disappearance of the species after 2005-2010) and the Wadden Sea (much more steady presence in the long run, but large fluctuations between years). Figure 11.1 illustrates the counting areas and the raw trends in the time series.

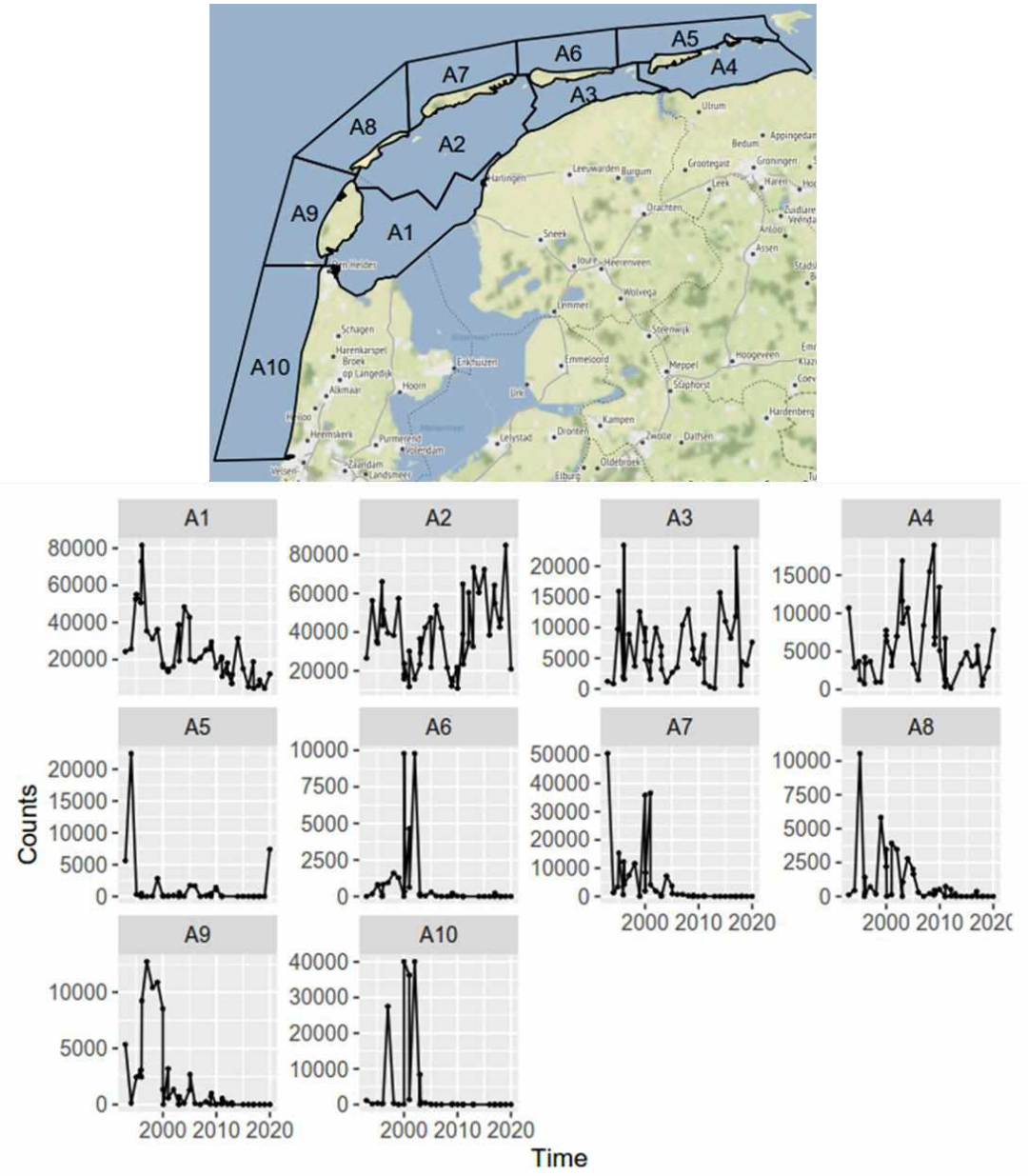


*Figure 11.1. Map of the counting areas (top) and raw time series of the counts in the 10 areas (bottom). Note the different y-scales used in the graphs. Observation points have been connected with lines within each area for clarity, but not all areas have been covered on all observation dates.*

For the model building every observation point (count of birds) is associated with an area, a moment in time and an observer (RWS or WMR). In all models fitted, it has been assumed that the data follow a negative binomial distribution. The first model uses a common trend for all areas. The areas can have a different intercept, which is modelled as a fixed factor, but the time course is the same. As this model did not capture the essence of the data, it was changed into a model where every area is allowed to have a different trend, with the trends independently sampled from a statistical distribution. This model improved the fit, but the assumption of (spatial) independence of the trends could not be maintained. Neighboring areas have more similar trends than areas far apart. Therefore, a final model fitted trends in the different areas that are spatially correlated. That provided a satisfactory model to the data.

The time trend is modelled as a Random Walk trend. Spatial correlation between trends of neighboring areas are modelled using CAR autocorrelation. (Chapter 4.5)

The final model fitted to the data has a negative binomial distribution, separate trends fitted to each area but with spatially correlated intercepts. The model is specified by the following prescription:

$$
\begin{aligned}
Counts_{is} &\sim NB(\mu_{is}, \theta) \\
E[Counts_{is}] &= \mu_{is} \\
var[Counts_{is}] &= \mu_{is} + \frac{\mu_{is}^2}{\theta} \\
\log(\mu_{is}) &= \beta_1 + f_i(Time_{is}) + Observer_s + u_i \\
f_i(Time_{is}) &= RW1 \\
u_i &\sim CAR
\end{aligned}
$$

Where NB stands for negative binomial distribution with parameters mean and dispersion parameter. E[Y] is the expected value of Y, given by the mean of the negative binomial. Var[] is the variance operator. Its specification follows the definition of the negative binomial distribution. The expected value is log-linked to a linear equation that contains an intercept, a Random Walk Trend smoother of time, and a spatially correlated random intercept that is specified according to CAR correlation.

The main result of the model is formed by the trends in the 10 counting areas (Figure 11.2). The time smoother in the four Wadden areas is relatively flat. It has 0 in its 95 % credible interval at all times. This indicates that in the longer run, there is little or no trend in the numbers of eider ducks in the Wadden Sea. This is very different for the North Sea counting areas. All of the time smoothers cross the y=0 line at some point, but the time is different for the different areas. It happened latest (around 2010 only) in areas A5 and A6, and in area A5 numbers have started to go up again as of 2017. The other areas A7 – A10 lost their ducks earlier (between 2005-2010), and no recovery is visible.

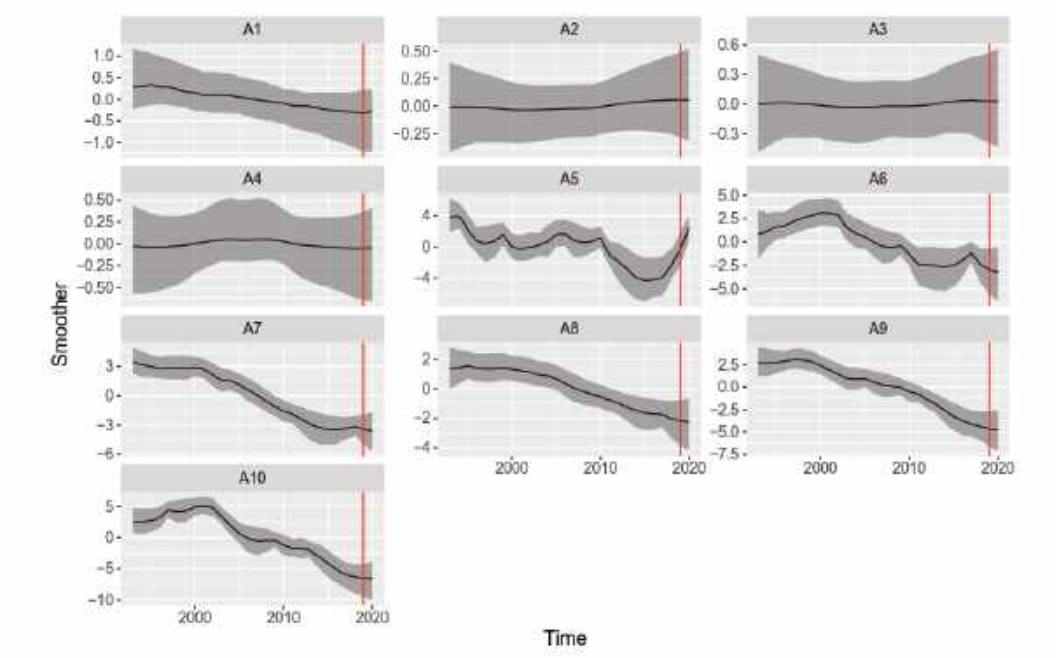


*Figure 11.2. Posterior mean values and 95 % credible intervals for all smoothers in the negative binomial GAM with CAR correlation. A vertical red line is drawn at January 2019 in each panel.*

The random intercepts of the ten areas are correlated in space, as is shown in Figure 11.3. The 'hotspot' for eider ducks is the western Wadden Sea and in particular the Vlie tidal basin.

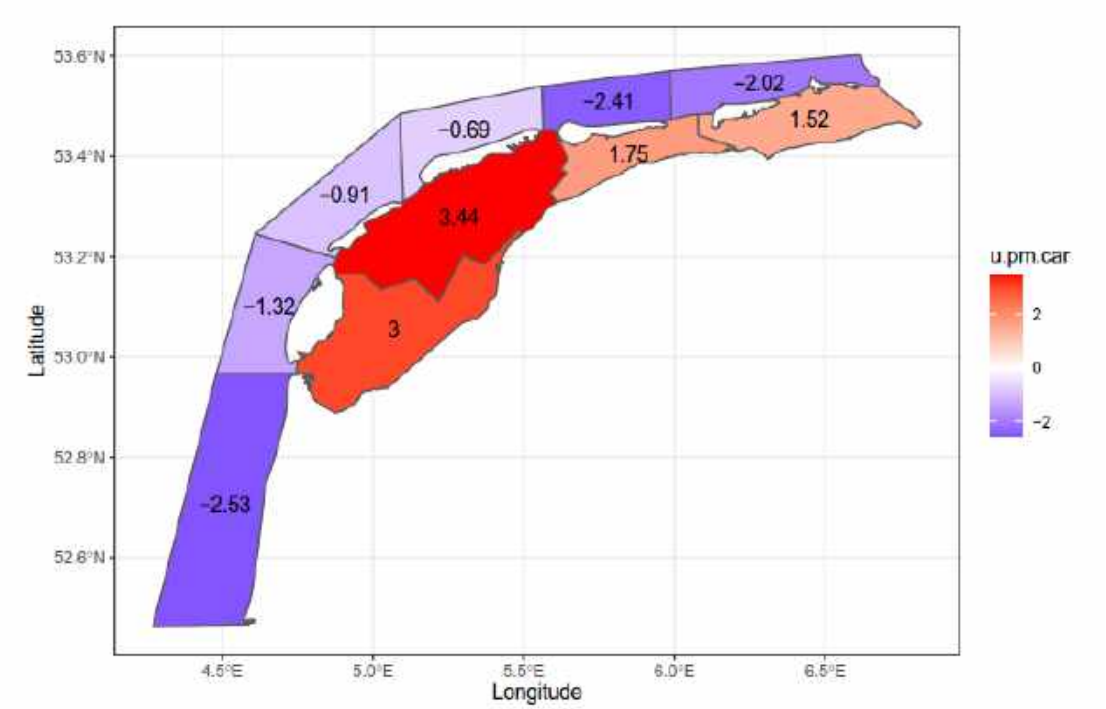


*Figure 11.3. Posterior mean values of the random intercept $u_i$. The NB GAM with CAR spatial correlation was used.*

Effects of the MSC Zoe incident are not apparent when inspecting the temporal smoothers in Figure 11.2 around the red line. The comparison has formally been executed by calculating, for each area, the posterior probability distribution of the difference between the trend in January 2019 with January 2018 on the one hand (T2019-T2018), and with January 2020 on the other hand (T2020-T2019). The results of this analysis are summarized in Figure 11.4. Only for area 5, the credible interval for the comparison with 2020 does not encompass zero. This area has an increasing trend since 2017 and that increasing trend is reflected in these differences. It is impossible, however, that a change that has been ongoing since several years before the Zoe incident, would be caused by the latter. For the other North Sea areas we see that there is in general a slight decrease of the trend from year to year, but the values of the comparisons with 2018 and 2020 are very similar and, again, do not point to any disturbance of the time series. Moreover, in these cases zero is a very likely value for the difference.

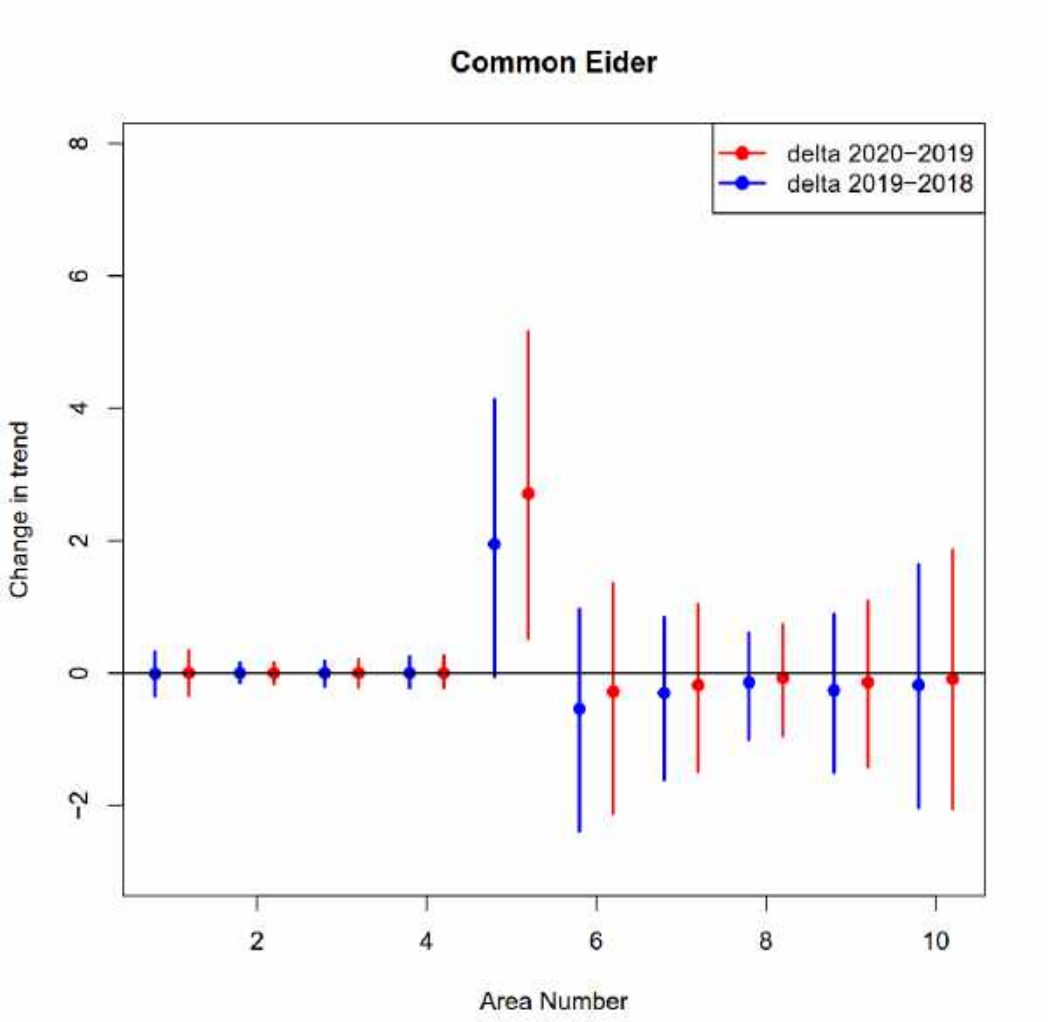


*Figure 11.4. Changes in the trend between 2019 and surrounding years. In blue the difference of the trend with 2018 (value in 2019 minus value in 2018) is shown for the 10 areas. In red the difference with 2020 (value 2020 minus value 2019). Shown are the 95 % credible intervals of the posterior distribution of the difference. Dots denote the mean difference.*

## 11.4 Discussion

Eiders and common scoters traditionally show quite different distribution patterns in the Netherlands, but these patterns have changed over time. Eiders are, largely, typical ducks of the Wadden Sea. They breed on the islands, and winter, in large numbers, in the Wadden Sea where their main prey species are mussels *Mytilus edulis* and cockles *Cerastoderma edule*. The wintering numbers are much larger than those of the local breeding population, as large numbers of migrants from the Baltic region come here in winter. Only very small numbers of eiders winter south of the Wadden Sea. Numbers of eiders in the Wadden Sea have probably increased significantly, in response of mussel culturing, which provided ample, readily available, and good quality food for these diving ducks. Only when stocks of both mussels and cockles were extremely low in the Wadden Sea in the early 1990's, did the eiders move to the North Sea, where they joined the large flocks of common scoters (Leopold 1993; Camphuysen et al. 2002).

Both species of sea duck swallow their prey whole, crush the shells in their muscular gizzard (stomach), digest the contents and defecate the shell fragments. Their foraging takes a lot of energy and they roughly consume a daily amount of shellfish, equal to their own body mass.

As they must dive for their food, and must obtain their prey partly by underwater digging, they are probably rather indiscriminatory while ingesting food. Therefore, small stones, sand, but also human artefacts such as pellets lost by the MSC Zoe, might be gobbled up by these diving ducks, when feeding at the seafloor. Both species are also easily disturbed by shipping, and the salvage operations for the lost containers and their contents, might have displaced the ducks. Therefore, it was conceivable that numbers of ducks might have dropped after the MSC Zoe had lost part of her cargo, either through the associated disturbance (North Sea coastal waters) or through detrimental effects of the lost cargo (North Sea and Wadden Sea).
Counting methods of sea ducks have changed for the North Sea coastal area, but not for the Wadden Sea, which is the most important area of eider ducks. The negative trend and disappearance of the eider duck from the North Sea cannot be a consequence of methodological changes, because the methods have improved over time and the possibility to detect isolated birds is higher in recent years than before.
The reason for the declining trend in the North Sea is not well known. The trend may find its cause in the Netherlands, but also in the summer staging areas of the species or in a change in wintering migration.
Analysis of the time trend did not reveal any change that can be linked to the MSC Zoe incident. In one area, there was an important difference between the trend value in 2019 and the surrounding values. This was, however, part of a trend that had been ongoing since 2017 and that was not visually changed in 2019 compared to the years before and the year after.

## 11.5 Conclusion

The data reveal an ongoing pattern of change in the winter distribution of the eider duck between the Wadden Sea and the coastal North Sea. In recent years, numbers are concentrated in the Wadden Sea, although recently one of the North Sea areas saw a small increase.
Trends were steady around the year 2019 when the MSC Zoe incident happened. In one area, the trend value of 2019 is different from the year before and the year after, but this difference is part of an ongoing trend that had started two years earlier.
We conclude that no effects of the MSC Zoe incident, caused by either the plastics lost or the salvage operations, is visible in the data.

# 12 The Common Scoter (*Melanitta nigra*)

## 12.1 Biology and ecology

Common scoters are medium-sized sea ducks that breed mostly in boreal and tundra habitats, from Greenland to Russia, and south to the British Isles (Voous 1960; Keller *et al*. 2020; BirdLife International 2021). The species does not breed in the Netherlands but is a common winter visitor here (Poot 2018). Common scoters are highly migratory. The largest concentrations of wintering birds are found in the Baltic (Durinck *et al.* 1994; Skov et al. 1995). Numbers in the Baltic, including Skagerrak/Kattegat are nearly ten times higher (up to 1 million birds; Durinck et al. 1994) than those wintering in the Netherlands (up to 135 000; Leopold *et al*. 1995) and in the UK (135 000; Robinson 2005). Wintering scoters may be found all along the Atlantic seaboard, south to Mauritania (BirdLife International 2021) but the largest numbers are found in the regions mentioned above.

In many parts of its ranges, particularly in the Baltic, the species appears to be declining significantly. A decline in wintering numbers is also seen in the Netherlands, where numbers peaked in the early 1990s (Leopold *et al*. 1995; Sluijter *et al*. 2020) but declined from then on. In the past ten years, numbers of wintering common scoters in the Netherlands fluctuated between 30 000 and 60 000 with most birds residing in a core area north of the eastern Wadden Islands (Terschelling-Ameland-Schiermonnikoog). While large numbers have incidentally also occurred elsewhere in Dutch coastal waters, such as off Texel (Leopold *et al*. 2014) or off the North-Holland mainland coast (Fijn *et al*. 2017), numbers in two other formerly important areas, Voordelta (28 000 in 1980; Leopold *et al*. 1995) and the western Wadden Sea (40 000 in the early 1960s; Swennen 1985) have been decimated, to only a few thousands at most in recent years in each of these two areas. Despite these declines, due to its large range and (still) large population size, the conservation status of the species does not approach the thresholds for Vulnerable and its status is kept as Least Concern. However, BirdLife International (2021) concludes that: “if surveys do not locate the numbers that appeared to be missing from the Baltic Sea in recent years (2007-2009), this species is likely to qualify for uplisting” (i.e. being given a conservation status).

There is some evidence, that common scoters were once very numerous in the western Wadden Sea (Swennen 1985) and blue mussels may have been the staple food here. Blue mussels are also the likely food of common scoters in the Baltic (Durinck et al. 1994). In both these areas, the scoters were usually found in slightly deeper waters (5-15 m) than the eiders. This is also true for the North Sea coastal zone in the Netherlands and Denmark, but here *Spisula subtruncata* is the most important food source (Durinck *et al*. 1993; Leopold *et al*. 1995). However, when *Spisula* is scarce, razor clams (*Ensis*) are a good alternative (Skov *et al*. 2008; Tulp *et al*. 2010; Leopold *et al*. 2010; 2014; Schwemmer *et al*. 2019).

## 12.2 Interaction with plastics and salvage operations

Common scoters take a large variety of food species and anything seems to be acceptable, as long as the prey occur at large densities and in the right size range (Fox 2003). If their prey contain contaminants, e.g. plastic particles from the Zoe spill, common scoters might ingest these. As scoters are used to foods that are hard-shelled, with lots of indigestible material, they might also ingest plastic particles directly, if these cover shellfish beds, or lie between shellfish on the sea floor. The large-scale, post-spill salvage operations, aimed at recovering as many lost containers as possible, will have disturbed the common scoters, the most numerous sea ducks in the area of operation at the time of the clean-up, and hampered feeding in the North Sea coastal waters north of the Dutch Wadden isles.

## 12.3 Data collection and analysis

The data set consists of aerial counts of the species (see chapter 3.4) collected between 1993 and 2020 by the observers Rijkswaterstaat and WMR. In the observation years, not all months are covered with countings. For the species, only the winter months are relevant. In order to avoid an excessive number of unavailable observations, the analysis has been restricted to the months December, January and February. In this series, there are also missing observations.
The focus of counting common scoters in the Netherlands was on North Sea coastal waters. In the Wadden Sea, the focus was on counting eiders, while common scoters were always counted in the margin of these eider counts, but in reality, coverage for common scoters in the Wadden Sea was often incomplete and these data are not used in the analyses for common scoters. Total numbers of common scoters counted in the Wadden Sea never exceeded a few thousand, while numbers in North Sea coastal waters were in the tens of thousands, in some years even over 100,000, so numbers in the Dutch Wadden Sea were relatively insignificant.
The countings have been grouped in 6 areas in the North Sea coastal area, which correspond exactly with the areas used in the analysis of eider duck data (chapter 11).
The earliest countings of common scoters were countings from boats, but since 1993 most countings were performed from airplanes. Since 2004 plane countings are the only source of information. Because the counting method is colinear with time, and to avoid contamination of the time trend with methodological aspects, only the plane countings were used in the analysis. Because of this restriction, only one observer (Rijkswaterstaat) has produced the data. No term for observer had to be included in the statistical model.

The raw time series in the different areas (Figure 12.1) reveal the strong variability of the number of common scoters in the Wadden Sea coastal area. In some years, peak numbers of more than 100,000 ducks have been counted, whereas in other years the numbers were very low. This extreme variability makes it difficult to discern clear trends in the data.

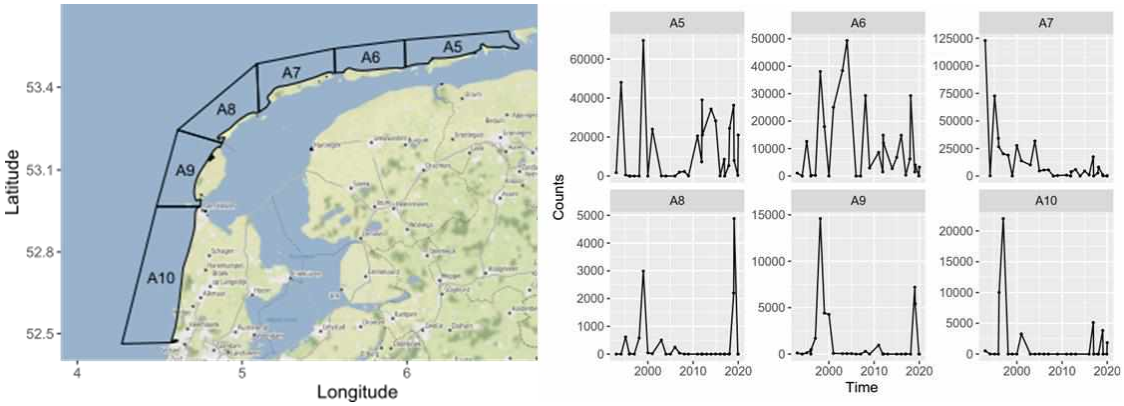


*Figure 12.1. Map of the counting areas (left) and raw time series of the counts of common scoters in the six areas. Note the different y-scales used in the graphs. Observation points have been connected with lines within each area for clarity, but not all areas have been covered on all observation dates.*

For the model building every observation point (count of birds) is associated with an area and a moment in time. In all models fitted, it has been assumed that the data follow a negative binomial distribution. As was the case for the eider duck, a first model with a common trend for all areas did not capture the dynamics very well. This model is not explicitly reported on. It has been changed into a model with a different intercept and different time trend smoother for each of the areas. There were no clear indications of spatial autocorrelation in the trends, which was fortunate because the low number of areas (6) made the inclusion of a spatial autocorrelation term in the model rather difficult.

The final model has a negative binomial distribution, separate trends fitted to each area but with spatially correlated intercepts. The model is specified by the following prescription:

$$\begin{aligned} Counts_{is} &\sim NB(\mu_{is}, \theta) \\ E[Counts_{is}] &= \mu_{is} \\ var[Counts_{is}] &= \mu_{is} + \frac{\mu_{is}^2}{\theta} \\ \log(\mu_{is}) &= \beta_1 + f_i(Time_{is}) + Area_i \end{aligned}$$

Where NB stands for negative binomial distribution with parameters mean and dispersion parameter. E[Y] is the expected value of Y, given by the mean of the negative binomial. Var[] is the variance operator. Its specification follows the definition of the negative binomial distribution. The expected value is log-linked to a linear equation that contains an intercept, a Random Walk Trend smoother of time, and a spatially uncorrelated random area intercept. The main result of the model is formed by the trends in the 6 counting areas (Figure 12.2). The most prominent feature of the time smoothers is the wide credibility interval. This is a reflection of the large, apparently unstructured, year-to-year variation that was visible in the raw data. The three areas in the north-east, which hold the highest numbers of birds, have no trend or (in the case of area 7) a slight indication of a negative trend over time. The three south-western areas, which hold fewer birds in general, have relatively high numbers around 2000 and in recent years, with a period of low countings around 2010 in between. However, the credible intervals around the time smoothers contain 0 in almost all cases, indicating that there is no real trend visible and that almost all variation is year-to-year variation which is no part of a trend at a longer time scale.

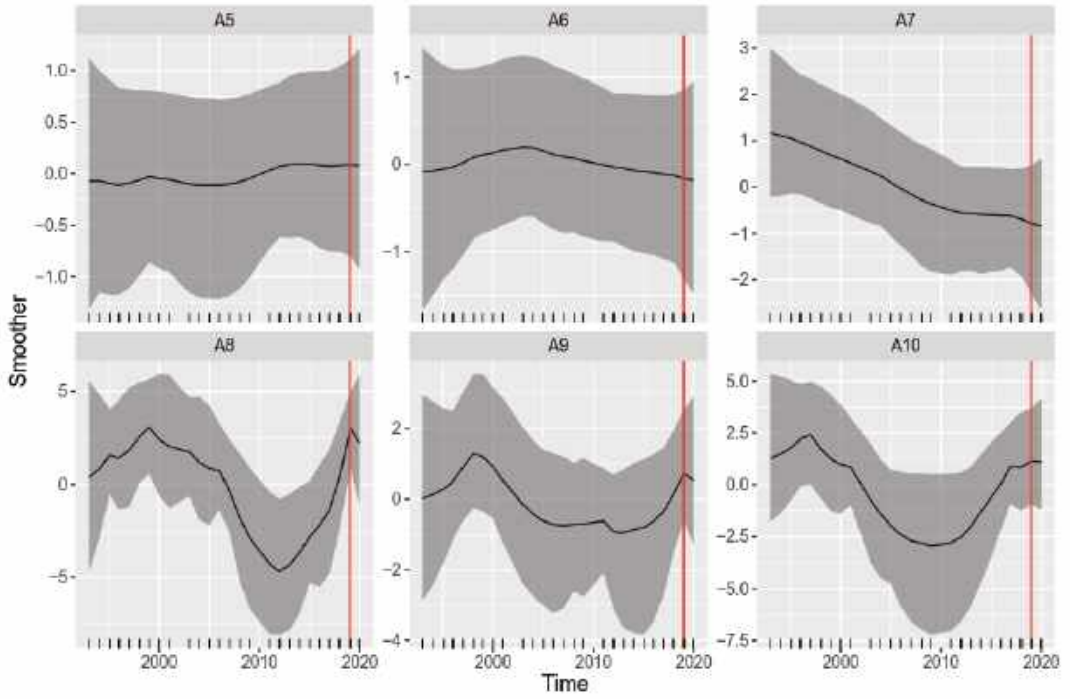


*Figure 12.2. Common scoter: posterior mean values and 95 % credible intervals for all smoothers in the negative binomial GAM with independent area intercepts. A vertical red line is drawn at January 2019 in each panel.*

Effects of the MSC Zoe incident are not apparent when inspecting the temporal smoothers in Figure 11.2 around the red line. The comparison has formally been executed by calculating, for each area, the posterior probability distribution of the difference between the trend in 2019, 2018 and 2020. As we have no January countings in 2018, and no February countings in 2020, the comparisons are made between January 2019 and January 2020 on the one hand, and between February 2019 and February 2018 on the other hand. The results of this analysis are summarized in Figure 12.3. All of the credible intervals encompass zero. The largest difference found is an increase from 2018 to 2019. There is no indication of a change in the trend related to the MSC Zoe incident.

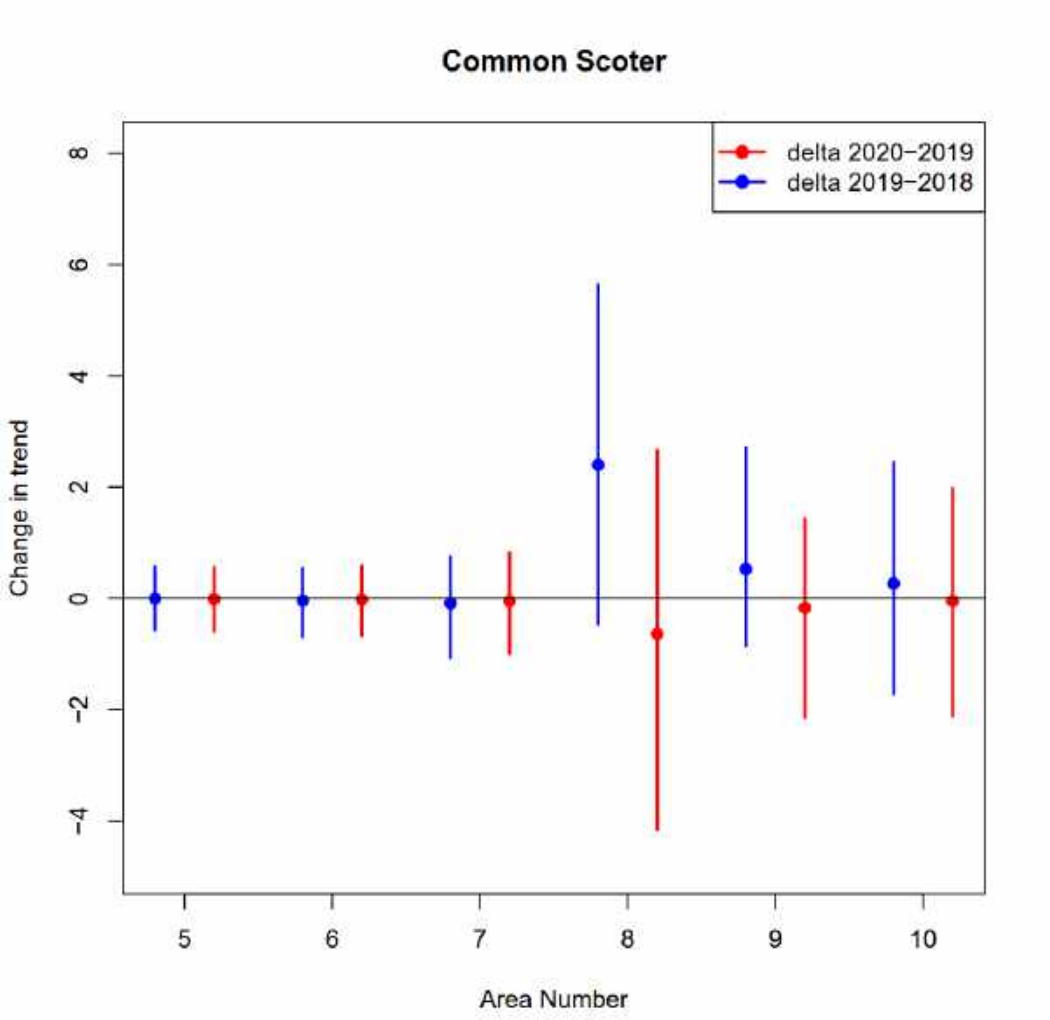


*Figure 12.3. Changes in the trend between 2019 and surrounding years. In blue the difference of the trend with 2018 (value in 2019 minus value in 2018) is shown for the 10 areas. In red the difference with 2020 (value 2020 minus value 2019). Shown are the 95 % credible intervals of the posterior distribution of the difference. Dots denote the mean difference.*

## 12.4 Discussion

In contrast to eider ducks, common scoters are (today) typical ducks of North Sea coastal waters in the Netherlands and not from the Wadden Sea. Their range extends from the Nordic countries all the way down to NW Africa. There is one (popular) publication that states that some 40 000 common scoters wintered in the Western Wadden Sea in the early 1960's (Swennen 1985), but after this period, only a few thousand birds have ever been found here. In the coastal waters of the North Sea just north of the Wadden Sea however, numbers >100 000 were found in the early 1990's, but these more or less halved in later years.

The likely staple food is *Spisula subtruncata*, but other shellfish, most notably American razor clams *Ensis leei* (formerly: *E. directus*) are also taken (Tulp et al. 2010), particularly when stocks of *Spisula* are low. The same applies to eiders (Ens et al. 2006): both species of sea duck are opportunistic foragers (Leopold et al. 2001; Fox 2003) but do have preferred foods in their wintering quarters in the Netherlands.
Due to their opportunistic feeding habits, the species may have swallowed plastic particles if these were present at the feeding location. However, as the species is well adapted to handling large quantities of undigestible material, such as shells and debris to which shells are attached, it is unlikely that this would pose a major problem.
The species is known to be easily disturbed by shipping. For this reason, the intense shipping activities involved in the salvage operation could have been a potential source of disturbance of the species, with the possibilities that ducks would have moved away from the Wadden area to elsewhere along the European coast. However, from the statistical analysis no such change has been detected. The trend value in 2019 does not differ from the trend values in 2018 or 2019. In the one case where the difference was rather large, the value in 2019 was higher than the value in 2018.

## 12.5 Conclusion

Numbers of common scoters in the Dutch coastal zone are variable from year to year, but without a strong overall trend. No differences have been found between the trend value in 2019, after disturbance by the MSC Zoe incident, and trend values in the preceding and in the following year. No evidence for negative effects of the incident has been found.

# 13 The Common Shelduck (*Tadorna tadorna*)

## 13.1 Biology and ecology

The Common Shelduck is a large, somewhat goose-like duck. Its breeding range extends across a wide band from Western Europe to China. The species is a partial migrant wintering from our latitudes south to the Mediterranean basin. In summer the species performs moult migration from breeding areas to wetlands up to 1000 km away to undergo a flightless period of wing moult.

Feeding

Shelduck prefer to forage in shallow muddy water, in intertidal areas such as the Wadden Sea but also in polder ditches and shallow pools and lakes elsewhere. Here they filter the muddy top layer of the soil in search of snails, worms, insects and other edible benthos. Usually they forage by walking on the mudflats or by upending in shallow water and making swinging their beak sideways through the muddy sediment. They may also create pits by trampling movements in shallow water to expose buried bivalves.
In NW European estuaries the most commonly reported prey are Mudsnails *Peringia ulvae*, Baltic Tellin *Limecola balthica*, brood of Mussel *Mytilus edulis* and Cockle *Cerastoderma edule* and other small bivalves, Ragworm *Hediste diversicolor* and the mud shrimp *Corophium volutator.* In the Wadden Sea *Corophium* is an important prey during summer and early autumn, probably also for the huge moult gatherings. In other situations, green algae, diatoms, insect larvae and small worms such as *Tubifex spp*. are taken as well. Plant materials generally make up only a small fraction of the diet.

Reproduction

In Europe, the main breeding populations of Shelduck are found in the United Kingdom, Sweden and the Netherlands. Shelduck prefer to nest in burrows (often rabbit burrows) or other covered sites. There is one clutch per year, comprising 8-10 eggs. The precocial young are taken to shallow wetlands or onto the mudflats; chick mortality can be considerable.
Population in the Wadden Sea
The Dutch Wadden Sea is an important area for breeding, moulting and wintering Shelduck. In July and August almost the entire W-European population congregates in the Wadden Sea to moult. Since the turn of the century the largest moult concentrations have shifted from the German to the Dutch part of the Wadden Sea, particularly off the Frisian mainland coast. Numbers are highest in July-November (c. 100,000) after which many birds migrate to the south and west for the winter. In recent years about 20,000-40,000 remain during winter (Hornman *et al.* 2020).
On the long-term (since 1990), the trend in year-round abundance of the Shelduck in the Dutch Wadden Sea has been moderately increasing; over the most recent 10 years it has been stable (https://www.sovon.nl/nl/gebieden).

## 13.2 Interaction with plastic

The main pathway through which Shelduck may be exposed to the plastic particles is when PS particles are ingested and perhaps accumulated by benthic organisms on which the ducks feed, e.g. bivalves or (rag)worms. A second potential pathway occurs when Shelduck filter these particles directly out from the sediment during foraging, but it is doubtful whether, if encountered, these will be actively ingested. Their very small size is likely to render them perceived by the birds as unprofitably small, and therefore rejected.

The larger HDPE particles are unlikely to be ingested by Shelduck as these do not usually skim the water's surface during foraging, and also do not habitually feed along the tideline or on seeds in saltmarshes where such particles may be concentrated.

## 13.3 Data collection and analysis

The data set consists of counts of the species (see chapter 3.5) collected between 1976 and 2020 by SOVON and volunteers. In the observation years, not all months are covered with countings. In order to avoid an excessive number of unavailable observations, the analysis has been restricted to the month of January in all years. Counts are available for all areas and all years, although some of the values used have been partially imputed by SOVON. These have been treated as if they were counts in the analysis.

The countings have been grouped in 13 areas covering the Wadden Sea. The raw time series in the different areas reveal that there are large differences between areas in the average number of birds counted. Figure 13.1 illustrates the counting areas and the raw trends in the time series. Note the differences in y-scales of the figures for the different areas.

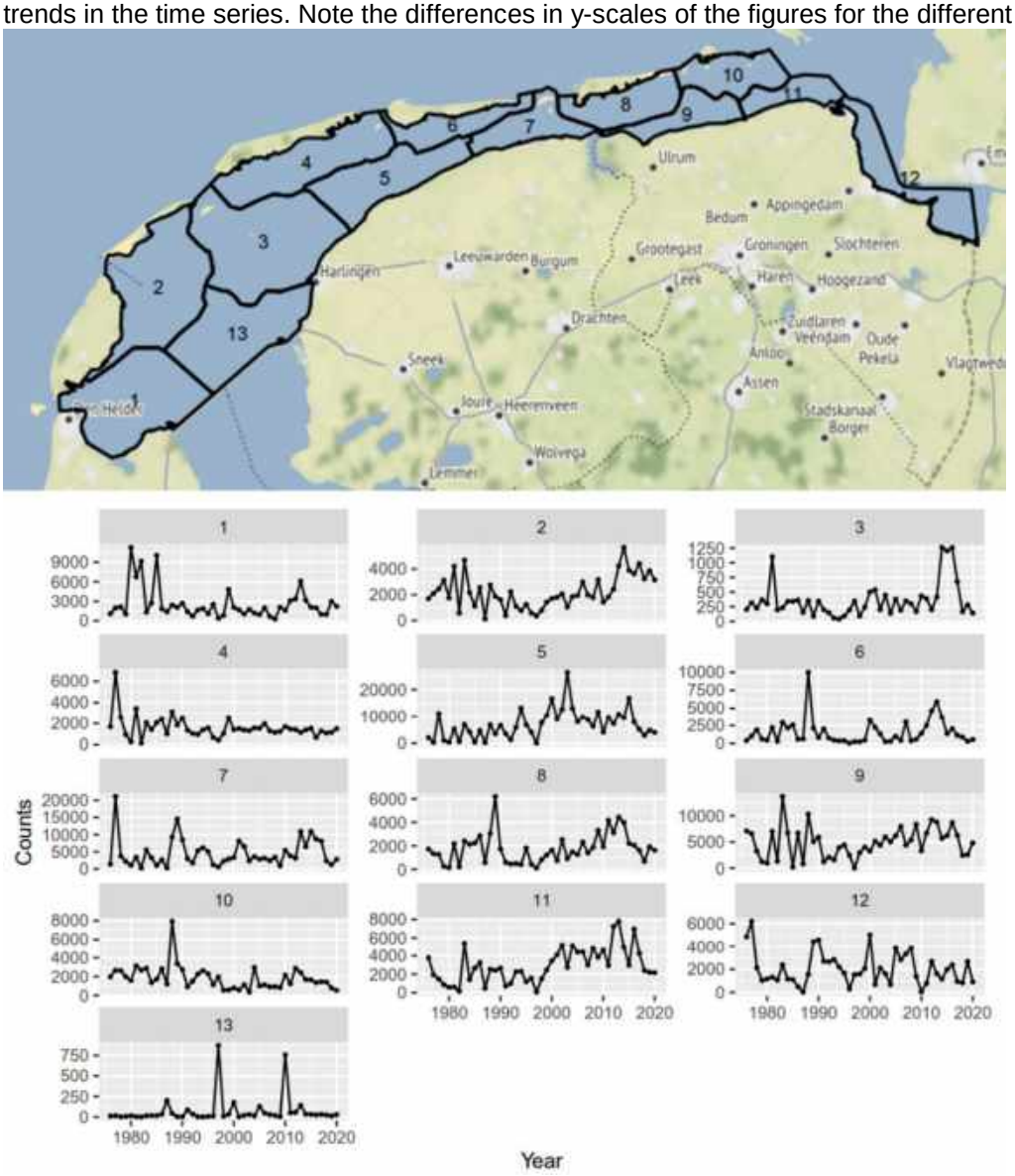


*Figure 13.1. Map of the counting areas (left) and raw time series of the counts in the 13 areas. Note the different y-scales used in the graphs. Observation points have been connected with lines within each area for clarity.*

For the model building every observation point (count of birds) is associated with an area and a moment in time. In all models fitted, it has been assumed that the data follow a negative binomial distribution. The first model uses a common trend for all areas. The areas can have a different intercept, which is modelled as a fixed factor, but the time course is the same. As this model did not capture the essence of the data, it was changed into a model where every area is allowed to have a different trend, with the trends independently sampled from a statistical distribution. This model improved the fit, but the assumption of (spatial) independence of the trends could not be maintained. Neighboring areas have more similar trends than areas far apart. Therefore, a final model fitted trends in the different areas that are spatially correlated. A CAR (conditional auto-regressive correlation) model was used. That provided a satisfactory model to the data.

The final model has a negative binomial distribution, separate trends fitted to each area but with spatially correlated intercepts. The model is specified by the following prescription:

$$
\begin{aligned}
Counts_{is} &\sim NB(\mu_{is}, \theta) \\
E[Counts_{is}] &= \mu_{is} \\
var[Counts_{is}] &= \mu_{is} + \frac{\mu_{is}^2}{\theta} \\
\log(\mu_{is}) &= \beta_1 + f_i(Time_s) + u_i \\
f_i(Time_s) &= RW1 \\
u_i &\sim CAR
\end{aligned}
$$

Where NB stands for negative binomial distribution with parameters mean and dispersion parameter. E[Y] is the expected value of Y, given by the mean of the negative binomial. Var[] is the variance operator. Its specification follows the definition of the negative binomial distribution. The expected value is log-linked to a linear equation that contains an intercept, a Random Walk Trend smoother of time, and a spatially correlated random intercept that is specified according to CAR correlation.
The main result of the model is formed by the trends in the 13 counting areas (Figure 6.2). Trends in time are fluctuating, but there is not a real dominant pattern. Note that it is relatively rare to find zero outside of the credible interval for the trend smoother in most series. Areas 6 (south of Ameland) and 13 (eastern Marsdiep basin), with normally relatively low numbers of birds, have the strongest fluctuations in numbers.

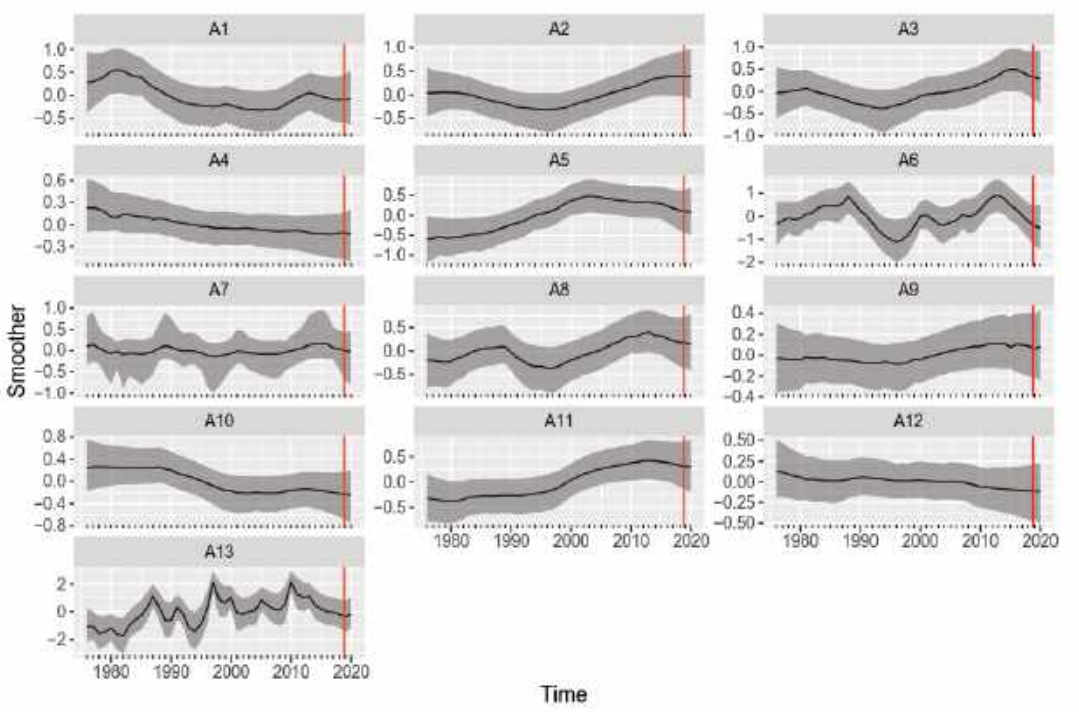


*Figure 13.2. Posterior mean values and 95 % credible intervals for all smoothers in the negative binomial GAM with CAR correlation. A vertical red line is drawn at January 2019 in each panel.*

The random intercepts of the counting areas are correlated in space, as is shown in Figure 13.3. Hotspots for the species are the rather muddy coasts of Friesland and Groningen. Deep areas with few tidal flats, such as the eastern part of the Marsdiep basin, have few birds.

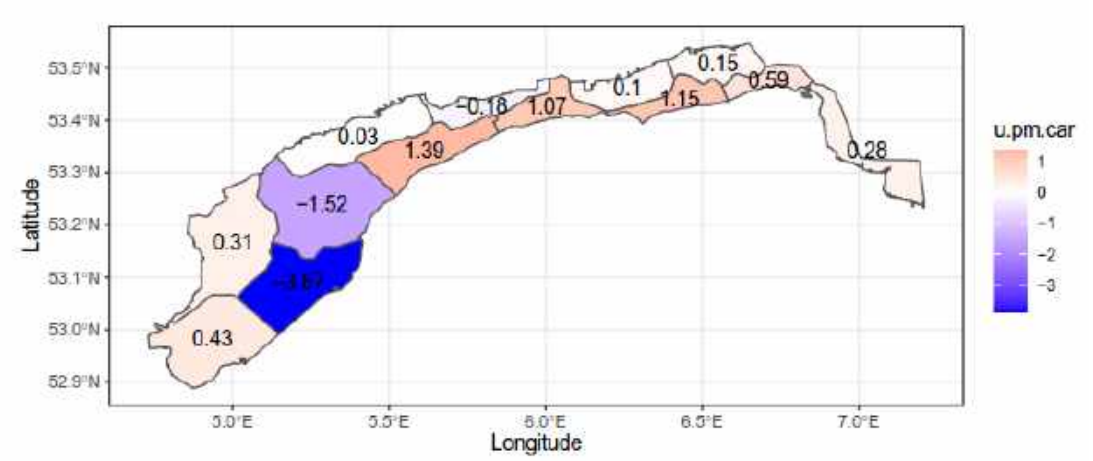


*Figure 13.3. Posterior mean values of the random intercept $u_i$. The NB GAM with CAR spatial correlation was used.*

Effects of the MSC Zoe incident are not apparent when inspecting the temporal smoothers in Figure 13.2 around the red line. The comparison has formally been executed by calculating, for each area, the posterior probability distribution of the difference between the trend in January 2019 with January 2018 on the one hand (T2019-T2018), and with January 2020 on the other hand (T2020-T2019). The results of this analysis are summarized in Figure 13.4. All credible intervals encompass zero. There are no indications of changes in the trend between 2019 and the surrounding years, for any of the counting areas.

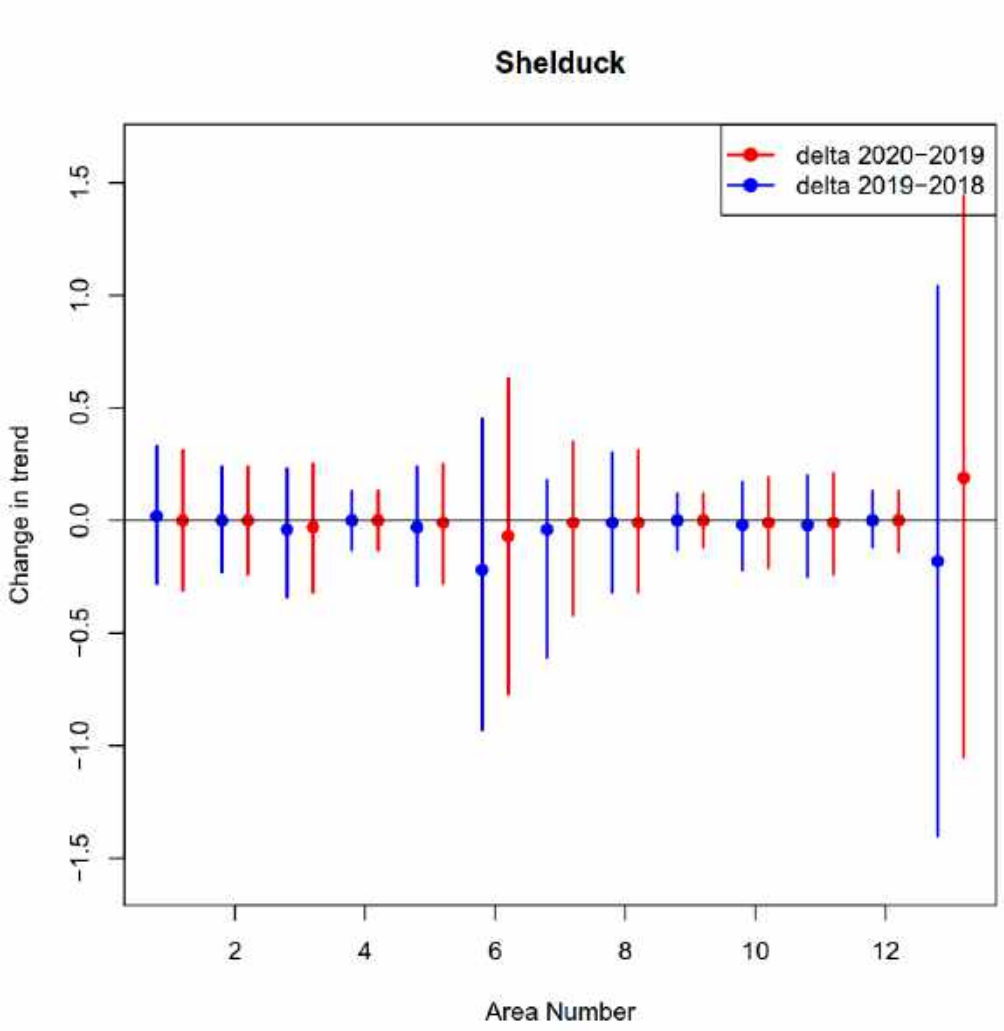


*Figure 13.4. Shelduck in the Wadden Sea. Changes in the trend between 2019 and surrounding years. In blue the difference of the trend with 2018 (value in 2019 minus value in 2018) is shown for the 10 areas. In red the difference with 2020 (value 2020 minus value 2019). Shown are the 95 % credible intervals of the posterior distribution of the difference. Dots denote the mean difference.*

## 13.4 Discussion

In general, results of the statistical analysis are in agreement with what is known of this species. The – in comparison to some of the other intertidal birds analyzed – fairly 'decent behavior' of the data with respect to temporal and spatial variability is explained by the Shelduck's large size, striking plumage, generally moderate flock sizes (in winter) and reasonably wide spacing between individuals enabling relatively accurate counts. In addition, Shelduck typically show a rather predictable distribution and limited spatial movements. The statistical analysis is therefore expected to capture existing patterns in Shelduck abundance well, leading to good confidence in the results. Moreover, results for the 13 separate areas show a consistent pattern of no discernible shift in the trend after the MS Zoe event. That no apparent effect of this event on Shelduck numbers was found also is in line with a rather low risk of exposure of the birds to MS Zoe plastic through the food chain.

## 13.5 Conclusion

Plastic particles originating from the MS Zoe incident have no discernible effect on the abundance and distribution of Common Shelduck.

# 14 The red knot (*Calidris canutus*)

## 14.1 Biology and ecology

The Red Knot is a fairly small (c. 120 g) shorebird. It is a long-distance migrant, breeding in the high arctic tundra and polar desert of Asia and North America and wintering in the world's larger intertidal areas, both temperate and tropical. Worldwide, five subspecies occur, two of which visit the Wadden Sea. "Nearctic" knots breeding in Greenland and NE Canada (*C. c. islandica*) winter along the coasts of NW Europe, with the Wadden Sea as one of the most important areas. The "Afrosiberian" population (*C. c. canutus*) breeds in Northern Siberia, winters along the coast of West Africa, and uses the Wadden Sea as a feeding station during their migrations in July-August and in May. The Red Knots is one of the best-researched shorebird species, with respect to aspects like feeding ecology, physiology and body reserve dynamics, and migratory behavior (e.g. Piersma 1994, 2007).
In the non-breeding season Knots are very gregarious birds which gather in large and dense groups, numbering up to thousands of individuals when foraging and up to tens of thousands when roosting at high tide. Nearctic knots wintering in the Wadden Sea have large activity areas (up to approximately 800 $km^2$), in which they exploit of spatial differences in the timing of the tidal cycle to maximize their foraging time (van Gils et al. 2005).

Feeding
Outside the breeding season, The Red Knot is a specialized shellfish-eater, feeding mainly on small bivalves, in the Wadden Sea mainly Baltic tellin *Limecola balthica* and small cockles *Cerastoderma edule* and mussels *Mytilus edulis*, but also other species, if small enough to be ingested. Buried bivalves are detected by probing the bill into the moist mudflat substrate, where pressure sensors in the tip detect hard objects at some distance. The bivalves are swallowed whole and their shells cracked in the muscular stomach. However, knots also eat more easily digestible benthic animals, such as shrimps and small crabs, mainly available in late summer. Worms do not feature extensively in the diet.

Reproduction
Red Knots breed in high arctic tundra and polar desert habitats and produce one clutch of four eggs. The precocial young are insectivorous. Adults as well feed mainly on insects during the breeding season, augmented by some plant material and leftover berries from previous years.
Population in the Wadden Sea
For both the subspecies *islandica* and *canutus*, the Wadden Sea is an important wintering and migratory staging area. In the autumn, birds from both populations are present and a maximum of 100,000-200,000 birds stage in the Dutch part. In winter, only Neartic *islandica* Knots are present; the 60,000-100,000 birds comprise roughly 15% of the total flyway population (Hornman et al. 2020). The Nearctic Knots also undergo their annual moult of flight feathers in the Wadden Sea. During the spring migration peak numbers are relatively modest; both subspecies staging mainly in the German and Danish parts of the Wadden Sea. On the long-term (since 1990), the trend in year-round abundance of red knot in the Dutch Wadden Sea has been stable; over the most recent 10 years it is classified as uncertain (https://www.sovon.nl/nl/gebieden).

## 14.2 Interaction with plastic

The one pathway through which red knot may be exposed to plastic particles lost by MS Zoe is when PS particles are ingested and accumulated by bivalves on which the birds feed. The larger HDPE particles are unlikely to be taken in by either bivalves or foraging red knots.

## 14.3 Data collection and analysis

Data on the abundance of red knot in the Dutch Wadden Sea originate from systematic waterbird counts which have been carried out since the 1970s by SOVON and volunteers (see chapter 3.5).
The data set consists of counts of the species collected between 1976 and 2020. In the observation years, not all months are covered with countings. In order to avoid an excessive number of unavailable observations, the analysis has been restricted to the month of January in all years. Counts are available for all areas and all years, although some of the values used have been partially imputed by SOVON. These have been treated as if they were counts in the analysis.

The countings have been grouped in 13 areas covering the Wadden Sea. The raw time series in the different areas reveal that there are large differences between areas in the average number of birds counted. Figure 14.1 illustrates the counting areas and the raw trends in the time series. Note the differences in y-scales of the figures for the different areas.

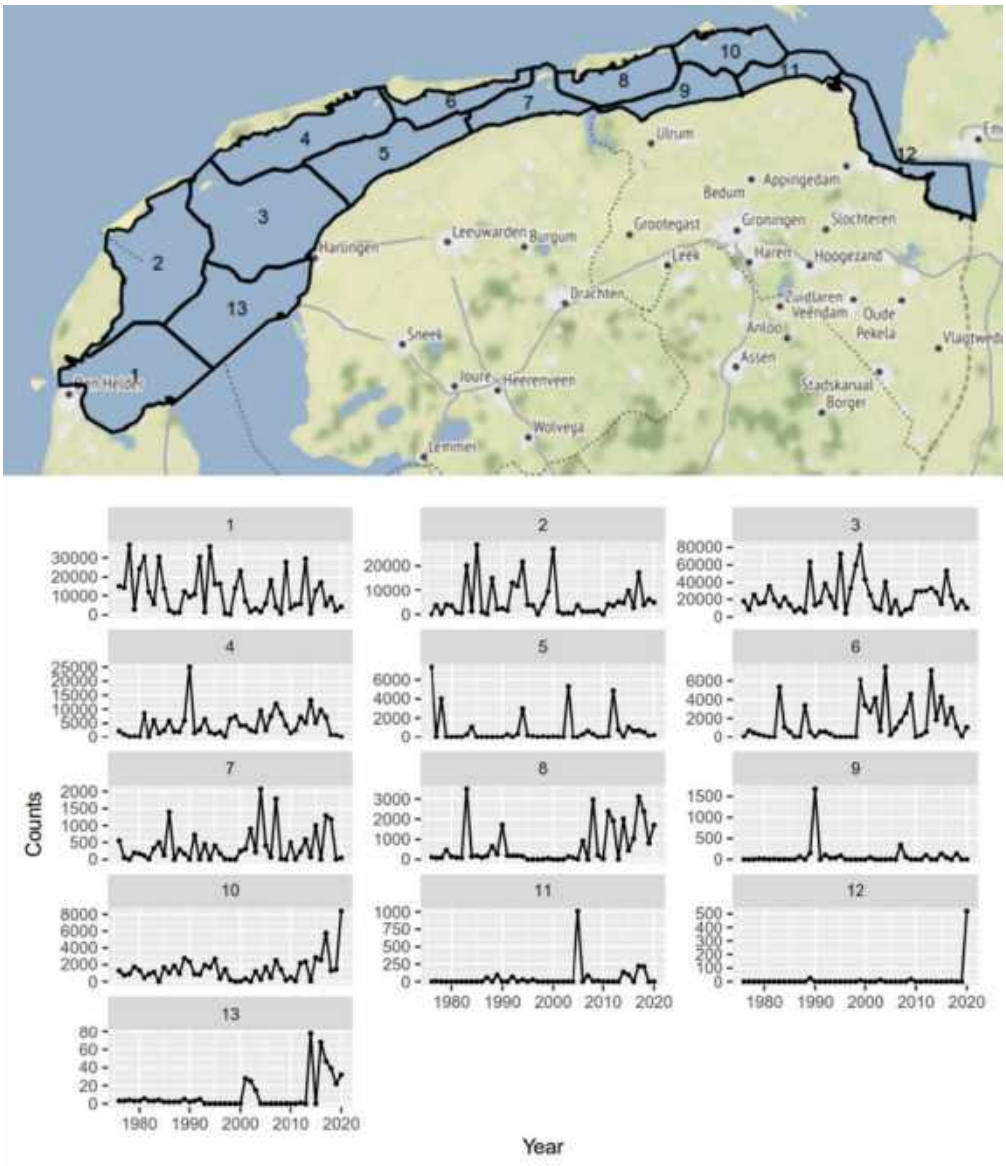


*Figure 14.1. Red knot in the Wadden Sea. Map of the counting areas (left) and raw time series of the counts in the 13 areas. Note the different y-scales used in the graphs. Observation points have been connected with lines within each area for clarity.*

For the model building every observation point (count of birds) is associated with an area and a moment in time. The number of zero observations in the data set is relatively high (around 20%), and therefore not only the negative binomial distribution but also the zero-inflated negative binomial have been considered. The first model fitted uses a common trend for all areas. The areas can have a different intercept, which is modelled as a fixed factor, but the time course is the same. As this model did not capture the essence of the data, it was changed into a model where every area is allowed to have a different trend, with the trends independently sampled from a statistical distribution. There were no indications of spatial correlation in the trends. No model with CAR correlation was fitted, as was done in other bird species. Instead, due to the high number of zero observations, a zero-inflated negative binomial distribution was fitted and found to be superior to the NB model, based on DIC.

The final model has a zero-inflated negative binomial distribution, separate trends fitted to each area with independent spatially uncorrelated intercepts. The model is specified by the following prescription:

$$
\begin{aligned}
Counts_{is} &\sim ZINB(\mu_{is}, \theta, \pi) \\
E[Counts_{is}] &= (1-\pi) \times \mu_{is} \\
var[Counts_{is}] &= (1-\pi) \times \mu_{is} \times (1 + \pi \times \mu_{is} + \frac{\mu_{is}}{\theta}) \\
\log(\mu_{is}) &= Intercept + f_i(Year_s) + u_i \\
logit(\pi) &= Constant \\
f_i(Year_s) &= RW1 \\
u_i &\sim N(0, \sigma_u^2)
\end{aligned}
$$

Where ZINB stands for zero-inflated negative binomial distribution with parameters mean, dispersion parameter and fraction excess zeroes π. E[Y] is the expected value of Y. Var[] is the variance operator. The expected value is log-linked to a linear equation that contains an intercept, a Random Walk Trend smoother of time, and independent area-specific random intercepts.
The main result of the model is formed by the trends in the 13 counting areas (Figure 14.2). Trends in time are fluctuating, but there is not a real dominant pattern. Note that it is relatively rare to find zero outside of the credible interval for the trend smoother in most series. It happens in the areas 9, 11, 12 and 13. All these areas have large numbers of zero observations and only occasional peaks in counts, although area 13 seems to have consistently higher numbers in the last years (see Figure 14.1).

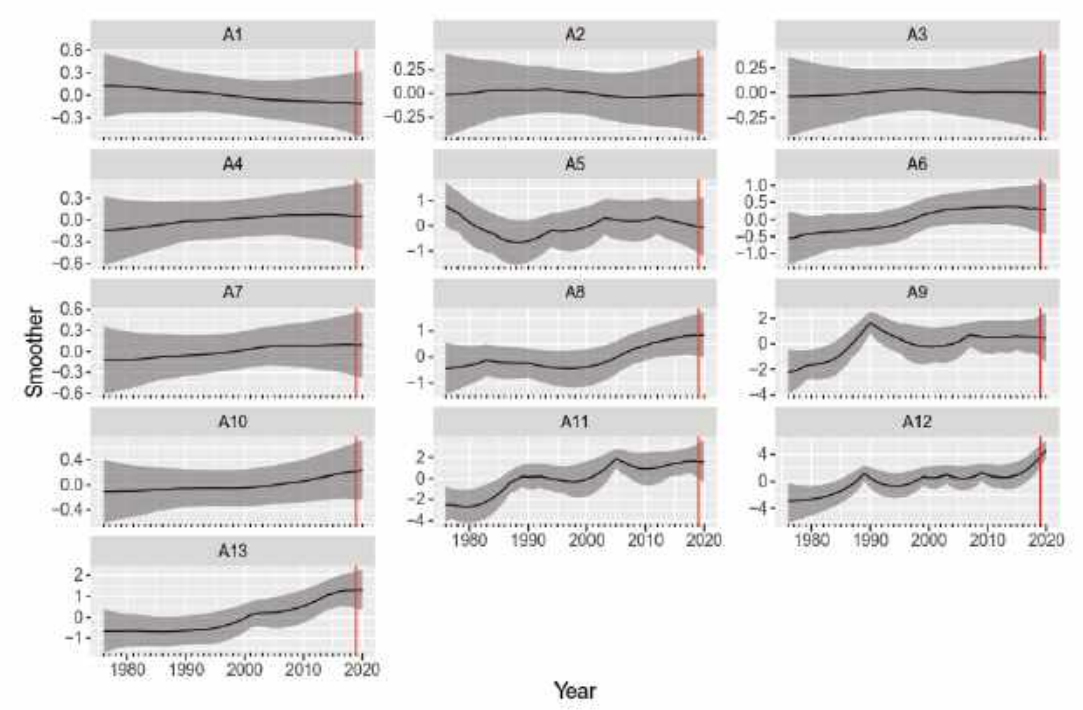


*Figure 14.2. Red knot. Posterior mean values and 95 % credible intervals for all smoothers in the negative binomial GAM with CAR correlation. A vertical red line is drawn at January 2019 in each panel.*

The random intercepts of the counting areas were found to be uncorrelated in space, but large differences are present, as is shown in Figure 14.3.

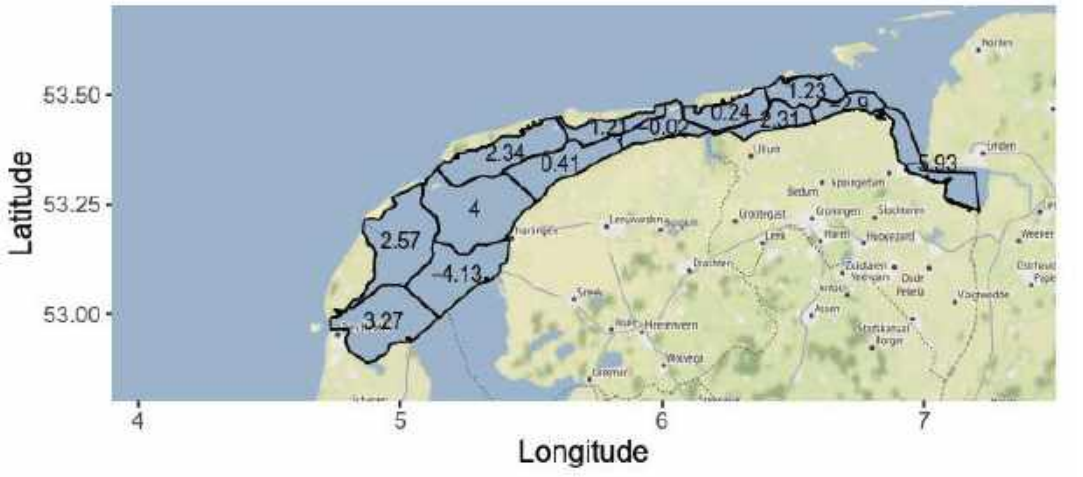


*Figure 14.3. Red knot. Posterior mean values of the random intercept $u_i$. The ZINB GAM without spatial correlation was used.*

Effects of the MSC Zoe incident are not apparent when inspecting the temporal smoothers in Figure 14.3 around the red line. The comparison has formally been executed by calculating, for each area, the posterior probability distribution of the difference between the trend in January 2019 with January 2018 on the one hand (T2019-T2018), and with January 2020 on the other hand (T2020-T2019). The results of this analysis are summarized in Figure 14.4. All credible intervals encompass zero. There are no indications of changes in the trend between 2019 and the surrounding years, for any of the counting areas.

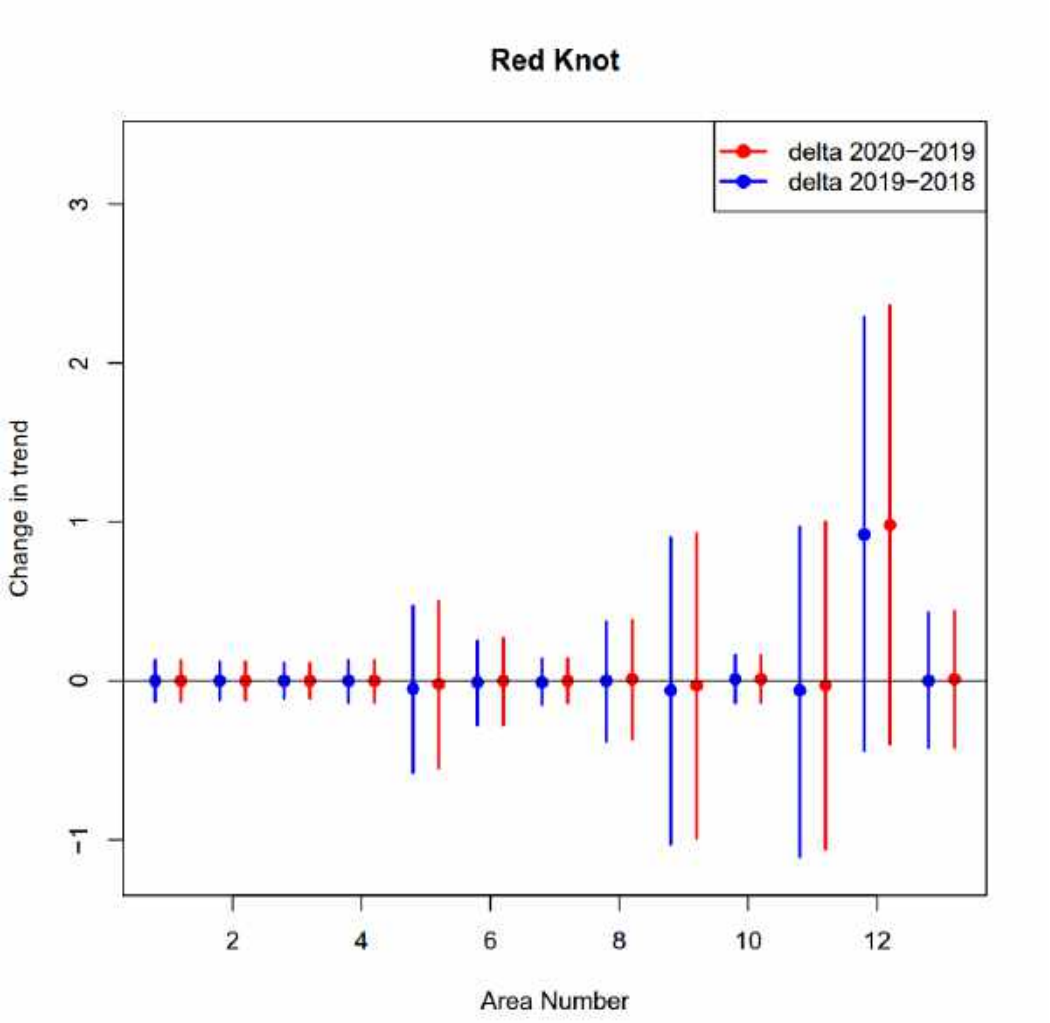


*Figure 14.4.Red knot in the Wadden Sea. Changes in the trend between 2019 and surrounding years. In blue the difference of the trend with 2018 (value in 2019 minus value in 2018) is shown for the 10 areas. In red the difference with 2020 (value 2020 minus value 2019). Shown are the 95 % credible intervals of the posterior distribution of the difference. Dots denote the mean difference.*

## 14.4 Discussion

In general, results of the statistical analysis are in agreement with what is known of this species. The large and seemingly random variability in the count data (similar to white noise) is explained by the red knots gregariousness leading to huge, densely packed flocks on the high tide roosts, which are difficult to count and lead to large random errors. In addition, wintering red knots roam widely over large areas in the Wadden Sea, often exceeding the average size of the counting areas used in the analysis even within a tidal cycle. Of the four intertidal bird species analyzed in this study, the red knot was therefore expected to show the largest spatiotemporal variability in the counts, and the analysis confirmed this. The variability will have reduced the power to discern effects of the MS Zoe event, but the results for the 13 separate areas were consistent in showing no statistically important shift in the trend after this event. The risk of exposure of the birds to MS Zoe plastics through the food chain must also have been rather low.

## 14.5 Conclusion

Plastic particles originating from the MS Zoe incident have no discernible effect on the abundance and distribution of red knot.

# 15 The Northern Pintail (*Anas acuta*)

## 15.1 Biology and ecology

The Northern Pintail is a dabbling, duck breeding in the boreal regions of Eurasia and North America. Situated on the southern edge of the breeding range, only a few pairs breed in the Netherlands. The species is mainly a migrant here; from August onwards large numbers of Pintails from Finland and Western Russia stage in the Wadden Sea. Some of the birds then migrate to more southern wintering areas (S to Mediterranean and N-Africa), while another part remains to winter here.

Feeding

Pintails eat both vegetable and animal matter that they extract from shallow water, water bottoms and mudflats, but also forage on harvest remains on arable fields. In coastal wetlands mainly seeds of water and salt marsh plants are eaten and parts of aquatic plants, including rhizomes and tubers. Animal food here includes amphipods and isopods, clams, gastropods and insects including larvae. Animal foods usually seems to represent a minority of the diet by mass, although it may be underestimated as remains are less easily detectable in faeces and stomach samples than plant material.

After the Shelduck, Northern Pintail is the duck species most often found foraging on the open mudflats of the Wadden Sea during low tide. Here they feed by slowly walking and filtering the muddy top layer, or by upending in shallow water. Food taken here includes mud shrimp *Corophium*, mudsnails *Peringia ulvae* and small bivalves. They also feed at sites with a well-developed layer of diatoms on the mud surface. On the rising tide Pintails concentrate at the edges and in shallowly submerged parts of saltmarshes, where they feed on saltmarsh plants (e.g. glasswort, *Salicornia europaea*) but probably mostly on seeds which are concentrated in the shallow water near the tide line. In stomachs of Pintails shot on Terschelling between December and February, seeds of 33 different plant species were found, including grasses, sedges *Carex*, glasswort, arrowgrass *Trichlogin*, sea-blite *Suaeda*, spike-rush *Eleocharis* and sheep's sorrel *Rumex acetosella* (de Vries 1939). Pintail also often leave the wetlands at night to forage in inland agricultural areas, where they consume harvest remains such as cereal grains. Opportunities for this are greater along the mainland shores of the Wadden Sea than on the islands.

Reproduction

Pintail breed in bogs, marshes and along lakes in the boreal and temperate zones. Also, in the breeding season, the diet is mixed with both plant and animal foods consumed. There is one brood per year numbering 6-12 eggs. Chicks are precocial and mainly insectivorous at first.

Population in the Wadden Sea

The Dutch Wadden Sea harbors 10,000-25,000 Pintail in October, increasing to 15,000-30,000 in January (Hornman et al. 2020). This amounts to 25-45% of the total flyway population wintering in NW Europe. Highest numbers are found along parts of the mainland coast of Friesland and Groningen and on the islands of Terschelling and Schiermonnikoog. At all these sites, extensive saltmarshes are present.

On the long-term (since 1990), the trend in year-round abundance of Northern Pintail in the Dutch Wadden Sea has been moderately increasing; over the most recent 10 years it is uncertain (https://www.sovon.nl/nl/gebieden).

## 15.2 Interaction with plastic

Northern Pintail in the Wadden Sea may be exposed to PS particles from MS Zoe accumulated by small bivalves eaten by the ducks, or if ingested accidentally when filtering for diatoms. Given the small contributions of these sources to the ducks' diet, this pathway does not seem to entail a high risk. The larger and floating HDPE particles may however be ingested by Pintail skimming the water's surface for plant seeds, particularly as they are likely to become concentrated along the tideline and in parts of saltmarshes in a similar way to those seeds. Of the four bird species of the intertidal considered in this study, the Northern Pintail may therefore well be the one most at risk to exposure to MS Zoe plastics.

## 15.3 Data collection and analysis

Data on the abundance of Northern Pintail in the Dutch Wadden Sea originate from systematic waterbird counts which have been carried out since the 1970s by SOVON and volunteers (see chapter 3.5).
The data set consists of counts of the species collected between 1976 and 2020. In the observation years, not all months are covered with countings. In order to avoid an excessive number of unavailable observations, the analysis has been restricted to the month of January in all years. Counts are available for all areas and all years, although some of the values used have been partially imputed by SOVON. These have been treated as if they were counts in the analysis.

The countings have been grouped in 13 areas covering the Wadden Sea. The raw time series in the different areas reveal that there are large differences between areas in the average number of birds counted. Figure 5.1 Figure 14.1 illustrates the counting areas and the raw trends in the time series. Note the differences in y-scales of the figures for the different areas.

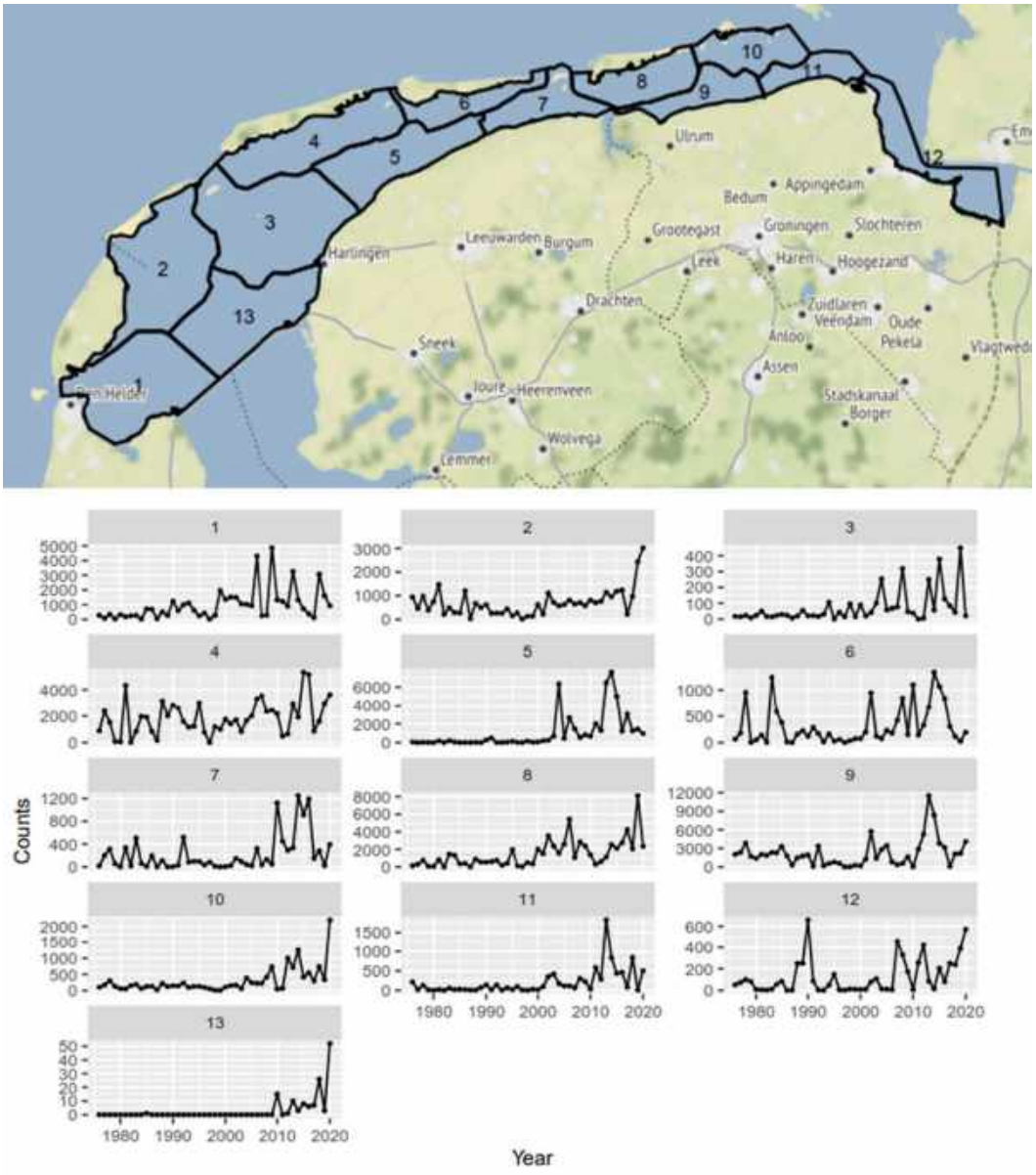


*Figure 15.1. Northern Pintail in the Wadden Sea. Map of the counting areas (left) and raw time series of the counts in the 13 areas. Note the different y-scales used in the graphs. Observation points have been connected with lines within each area for clarity.*

For the model building every observation point (count of birds) is associated with an area and a moment in time. The number of zero observations in the data set is relatively low (around 9%). It differs by area and is only elevated in area 13. The first model fitted uses a common trend for all areas. The areas can have a different intercept, which is modelled as a fixed factor, but the time course is the same. As this model did not capture the essence of the data, it was changed into a model where every area is allowed to have a different trend, with the trends independently sampled from a statistical distribution. There were no indications of spatial correlation in the trends. No model with CAR correlation was fitted.
The final model has a negative binomial distribution, separate trends fitted to each area with spatially uncorrelated intercepts. The model is specified by the following prescription:

$$
\begin{aligned}
Counts_{is} &\sim NB(\mu_{is}, \theta) \\
E[Counts_{is}] &= \mu_{is} \\
var[Counts_{is}] &= \mu_{is} + \frac{\mu_{is}^2}{\theta} \\
\log(\mu_{is}) &= \beta_1 + f_i(Time_{is}) + u_i \\
f_i(Time_{is}) &= RW1 \\
u_i &\sim N(0, \sigma_u^2)
\end{aligned}
$$

Where NB stands for negative binomial distribution with parameters mean and dispersion parameter. E[Y] is the expected value of Y. Var[] is the variance operator. The expected value is log-linked to a linear equation that contains an intercept, a Random Walk Trend smoother of time, and independent area-specific random intercepts.
The main result of the model is formed by the trends in the 13 counting areas (Figure 15.2). Trends in time are fluctuating, but in general an increase is seen since 2000.

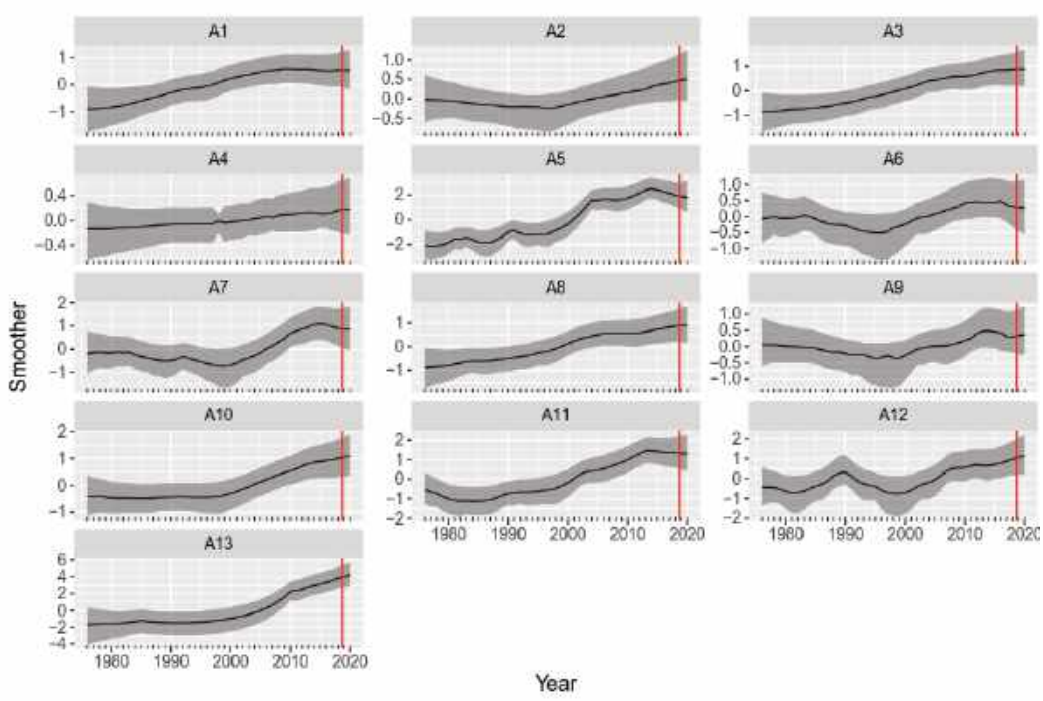


*Figure 15.2. Northern Pintail. Posterior mean values and 95 % credible intervals for all smoothers in the negative binomial GAM with CAR correlation. A vertical red line is drawn at January 2019 in each panel.*

The random intercepts of the counting areas are shown in Figure 15.3.

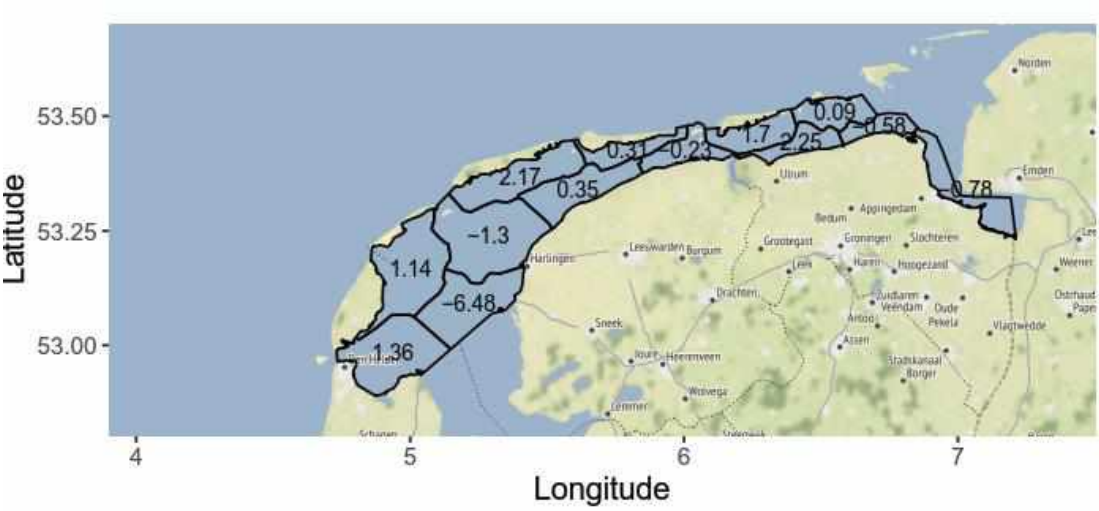


*Figure 15.3. Northern Pintail. Posterior mean values of the random intercept $u_i$. The ZINB GAM without spatial correlation was used.*

Effects of the MSC Zoe incident are not apparent when inspecting the temporal smoothers in Figure 14.3 around the red line. The comparison has formally been executed by calculating, for each area, the posterior probability distribution of the difference between the trend in January 2019 with January 2018 on the one hand (T2019-T2018), and with January 2020 on the other hand (T2020-T2019). The results of this analysis are summarized in Figure 14.4. All credible intervals encompass zero. There are no indications of changes in the trend between 2019 and the surrounding years, for any of the counting areas.

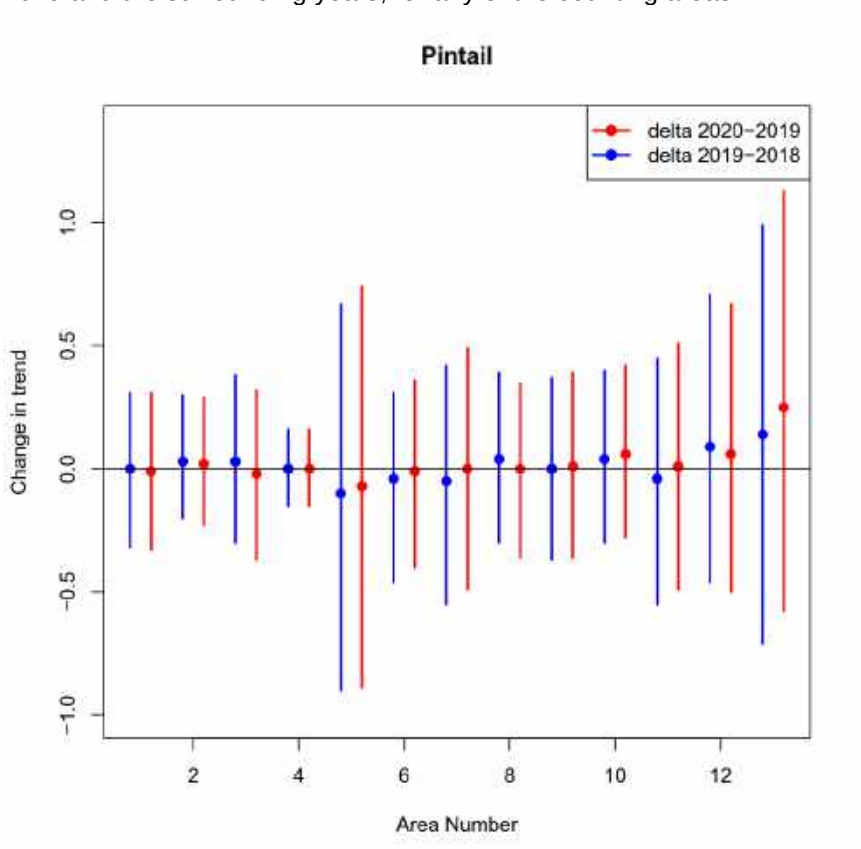


*Figure 15.4. Northern Pintail in the Wadden Sea. Changes in the trend between 2019 and surrounding years. In blue the difference of the trend with 2018 (value in 2019 minus value in 2018) is shown for the 10 areas. In red the difference with 2020 (value 2020 minus value 2019). Shown are the 95 % credible intervals of the posterior distribution of the difference. Dots denote the mean difference.*

## 15.4 Discussion

In general, results of the statistical analysis are in agreement with what is known of this species. The increasing trend since the start of this century has also been noted elsewhere (Hornman et al. 2020). Although counting numbers of Pintails can sometimes be difficult when they are partly hidden in saltmarsh vegetation, Pintail typically shows a predictable distribution and limited spatial movements. However, there are relatively many of the 13 areas analyzed have fairly low numbers, which will reduce the power to discern effects of the MS Zoe event, but the results for the 13 separate areas were consistent in this respect and showed no statistically important shift in the trend after this event.

## 15.5 Conclusion

Plastic particles originating from the MS Zoe incident have no discernible effect on the abundance and distribution of Northern Pintail in the Dutch Wadden Sea.

# 16 The Bar-tailed Godwit (*Limosa lapponica*)

## 16.1 Biology and ecology

The Bar-tailed godwit is a fairly large (300-500 g) long-distance migratory wader. Two subspecies occur along the East Atlantic flyway (Duijns et al. 2012). The "European" subspecies *L. l. lapponica* breeds in northern Scandinavia and adjacent north-western Russia and winters along the coasts of W-Europe, including the Wadden Sea. The "Afro-Siberian" population of *L. l. taimyrensis* breeds in Northern Siberia and overwinters in West Africa, using the Wadden Sea during migration in autumn and spring.

Feeding

The bar-tailed godwit's diet consists mainly of different types of worms and shellfish that are extracted from the mudflats with the long beak. Bristle worms make up the bulk of the food in most areas; in the Wadden Sea, for example, 80% of the winter diet consists of ragworms *Hediste diversicolor*, armed bristleworm *Scoloplos armiger*, catworm *Nephtyis hombergi* and lugworm *Arenicola marina* and are also often taken. Smaller worms, bivalves, shrimp and crabs are less important in the diet (Scheiffarth 2001, Duijns et al. 2013). Lugworms are less important in winter when most are buried too deep to be reached by the godwits but seem to be a critical prey for spring-staging for the Afrosiberian Godwits; variation in lugworm abundance is correlated with the rate of body mass gain and with survival (Rakhimberdiev et al. 2018).

Reproduction

Bar-tailed godwits breed on forest tundra bogs and in arctic tundra, where they lay a single clutch of four eggs annually. While adults feed partly on soil invertebrates and berries during the breeding season, the precocial chicks are insectivorous.

Population in the Wadden Sea

The taimyrensis subspecies uses the Dutch Wadden Sea as a migratory staging site in late summer (August) and spring (May), on their way to and from African wintering sites. For L. l. lapponica, the Wadden Sea is also an important moulting and wintering area, holding some 40,000-70,000 birds in midwinter, 25-45% of the entire population. During late summer and spring migration the occurrence of both subspecies overlaps, leading to larger numbers reaching on average to c. 100,000 in September and 150,000 in May.
The long-term (since 1990) trend in year-round abundance of the Bar-tailed Godwit in the Dutch Wadden Sea is a moderate increase; over the most recent 10 years it has been stable (https://www.sovon.nl/nl/gebieden).

## 16.2 Interaction with plastic

The one pathway through which Bar-tailed Godwits may become exposed to plastic particles lost by MS Zoe occurs when PS particles are ingested and accumulated by benthic organisms on which the birds feed, particularly Ragworms and Lugworms. The larger HDPE particles are unlikely to be taken in by either species, or directly by foraging godwits.

## 16.3 Data collection and analysis

Data on the abundance of Bar-tailed Godwit in the Dutch Wadden Sea originate from systematic waterbird counts which have been carried out since the 1970s by SOVON and volunteers (see chapter 3.5).

The data set consists of counts of the species collected between 1976 and 2020. In the observation years, not all months are covered with countings. In order to avoid an excessive number of unavailable observations, the analysis has been restricted to the month of January in all years. Counts are available for all areas and all years, although some of the values used have been partially imputed by SOVON. These have been treated as if they were counts in the analysis.

The countings have been grouped in 13 areas covering the Wadden Sea. The raw time series in the different areas reveal that there are large differences between areas in the average number of birds counted. Figure 16.1 illustrates the counting areas and the raw trends in the time series. Note the differences in y-scales of the figures for the different areas.

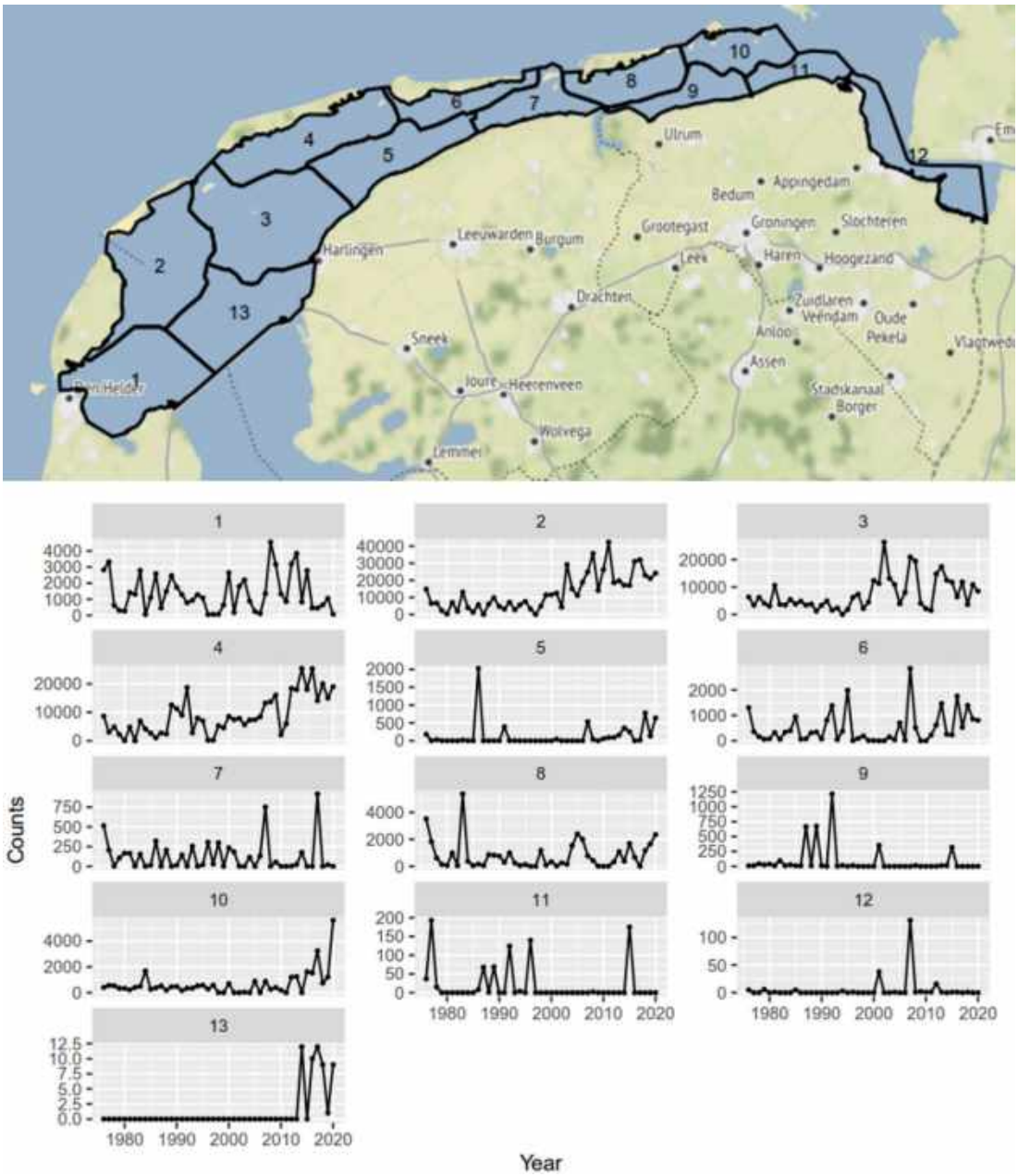


*Figure 16.1. Bar-tailed Godwit in the Wadden Sea. Map of the counting areas (left) and raw time series of the counts in the 13 areas. Note the different y-scales used in the graphs. Observation points have been connected with lines within each area for clarity.*

For the model building every observation point (count of birds) is associated with an area and a moment in time. The number of zero observations in the data set is relatively low (around 27%). It is highest in area 13. In area 13 only 6 non-zero observations are available, and none of the observations is higher than 12 birds. For that reason, the area has been dropped from the analysis. For the remainder of this chapter, only the 12 other areas will be discussed. The number of zero observations then drops but remains relatively elevated with approximately 22 %.
The first model fitted uses a common trend for all areas. The areas can have a different intercept, which is modelled as a fixed factor, but the time course is the same. As this model did not capture the essence of the data, it was changed into a model where every area is allowed to have a different trend, with the trends independently sampled from a statistical distribution. Because of the elevated number of zero observations, the negative binomial and zero-inflated negative binomial were compared. Based on the DIC, the negative binomial performed better than the zero-inflated negative binomial and was used as the final model. There were no indications of spatial correlation in the trends. No model with CAR correlation was fitted

The final model has a negative binomial distribution, separate trends fitted to each area with spatially uncorrelated intercepts. The model is specified by the following prescription:

$$\begin{aligned} Counts_{is} &\sim NB(\mu_{is}, \theta) \\ E[Counts_{is}] &= \mu_{is} \\ var[Counts_{is}] &= \mu_{is} + \frac{\mu_{is}^2}{\theta} \\ \log(\mu_{is}) &= \beta_1 + f_i(Time_{is}) + u_i \\ f_i(Time_{is}) &= RW1 \\ u_i &\sim N(0, \sigma_u^2) \end{aligned}$$

Where NB stands for negative binomial distribution with parameters mean and dispersion parameter. E[Y] is the expected value of Y. Var[] is the variance operator. The expected value is log-linked to a linear equation that contains an intercept, a Random Walk Trend smoother of time, and independent area-specific random intercepts.
The main result of the model is formed by the trends in the 12 counting areas (Figure 16.2). Some areas are flat, others have an increasing trend or show fluctuations that go up and down. No single general trend is visible.

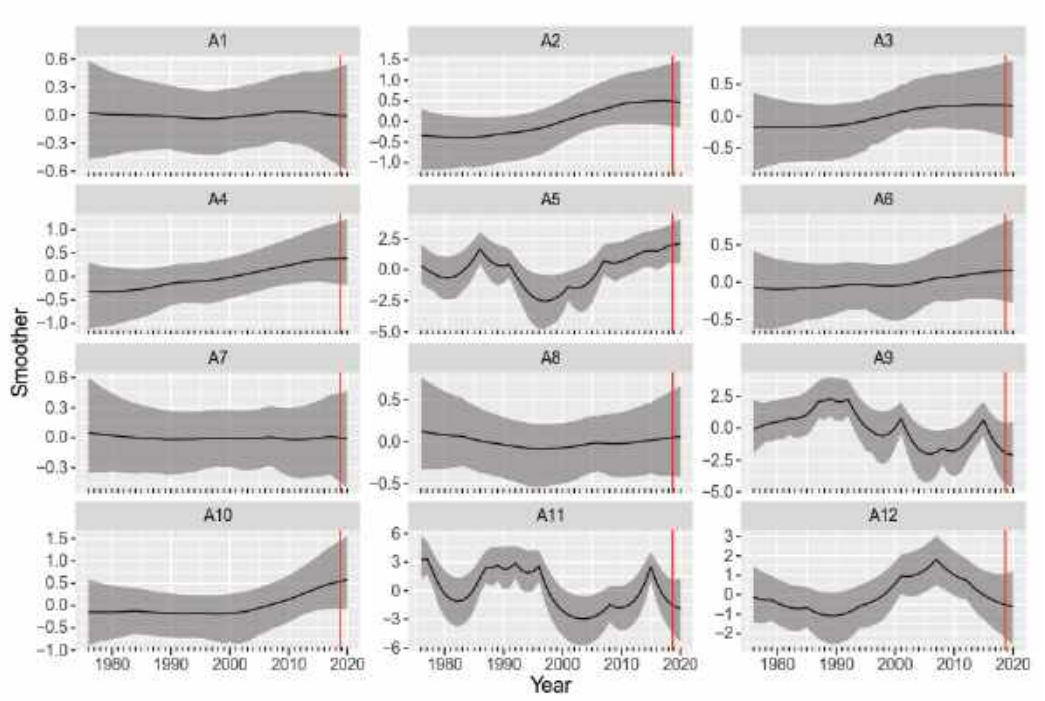


*Figure 16.2. Bar-tailed Godwit. Posterior mean values and 95 % credible intervals for all smoothers in the negative binomial GAM with CAR correlation. A vertical red line is drawn at January 2019 in each panel.*

The random intercepts of the counting areas are shown in Figure 16.3.

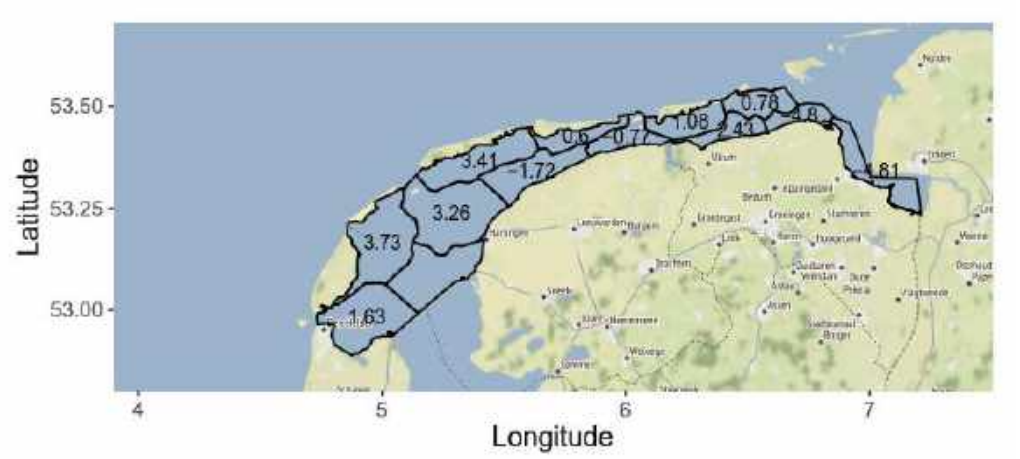


*Figure 16.3. Bar-tailed Godwit. Posterior mean values of the random intercept $u_i$. The ZINB GAM without spatial correlation was used.*

Effects of the MSC Zoe incident are not apparent when inspecting the temporal smoothers in Figure 14.3 around the red line. The comparison has formally been executed by calculating, for each area, the posterior probability distribution of the difference between the trend in January 2019 with January 2018 on the one hand (T2019-T2018), and with January 2020 on the other hand (T2020-T2019). The results of this analysis are summarized in Figure 16.4Figure 14.4. All credible intervals encompass zero. There are no indications of changes in the trend between 2019 and the surrounding years, for any of the counting areas.

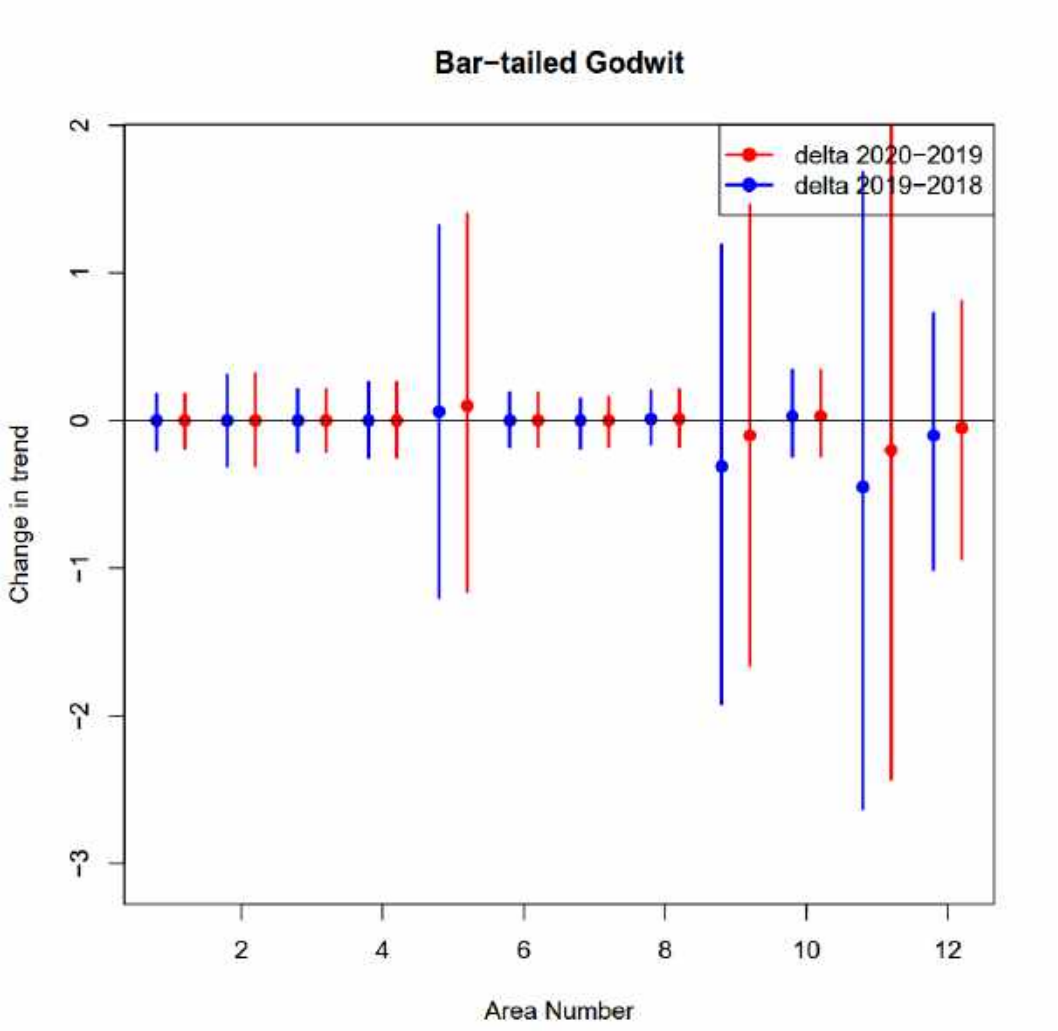


*Figure 16.4. Bar-tailed Godwit in the Wadden Sea. Changes in the trend between 2019 and surrounding years. In blue the difference of the trend with 2018 (value in 2019 minus value in 2018) is shown for the 10 areas. In red the difference with 2020 (value 2020 minus value 2019). Shown are the 95 % credible intervals of the posterior distribution of the difference. Dots denote the mean difference.*

## 16.4 Discussion

In general, results of the statistical analysis are in agreement with what is known of this species. Although Bar-tailed Godwits often roost in large and dense flocks, counting these is made easier by the birds' relatively large size, fairly patterned plumage, and particularly by their proneness to take flight temporarily (flying shorebird flock are usually counted with greater accuracy than standing flocks; Rappoldt et al. 1985). Compared to red knots, Bar-tails also show a more predictable spatial distribution. The statistical analysis is therefore expected to capture existing patterns in their abundance fairly well, leading to confidence in the results. Moreover, results for the 13 separate areas show a consistent pattern of no discernible shift in the trend after the MS Zoe event. That no apparent effect of this event on godwit numbers was found also is in line with a rather low risk of exposure of the birds to MS Zoe plastic through the food chain.

## 16.5 Conclusion

Plastic particles originating from the MS Zoe incident have no discernible effect on the abundance and distribution of Bar-tailed Godwit in the Dutch Wadden Sea.

# 17 General discussion and conclusion

For this analysis of possible effects of the MSC Zoe incident on protected and typical species of the Wadden Sea and coastal North Sea, some of the most extensive ecological monitoring databases of the Netherlands have been used. The number of data points used for the analyses is impressive. For the benthic species in the order of 10000 samples have been used. For the birds, the number of individual count data is not always traceable, as the counts have been assembled in larger areas. Nevertheless, also these data rest on a solid observational basis of many thousands of individual data.

## 17.1 Changes in the populations

For the six benthic species, both numerical abundance and biomass were statistically analyzed, yielding 12 analyses in total. In four of these, an important difference between the spatial random field of 2018 and that of 2019 was shown, as a model with separate random fields for the two years had a lower DIC than a model with a joint random field. In two out of the four cases, the change in spatial field was clearly linked to a strong recruitment event. This concerns the cockle, where 2018 was a strong recruitment year, yielding very similar patterns in the spatial field as the other strong recruitment year in the series, 2011. It was seen that the development of biomass spatial distribution followed a repeatable pattern between these two years. That makes a link to the MSC Zoe most unlikely. Also, for the razor clam, the change in the spatial random field was very clearly linked to the massive recruitment in 2018, first detected in the data of 2019, as the coastal zone is sampled in spring before the recruits-of-the-year can be sampled. For the razor clam, it is interesting that the recruitment event is visible in the abundance, where very high numbers are found in 2019, but not (yet) in the biomass, which has different hotspots and coldspots and little change due to the addition of many very small organisms. The other two cases where a change in the spatial random fields was observed concern the mussel and the Baltic tellin. Both species are characterized by a spatial random field that is rather patchy at a relatively small scale. For mussels this is most probably linked to the occurrence of intertidal beds that have high local density and that occur in only part of the suitable habitat. For Baltic tellin the mechanism behind the small-scale patchy nature of the random field is less clear, but the fluctuations in this species were small in magnitude, suggesting it occurs relatively homogeneously across the area that, on basis of the physical cofactors, can be considered suitable habitat. In both species the differences detected between the random fields concerned a few small places, where about half of the changes were increases and the other half decreases. They provide no evidence for an exceptional external cause, such as the MSC Zoe incident.

## 17.2 Variability and power of the analysis

Although based on a solid set of observations, variability remains an important result of the analysis across the species. The variability has two distinct sources: part of it is a consequence of observational uncertainty; another part is linked to biological processes that are variable from year to year or from place to place.
Despite all efforts, variability still arises from observational uncertainty. Where abundance of a benthic species is relatively low, it is a matter of chance whether the species will be present in a particular sample or not. However, the variability arising from biological processes in the populations, such as recruitment or migration processes, is usually much larger than observational uncertainty.

In contrast to the observational uncertainty, that decreases with increasing sampling effort, the process-related part of the variability cannot be reduced by further increasing the observational effort. No matter how the measurements are made or how many measurements are available, a good recruitment year of cockles will always show much larger numbers throughout the Wadden Sea than a bad recruitment year.
For the benthic species, and in particular for the shellfish, the recruitment process is the major source of stochasticity in the population strength. Years standing out because of strong recruitment have been identified in the data of the cockle, the Baltic tellin, the razor clam, the cut-through shell and the mussel. Strong recruitment leads to particular patterns in the data. During the year of strong recruitment, numbers go up, but biomass does not yet follow. In subsequent years, numbers go down and biomass tends to remain stable or increase as the individuals grow. It was, moreover, also observed that the spatial random fields, which indicate spatially autocorrelated unresolved latent factors driving the population, can differ substantially during years of strong recruitment. The reason is variable between species. In the razor clam, recruitment peaked close to the coast, but biomass usually peaked in slightly offset areas, probably areas of good food supply or other factors favoring long-term growth and survival. These areas are different from the areas of maximal recruitment, causing the spatial random fields to vary between good and bad recruitment years. A similar shift was also observed in the cockle, which tends to develop an unusually high biomass in the north-eastern Wadden Sea during years of high recruitment but shifts the centers of high biomass towards the central Wadden Sea when recruitment is lower, and growth and survival dominate the distribution of biomass.
The variability in the bird count time series is not the same for all species. The sea ducks (eider and scoter) show extreme variability from year to year. Among the Wadden Sea birds, the shelduck is rather predictable in occurrence and numbers, whereas other species, e.g. the red knot, are also very variable. Besides conditions in the Wadden Sea, e.g. food availability or disturbance, also conditions elsewhere may determine whether the birds are massively present in the Dutch waters or not. We refer to the individual species' chapters for details most relevant to each of the species.
In view of the natural variability, it is not easy to find clear statistical signs of a disturbance by the MSC Zoe incident, should such a disturbance have happened. The more variable the background is, the more difficult it becomes to see an additional signal. As argued above, this variability is mostly an inherent consequence of biological processes, and variability stemming from those processes cannot be reduced by further increasing the sampling effort. The data bases used for this analysis are amongst the spatially most intensive monitoring programs in the world. There are no equivalents known to the SIBES program, and also the WOT shellfish survey is extremely intensive. The results of the analysis, showing very distinct reactions to physical co-factors and distinct patterns and trends linked to biological processes, also show that the data base does not yield random, stochastically-dominated results. Consequently, we estimate that the conclusions of this study are not determined by inherent methodological weaknesses of the approach as a whole (i.e. including the devoted monitoring effort) but reflect the true situation of no effect with a high likelihood. Given the complexity of the analysis, it is not possible to quantify the power of the analysis without performing extensive Monte Carlo simulations, which were outside the scope of the present project. We do not recommend extending the project to such exercise, as it is unlikely to change the outcome of the analysis and would involve major efforts, considering that a single run of the current model fitting takes between 12 and 24 hours per data set on a very fast PC.

## 17.3 Uncertainty of microplastics distribution

The analysis was complicated by the fact that no clear picture was available of the potential disturbance by the MSC Zoe incident in space and time. The likely spatial distribution of the large floating HDPE pellets is relatively well known from modelling and ground truthing, but these particles have a low probability of being taken up by any of the organisms studied here.

The northern pintail was added to the list of studied species for the single reason that for this bird, at least in principle there was a mechanistic reason why it could have taken up the pellets, as it might have mistaken them for seeds of saltmarsh plants. There was, however, no sign of disturbance of the northern pintail population at all in the statistical analysis. For the smaller PS granules, it was not possible to even remotely indicate their most probable distribution in space and time. We demonstrated (Chapter 2) that this distribution could range from diluted over a large area, to relatively concentrated in a small but unknown area. Given this uncertainty, the statistical analysis took a broad view to detect any conspicuous change in spatial pattern of the populations before and after the MSC Zoe incident.
If the distribution would have been known much more precisely, a different statistical approach would have been possible. The presence of the particles would then have been added to the model as a factor to be investigated for effect on the density or biomass of the populations. The clarity of the analysis would have profited from that situation, but it is questionable if it would have strongly increased the power of the analysis, i.e. the ability to detect an effect if one exists. The main difference would be that, whereas in the present analysis any detected change requires thorough ecological analysis and discussion, the interpretation would have been more straightforward in a regression-type of approach.

## 17.4 Short-term versus long-term effects

This study has only been able to investigate effects at relatively short time scales. The incident happened relatively recently, and moreover the working up of data sets requires time. For that reason, in benthic species there was only the possibility to detect an effect in summer 2019, about half a year after the incident. For the birds, additional data were available in 2020. At this short term, no effects were visible in the data. In theory it is possible that effects at longer term play a role for the populations. The microplastics, which were mostly in a size range that could not be ingested easily by the studied animals, could wear down to smaller size classes and moreover, adsorb toxic substances while ageing. In that form, their effect could then become stronger than the short-term effect. However, at the same time, it is likely that dilution would take place, either in the sediment or through the water column to other areas. Even if the effect would then contribute to the background stress on natural systems, it is not very likely that it would ever become detectable by analyzing the populations. Further dilution would make it even less clear where and when to look for an effect, so that confusion with natural variability becomes likely. For that reason, we do not recommend repeating this exercise at a later stage.

## 17.5 Direct and cumulative effects

The research of the ecological data series has attempted to detect a short-term, direct effect of the MSC Zoe incident on the populations of the studied species. Such effect could have been detected if it had been strong compared to variation stemming from biological processes and from other anthropogenic disturbance, including ongoing (background) plastic pollution. The analysis has not been able to demonstrate the existence of such strong direct effect. However, this does not necessarily imply that no effect at all has been exerted on the protected and flagship populations. Besides other anthropogenic stresses, plastic pollution is a chronic source of stress with a still badly quantified effect on biological populations. The microplastic pollution stemming from the MSC Zoe incident has been added to this existing stress and has increased its pressure by increasing the total amount of plastics in the environment. In that sense, it is a contribution to the existing cumulative pressure. We do not have a very precise estimate of the total amount of plastic in the natural environment of the Wadden Sea. Such estimate would be needed to evaluate the relative contribution of the plastic stemming from the incident to the total cumulative effect.

## 17.6 Fate of microplastics in the food web

Neither of the two types of pellets have a high probability of entering the food web *via* the benthic species described here. For the natural range of particle sizes ingested by the lugworm *Arenicola marina*, or by the shellfish studied here, even the small plastic granules are too large, at least based on their average size. As the particles have a size distribution, it cannot be excluded that some small particles can be ingested and, in fact, this has been observed for *Arenicola marina* in high-concentration mesocosm experiments (Foekema et al., 2021). The main effect of these plastic particles on the physiology of the animal is occupation of idle space in the digestive tract. This implies that effects on the animal can only be expected at elevated concentrations in the digestive tract. Due to the spatial distribution of the particles, this is unlikely to impossible to have occurred over large areas of the Wadden Sea or the coastal North Sea.

Over all bird species, there was only one population where an important difference in the trend value between 2019 and 2018 or 2020 was found. This was in one counting area for the eider duck, but this was part of a sharp bend in the time trend that had been ongoing since 2017 and that seems to be related to a shift in the spatial distribution of the birds in recent years. In none of the other species was there any statistical indication that something special had happened in the first months of 2019. Neither by uptake of plastics coming from the MSC Zoe, nor by the disturbance that might have been caused due to salvage operations, were consistent disruptions in the time series of bird counts visible.

In summary, we have analyzed population density and (for benthic species) biomass of some of the best documented populations in the Netherlands, taking into account natural dynamics in at least the preceding decade. Compared to the dynamics revealed in that period that was undisturbed by the MSC Zoe incident, no deviating dynamics or patterns were detected in the data. No evidence has been found for negative effects of the MSC Zoe incident on flagship protected and typical species of the protected habitats in the Wadden Sea and Dutch coastal waters of the North Sea.

# 18 References


Agüera García, A., 2015. The role of the starfish (Asterias rubens L.) predation in blue mussel (Mytilus edulis L.) seedbed stability. Wageningen University.

André, C., Jonsson, P., Lindegarth, M., 1993. Predation on settling bivalve larvae by benthic suspension feeders: the role of hydrodynamics and larval behaviour. Marine Ecology Progress Series, 183-192.

André, C., Rosenberg, R., 1991. Adult-larval interactions in the suspension-feeding bivalves Cerastoderma edule and Mya arenaria. Marine Ecology Progress Series, 227-234.

Ansell, A., Barnett, P., Bodoy, A., Massé, H., 1981. Upper temperature tolerances of some European molluscs. Marine Biology 65, 177-183.

Ardamatskaya T.B. 2001. The expansion of the common eider Somateria mollissima at Ukrainian Coast of the Black Sea. Acta Ornithologica 36: 53-54.

Armonies, W., Hellwig-Armonies, M., 1992. Passive settlement of Macoma balthica spat on tidal flats of the Wadden Sea and subsequent migration of juveniles. Netherlands Journal of Sea Research 29, 371-378.

Armonies, W., Herre, E., Sturm, M., 2001. Effects of the severe winter 1995/96 on the benthic macrofauna of the Wadden Sea and the coastal North Sea near the island of Sylt. Helgoland Mar Res 55, 170-175.

Armonies, W., Reise, K., 1999. On the population development of the introduced razor clam Ensis americanus near the island of Sylt (North Sea). Helgolander Meeresun 52, 291-300.

Baptist, M.J., Leopold, M.F., 2009. The effects of shoreface nourishments on Spisula and scoters in The Netherlands. Mar Environ Res 68, 1-11.

Bayne, B., 1971. Some morphological changes that occur at the metamorphosis of the larvae of Myths edulis. 4th European Marine Biology Symposium. Cambridge University Press, Cambridge.

Bayne, B., 1976. Marine mussels: their ecology and physiology.

Bayne, B., 1998. The physiology of suspension feeding by bivalve molluscs: an introduction to the Plymouth “TROPHEE” workshop. Journal of Experimental Marine Biology and Ecology 219, 1-19.

Belgrano, A., Legendre, P., Dewarumez, J.-P., Frontier, S., 1995. Spatial structure and ecological variation of meroplankton on the French-Belgian coast of the North Sea. Mar Ecol Prog Ser 128, 43-50.

Bell M.C. 1995. UINDEX 4. A computer programme for estimating population index numbers by the Underhill method. The Wildfowl & Wetlands Trust, Slimbridge.

Besseling, E., Wegner, A., Foekema, E.M., Van den Heuvel-Greve, M.J. & Koelmans, A.A., 2013. —Environmental Science and Technology 47: 593-600.

Beukema, J., 1974. The efficiency of the Van Veen grab compared with the Reineck box sampler. ICES Journal of Marine Science 35, 319-327.

Beukema, J., 1990. Expected effects of changes in winter temperatures on benthic animals living in soft sediments in coastal North Sea areas, Expected effects of climatic change on marine coastal ecosystems. Springer, pp. 83-92.

Beukema, J., 1993. Successive changes in distribution patterns as an adaptive strategy in the bivalveMacoma balthica (L.) in the Wadden Sea. Helgoländer Meeresuntersuchungen 47, 287-304.

Beukema, J.J., Dekker, R., 1995. Dynamics and growth of a recent invader into European coastal waters: the Amerikan razor clam, Ensis directus. Journal of the Marine Biology Association of the United Kingdom 75, 351-362.

Bijkerk, R & Dekker, P.I., 1991. De wadpier Arenicola marina (Polychaeta). Ecologisch profiel. Report RDD Aquatic Ecosystems, 77p.

Bijleveld, A.I., van Gils, J.A., van der Meer, J., Dekinga, A., Kraan, C., van der Veer, H.W. & Piersma, T. (2012) Designing a benthic monitoring programme with multiple conflicting objectives. Methods in Ecology and Evolution, 3, 526-536.

BirdLife International 2021. Species factsheet: Melanitta nigra. http://www.birdlife.org, visited on 11/02/2021.

Bos, O.G., Hendriks, I.E., Strasser, M., Dolmer, P., Kamermans, P., 2006. Estimation of food limitation of bivalve larvae in coastal waters of north-western Europe. Journal of Sea Research 55, 191-206.
Bouma, T.J., Olenin, S., Reise, K., Ysebaert, T., 2009. Ecosystem engineering and biodiversity in coastal sediments: posing hypotheses. Helgoland Marine Research 63, 95-106.
Brafield, A., Newell, G., 1961. The behaviour of Macoma balthica (L.). Journal of the Marine Biological Association of the United Kingdom 41, 81-87.
Bregnballe T. 2002. Clutch size in six Danish common eider Somateria mollissima colonies: variation in egg production. In H. Noer & G. Nehls (eds.): Population processes in the common eider Somateria mollissima. Danish Review of Game Biology 16. Rønde, Denmark.
Brenko, M.H., Calabrese, A., 1969. The combined effects of salinity and temperature on larvae of the mussel Mytilus edulis. Marine Biology 4, 224-226.
Brinkman, A., Dankers, N., and van Stralen, M. (2002). An analysis of mussel bed habitats in the Dutch Wadden Sea. *Helgoland Marine Research* 56(1)**,** 59-75. doi: 10.1007/s10152-001-0093-8.
Brock, V., 1980. The geographical distribution of Cerastoderma [Cardium] edule (L.) and C. lamarcki (Reeve) in the Baltic and adjacent seas related to salinity and salinity fluctuations. Ophelia 19, 207-214.
Browne, M.A., Dissanayake, A., Galloway, T.S., Lowe, D.M., Thompson, R.C., 2008. Ingested microscopic plastic translocates to the circulatory system of the mussel, Mytilus edulis (L.). Environmental science & technology 42, 5026-5031.
Bruyne, R.d., van Leeuwen, S., Meyling, A.G., Daan, R., 2013. Schelpdieren van het Nederlandse Noordzeegebied. Ecologische atlas van de mariene weekdieren (Mollusca). Tirion Uitgevers, Utrecht en Stichting Anemoon, Lisse 414.
Bubnova, N., 1972. Nutrition of detritus-feeding mollusks Macoma-baltica (L) and Portlandia-arctica (Gray) and their influence on bottom sediments. OCEANOLOGY-USSR 12, 899-905.
Budd, G., Rayment, W., 2001. Limecola balthica Baltic tellin. In Tyler-Walters H. and Hiscock K. (eds) Marine Life Information Network: Biology and Sensitivity Key Information Reviews, [on-line]. Plymouth: Marine Biological Association of the United Kingdom. [cited 10-02-2021]. Available from: https://www.marlin.ac.uk/species/detail/1465.
Cadée G.C., 1976. Sediment reworking by Arenicola marina on tidal flats in th Dutch Wadden Sea. —Netherlands Journal of Sea Research 10: 440-460.
Cadée, G., 2001. Zilvermeeuwen profiteren van sterven van Ensis directus. Het Zeepaard 61, 133-140.
Camphuysen C.J., Berrevoets C.M., Cremers H.J.W.M., Dekinga A., Dekker R., Ens B.J., van der Have T.M., Kats R.K.H., Kuiken T., Leopold M.F., van der Meer J. & Piersma T. 2002. Mass mortality of common eiders (Somateria mollissima) in the Dutch Wadden Sea, winter 1999/2000: starvation in a commercially exploited wetland of international importance. Biological Conservation 106: 303-317.
Cardoso, J.F.M.F., 2007. Growth and reproduction in bivalves: an energy budget approach.
Cardoso, J.F.M.F., Witte, J.I.J., van der Veer, H.W., 2007. Growth and reproduction of the bivalve Spisula subtruncata (da Costa) in Dutch coastal waters. J Sea Res 57, 316-324.
Cervencl, A., Troost, K., Dijkman, E., de Jong, M., Smit, C.J., Leopold, M.F., Ens, B.J., 2015. Distribution of wintering Common Eider Somateria mollissima in the Dutch Wadden Sea in relation to available food stocks. Marine Biology 162, 153-168.
Clay, E., 1967. Literature survey of the common fauna of estuaries, 10. Macoma balthica and Tellina tenuis. Imperial Chemical Industries Limited, Brixham Laboratory. BL/A/705.
Compton, T.J., Holthuijsen, S., Koolhaas, A., Dekinga, A., ten Horn, J., Smith, J., Galama, Y., Brugge, M., van der Wal, D., van der Meer, J., van der Veer, H.W. & Piersma, T. (2013) Distinctly variable mudscapes: distribution gradients of intertidal macrofauna across the Dutch Wadden Sea. Journal of Sea Research, 82, 103-116.
Compton, T.J., Rijkenberg, M.J., Drent, J., Piersma, T., 2007. Thermal tolerance ranges and climate variability: a comparison between bivalves from differing climates. Journal of Experimental Marine Biology and Ecology 352, 200-211.
Costil, K., Dauvin, J.-C., Duhamel, S., Hocdé, R., Mouny, P., Akopian, M., 2006. Biological heritage and food chains. Seine-Aval scientific programme.

Cozzoli, F., T. J. Bouma, T. Ysebaert, and P.M.J. Herman. 2013. 'Application of non-linear quantile regression to macrozoobenthic species distribution modelling: comparing two contrasting basins', Marine Ecology Progress Series, 475: 119-33.
Craeymeersch, J., van Stralen, M., Wijsman, J., Kesteloo, J., Perdon, K., de Mesel, I., 2007. Ontwikkeling van een monstertuig voor bestandsopnames van mesheften. IMARES.
Craeymeersch, J.A., Escaravage, V., Adema, J., van Asch, M., Tulp, I., Prins, T., 2015. PMR Monitoring natuurcompensatie Voordelta - bodemdieren 2004-2013. IMARES Rapport C091/15. 171pp.
Craeymeersch, J.A., Leopold, M.F., van Wijk, M., 2001. Halfgeknotte strandschelp en Amerikaanse zwaardschede: een overzicht van bestaande kennis over visserij, economische betekenis, regelgeving, ecologie van de beviste soorten en effecten op het ecosysteem. RIVO Nederlands Instituut voor Visserijonderzoek, IJmuiden, p. 34.
Craeymeersch, J.A., Perdon, J., 2006. De halfgeknotte strandschelp, Spisula subtruncata, in de Nederlandse kustwateren in 2005. Wageningen IMARES BV (RIVO). Rapport C036/06. 22 pp.
Creek, G.A., 1960. The development of the lamellibranch Cardium edule L, Proceedings of the Zoological Society of London. Wiley Online Library, pp. 243-260.
Crisp, D.J., 1964. The effects of the winter of 1962/63 on the British marine fauna. Helgolaender Wissenschaftliche Meeresuntersuchungen 10, 313-327.
Dankers, N., Fey-Hofstede, F., 2015. Een zee van Mosselen. Handboekecologie, bescherming, beleid en beheer van mosselbanken in de Waddenzee. Stichting Anemoon, Lisse, The Netherlands.
Dauvin, J., Ruellet, T., Thiebaut, E., Gentil, F., Desroy, N., Janson, A., Duhamel, S., Jourde, J., Simon, S., 2007. The presence of Melinna palmata (Annelida: Polychaeta) and Ensis directus (Mollusca: Bivalvia) related to sedimentary changes in the Bay of Seine (English Channel, France). CBM-Cahiers de Biologie Marine 48, 391-401.
De Boer, T.W., De Bruyne, R., 1983. De amerikaanse zwaardschede Ensis directus (Conrad, 1843) in Nederland. Basteria 47, 154-154.
De Mesel, I., Craeymeersch, J., Schellekens, T., van Zweeden, C., Wijsman, J., Leopold, M., Dijkman, E., Cronin, K., 2011. Kansenkaarten voor schelpdieren op basis van abiotiek en hun relatie tot het voorkomen van zwarte zee-eenden. IMARES Wageningen UR, Rapport C042/11. .
De Montaudouin, X., Bachelet, G., 1997. Experimental evidence of complex interactions between biotic and abiotic factors in the dynamics of an intertidal population of the bivalve Cerastoderma edule. Oceanographic Literature Review 2, 127.
de Vries V. 1939. Bijdrage tot de voedselbiologie van een viertal eenden-soorten, naar aanleiding van materiaal, afkomstig van Vlieland en Terschelling. Limosa 12: 87-98.
Degraer, S., Meire, P., Vincx, M., 2007. Spatial distribution, population dynamics and productivity of Spisula subtruncata: implications for Spisula fisheries in seaduck wintering areas. Mar Biol 152, 863-875.
Drent, J., 2004. Life history variation of a marine bivalve (Macoma balthica) in a changing world.
Duijns S, Hidayati NA & Piersma T. 2013. Bar-tailed Godwits Limosa l. lapponica eat polychaete worms wherever they winter in Europe. Bird Study 60: 1-9.
Durinck J., Christensen K.D., Skov H. & Danielsen F. 1993. Diet of Common scoter Melanitta nigra and velvet scoter M. fusca wintering in the North Sea. Ornis Fennica 70: 215-218.
Durinck J., Skov H., Jensen F.P. & Pihl S. 1994. Important marine areas for wintering birds in the Baltic Sea. EU DG XI research contract no. 224/90-09-01, Ornis Consult Report 1994: 1-110, Copenhagen.
Ellien, C., Thiébaut, E., Dumas, F., Salomon, J.-C., Nival, P., 2004. A modelling study of the respective role of hydrodynamic processes and larval mortality on larval dispersal and recruitment of benthic invertebrates: example of Pectinaria koreni (Annelida: Polychaeta) in the Bay of Seine (English Channel). Journal of Plankton Research 26, 117-132.
Ens B.J., Kats R.K.H. & Camphuysen C.J. 2006. Waarom zijn Eiders niet massaal gestorven in de winter van 2005/2006? Limosa 79: 95-106.
Essink, K., 1994. Foreign species in the Wadden Sea, do they cause problems. Wadden Sea Newsletter 1, 9-11.
Fijn R., Leopold M., Dirksen S., Arts F., van Asch M., Baptist M., Craeymeersch J., Engels B., van Horssen P., de Jong J., Perdon J., van der Zee E. & van der Ham N. 2017. Een

onverwachte concentratie van Zwarte Zee-eenden in de Hollandse kustzone in een gebied met hoge dichtheden van geschikte schelpdieren. Limosa 90: 97-117.
Foekema, E., van der Molen, J., Asjes, A., Bijleveld, A., Brasseur, S., Camphuysen, K., van Franeker, J.A., Holthuijsen, S., Kentie, R., Kühn, S., Leopold, M., Kleine Schaars, L., Lok, T., Niemann, H., Schop, J. (2021). Ecologische effecten van het ongeluk met de MSC Zoe op het Nederlandse Waddengebied, met focus op microplastics. NIOZ Rapport 2021-03. NIOZ Royal Netherlands Institute for Sea Research, 't Horntje, Texel, The Netherlands. 98pp. DOI: 10.25850/nioz/7b.b.mb
Folmer, E., Büttger, H., Herlyn, M., Markert, A., Millat, G., Troost, K., Wehrmann, A., 2017. Beds of blue mussels and Pacific oysters.
Fox A.D. 2003. Diet and habitat use of scoters Melanitta in the Western Palearctic - a brief overview. Wildfowl 54: 163-182.
Fox A.D. 2003. Diet and habitat use of scoters Melanitta in the Western Palearctic - a brief overview. Wildfowl 54: 163-182.
Fransson T., Jansson L., Kolehmainen T., Kroon C. & Wenninger T. 2017. EURING list of longevity records for European birds. https://euring.org/data-and-codes/longevity-list, visited on 11/02/2021.
Frechette, M., Butman, C.A., Geyer, W.R., 1989. The importance of boundary-layer flows in supplying phytoplankton to the benthic suspension feeder, Mytilus edulis L. Limnology and oceanography 34, 19-36.
Gebhardt, C., Forster, S., 2018. Size-selective feeding of Arenicola marina promotes long-. term buriel of microplastic particles in marine sediments. —Environmental pollution 242, B: 1777-1786.
Gollasch, S., Kerckhof, F., Craeymeersch, J., Goulletquer, P., Jensen, K., Jelmert, A., Minchin, D., 2015. Alien Species Alert: Ensis directus. Current status of invasions by the marine bivalve Ensis directus. ICES COOPERATIVE RESEARCH REPORT NO. 323, p. 36.
Gollasch, S., Minchin, D., Rosenthal, H., Voigt, M., 1999. Exotics across the ocean. Case histories on introduced species: their general biology, distribution, range expansion and impact. Logos-Verlag.
Gosling, E., 2003. Bivalve molluscs: biology, ecology and culture. John Wiley & Sons.
Green, D.S., Boots, B.,Sigwart, J., Jiang, S. & Rocha, C., 2016. Effects of conventional and biodegradable microplastics on a marine microsystem engineer (Arenicola marina) and sediment nutrient cycling. —Environmental Pollution 208, B: 426-434.
Guilhermino, L., Vieira, L.R., Ribeiro, D., Tavares, A.S., Cardoso, V., Alves, A., Almeida, J.M., 2018. Uptake and effects of the antimicrobial florfenicol, microplastics and their mixtures on freshwater exotic invasive bivalve Corbicula fluminea. Science of the Total Environment 622, 1131-1142.
Guillou, J., Tartu, C., 1994. Post-larval and juvenile mortality in a population of the edible cockle Cerastoderma edule (L.) from northern Brittany. Netherlands Journal of Sea Research 33, 103-111.
Hancock, D., Urquhart, A., 1964. Mortalities of edible cockles (Cardium edule L.) during the severe winter of 1962-64. Journal of the Marine Biological Association of the United Kingdom 33, 176-178.
Hayward PJ & Ryland JS. (1995) Handbook of the marine fauna of North-West Europe. Oxford University Press.
Helm, M.M., 2004. Hatchery culture of bivalves: a practical manual. FAO.
Herman, P. and R. van Weerdenburg. 2020. Cofactoren voor bodemdieren in de Waddenzee Beschrijving van data en modeluitvoer. Deltares report.
Hiddink, J., Marijnissen, S., Troost, K., Wolff, W., 2002. Predation on 0-group and older year classes of the bivalve Macoma balthica: interaction of size selection and intertidal distribution of epibenthic predators. Journal of Experimental Marine Biology and Ecology 269, 223-248.
Hiddink, J., Wolff, W., 2002. Changes in distribution and decrease in numbers during migration of the bivalve Macoma balthica. Marine Ecology Progress Series 233, 117-130.
Hiddink, J.G., 2002. The adaptive value of migrations for the bivalve Macoma balthica. University of Groningen Groningen, The Netherlands.
Hill, J., 2006. Ensis ensis. A razor shell. In Tyler-Walters H. and Hiscock K. (eds) Marine Life Information Network: Biology and Sensitivity Key Information Reviews, [on-line].

Plymouth: Marine Biological Association of the United Kingdom. [cited 09-02-2021]. Available from: https://www.marlin.ac.uk/species/detail/1419.
Holland, A., Dean, J., 1977. The biology of the stout razor clam Tagelus plebeius: I. Animal-sediment relationships, feeding mechanism, and community biology. Chesapeake Science 18, 58-66.
Honkoop, P., Van der Meer, J., 1998. Experimentally induced effects of water temperature and immersion time on reproductive output of bivalves in the Wadden Sea. Journal of Experimental Marine Biology and Ecology 220, 227-246.
Hornman M, Hustings F, van Roomen M, Koffijberg K, van Winden E, Soldaat L 2012. Populatietrends van overwinterende en doortrekkende watervogels in Nederland in 1975-2010. Limosa 85: 97-116.
Hornman M., Hustings F., Koffijberg K., van Winden E, van Els P., Kleefstra R., Sovon Ganzen- en Zwanenwerkgroep & Soldaat L. 2020. Watervogels in Nederland in 2017/2018. Sovon rapport 2020/01, RWS-rapport BM 19.18. Sovon Vogelonderzoek Nederland, Nijmegen.
Houziaux, J., Craeymeersch, J., Merckx, B., Kerckhof, F., Van Lancker, V., Courtens, W., Stienen, E., Perdon, J., Goudswaard, P., Van Hoey, G., 2011. EnSIS'-Ecosystem Sensitivity to Invasive Species. Final Report. Brussels: Belgian Science Policy Office. Research Programme Science for a Sustainable Development: 0-105.
Hulscher, J.B., 1982. The oystercatcher Haematopus ostralegus as a predator of the bivalve Macoma balthica in the Dutch Wadden Sea. Ardea 55, 89-152.
Hummel, H., 1985a. Food intake and growth in Macoma balthica (Mollusca) in the laboratory. Netherlands journal of sea research 19, 77-83.
Hummel, H., 1985b. Food intake of Macoma balthica (Mollusca) in relation to seasonal changes in its potential food on a tidal flat in the Dutch Wadden Sea. Netherlands Journal of Sea Research 19, 52-76.
Jensen, K.T., Jensen, J.N., 1985. The importance of some epibenthic predators on the density of juvenile benthic macrofauna in the Danish Wadden Sea. Journal of Experimental Marine Biology and Ecology 89, 157-174.
Kamermans, P., Brummelhuis, E., Dedert, M., 2013. Effect of algae-and silt concentration on clearance-and growth rate of the razor clam Ensis directus, Conrad. Journal of experimental marine biology and ecology 446, 102-109.
Kamermans, P., Brummelhuis, E., Wijsman, J.W.M., 2011. First pioneering laboratory experiments on filtration, respiration and growth of the razor clam (Ensis directus, Conrad). IMARES.
Kamermans, P., Bult, T., Kater, B., Baars, J., Kesteloo-Hendrikse, J., Perdon, K., Schuiling, E., 2004. Eindrapport EVA II (Evaluatie Schelpdiervisserij tweede fase) Deelproject H4: Invloed van natuurlijke factoren en kokkelvisserij op de dynamiek van bestanden aan kokkels (Cerastoderma edule) en nonnen (Macoma balthica) in de Waddenzee, Ooster-en Westerschelde. RIVO.
Karlsson, Ö., Jonsson, P.R., Larsson, A.I., 2003. Do large seston particles contribute to the diet of the bivalve Cerastoderma edule? Marine Ecology Progress Series 261, 161-173.
Kater, B., van Kessel, A.G., Baars, J., 2006. Distribution of cockles Cerastoderma edule in the Eastern Scheldt: habitat mapping with abiotic variables. Marine Ecology Progress Series 318, 221-227.
Kats R.K.H. Common eiders Somateria mollissima in the Netherlands. The rise and fall of breeding and wintering populations in relation to the stocks of shellfish. PhD thesis, Univ. Groningen.
Keller V., Herrando S., Voříšek P., Franch M., Kipson M., Milanesi P., Martí D., Anton M., Klvaňová A., Kalyakin M.V., Bauer H.-G. & Foppen R.P.B. 2020. European Breeding Bird Atlas 2: Distribution, Abundance and Change. European Bird Census Council & Lynx Edicions, Barcelona.
Kenchington, E., Duggan, R., Riddell, T., 1998. Early Life History Characteristics of the Razor Clam, Ensis Directus, and the Moonsnails, Euspira Spp., with Applications to Fisheries and Aquaculture. Department of Fisheries & Oceans, Science Branch, Maritimes Region ….
Keus, B., 1986. De predatie van de garnaal (Crangon crangon) op het broed van het nonnetje (Macoma balthica). Interne verslagen Nederlands Instituut voor Onderzoek der Zee.

Kingston, P., 1974. Some observations on the effects of temperature and salinity upon the growth of Cardium edule and Cardium glaucum larvae in the laboratory. Journal of the Marine Biological Association of the United Kingdom 54, 309-317.
Kristensen, I., 1958. Differences in density and growth in a cockle population in the Dutch Wadden Sea. Archives neerlandaises de Zoologie 12, 351-453.
Leonard, G.H., Bertness, M.D., Yund, P.O., 1999. Crab predation, waterborne cues, and inducible defenses in the blue mussel, Mytilus edulis. Ecology 80, 1-14.
Leopold M.F, Verdaat H., Spierenburg P. & van Dijk J. 2010. Zee-eendenvoedsel op een recente zandsuppletie bij Noordwijk. IMARES Rapport C021/10.
Leopold M.F. 1993. Spisula's, zeeëenden en kokkelvissers: een nieuw milieuprobleem op de Noordzee. Sula 7: 24-28.
Leopold M.F. 2005. Hoog-noordelijke eiders met vlaggetjes: wie ziet de eerste? Nieuwsbrief Nederlandse Zeevogelgroep 6(3): 10.
Leopold M.F., Baptist H.J.M. , Wolf P.A. & Offringa H. 1995. De zwarte Zeeëend Melanitta nigra in Nederland. Limosa 68: 49-64.
Leopold M.F., Kats R.K.H. & Ens B.J. 2001. Diet (preferences) of common eiders Somateria mollissima. Wadden Sea Newsletter 2000-1: 25-31.
Leopold M.F., M. van Asch, E. Dijkman, K. Goudswaard, S. Lagerveld, H. 2014. Zwarte zee-eenden bij Texel, een reactie op overvloedig voorkomen van Ensis? IMARES-report C084/14.
Leopold M.F., van Bemmelen R., Perdon J., Poot M., Heunks C., Beuker D., Jonkvorst R.J. & de Jong J. 2013. Zwarte zee-eenden in de Noordzeekustzone benoorden de Wadden: verspreiding en aantallen in relatie tot voedsel en verstoring. IMARES Rapport C023/13.
Loosanoff, V.L., Davis, H.C., 1963. Rearing of bivalve mollusks, Advances in marine biology. Elsevier, pp. 1-136.
Maurer, D., Watling, L., Aprill, G., 1974. The distribution and ecology of common marine and estuarine pelecypods in the Delaware Bay area. Nautilus 88, 38-45.
Meire, P.M., 1993. The impact of bird predation on marine and estuarine bivalve populations: a selective review of patterns and underlying causes. Bivalve filter feeders, 197-243.
Møhlenberg, F., Riisgård, H., 1979. Filtration rate, using a new indirect technique, in thirteen species of suspension-feeding bivalves. Marine Biology 54, 143-147.
Møhlenberg, F., Riisgård, H.U., 1978. Efficiency of particle retention in 13 species of suspension feeding bivalves. Ophelia 17, 239-246.
Muir, S.D., 2003. The biology of razor clams ('Ensis' spp.) and their emergent fishery on the west coast of Scotland. University of London.
Oertzen, J.V., 1969. Erste Ergebrisse zur experimentellen ökologie von postglazialen Relikten (Bivalvia) der Ostsee. Limnologica (Berlin) 7, 129-137.
Olafsson, E., 1986. Density dependence in suspension-feeding and deposit-feeding populations of the bivalve Macoma balthica: a field experiment. The Journal of animal ecology, 517-526.
Paul-Pont, I., Lacroix, C., Fernández, C.G., Hégaret, H., Lambert, C., Le Goïc, N., Frère, L., Cassone, A.-L., Sussarellu, R., Fabioux, C., 2016. Exposure of marine mussels Mytilus spp. to polystyrene microplastics: toxicity and influence on fluoranthene bioaccumulation. Environmental pollution 216, 724-737.
Payne, B.S., Miller, A.C., Lei, J., 1995. Palp to gill area ratio of bivalves: a sensitive indicator of elevated suspended solids. Regulated Rivers: Research & Management 11, 193-200.
Perdon, K.J., Troost, K., Zwol, J.v., Asch, M.v., Pool, J.v.d., Perdon, K.J., Troost, K., Zwol, J.v., Asch, M.v., Pool, J.v.d., 2019. Schelpdierbestanden in de Nederlandse kustzone in 2019. Stichting Wageningen Research, Centrum voor Visserijonderzoek (CVO), IJmuiden.
Piersma T 1994. Close to the edge: energetic bottlenecks and the evolution of migratory pathways in Knots. Proefschrift, Rijksuniversiteit Groningen / Uitgeverij Het Open Boek, Den Burg, Texel.
Piersma T 2007. Using the power of comparison to explain habitat use and migration strategies of shorebirds worldwide. Journal of Ornithology 148: S45-S59.
Piersma, T., Verkuil, Y., Tulp, I., 1994. Resources for long-distance migration of knots Calidris canutus islandica and C. c. canutus: how broad is the temporal exploitation window of benthic prey in the western and eastern Wadden Sea? Oikos, 393-407.

Poot M. 2018. Zwarte Zee-eend Melanitta nigra. P. 129 in: SOVON Vogelonderzoek Nederland. Vogelatlas van Nederland. Broedvogels, wintervogels en 40 jaar verandering. Kosmos Uitgevers, Utrecht/Antwerpen.

Prins T.C., van der Kolff G.H., Boon A.R., Reinders J., Kuijper C., Hendriksen G., Holzhauer H., Langenberg V.T., Craeymeersch J.A.M., Tulp I.Y.M., Poot M.J.M., Seegers H.C.M. & Adema J. 2014. PMR Monitoring natuurcompensatie Voordelta. Deltares, Eindrapport 1e fase 2009-2013.

Prins, T., Meer, J.v.d., Herman, P., Spek, A.v.d., Chen, C., Wymenga, E., Zee, E.v.d., Stienen, E., Aarts, G., Meijer-Holzhauer, H., Adema, J., Craeymeersch, J., Wolfshaar, K.v., Bolle, L., Poot, M., Hintzen, N., Horssen, P.v., Fijn, R., Glorius, S., Beier, U., Courtens, W., Neitzel, S., Hoof, L.v., Prins, T., Meer, J.v.d., Herman, P., Spek, A.v.d., Chen, C., Wymenga, E., Zee, E.v.d., Stienen, E., Aarts, G., Meijer-Holzhauer, H., Adema, J., Craeymeersch, J., Wolfshaar, K.v., Bolle, L., Poot, M., Hintzen, N., Horssen, P.v., Fijn, R., Glorius, S., Beier, U., Courtens, W., Neitzel, S., Hoof, L.v., 2020. Eindrapportage monitoring- en onderzoeksprogramma Natuurcompensatie Voordelta (PMR-NCV). Wageningen Marine Research, Den Helder.

Rakhimberdiev E., Duijns S., Karagicheva J., Camphuysen C.J., VRS Castricum, Dekinga A. , Dekker R., Gavrilov A., ten Horn J., Jukema J., Saveliev A., Soloviev M., Tibbitts T.L., van Gils J.A. & Piersma T. 2018. Fuelling conditions at staging sites can mitigate Arctic warming effects in a migratory bird. Nature Communications 9: 4263.

Rappoldt C., M. Kersten & C. Smit 1985. Errors in large-scale shorebird counts. Ardea 73: 13-24.

Ratcliffe, P., Jones, N., Walters, N., 1981. The Survival of MacomaBalthica (L.) in Mobile Sediments, Feeding and Survival Srategies of Estuarine Organisms. Springer, pp. 91-108.

Read, K.R., Cumming, K.B., 1967. Thermal tolerance of the bivalve molluscs Modiolus modiolus L., Mytilus edulis L. and Brachidontes demissus Dillwyn. Comparative biochemistry and physiology 22, 149-155.

Richards, H.G., 1938. Animals of the seashore.

Riera, P., 2007. Trophic subsidies of Crassostrea gigas, Mytilus edulis and Crepidula fornicata in the Bay of Mont Saint Michel (France): a δ13C and δ15N investigation. Estuarine, Coastal and Shelf Science 72, 33-41.

Riisgård, H.U., 2001. On measurement of filtration rates in bivalves—the stony road to reliable data: review and interpretation. Marine Ecology Progress Series 211, 275-291.

Riisgard, H.U., Randløv, A., Kristensen, P.S., 1980. Rates of water processing, oxygen consumption and efficiency of particle retention in veligers and young post-metamorphic Mytilus edulis. Ophelia 19, 37-46.

Robinson R.A. 2005. BirdFacts: profiles of birds occurring in Britain & Ireland. BTO, Thetford http://www.bto.org/birdfacts, visited on 11 February 2021

Sala, A., Nielsen, J.R., Rijnsdorp, A.D., Polet, H., Laffargue, P., Smith, C., Zengin, M., 2016. Report on results of sea trials in the regional seas.

Sanchez-Salazar, M., Griffiths, C., Seed, R., 1987. The interactive roles of predation and tidal elevation in structuring populations of the edible cockle, Cerastoderma edule. Estuarine, Coastal and Shelf Science 25, 245-260.

Scheiffarth G. 2001. The diet of Bar-tailed Godwits Limosa lapponica in the Wadden Sea: combining visual observations and faeces analyses. Ardea 89: 481-494.

Schelpdiermonitor, 2021. Schelpdiermonitor. Wageningen Marine Research. Available from: https://shiny.wur.nl/Schelpdiermonitor_WaddenSublit/.

Schwemmer P., Volmer H., Enners L., Reimers H.-C., Binder K., Horn S., Adler S., Fox A.D. & Garthe S. 2019. Modelling distribution of common scoter (Melanitta nigra) by its predominant prey, the American razor clam (Ensis leei) and hydrodynamic parameters. Estuarine, Coastal and Shelf Science 225 (2019) 106260.

Seed, R., 1969. The ecology of Mytilus edulis L.(Lamellibranchiata) on exposed rocky shores. Oecologia 3, 277-316.

Seed, R., Brown, R., 1977. A comparison of the reproductive cycles of Modiolus modiolus (L.), Cerastoderma (= Cardium) edule (L.), and Mytilus edulis L. in Strangford Lough, Northern Ireland. Oecologia 30, 173-188.

Shumway, S.E., Cucci, T.L., Newell, R.C., Yentsch, C.M., 1985. Particle selection, ingestion, and absorption in filter-feeding bivalves. Journal of experimental marine biology and ecology 91, 77-92.

Skilleter, G.A., Peterson, C.H., 1994. Control of foraging behavior of individuals within an ecosystem context: the clam Macoma balthica and interactions between competition and siphon cropping. Oecologia 100, 268-278.
Skov H., Durinck J., Erichsen A., Kloster R.M., M/ohlenberg F. & Leonard S.B. 2008. Horns Rev II offshore wind farm food basis for common scoter. Baseline studies 2007-2008. Report commissioned by DONG energy, Orbicon/DHI/Marine Observers, 46p.
Skov H., Durinck J., Leopold M.F. & Tasker M.L. 1995. Important bird areas in the North Sea, including the Channel and the Kattegat. BirdLife International, Cambridge, 156p.
Sluijter M., Arts F.A., Lilipaly S.J., & Wolf P.A. 2020. Midwintertelling van zee-eenden in de Waddenzee en Nederlandse kustwateren in augustus en november 2019 en januari 2020. Rapport RWS - Centrale Informatievoorziening. Rapport BM 20.20 / Deltamilieu Projecten rapport 2020-6, Vlissingen.
Sluijter M., Arts F.A., Lilipaly S.J., & Wolf P.A. 2020. Midwintertelling van zee-eenden in de Waddenzee en Nederlandse kustwateren in augustus en november 2019 en januari 2020. Rapport RWS - Centrale Informatievoorziening. Rapport BM 20.20 / Deltamilieu Projecten rapport 2020-6, Vlissingen.
Smaal, A., Craeymeersch, J., Drent, J., Jansen, J., Glorius, S., Van Stralen, M., 2013. Effecten van mosselzaadvisserij op sublitorale natuurwaarden in de westelijke Waddenzee: samenvattend eindrapport. IMARES.
Smit C. 2018. Eider Somateria mollissima. Pp. 126-127 in: SOVON Vogelonderzoek Nederland. Vogelatlas van Nederland. Broedvogels, wintervogels en 40 jaar verandering. Kosmos Uitgevers, Utrecht/Antwerpen.
Smit C.J. & de Jong M. 2011 Aantallen en verspreiding van eiders, toppers en zee-eenden in de winter van 2011-2011. IMARES Rapport C196/11.
Sörlin, T., 1988. Floating behaviour in the tellinid bivalve Macoma balthica (L.). Oecologia 77, 273-277.
Sprung, M., 1984. Physiological energetics of mussel larvae (Mytilus edulis). 11. Food uptake. Marine Ecology-Progress Series 17, 295-305.
Stralen, M.v., 2002. De ontwikkeling van mosselbestanden op droogvallende platen en in het sublitoraal van de Waddenzee vanaf 1955: een reconstructie op basis van gegevens uit de mosselzaadvisserij. Marinx.
Strohmeier, T., Strand, Ø., Alunno-Bruscia, M., Duinker, A., Cranford, P.J., 2012. Variability in particle retention efficiency by the mussel Mytilus edulis. Journal of Experimental Marine Biology and Ecology 412, 96-102.
Suykerbuyk, W., Van den Bogaart, L., Hamer, A., Walles, B., Troost, K., Tangelder, M., In prep. Hittestress op intergetijdenplaten van de Oosterschelde. Wageningen Marine Research.
Swennen C. & Spaans A.L. 1970. De sterfte van zeevogels door olie in februari 1969 in het Waddengebied. Het Vogeljaar 18: 233-245.
Swennen C. 1972. Clorinated hydrocarbons attacked the Eider population in The Netherlands. TNO-nieuws 12: 556-560.
Swennen C. 1976. Populatiestructuur en voedsel van de eidereend Somateria mollissima in de Nederlandse Waddenzee. Ardea 64: 311-371.
Swennen C. 1985. Iets over de vogels van het open water van IJsselmeer, Waddenzee en Noordzee. Vogeljaar 33: 208-214.
Swennen C., Nehls G. & Laursen K. 1989. Numbers and distribution of eiders Somateria mollissima in the Wadden Sea. Neth. J. Sea Res. 24: 83-92.
Swennen, C., Leopold, M., Stock, M., 1985. Notes on growth and behaviour of the American razor clamEnsis directus in the Wadden Sea and the predation on it by birds. Helgoländer Meeresuntersuchungen 39, 255-261.
Tebble, N., 1966. British bivalve seashells. Birtish museum (Natural History). London.
Theisen, B.F., 1968. Growth and mortality of culture mussels in the Danish Wadden Sea. Andr. Fred. Høst & Søn.
Thieltges, D.W., Engelsma, M.Y., Wendling, C.C., Wegner, K.M., 2013. Parasites in the Wadden Sea food web. Journal of Sea Research 82, 122-133.
Troost, K., 2009. Pacific oysters in Dutch estuaries: causes of success and consequences for native bivalves.
Troost, K., Drent, J., Folmer, E., van Stralen, M., 2012. Ontwikkeling van schelpdierbestanden op de droogvallende platen van de Waddenzee. De Levende Natuur 113, 83-88.

Troost, K., Stamhuis, E.J., van Duren, L.A., Wolff, W.J., 2009. Feeding current characteristics of three morphologically different bivalve suspension feeders, Crassostrea gigas, Mytilus edulis and Cerastoderma edule, in relation to food competition. Marine Biology 156, 355-372.
Troost, K., Van Asch, M., 2018. Herziene schatting van het kokkelbestand in de Waddenzee en Oosterschelde in het najaar van 2018. Stichting Wageningen Research, Centrum voor Visserijonderzoek (CVO).
Troost, K., Van Asch, M., Brummelhuis, E., Van den Ende, D., Van Es, Y., Perdon, J., Van der Pool, J., Van Zweeden, C., Van Zwol, J., 2021. Schelpdierbestanden in de Nederlandse kustzone, Waddenzee en zoute deltawateren in 2020. Stichting Wageningen Research, Centrum voor Visserijonderzoek (CVO).
Troost, K., Veldhuizen, R., Stamhuis, E.J., Wolff, W.J., 2008. Can bivalve veligers escape feeding currents of adult bivalves? Journal of Experimental Marine Biology and Ecology 358, 185-196.
Trueman, E., 1967. The dynamics of burrowing in Ensis (Bivalvia). Proceedings of the Royal Society of London. Series B. Biological Sciences 166, 459-476.
Tulp I., Craeymeersch J., Leopold M., van Damme C., Fey F. & Verdaat H. 2010. The role of the invasive bivalve Ensis directus as food source for fish and birds in the Dutch coastal zone. Estuarine, Coastal and Shelf Science 90: 116-128.
Tulp, I., Glorius, S., Rippen, A., Looije, D., Craeymeersch, J., 2020. Dose-response relationship between shrimp trawl fishery and the macrobenthic fauna community in the coastal zone and Wadden Sea. J Sea Res 156.
Tyler-Walters, H., 2007. *Cerastoderma edule* Common cockle. In Tyler-Walters H. and Hiscock K. (eds) *Marine Life Information Network: Biology and Sensitivity Key Information Reviews*, [on-line]. Plymouth: Marine Biological Association of the United Kingdom. DOI https://dx.doi.org/10.17031/marlinsp.1384.1.
Tyler-Walters, H., 2008. Mytilus edulis Common mussel. In Tyler-Walters H. and Hiscock K. (eds) Marine Life Information Network: Biology and Sensitivity Key Information Reviews, [on-line]. Plymouth: Marine Biological Association of the United Kingdom. [cited 04-02-2021]. Available from: https://www.marlin.ac.uk/species/detail/1421.
van Asch, M., van den Ende, D., van der Pool, J., Brummelhuis, E. B. M., van Zweeden, C., van Es, Y., Troost, K., 2019. Het kokkelbestand in de Nederlandse kustwateren in 2019. CVO report; No. 19.009 Wageningen UR - Centrum voor Visserijonderzoek (CVO) en Wageningen Marine Research.
van Cauwenberghe, L., Claessens, M., Vandegehuchte, M.B. & Janssen, C.R., 2015. Microplastics are taken up by mussels (Mytilus edulis) and lugworms (Arenicola marina) living in natural habitats. —Environmental pollution 199: 10-17.
Van Cauwenberghe, L., Devriese, L., Galgani, F., Robbens, J., Janssen, C.R., 2015. Microplastics in sediments: a review of techniques, occurrence and effects. —Marine Environmental Research 111: 5-17.
Van den Ende, D., Troost, K., Van Asch, M., Perdon, J., Van Zweeden, C., 2020. Mosselbanken en oesterbanken op droogvallende platen van de Nederlandse zoute getijdenwateren in 2019: bestand en arealen. Stichting Wageningen Research, Centrum voor Visserijonderzoek (CVO).
van der Hout, C.M., Witbaard, R., Bergman, M.J.N., Duineveld, G.C.A., Rozemeijer, M.J.C., and Gerkema, T. (2017). The dynamics of suspended particulate matter (SPM) and chlorophyll-a from intratidal to annual time scales in a coastal turbidity maximum. Journal of Sea Research 127, 105-118. doi: https://doi.org/10.1016/j.seares.2017.04.011.
van der Meer, J., Dankers, N., Ens, B.J., van Stralen, M., Troost, K., Waser, A.M., 2018. The Birth, Growth and Death of Intertidal Soft-Sediment Bivalve Beds: No Need for Large-Scale Restoration Programs in the Dutch Wadden Sea. Ecosystems, 1-11.
van der Veer, H.W., Cardoso, J.F., van der Meer, J., 2006. The estimation of DEB parameters for various Northeast Atlantic bivalve species. Journal of Sea Research 56, 107-124.
van Gils JA, Dekinga A, Spaans B, Vahl WK, Piersma T 2005. Digestive bottleneck affects foraging decisions in red knots Calidris canutus. II. Patch choice and length of working day. Journal of Animal Ecology 74: 120-130.
van Roomen M., C. van Turnhout, J. Nienhuis, F. Willems & E. van Winden 2002. Monitoring van watervogels als niet-broedvogel in de Nederlandse Waddenzee: evaluatie huidige

opzet en voorstellen voor de toekomst. Sovon-onderzoeksrapport 2002/01. Sovon, BeekUbbergen.
Vaquer, C.D.A., Lam-Höai, T., Rougier, C., Mazouni, N., Lautier, J., Collos, Y., Le Gall, S., 2000. Feeding rate of the oyster Crassostrea gigas in a natural planktonic community of the Mediterranean Thau Lagoon. Marine Ecology Progress Series 205, 171-184.
Verdelhos, T., Marques, J., Anastácio, P., 2015. Behavioral and mortality responses of the bivalves Scrobicularia plana and Cerastoderma edule to temperature, as indicator of climate change's potential impacts. Ecological Indicators 58, 95-103.
Von Cosel, R., 2009. The razor shells of the eastern Atlantic, part 2. Pharidae II: the genus Ensis Schumacher, 1817 (Bivalvia, Solenoidea). Basteria 73, 9-56.
Von Cosel, R., Dörjes, J., Mühlenhardt-Siegel, U., 1982. Die amerikanische Schwertmuschel Ensis directus (Conrad) in der Deutschen Bucht: I. Zoogeographie und Taxonomie im Vergleich mit den einheimischen Schwertmuschel-Arten= The american jackknife clam Ensis directus (Conrad) in the German Bight: I. Zoogeography and taxonomy in comparison with the native jackknife and razor clams. Senckenbergiana Maritima: wissenschaftliche Mitteilungen der Senckenbergischen naturforschenden Gesellschaft.
Voous K.H. 1960. Atlas of European Birds. Nelson and sons Ltd, London 284p.
Vroom, J., R. van Weerdenburg, B.P. Smits, and P.M.J. Herman. 2020. "Modellering slibdynamiek voor de Waddenzee. Kalibratie voor KRW slib." Deltares report.
Ward, J., Sanford, L., Newell, R., MacDonald, B., 1998. A new explanation of particle capture in suspension-feeding bivalve molluscs. Limnology and Oceanography 43, 741-752.
Ward, J.E., Shumway, S.E., 2004. Separating the grain from the chaff: particle selection in suspension-and deposit-feeding bivalves. Journal of Experimental Marine Biology and Ecology 300, 83-130.
Widdows, J., 1991. Physiological ecology of mussel larvae. Aquaculture 94, 147-163.
Wijsman, J.W.M., Kesteloo-Hendrikse, J., Craeymeersch, J., 2006. Ecologie, visserij en monitoring van mesheften in de Voordelta. RIVO.
Witbaard, R., Duineveld, G.C.A., Bergman, M.J.N., Witte, H.I.J., Groot, L., Rozemeijer, M.J.C., 2015. The growth and dynamics of Ensis directus in the near-shore Dutch coastal zone of the North Sea. J Sea Res 95, 95-105.
Witbaard, R., Kamermans, P., 2009. De bruikbaarheid van de klepstandmonitor op Ensis directus ten behoeve van de monitoring van aan zandwinning gerelateerde effecten. NIOZ rapport 10, 2010.
Yonge, M., 1949. On the structure and adaptions of the Tellinacea, deposit-feeding Eulamellibranchia. Philosophical Transactions of the Royal Society of London. Series B, Biological Sciences 234, 29-76.
Ysebaert, T., P. Meire, P.M.J. Herman, and H. Verbeek. 2002. 'Macrobenthic species response surfaces along estuarine gradients: prediction by logistic regression', Marine Ecology Progress Series, 225: 79-95.
Zuur A.F. & Ieno E.N. 2021. Statistical analysis investigation the effects of the container loss by the MSC Zoe in January 2019. Highland Statistics Ltd., Newburgh, Scotland & Alicante, Spain.
Zwarts, L., Cayford, J., Hulscher, J., Kersten, M., Meire, P., Triplet, P., 1996. Prey size selection and intake rate. In ‘Oystercatcher: From Individuals to Populations’.(Ed. JD Gross-Custard.) pp. 30–55. Oxford University Press: Oxford.

# Appendix I. Internal memo Rijkswaterstaat underlying the research and the legal context

**INTERNE NOTITIE VOOR RIJKSWATERSTAAT** **20 juli 2020**

**THE INCIDENT WITH THE MSC ZOE**

**APPLYING THE EU ENVIRONMENTAL LIABILITY DIRECTIVE. ASSESSING DAMAGE AND COMPENSATION**

*Prof. dr ir Katja Philippart[abc] & Dr Edward Brans[d]*

[a] Waddenacademie, Ruiterskwartier 121a, 8911 BS Leeuwarden

[b] Royal Netherlands Institute for Sea Research, Coastal Systems, P.O. Box 59, 1790 AB Den Burg

[c] Utrecht University, Physical Geography, P.O. Box 80.115, 3508 TC Utrecht

[d] Pels Rijcken & Droogleever Fortuijn N.V., P.O. Box 11756, 2502 AT Den Haag

## 1 Introduction

On 2 January 2019 the containership MSC Zoe lost over 340 containers, including the contents of these containers. The containers were lost on the North Sea, north of the Dutch and German Wadden Islands. Due to wind and tides, a large amount of the contents of the containers ended up on the shores of the Dutch Wadden Islands and in the Wadden Sea. MSC and others have taken measures to retrieve debris from the North Sea seafloor, the beaches of the impacted Wadden Islands and other shores. Likely, almost 75% of the lost cargo has been retrieved.

The Wadden Sea-area, including part of the North Sea coastal zone north of the Wadden Islands, has been designated as Natura 2000 area. In fact, the area consists of seven Natura 2000 sites.[1] Due to the incident with the MSC Zoe several of these Natura 2000 sites were polluted. It is not unlikely that the pollution affected and continues to affect habitats and species protected under the Wild Birds and Habitats Directives.[2]

## 2 Polluter pays principle

According to the preamble of the EU Directive 2004/35/EC, on environmental liability with regard to the prevention and remediation of environmental damage ('Directive' or 'ELD')[3], the 'Polluter pays' principle requires an operator – such as MSC – who caused environmental damage or creates an imminent threat of such damage, in principle, to

[1] See Min. I&M, Natura 2000-beheerplan Waddenzee. Periode 2016-2022, juli 2016, p. 19 and Min I&M, Natura 2000-beheerplan Noordzeekustzone. Periode 2016-2022, juli 2016 (resp.: http://publicaties.minienm.nl/documenten/natura-2000-beheerplan-waddenzee-periode-2016-2022 en http://publicaties.minienm.nl/documenten/natura-2000-beheerplan-noordzeekustzone-periode-2016-2022). See also: https://www.synbiosys.alterra.nl/natura2000/documenten/gebieden/A0_RVO_N2000_RV_20180503.pdf.

[2] Respectively Directive 79/409/EEG on the conservation of wild birds [1979] OJ L 103/1 and Directive 92/43/EEG on the conservation of natural habitats and of wild fauna and flora [1992] OJ L206/7.

[3] Directive 2004/35/EC on environmental liability with regard to the prevention and remediation of environmental damage [2004] OJ L143/56.

bear the cost of the necessary preventive or remedial measures.[4] This is also the case if public authorities act in place of the operator. Starting point is that costs incurred by the public authorities are recovered from the operator. In addition, it is noted in the preamble of the Directive that it is appropriate that the operator ultimately bears the cost of assessing environmental damage and, as the case may be, assessing an imminent threat of such damage occurring.[5] The ELD contains provisions further specifying these starting points and principles.

The Directive is implemented in Dutch law by introducing Title 17.2 in the Environmental Management Act ("Wet milieubeheer").

In this memo, we describe a work plan on the basis of which it should be possible to investigate whether due to the incident with the MSC Zoe, significant damage is caused or likely to be caused to the EU protected habitats and species located in (some of) the above-mentioned Natura 2000 sites.

The first part of this memo (shortly) describes the legal fundamentals of the ELD. The second part describes the work plan and time frame needed to describe the baseline condition of the impacted protected species and habitats and for determining the possible effects of the incident with the MSC Zoe on these species and habitats. The third part contains a cost estimation.

# 3 Fundamentals ELD

## *3.1 Goal*

One of the primary goals of the ELD is to establish a regime which makes it possible to force polluters to take remedial measures once environmental damage has been caused. So the Directive requires persons liable for causing damage to protected habitats and species above a certain threshold, to take remediation measures in order to bring back the impacted habitats and species to baseline condition and to compensate for interim losses.

The ELD does not cover all types of environmental damage. The scope of the ELD is limited to the natural habitats and species protected by the Wild Birds and Habitats Directives, certain waters and soil pollution. The focus here is on protected habitats and species as the container incident may have affected several Natura 2000 areas in the Wadden Sea and North Sea.

## *3.2 Threshold*

The ELD can be applied only in cases where damage was caused or is threatened to be caused to covered natural resources. The ELD defines 'damage' as a "measurable

[4] Paragraph 18 of the preamble of the ELD.
[5] Id.

adverse change in a natural resource or measurable impairment of a natural resource service which may occur directly or indirectly". However, not every measurable adverse change constitutes a claim under the ELD. This is only the case if certain threshold criteria are met. For example, with regard to damage to protected natural habitats and species, the ELD applies only if the damage has "significant adverse effects on reaching or maintaining the favourable conservation status" of the habitats and species concerned. The significance of such effects is to be assessed with reference to the baseline condition, considering the criteria set out in an annex of the ELD.[6]

The term "conservation status" refers to language used in Article 1 of the Habitats Directive. The Directive also determines when a conservation status is considered "favourable".

The conservation status of a **natural habitat** is considered to be 'favourable' when:

— its natural range and the areas it covers within that range are stable or increasing,
— the specific structure and functions which are necessary for its long-term maintenance exist and are likely to continue to exist for the foreseeable future, and
— the conservation status of its typical species is favourable.

The conservation status of a **species** is considered to be 'favourable' when:

— population dynamics data on the species concerned indicate that it is maintaining itself on a long-term basis as a viable component of its natural habitats,
— the natural range of the species is neither being reduced nor is likely to be reduced for the foreseeable future, and
— there is, and will probably continue to be, a sufficiently large habitat to maintain its populations on a long-term basis.

### *3.3 Baseline*

Baseline condition is the condition of a species or habitat that would have been present had the incident in question not occurred, taking into account natural fluctuations and other influences or occurrences not caused by the incident. So, a baseline condition does not imply a pristine condition.

Baseline conditions can be quantified using pre-incident data from the damaged site or from sites similar to the one unaffected by the incident. In the US often reference sites are used to determine baseline conditions.[7] Based on EU law, member states are

[6] Bergkamp, L., Goldsmith, B.J., The EU Environmental Liability Directive. A Commentary, OUP 2013.
[7] Lipton, J., (et al), Equivalency Methods for Environmantal Liability. Assessing Damage and Compensation Under the European Environmental Liability Directive, Springer Verlag 2018.

required to report on a regular basis the status the Natura 2000 sites within their territory are in. Likely, with regard to the Wadden Sea area a lot of data is available to determine baseline conditions, including population dynamics data.

Thus, after the nature of the damage has been identified and determined, the damage has to be qualified. This includes a comparison to the baseline condition. It is an evaluation of the spatial extent and/or degree of damage caused (i.e. loss of habitat, resources and/or natural resource services). It provides the basis for determining the significance of the environmental damage caused, and for establishing remediation goals.

### 3.4 *Remediation*

One of the primary objectives of the ELD is to restore damage to the species and natural habitats protected under the Habitats and Wild Birds Directives. The ELD therefore emphasizes restoration and chooses restoration costs as the primary and preferred method to assess damages. However, because it takes time to restore the damaged protected habitats and species to baseline condition - that is the condition the natural resources and services would have been in, had the damage not occurred - the operator will also be held liable for the loss or impairment of natural resources and natural resource services during the restoration period (interim losses). This is further illustrated by the next figure.

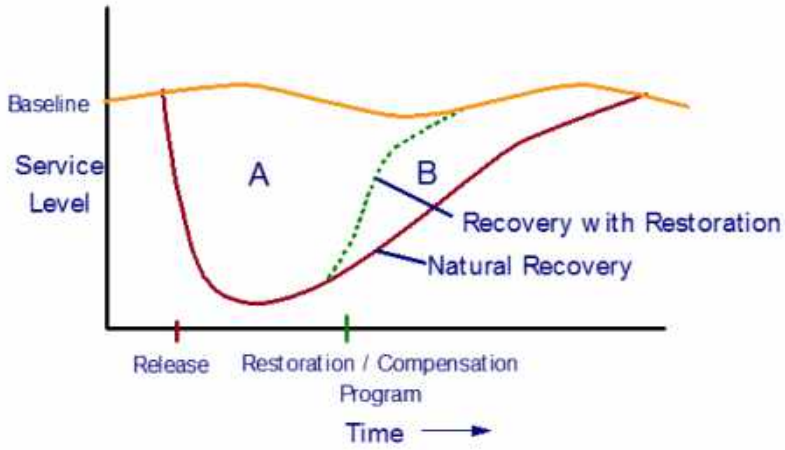


*Figure 1. Definition of damage (A) due to an incident as the difference between base line and actual conditions (e.g. service level), which can be partly restored or compensated (B) by means of primary, complementary or compensatory remediation.*

According to Annex II of the ELD, restoration of damage to protected habitats and species is to be achieved by way of so-called primary, complementary and

compensatory remediation measures. **Primary remediation** is defined as "any remedial measure which returns the damaged natural resources and/or impaired services to, or towards, baseline condition". The focus of these measures is thus on directly restoring the natural resources and services that have been impacted to baseline condition.

**Complementary remediation** is defined in the ELD as "any remedial measure taken in relation to natural resources and/or services to compensate for the fact that primary remediation does not result in fully restoring the damaged natural resources and/or services". The purpose of this type of remediation measures is to provide a similar level of natural resources and/or services at an *alternative site*, as would have been provided if the damaged site had been returned to its baseline condition.

Because neither of these remediation measures compensate for the loss of natural resource and/or human services during the remediation period, **compensatory remediation** measures also need to be taken to compensate for such interim loss of natural resources and services pending recovery. This compensation often consists of additional improvements to protected natural habitats and species or waters at either the damaged site or at an alternative site.

Without going into detail here, methods such as the Habitat Equivalency Method (HEA) and Resource Equivalence Method (HEA) have been developed to determine the scale of the complementary and compensatory remediation measures.

### *3.5 Finally*

Liability under the ELD is in principle unlimited. However, because MSC has the option under the 1996 LLMC to limit liability by establishing a fund, liability is limited (provided relevant requirements are fulfilled).

## 4 Work plan Phase I: identification baseline condition and nature, degree and extent damage

### *4.1 MICROPLASTICS LOST BY THE MSC ZOE*

Much of the cargo lost by the MSC Zoe consisted of plastic items, ranging from relatively large car parts to microplastics (consisting of HDPE-pellets and polystyrene beads). Based upon what is presently known of the cargo list and of the potential risk for protected species and habitats, the Waddenacademie advised Rijkswaterstaat to focus on the possible impacts of the microplastics[8].

[8] https://www.waddenacademie.nl/organisatie/publicatie-lijst/publicatie-detail/wat-zijn-de-gevolgen-van-de-door-de-msc-zoe-verloren-lading-voor-de-noordzeekustzone-en-de-waddenzee

Ingested plastics can have lethal and sub-lethal impacts on a wide range of marine organisms, resulting from physical harm including induction of inflammation and stress. Furthermore, plastic fragments can additionally absorb and/or adsorb contaminants, which may interfere with an individual's physiology and therefore have negative consequences on reproduction (e.g. breeding success) and survival[9].

The so-called primary microplastics (plastic items smaller than 5 mm when entering the natural environment) include HPDE-pellets which were washed ashore in unprecedentedly large quantities directly after the cargo loss by the MSC Zoe (both as single pellets and as pellets packed within 25kg bags), and polystyrene beads which were documented as being lost from the MSC Zoe by the German Central Command for Maritime Emergencies[10].

At present, 299 containers and 2.424.930 kg (sum of containers and their contents) are recovered of the 342 containers and 3.257.000 kg lost[11]. This implies that more than 25% (832.070 kg, including the weight of 43 containers) of the lost cargo is still within the natural environment. Assuming an average weight of 3500kg per container, the net weight of the not yet recovered cargo is 681.570 kg. All plastic items of this cargo will rapidly or slowly (depending on the size, shape and properties of these items, and on the environmental conditions) deteriorate into so-called secondary microplastics[12].

Plastic pollution affects marine species in two main ways, through entanglement and ingestion. Here, we focus on potential damage due to ingestion of microplastics, which can be direct (purposefully ingestion by mistaking it for food) or indirect (inadvertently consuming plastic while foraging on other prey items).

The HDPE-pellets more or less mimic the size and shape of (juvenile) bivalves, including Cockles (*Cerastoderma edule*), Surf Clams (*Spisula subtruncata*), Blue Mussels (*Mytilus edulis*) and Baltic Tellins (*Limecola balthica*), that commonly occur in the Wadden Sea and North Sea coastal zone. In addition to inadvertent ingestion, these pellets might therefore be purposely consumed by shellfish-eating birds, including N2000 species.

The polystyrene beads more or less mimic the size (0.68 ± 0.09 mm) and shape of grains of coarse sand (0.5–1 mm). In addition to direct ingestion by benthos-eating fish and birds, these beads might therefore first be inadvertently consumed by deposit-feeding macrozoobenthos (including polychaetes and bivalves) that can be subsequently consumed by N2000 species.

---

[9] SAPEA, Science Advice for Policy by European Academies (2019) A Scientific Perspective on Microplastics in Nature and Society. Berlin: SAPEA.
[10] https://www.havariekommando.de/SharedDocs/Downloads/DE/Infotexte_Containerverlust_MSC_ZOE/Info_Verpackung_Gefahrstoffe.pdf?__blob=publicationFile&v=1
[11] Update 23, t/m 8 oktober – Afhandeling incident containers MSC Zoe (published by Rijkswaterstaat)
[12] Veiga JM et al. 2016. Identifying sources of marine litter. MSFD GES TG Marine Litter Thematic Report; JRC Technical Report; EUR 28309; doi:10.2788/018068

Additionally, if a particular polychaete or bivalve species performs key functions within a particular habitat, plastic-related impacts on these functions might reduce the quality of this habitat. Plastic ingestion by Lugworms (*Arenicola marina*), for example, has been found to reduce its bioturbation activities[13], subsequently affecting the natural dynamics (quality) of habitat type H1140 (mudflats and sandflats not covered by seawater at low tide)[14].

If plastic ingestion by bivalves reduces their health, as has been found for Blue Mussels (*Mytilus edulis*)[15], then this might reduce the typical species and biogenic structures (mussel beds) stated to be crucial for habitat types H1140 (mudflats and sandflats not covered by seawater at low tide) and H1110 (sandbanks which are slightly covered by sea water all the time)[16].

Typical species of H1140 include Lugworm (*Arenicola marina*), Common Cockle (*Cerastoderma edule*), Baltic Tellin (*Macoma balthica*) and Blue Mussel (*Mytilus edulis*)[17]. Typical species of H1110 include Baltic Tellin (*Macoma balthica*), Blue Mussel (*Mytilus edulis*) and Surf clam (*Spisula subtrucata*)[18].

## 4.2 SPECIES SELECTION

### 3.2.1 SELECTION CRITERIA

For the assessment of damage due to the loss of cargo by the MSC Zoe, it is proposed to focus on a small selection of "flagship" bird species that are protected under the Wild Birds Directive within the Natura 2000 areas of the Wadden Sea and North Sea coastal zone[19].

Each of these bird species represents a larger group ("fleet") with respect to pathways of pollution (e.g. via direct or indirect ingestion) within the food web, their present status with respect to conservation objectives[20], the potential damage caused by microplastics and the options for remediation.

With respect to species indicating the quality of the habitat types H1140 and H1110, selection of "typical species" was restricted to those polychaetes and bivalves that are considered to be an important prey for the selected flagship bird species.

[13] Wright SL et al. 2016. Microplastic ingestion decreases energy reserves in marine worms. Current Biology 23, R1031-R1033
[14] See further https://www.synbiosys.alterra.nl/natura2000/gebiedendatabase.aspx?main=natura2000&subj=habtypen&groep=0
[15] von Moos et al. 2012. Uptake and effects of microplastics on cells and tissue of the blue mussel Mytilus edulis after an experimental exposure. Environ. Sci. Technol. 2012, 46, 20, 11327-11335.
[16] https://www.synbiosys.alterra.nl/natura2000/documenten/profielen/habitattypen/Profiel_habitattype_1110_2008.pdf
[17] https://www.synbiosys.alterra.nl/natura2000/documenten/profielen/habitattypen/Profiel_habitattype_1140.pdf
[18] https://www.noordzeeloket.nl › pages › annex_2888
[19] http://publicaties.minienm.nl/documenten/natura-2000-beheerplan-waddenzee-periode-2016-2022
[20] Foppen R, et al. 2016. De ecologische haalbaarheid van de Natura 2000 instandhoudingsdoelen voor vogels. Sovon-rapport 2016/51. Sovon Vogelonderzoek Nederland, Nijmegen.

### 3.2.2 CANDIDATE "FLEET" AND "FLAGSHIP" BIRD SPECIES

*SHELLFISH-EATING DUCKS*

The **Common Scoter (*Melanitta nigra*)** is a medium-large sea duck that winters in the coastal zone north of the Wadden islands, where they feed (by diving) on suspension-feeding bivalves such as surf clams (*Spisula subtruncata*) and razor clams (*Ensis directus*)[21], which in general are able to ingest microplastics from the water and the sediment[22].

The group of diving sea ducks also includes the **Common Eider (*Somateria mollissima*)**, which breeds in the Wadden Sea area. Within the Wadden Sea, Eiders feed predominantly on mussels (*Mytilus edulis*), cockles (*Cerastoderma edule*) and razor clams (*Ensis directus*)[23]. Such suspension-feeding bivalves have been observed to ingest microplastics, e.g. mussels[24]. In addition, Eider ducks have been observed to ingest plastic items during feeding[25].

*FILTER-FEEDING DUCKS*

The **Shelduck (*Tadorna tadorna*)** obtains its prey mainly by moving its bill in a scything action through the mud and sieving small benthic organisms (< 8 mm), such as mudsnails (*Hydrobia ulvae*)[26], mudshrimps (*Corophium volutator*)[27] and small bivalves (*Macoma balthica*, *Cerastoderma edule*)[28], from the upper two centimeters of the sediment surface. Because droppings of these ducks include indigestible items such as seeds of widgeongrass (*Ruppia maritima*)[29], these ducks might be considered to be particularly vulnerable to ingesting microplastics when present within the birds' foraging depth of the sediment (as has been observed for shelducks foraging in Spanish lakes[30]).

*SHELLFISH-EATING WADERS*

---

[21] Leopold MF et al. 1995. De Zwarte Zeeëend *Melanitta nigra* in Nederland. Limosa 68, 49-64.
[22] Ward JE, et al. 2019. Capture, ingestion, and egestion of microplastics by suspension-feeding bivalves: a 40-year history. Anthropocene Coasts 2: 39-49. dx.doi.org/10.1139/anc-2018-0027.
[23] Nehls G & Ketzenberg C, 2002. Do eiders, *Somateria mollissima*, exhaust their food resources? A study on natural mussel *Mytilus edulis* beds in the Wadden Sea. Danish Review of Game Biology 16, 47-61.
[24] Van Cauwenberghe L, et al. 2013. Selective uptake of microplastics by a marine bivalve (*Mytilus edulis*). Commun. Agric. Appl. Biol. Sci. 78: 25–27. PMID: 23875293.
[25] Baptist MJ et al. 2019. Mogelijke ecologische gevolgen containerramp MSC Zoe voor Waddenzee en Noordzee. Een quickscan. Wageningen University Research.
[26] Anders NR et al 2009. Predation of the shelduck *Tadorna tadorna* on the mud snail *Hydrobia ulvae*. Aquatic Ecology 43, 1193-1199.
[27] Kraan C et al. 2006. Bergeenden vinden Slijkgarnaaltjes en rust op nieuwe ruiplaats bij Harlingen. Limosa 79, 19-24.
[28] Nehls et al. 1992. Bestand und Verteilung mausernder Brandenten (*Tadorna tadorna*) im Deutschen Wattenmeer. Die Vogelwarte 36, 221-232.
[29] Figuerola J et al. 2002. Comparative dispersal effectiveness of wigeongrass seeds by waterfowl wintering in south-west Spain: quantitative and qualitative aspects. Journal of Ecology 90, 989–1001.
[30] Gil-Delgado JA et al. 2017. Presence of plastic particles in waterbirds faeces collected in Spanish lakes. Environmental Pollution 220, 732-736.

The **Red Knot (*Calidris canutus*)** is a small wader that stays part of the year in the Wadden Sea, to overwinter (*C.c. islandica*) or to fuel during migration in spring and autumn (*C.c. canutus*). In the Wadden Sea, the knots feed mainly upon small buried macrozoobenthic species[31], which are swallowed whole. Red Knots have been observed to prey on juvenile bivalves and mudsnails with sizes similar to those of the HPDE-pellets, i.e., 4-5 mm[32].

*POLYCHAETE-EATING WADERS*

The **Bar-tailed Godwit (*Limosa lapponica*)** breeds in northern Scandinavia and western Siberia, and part of the population overwinters in the Wadden Sea whilst others use this area to fuel for their long-distance migration. For the females of this bird species, the lugworm (*Arenicola marina*) is the main component of the diet ranging between more than 20% in March to more than 60% in August of the total biomass of the identified prey[33]. Lugworms were observed to accumulate microplastics, both in the laboratory[34] as under natural conditions[35]. Bar-tailed godwits may, therefore, consume plastic while foraging on lugworms.

### 3.2.3 "TYPICAL" SPECIES (H1140, H1110)

Based upon the prey preferences of the flagship bird species, we selected the following macrozoobenthic species which are considered to be typical for habitat types H1140 and H1110 and common in the study area.

Polychaetes

- Lugworm (*Arenicola marina*)

Bivalves

- Baltic Tellin (*Macoma balthica*)
- Common Cockle (*Cerastoderma edule*)
- Blue Mussel (*Mytilus edulis*)
- Surf clam (*Spisula subtruncata*)

## 4.3 CONSERVATION STATES AND OBJECTIVES

**Common Scoters** are presently considered to be in an unfavourable conservation status (EU N2000)[36] but are listed to be of "least concern" on the IUCN Red List[37]. Wintering numbers in The Netherlands constitute 5-10% of the European population.

[31] Piersma T, et al. 1994. Resources for long-distance migration of knots *Calidris canutus islandica* and *C. c. canutus*: how broad is the temporal exploitation window of benthic prey in the western and eastern Wadden Sea? Oikos 71, 393-407.
[32] Dekinga A & Piersma T, 1993. Reconstructing diet composition on the basis of faeces in a mollusc-eating wader, the Knot *Calidris canutus*. Bird Study 40, 144-156
[33] Scheiffarth G, 2001. The diet of Bar-tailed Godwits *Limosa lapponica* in the Wadden Sea: combining visual observations and faeces analyses. Ardea 89, 481-494.
[34] Besseling E et al. 2013. Effects of microplastic on performance and PCB bio- accumulation by the lugworm *Arenicola marina* (L.). Environ. Sci. Technol. 47, 593-600.
[35] Fischer E, 2019. Distribution of microplastics in marine species of the Wadden Sea along the coastline of Schleswig-Holstein, Germany. University of Hamburg, 65 pp.
[36] http://publicaties.minienm.nl/documenten/natura-2000-beheerplan-waddenzee-periode-2016-2022
[37] https://www.iucnredlist.org

**Common Eiders** are presently considered to be in a highly unfavourable conservation status (EU N2000), the birds in the Wadden Sea contribute to more than >50% to the national conservation objective[38] and is listed as "near threatened" on the IUCN Red List[39].

**Shelducks** are presently considered be in a favourable conservation status (EU N2000), the birds in the Wadden Sea contribute to more than >50% to the national conservation objective[40] and this species is listed to be of "least concern" on the IUCN Red List[41].

**Red Knots** are presently considered to be in an unfavourable conservation status (EU N2000), the birds in the Wadden Sea contribute to more than >50% to the national conservation objective[42], and this species is considered to be "near threatened" on the IUCN Red List[43].

**Bar-tailed Godwits** are presently considered to be in a favourable conservation status (EU N2000), the birds in the Wadden Sea contribute to more than >50% to the national conservation objective[44], and this species is considered to be "near threatened" on the IUCN Red List[45].

The EU Natura-2000 conservation objectives for these five flagship bird species are given in Table 1.

*Table 1. Conservation objectives for bird species that are protected under the Wild Birds Directive within the Natura 2000 areas of the Wadden Sea and North Sea coastal zone[46].*

| N2000 code | Bird Species | Conservation objective (number of birds/breeding pairs) | |
|---|---|---|---|
| **North Sea coastal zone** | | | |
| A065 | Common Scoter | 68.500 | Carrying capacity in winter |
| **Wadden Sea** | | | |
| A048 | Shelduck | 38.400 | Seasonal average |
| A063 | Common Eider | 5.000 | Breeding pairs |
| | | 90.000-115.000 | Seasonal average |
| A143 | Red Knot | 44.400 | Seasonal average |
| A157 | Bar-tailed Godwit | 54.400 | Seasonal average |

## 4.4 DETERMINATION OF BASELINE CONDITIONS ($T_0$)

### Microplastics

[38] http://publicaties.minienm.nl/documenten/natura-2000-beheerplan-waddenzee-periode-2016-2022
[39] https://www.iucnredlist.org
[40] http://publicaties.minienm.nl/documenten/natura-2000-beheerplan-waddenzee-periode-2016-2022
[41] https://www.iucnredlist.org
[42] http://publicaties.minienm.nl/documenten/natura-2000-beheerplan-waddenzee-periode-2016-2022
[43] https://www.iucnredlist.org
[44] http://publicaties.minienm.nl/documenten/natura-2000-beheerplan-waddenzee-periode-2016-2022
[45] https://www.iucnredlist.org
[46] http://publicaties.minienm.nl/documenten/natura-2000-beheerplan-waddenzee-periode-2016-2022

Following the incident with the MSC Zoe, a considerable number of samples were taken, varying from microplastic densities (on the beach, at the shores, in the water and on the seafloor) to marine organisms which will be analysed for contamination with microplastics[47]. These samples do allow for analysis of concentrations of microplastics in habitats, typical species of these habitats and species that are protected under the Wild Birds Directive within the Natura 2000 areas of the Wadden Sea and North Sea coastal zone before and after the incident in January 2019. In addition, spatial distribution within several programs on the environment and organisms allow for mapping the contamination patterns with microplastics within the Wadden Sea and North Sea coastal zone.

Immediately after the incident, unprecedentedly large quantities of High-Density Polyethylene (HDPE) pellets (4-5 mm) washed ashore in the North Sea and Wadden Sea area, both single and packed in bags of 25 kg, with highest densities and amounts found at the beaches of the island of Schiermonnikoog[48]. On the basis of 300 pellet density measurements on the beaches of the Wadden Islands and the mainland coasts, it is estimated that around 24 million pellets (with a total weight of around 600 kilos) washed ashore[49]. Backtracking of the pellets by means of an oceanographical model revealed that the source of these microplastics fits with the location and timing of the cargo loss by the MSC Zoe[50].

Comparison of commissioned beach litter surveys at "Zuiderduintjes" (a small island south of Rottumeroog) in 2018 and 2019 showed that industrial plastic HDPE-granulates were totally absent in all 2018 surveys and omni-present in March 2019[51]. Furthermore, litter has been collected from the sea floor in the North Sea coastal zone in 2019 and in 2018 as part of a scientific monitoring program on fish.

Comparison of samples taken during long-term monitoring programs (including microplastics) by NIOZ[52] will enable identification and spatial distribution of enhanced plastic contamination in sediments and macrozoobenthos of tidal flats of the Wadden Sea (habitat type H1140) in 2019 (> 700 and 200 samples, respectively) compared to 2018 (> 700 and 200 samples, respectively).

Analyses of stomach contents of fish caught by fishermen as bycatch and by scientists as part of a long-term monitoring programs on fish and commercial fish stocks in 2019 (> 3000 samples) compared to previous years (> 2000 samples) by NIOZ and WMR[53] will be informative on microplastic pollution in the North Sea coastal zone (habitat type H1110).

---

[47] Personal comments by Johan van der Molen (NIOZ) and Martin Baptist (WMR)
[48] Doze J, 2019. Analyse HDPE pellets. Notitie Rijkswaterstaat Noord-Nederland, 23 mei 2019.
[49] Van der Heide T, 2019. Position paper Ecologie voor rondetafelgesprek "Afhandeling van de containerramp MSC Zoe"
[50] Bert van Munster (RWS WVL), 2019.
[51] Bureau Waardenburg, 2019. Beach litter survey Zuiderduintjes 2018-2019. Report 18-0988/19.04503/RubFi.
[52] Royal Netherlands Institute of Sea Research
[53] Wageningen Marine Research

Furthermore, analyses of samples of faeces and pellets and stomach contents of several bird species that are visiting (e.g., Red Knots) or breeding in (e.g., Spoonbills) the Wadden Sea area from 2019 (> 2000 samples) and from previous years (> 1500 samples) by NIOZ will be informative on enhanced pollution by microplastics in birds that are protected under the Wild Birds Directive within the Natura 2000 areas of the Wadden Sea and North Sea coastal zone.

In addition, analyses of stomach contents of stranded harbour seals and harbour porpoises collected in 2019 (> 10 and 50, respectively) and in previous years (> 150 and 400, respectively) by WMR can be informative if pollution with microplastics was enhanced at higher trophic levels after the cargo loss by the MSC Zoe.

**Birds**

Baseline conditions (total numbers within the study area) of **Common Scoter** and **Common Eider** can be assessed from aerial annual bird counts (in January) since 1987 in the Dutch North Sea coastal zone and the Wadden Sea[54]. Furthermore, the baseline condition on breeding success of the **Common Eider** can be derived from annual monitoring since 1990 at several locations within the Wadden Sea area (Groningen, Texel, Vlieland, Griend, Ameland, Schiermonnikoog)[55].

Baseline conditions (total numbers within the study area) of **Shelduck, Red Knot** and **Bar-tailed Godwit** can be assessed from counts of high tide roosts (multiple times per year) since 1975[56]. Furthermore, the baseline condition on breeding success of the **Shelduck** can be derived from annual monitoring since 1998[57].

**Benthos**

Baseline conditions of selected "typical" polychaete and bivalve species can be derived from annual monitoring programs on dynamics intertidal benthos (including **Lugworms** and **Baltic Tellins**) since 2007[58], and on commercial shellfish species in the Wadden Sea since 1991 (**Cockles**[59] and **Mussels**[60]) and in the North Sea coastal zone since 1995 (**Surf Clams**)[61]. These data not only allow for analysis of variation in time and space, but also for calculation of possible long-term changes in food availability for the "flagship" bird species.

[54] https://www.clo.nl/indicatoren/nl1382-aantalsontwikkeling-van-overwinterende-watervogels
[55] Koffijberg K., et al. 2018. Breeding success of coastal breeding birds in the Wadden Sea in 2017. WOT Technical Report 136, Sovon report 2018/72, WMR report C089/18.
[56] https://qsr.waddensea-worldheritage.org/reports/migratory-birds
[57] https://www.sovon.nl/nl/soort/1730
[58] https://www.nioz.nl/en/research/projects/4126-0
[59] https://www.wur.nl/nl/show/Kokkelbestand-in-Nederlandse-kustwateren.htm
[60] https://www.wur.nl/nl/show/Mosselbanken-in-de-getijdenzone.htm
[61] https://www.wur.nl/nl/nieuws/Twee-soorten-schelpdieren-spectaculair-toegenomen-in-Nederlandse-kustwateren.htm

**ACKNOWLEDGEMENTS**

We are most grateful to Roeland Bom (NIOZ), Jacco Doze (RWS), Jan van Gils (NIOZ), Mardik Leopold (WMR), Johan van der Molen (NIOZ), Lies van Nieuwerburgh (RWS) and Eric Ravestein (RWS), who have commented on a previous version of this document.

Deltares is een onafhankelijk kennisinstituut voor toegepast onderzoek op het gebied van water en ondergrond. Wereldwijd werken we aan slimme oplossingen voor mens, milieu en maatschappij.

Deltares

www.deltares.nl